

Mycotoxins - An analysis of their immunomodulatory effects and methods for their detection

A thesis submitted for the degree of Ph.D.

by

Jonathan Loftus B.Sc. (Hons.)

August 2018

Based on research carried out at

School of Biotechnology,

Dublin City University,

Dublin 9,

Ireland.

Under the supervision of Professor Christine Loscher and

Professor Richard O' Kennedy

Declaration

I hereby certify that this material, which I now submit for assessment on the programme of study leading to the award of PhD is entirely my own work, and that I have exercised reasonable care to ensure that the work is original, and does not to the best of my knowledge breach any law of copyright, and has not been taken from the work of others save and to the extent that such work has been cited and acknowledged within the text of my work.

Signed:

ID No.:

Date:

“Great for the town”

Acknowledgements

I would like to start by thanking my supervisors, Prof. Richard O’Kennedy and Prof. Christine Loscher, for the wonderful opportunity to undertake this research, and for their constant encouragement and enthusiasm throughout my PhD.

Thanks to all the members of the Applied Biochemistry Group, Dan, Kara, Aoife, Arabelle, Julie-Ann, Caroline, Fay, and all the past members during my time in the group for the morning coffees, lunch time football and the ridiculous nights out, but especially to Jenny for everything over the last three years.

My thanks to the members of Immunomodulation Group, Niamh, Conor, all the past members for adopting me as one of their own, and particularly Kim for her help all the way through, even up to proofreading this thesis!

Thanks also to Gregor for the help and guidance with my first research publication, and to Albina and Damien for their help with experimental work at a crucial time.

A special mention to all the members, past and present, of the BRS for the nights out, tag rugby, great trips away and for the support during my time as Chairperson.

I must also acknowledge my friends from outside DCU, especially Evin and Alan, who helped me maintain my sanity for the past four years.

Importantly, I need to thank my family. My brother, Graham, my cousins, Amy and Vicky, and my aunt and uncle, Tom and Ann, in particular, provided me with an invaluable support network without which this would not have been possible.

Most of all, I simply cannot thank my parents, Patsy and Hugh, enough. Their love, support and encouragement has given me opportunities in life that I could not have imagined. I am forever in their debt and I can only hope I have made them proud.

Finally, a very special thanks to Sligo Rovers Football Club for reminding me that no matter how bad things got in the lab, they could always get worse on the pitch!

This project was funded by the Irish Research Council.

Table of Contents

Declaration	ii
Acknowledgements	iv
List of figures	x
List of tables	xvi
Abbreviations	xvii
Units	xxii
Publications	xxiv
Presentations and posters	xxv
Educational and outreach work	xxvi
Abstract	xxvii
Chapter 1: Introduction	1
1.1 Overview	2
1.1.1 History of mycotoxins	2
1.2 Classification, sources and chemical properties of mycotoxins	3
1.3 Mycotoxins, food safety and economic impact	5
1.3.1 Mycotoxin occurrence and exposure	5
1.3.2 Mycotoxin risk management	7
1.3.3 Legislative limits for mycotoxins	8
1.4 Effects of mycotoxins on human and animal health	11
1.4.1 Mycotoxicosis and toxicological studies for mycotoxins	11
1.4.2 Mycotoxins and the immune system	14
1.4.2.1 Inflammatory response	15
1.5 Mycotoxin detection methods	17
1.5.1 Analytical techniques	17
1.5.2 Immunological techniques	17
1.5.3 Limitations of current techniques	18
1.6 Novel mycotoxin binders	19
1.6.1 Antibodies	19
1.6.2 Recombinant antibody production	21
1.6.3 Phage Display Technology	21
1.6.4 Biopanning of phage display libraries	23
1.7 Analysis of multiple mycotoxin contamination	25
1.8 Thesis Aims	26

2.1 Materials	28
2.1.1 General reagents	28
2.1.2 Buffer and Media preparation	31
2.1.3 Commercial antibodies, antigens and mycotoxins	33
2.1.4 Commercial kits	34
2.1.5 Cell culture materials	35
2.1.6 Equipment	36
2.2 Methods	40
2.2.1 Cell culture	40
2.2.1.1 Culture of cell line	40
2.2.1.2 Long-term storage of cell line	40
2.2.1.3 Resuscitation of frozen cell line stocks	40
2.2.1.4 Cell counting	41
2.2.1.5 Cell authentication and mycoplasma testing	41
2.2.2 Effects of mycotoxin exposure on murine macrophage cell line	41
2.2.2.1 Mycotoxin treatments	41
2.2.2.2 Analysis of effect of individual mycotoxins on cell viability (MTS assay) in the J774A.1 murine macrophage cell line	41
2.2.2.3 Analysis of effects of individual mycotoxins on cytokine (IL-6, IL-10, IL-27, IL-12p40, IL-1 β and TNF- α) release in the J774A.1 murine macrophage cell line	42
2.2.2.4 Analysis of effects of mycotoxin combinations on cytokine (IL-6, IL-10, IL-12p40 and TNF- α) release in the J774A.1 murine macrophage cell line	42
2.2.2.5 Statistical analysis	43
2.2.2.6 Analysis of effects of mycotoxin combinations on cell surface marker (CD80, CD86, TLR4 and MHCII) expression in the J774A.1 murine macrophage cell line using flow cytometry	43
2.2.2.7 Analysis of effects of mycotoxin combinations on phagocytosis in the J774A.1 murine macrophage cell line using flow cytometry	44
2.2.2.8 Analysis of effects of mycotoxin combinations on cell surface marker (CD80 and CD86) expression from the J774A.1 murine macrophage cell line using Lab-in-a-Trench	44
2.2.3 Generation of an avian immune library for Aflatoxin M1, Patulin and Ochratoxin A	48
2.2.3.1 Immunisation of a leghorn chicken with AFM1-BSA and Patulin-HG-KLH	48
2.2.3.2 Serum titre of AFM1-BSA and Patulin-HG-KLH-immunised chickens by ELISA	48
2.2.3.3 Phenol-chloroform extraction of RNA	49
2.2.3.4 cDNA synthesis by reverse transcription	50
2.2.3.5 Amplification of antibody variable domain sequences using PCR	51

2.2.3.6 SOE-PCR optimisation	53
2.2.3.7 Agarose gel electrophoresis	54
2.2.3.8 DNA agarose gel purification	55
2.2.3.9 Digestion of scFv insert and pComb3XSS vector using Sfil	55
2.2.3.10 Treatment of pComb3XSS vector with antarctic phosphatase	57
2.2.3.11 Ligation of SOE insert into pComb3XSS vector	58
2.2.3.12 Library transformation and rescue of chicken scFv-displaying phage	58
2.2.3.13 Enrichment of chicken phage library by bio-panning	60
2.2.3.14 Polyclonal phage ELISA	61
2.2.3.15 Colony-pick PCR	61
2.2.3.16 Direct monoclonal ELISA of solubly-expressed scFv fragments	62
2.2.3.17 Analysis of scFv clones by direct and competition ELISA	63
2.2.3.18 Expression optimisation of scFv clones	63
2.2.3.19 scFv purification using immobilised metal affinity chromatography	64
2.2.3.20 scFv purification analysis by SDS-PAGE and western blotting	64
2.2.4 Synthesis of Pautlin-Hemisuccinate-Bovine Serum Albumin (Patulin-HS-BSA) Conjugate	66
2.2.5 Ethical authorisation for animal experimentation	66
2.2.6 Safety precautions and protocols for handling mycotoxin material and waste	66
Chapter 3: Effect of individual mycotoxin exposure on murine macrophage viability and cytokine production	67
3.1 Introduction	68
3.1.1 Mycotoxins as immunomodulatory agents	68
3.1.2 Chapter aims	70
3.2 Results	71
3.2.1 Analysis of mycotoxin exposure on J774A.1 murine macrophage viability using MTS assay	71
3.2.1.1 J774A.1 macrophage viability after exposure to patulin, zearalenone, deoxynivalenol and T-2 toxin with LPS challenge	71
3.2.2 Analysis of mycotoxin exposure on J774A.1 murine macrophage cytokine production	74
3.2.2.1 J774A.1 macrophage cytokine production after exposure to patulin, zearalenone, deoxynivalenol and T-2 toxin with LPS challenge	74
3.3 Discussion	84
Chapter 4: Effect of mycotoxin combinations on murine macrophage cytokine production	89
4.1 Introduction	90
4.1.1 Co-occurrence of multiple mycotoxins	90
4.1.2 Chapter aims	91

4.2 Results	92
4.2.1 Analysis of multiple mycotoxin exposure on J774A.1 murine macrophage cytokine production	92
4.2.1.1 J774A.1 macrophage cytokine production after exposure to deoxynivalenol and T-2 toxin with LPS challenge	92
4.2.1.2 J774A.1 macrophage cytokine production after exposure to patulin and deoxynivalenol with LPS challenge	94
4.2.1.3 J774A.1 macrophage cytokine production after exposure to zearalenone and deoxynivalenol with LPS challenge	96
4.2.1.4 J774A.1 macrophage cytokine production after exposure to zearalenone and T-2 toxin with LPS challenge	98
4.2.1.5 J774A.1 macrophage cytokine production after exposure to patulin and T-2 toxin with LPS challenge	100
4.2.1.6 J774A.1 macrophage cytokine production after exposure to patulin and zearalenone with LPS challenge	102
4.3 Discussion	104
Chapter 5: Effect of mycotoxin combinations on murine macrophage phagocytosis and cell surface marker expression	109
5.1 Introduction	110
5.1.1 Phagocytosis	111
5.1.2 Cell surface makers	111
5.1.3 Lab-in-a-Trench	112
5.1.4 Chapter aims	113
5.2 Results	114
5.2.1 Analysis of multiple mycotoxin exposure on J774A.1 murine macrophage phagocytosis using flow cytometry	114
5.2.1.1 J774A.1 macrophage phagocytosis after exposure to patulin, zearalenone, deoxynivalenol and T-2 toxin with LPS challenge	114
5.2.2 Analysis of multiple mycotoxin exposure on J774A.1 murine macrophage cell surface marker expression using flow cytometry	118
5.2.2.1 J774A.1 macrophage cell surface marker expression after exposure to patulin, zearalenone, deoxynivalenol and T-2 toxin with LPS challenge	118
5.2.3 Analysis of multiple mycotoxin exposure on J774A.1 murine macrophage cell surface marker expression using Lab-in-a-Trench	124
5.2.3.1 J774A.1 macrophage cell surface marker expression after exposure to patulin, zearalenone, deoxynivalenol and T-2 toxin with LPS challenge	124
5.3 Discussion	132
Chapter 6: Generation of avian recombinant antibody libraries to the mycotoxins; patulin, ochratoxin A and aflatoxin M1	138
6.1 Introduction	139

6.1.1	Detection methodologies for mycotoxins	139
6.1.2	Chapter aims	141
6.2	Results	142
6.2.1	Production of an avian recombinant scFv library for aflatoxin M1 and patulin	142
6.2.1.1	Avian immune response generation to mycotoxin conjugates	142
6.2.1.2	Extraction of RNA and reverse transcription to cDNA	144
6.2.1.3	Amplification of avian heavy and light chains and PCR optimisation	145
6.2.1.4	SOE-PCR optimisation of variable heavy and light chains from the avian library	148
6.2.1.5	Digestion of SOE product and ligation into pComb3xSS vector	154
6.2.1.6	Transformation of pComb3xSS vector in electro-competent E. coli XL1-Blue cells	155
6.3	Discussion	157
Chapter 7: Isolation and characterisation of avian antibodies to target the mycotoxins; patulin, ochratoxin A and aflatoxin M1		161
7.1	Introduction	162
7.1.1	Phage Display	162
7.1.2	Chapter aims	164
7.2	Results	164
7.2.1	Synthesis of Patulin-HS-BSA conjugate	164
7.2.2	Phage display bio-panning to isolate scFv clones to target patulin, AFM1 and OTA	165
7.2.2.1	Bio-panning of the immune avian libraries	165
7.2.2.2	Verification of scFv inserts by colony-pick PCR	166
7.2.2.3	Polyclonal phage ELISA	170
7.2.2.4	Direct monoclonal ELISA of solubly-expressed scFv fragments	172
7.2.3	Analysis of scFv clones	175
7.2.3.1	Analysis of clones using direct and competitive ELISA	175
7.2.3.2	Optimisation of scFv expression	176
7.2.3.3	IMAC purification of scFv clone and analysis using SDS-PAGE and Western Blotting	177
7.3	Discussion	179
Chapter 8: Overall Conclusions		183
8.1	Overall conclusions	184
Chapter 9: Bibliography		192

List of figures

Figure 1.1:	Chemical structures of aflatoxin B1, B2, M1, deoxynivalenol, T-2 toxin and patulin	5
Figure 1.2:	Immunoglobulin formats	20
Figure 1.3:	pComb phagemid vector and filamentous phage structure	22
Figure 1.4:	Biopanning of a scFv library using phage display technology	24
Figure 2.1:	Structure of the Lab-in-a-Trench platform	45
Figure 2.2:	Cell capture in the Lab-in-a-Trench platform	46
Figure 2.3:	Process for opto-microfluidic monitoring of cell expression dynamics	47
Figure 2.4:	Details of the pComb3X phagemid vector	56
Figure 3.1:	MTS proliferation assay to analyse the effect of patulin on the J774A.1 macrophage cell line	72
Figure 3.2:	MTS proliferation assay to analyse the effect of DON on the J774A.1 macrophage cell line	72
Figure 3.3:	MTS proliferation assay to analyse the effect of ZEN on the J774A.1 macrophage cell line	73
Figure 3.4:	MTS proliferation assay to analyse the effect of T-2 toxin on the J774A.1 macrophage cell line	73
Figure 3.5:	Cytokine production in the supernatants of J774A.1 murine macrophage cells cultured for 24 hours in the presence of patulin ranging in concentration from 0.001 to 100 pg/mL, with and without LPS stimulation	76
Figure 3.6:	Cytokine production in the supernatants of J774A.1 murine macrophage cells cultured for 24 hours in the presence of DON ranging in concentration from 0.001 to 100 pg/mL, with and without LPS stimulation	77
Figure 3.7:	Cytokine production in the supernatants of J774A.1 murine macrophage cells cultured for 24 hours in the presence of ZEN ranging in concentration from 0.001 to 100 pg/mL, with and without LPS stimulation	78

Figure 3.8:	Cytokine production in the supernatants of J774A.1 murine macrophage cells cultured for 24 hours in the presence of T-2 toxin ranging in concentration from 0.001 to 100 pg/mL, with and without LPS stimulation	79
Figure 4.1:	Production of IL-12p40 and TNF- α in the supernatants of J774A.1 murine macrophage cells, cultured for 24 hours in the presence of DON and T-2 Toxin, with and without LPS (100 ng/mL)	93
Figure 4.2:	Production of IL-6 and IL-12p40 in the supernatants of J774A.1 murine macrophage cells, cultured for 24 hours in the presence of Patulin and DON, with and without LPS (100 ng/mL)	95
Figure 4.3:	Production of IL-6 and TNF- α in the supernatants of J774A.1 murine macrophage cells, cultured for 24 hours in the presence of DON and ZEN, with and without LPS (100 ng/mL)	97
Figure 4.4:	Production of IL-6 and TNF- α in the supernatants of J774A.1 murine macrophage cells, cultured for 24 hours in the presence of ZEN and T-2 Toxin, with and without LPS (100 ng/mL)	99
Figure 4.5:	Production of IL-6, IL-10, IL-12p40 and TNF- α in the supernatants of J774A.1 murine macrophage cells, cultured for 24 hours in the presence of Patulin and T-2 Toxin, with and without LPS (100 ng/mL)	101
Figure 4.6:	Production of IL-6, IL-10, IL-12p40 and TNF- α in the supernatants of J774A.1 murine macrophage cells, cultured for 24 hours in the presence of Patulin and ZEN, with and without LPS (100 ng/mL)	103
Figure 5.1:	Controls for the effect of mycotoxin exposure on phagocytosis	115
Figure 5.2:	The effect of mycotoxin exposure on phagocytosis. J774A.1 murine macrophage cells, cultured for 24 hours in the presence of patulin, DON, ZEN and T-2 Toxin, with and without LPS (100 ng/mL) stimulation, followed by incubation with 1 μ m FITC-labelled latex beads for 1 hour	116

Figure 5.3:	The effect of mycotoxin exposure on phagocytosis. J774A.1 murine macrophage cells, cultured for 24 hours in the presence of patulin, DON and ZEN combinations, with and without LPS (100 ng/mL) stimulation, followed by incubation with 1 μ m FITC-labelled latex beads for 1 hour	117
Figure 5.4:	Expression of MHCII and TLR4 on the surface of J774A.1 murine macrophage cells, cultured for 24 hours in the presence of patulin, DON, ZEN and T-2 Toxin, with and without LPS (100 ng/mL) stimulation	119
Figure 5.5:	Expression of CD80 and CD86 on the surface of J774A.1 murine macrophage cells, cultured for 24 hours in the presence of patulin, DON, ZEN and T-2 Toxin, with and without LPS (100 ng/mL) stimulation	120
Figure 5.6:	Expression of CD80 and CD86 on the surface of J774A.1 murine macrophage cells, cultured for 24 hours in the presence of patulin, DON, ZEN and T-2 Toxin, with and without LPS (100 ng/mL) stimulation	121
Figure 5.7:	Expression of CD80 and CD86 on the surface of J774A.1 murine macrophage cells, cultured for 24 hours in the presence of patulin, DON, ZEN and T-2 Toxin, with and without LPS (100 ng/mL) stimulation	123
Figure 5.8:	Opto-microfluidic monitoring of CD80 and CD86 expression dynamics on J774A.1 murine macrophage cells. Cells were captured in a microfluidic Lab-in-a-Trench device and stimulated with LPS (200 ng/mL)	125
Figure 5.9:	'Real-time' monitoring for CD80 expression on the surface of J774A.1 murine macrophage cells captured in a microfluidic Lab-in-a-Trench device, exposed to ZEN and T-2 Toxin then stimulated with 200 ng/mL LPS	126

Figure 5.10:	'Real-time' monitoring for CD80 expression on the surface of J774A.1 murine macrophage cells captured in a microfluidic Lab-in-a-Trench device, exposed to DON and T-2 Toxin then stimulated with 200 ng/mL LPS	126
Figure 5.11:	'Real-time' monitoring for CD80 expression on the surface of J774A.1 murine macrophage cells captured in a microfluidic Lab-in-a-Trench device, exposed to DON and ZEN then stimulated with 200 ng/mL LPS	127
Figure 5.12:	'Real-time' monitoring for CD80 expression on the surface of J774A.1 murine macrophage cells captured in a microfluidic Lab-in-a-Trench device, exposed to patulin and DON then stimulated with 200 ng/mL LPS	127
Figure 5.13:	'Real-time' monitoring for CD80 expression on the surface of J774A.1 murine macrophage cells captured in a microfluidic Lab-in-a-Trench device, exposed to patulin and T-2 Toxin then stimulated with 200 ng/mL LPS	128
Figure 5.14:	'Real-time' monitoring for CD80 expression on the surface of J774A.1 murine macrophage cells captured in a microfluidic Lab-in-a-Trench device, exposed to patulin and ZEN then stimulated with 200 ng/mL LPS	128
Figure 5.15:	'Real-time' monitoring for CD86 expression on the surface of J774A.1 murine macrophage cells captured in a microfluidic Lab-in-a-Trench device, exposed to ZEN and T-2 Toxin then stimulated with 200 ng/mL LPS	129
Figure 5.16:	'Real-time' monitoring for CD86 expression on the surface of J774A.1 murine macrophage cells captured in a microfluidic Lab-in-a-Trench device, exposed to DON and T-2 Toxin then stimulated with 200 ng/mL LPS	129
Figure 5.17:	'Real-time' monitoring for CD86 expression on the surface of J774A.1 murine macrophage cells captured in a microfluidic Lab-in-a-Trench device, exposed to DON and ZEN then stimulated with 200 ng/mL LPS	130

Figure 5.18:	'Real-time' monitoring for CD86 expression on the surface of J774A.1 murine macrophage cells captured in a microfluidic Lab-in-a-Trench device, exposed to patulin and DON then stimulated with 200 ng/mL LPS	130
Figure 5.19:	'Real-time' monitoring for CD86 expression on the surface of J774A.1 murine macrophage cells captured in a microfluidic Lab-in-a-Trench device, exposed to patulin and T-2 Toxin then stimulated with 200 ng/mL LPS	131
Figure 5.20:	'Real-time' monitoring for CD86 expression on the surface of J774A.1 murine macrophage cells captured in a microfluidic Lab-in-a-Trench device, exposed to patulin and ZEN then stimulated with 200 ng/mL LPS	131
Figure 6.1:	Serum titre of an AFM1-BSA immunised chicken	143
Figure 6.2:	Serum titre of a patulin-HG-KLH immunised chicken	144
Figure 6.3:	First round PCR amplifications in duplicate of V _H and V _L using cDNA from an AFM1-immunised chicken	145
Figure 6.4:	First round PCR amplifications in duplicate of V _H and V _L using cDNA from an OTA-immunised chicken	146
Figure 6.5:	First round PCR amplifications in duplicate of V _H and V _L using cDNA from a patulin-immunised chicken	147
Figure 6.6:	Optimisation of MgCl ₂ concentration for V _H amplification	148
Figure 6.7:	SOE amplification of SOE-PCR product in duplicate for AFM1	149
Figure 6.8:	Gradient SOE for AFM1 to optimise annealing temperature	149
Figure 6.9:	Gradient SOE for AFM1 to optimise annealing temperature repeat	150
Figure 6.10:	Gradient SOE for patulin to optimise annealing temperature	151
Figure 6.11:	PCR enhancer optimisation for patulin and AFM1 SOE-PCR	151
Figure 6.12:	Gradient SOE using MyTaq™ Red Mix (Bioline) for OTA to optimise annealing temperature	152
Figure 6.13:	Gradient SOE using Platinum® PCR SuperMix (Thermo Fisher) for OTA to optimise annealing temperature	153
Figure 6.14:	Comparison of a two-step and three-step SOE-PCR for OTA	153
Figure 6.15:	Gradient SOE for OTA to optimise annealing temperature	154

Figure 6.16:	<i>Sfi</i> I digestion of pComb3xSS vector	155
Figure 6.17:	PCR insert check for successful cloning of patulin SOE products into the pComb3XSS vector system	156
Figure 6.18:	PCR insert check for successful cloning of AFM1 (top) and OTA (bottom) SOE products into the pComb3XSS vector system	156
Figure 7.1:	Testing of Patulin-HS-BSA conjugate synthesis using direct ELISA.	165
Figure 7.2:	PCR insert check for patulin panning selection rounds. Colonies were picked at random and incorporated into the PCR	168
Figure 7.3:	PCR insert check for OTA panning selection rounds. Colonies were picked at random and incorporated into the PCR	169
Figure 7.4:	PCR insert check for AFM1 panning selection rounds. Colonies were picked at random and incorporated into the PCR	170
Figure 7.5:	Polyclonal phage ELISA screening for anti-AFM1 scFv displayed on phage, following three rounds of panning	171
Figure 7.6:	Polyclonal phage ELISA screening for anti-OTA scFv displayed on phage, following three rounds of panning	172
Figure 7.7:	Monoclonal ELISA with 192 randomly selected clones from round two of panning	174
Figure 7.8:	Competitive ELISA of 19 scFv clones	175
Figure 7.9:	Titration analysis of six AFM1-specific clones	176
Figure 7.10:	Expression optimisation analysis of the AFM1-specific clone, H1	177
Figure 7.11:	SDS-PAGE (left) and Western Blotting (right) analysis of IMAC-purified H1 scFv	178

List of tables

Table 1.1:	Major mycotoxins and their producing fungal species	4
Table 1.2:	Maximum levels for mycotoxin contaminants in foodstuffs	9
Table 1.3:	Pathological effects of major mycotoxins	13
Table 1.4:	IARC classification of carcinogenic mycotoxins	14
Table 2.1:	Bio-panning conditions	60
Table 3.1:	The effect of increasing concentrations of patulin on the production levels of cytokines from J774A.1 macrophages with and without LPS treatment	80
Table 3.2:	The effect of increasing concentrations of DON on the production levels of cytokines from J774A.1 macrophages, with and without LPS treatment	81
Table 3.3:	The effect of increasing concentrations of ZEN on the production levels of cytokines from J774A.1 macrophages, with and without LPS treatment	82
Table 3.4:	The effect of increasing concentrations of T-2 toxin on the production levels of cytokines from J774A.1 macrophages, with and without LPS treatment	83
Table 5.1:	Expression of CD80, CD86, MHCII and TLR4 on the surface of J774A.1 murine macrophage cells, cultured for 24 hours in the presence of patulin, DON, ZEN and T-2 Toxin, with and without LPS (100 ng/mL) stimulation	123
Table 7.1:	Panning conditions employed for each round of the repeated selection for the avian anti-patulin scFv library	166
Table 7.2:	Panning conditions employed for each round of the repeated selection for the avian anti-OTA scFv library	166
Table 7.3:	Panning conditions employed for each round of the repeated selection for the avian anti-AFM1 scFv library	166

Abbreviations

α	Alpha
Ab	Antibody
AFB1	Aflatoxin B1
AFB2	Aflatoxin B2
AFG1	Aflatoxin G1
AFG2	Aflatoxin G2
AFM1	Aflatoxin M1
APC	Antigen presenting cell
AOAC	Association of Analytical Communities
β	Beta
bp	Base pair
BSA	Bovine serum albumin
CAST	Council for Agricultural Science and Technology
CD	Cluster of differentiation
cDNA	Complementary DNA
CDRs	Complementarity determining regions
C _H	Constant heavy chain of an antibody
C _L	Constant light chain of an antibody
CO ₂	Carbon dioxide
dH ₂ O	Distilled water
DMEM	Dulbecco's modified Eagle's medium
DMSO	Dimethyl sulfoxide

DNA	Deoxyribonucleic acid
dNTPs	Deoxynucleotide triphosphates
Da	Dalton
DON	Deoxynivalenol
DPBS	Dulbecco's phosphate buffered saline
<i>E.coli</i>	<i>Escherichia coli</i>
EU	European Union
ECACC	European Collection of Cell Cultures
EDTA	Ethylenediaminetetra acetic acid
ELISA	Enzyme-linked immunosorbent assay
EPA	Environmental Protection Agency
Fab	Fragment antigen-binding of antibody
FACS	Fluorescence-activated cell sorting
FAO	Food and Agriculture Organisation
FB1	Fumonisin B1
FBS	Fetal bovine serum
Fc	Fragment-crystallisable region of antibody
GC	Gas chromatography
HACCP	Hazard analysis and critical control points
HCC	Hepatocellular carcinoma
HCl	Hydrochloric acid
HPLC	High-performance liquid chromatography
HRP	Horseradish peroxidase

IARC	International Agency for Research on Cancer
Ig	Immunoglobulin
IgG	Immunoglobulin G
IgY	Immunoglobulin Y
IL	Interleukin
IMAC	Immobilised metal affinity chromatography
IPTG	Isopropyl- β -D galactopyranoside
kDa	Kilodalton
KLH	Keyhole limpet haemocyanin
LB	Lysogeny broth
LC	Liquid chromatography
LC-MS	Liquid chromatography-mass spectrometry
LOD	Limit of detection
Log	Logarithmic
LPS	Lipopolysaccharide
mAb	Monoclonal antibody
MALDI-TOF spectrometry	Matrix-assisted laser desorption time of flight mass spectrometry
MG	Molecular grade
MgCl ₂	Magnesium chloride
MHC	Major histocompatibility complex
mRNA	messenger RNA
MS	Mass spectrometry

MTS	3-(4,5-dimethylthiazol-2-yl)-5-(3-carboxymethoxyphenyl)-2-(4-sulfophenyl)-2H-tetrazolium
μ	Mu
Mw	Molecular weight
NaCl	Sodium chloride
OD	Optical density
OTA	Ochratoxin A
pAb	Polyclonal antibody
PAGE	Polyacrylamide gel electrophoresis
PBS	Phosphate buffered saline
PBST	Phosphate buffered saline with Tween 20
PCR	Polymerase chain reaction
PEG	Polyethylene glycol
pH	Log of the hydrogen ion concentration
POC	Point-of-care
PON	Point-of-need
PRRs	Pattern recognition receptors
rAb	Recombinant antibody
RNA	Ribonucleic acid
RNase	Ribonuclease
RPM	Revolutions per minute
RT	Room temperature
RU	Response units

SB	Super broth
scFv	Single chain fragment variable
SDS	Sodium dodecyl sulphate
SOC	Super optimal catabolites
SOE	Splice overlap extension
SPR	Surface plasmon resonance
TAE	Tris-acetate-EDTA
TB	Terrific broth
TLC	Thin layer chromatography
TLR	'Toll-like' receptor
TMB	3, 3', 5, 5' tetramethylbenzidine
TNF	Tumor necrosis factor
UV	Ultraviolet
V _H	Variable heavy (chain of antibody)
V _L	Variable light (chain of antibody)
WHO	World Health Organisation
ZEN	Zearalenone

Units

%	Percent
A	Absorbance
ANOVA	Analysis of variance
C	Concentration
°C	Degrees Celsius
Da	Dalton
g	Gram
kg	Kilogram
L	Litre
M	Molar
mg	Milligram
mL	Millilitre
mM	Millimolar
mmol	Millimoles
n	Number of observations
ng	Nanogram
nm	Nanometre
nM	Nanomolar
OD	Optical density
pg	Picogram
pH	Negative logarithm of the hydrogen ion concentration
SD	Standard deviation

SE	Standard error
SEM	Standard error of the mean
μg	Microgram
μL	Microlitre
v/v	Volume per unit volume
w/v	Weight per unit volume
xg	Centrifugal acceleration

Publications

Loftus, J.H., Moran, K.L.M., Murphy, C., O’Kennedy, R. (Submitted to CRC Press). “Current and emerging technologies for the analysis of fungal and marine toxin contaminants in food.” Nano-Inspired biosensors for Improved Healthcare.

Moran, K.L.M, Fitzgerald J., McPartlin D.A., **Loftus J.H.**, O’Kennedy R. (2016). Biosensor-Based Technologies for the Detection of Pathogens and Toxins. *Comprehensive Analytical Chemistry*, 74: 93-120.

Loftus, J.H., Kijanka, G.S., O’Kennedy, R., Loscher, C.E. (2016). Patulin, Deoxynivalenol, Zearalenone and T-2 toxin affect viability and modulate cytokine secretion in J774A.1 Murine Macrophages. *International Journal of Chemistry*, 8(2): 22-32.

McPartlin D.A., **Loftus J.H.**, Crawley A.S., Silke J., Murphy C.S., O’Kennedy R.J. (2017) Biosensors for the monitoring of harmful algal blooms. *Current Opinion in Biotechnology*, 45:164-169.

Loftus J.H., Kijanka G.S., O’Kennedy R.J. (2017) Mycofluidics: Miniaturization of Mycotoxin Analysis. *Diagnostic Devices with Microfluidics*. CRC Press Jul 2017 , 75 -88.

Loftus, J.H., O’Kennedy, R., Loscher, C.E. (Manuscript submitted, 2018) Immunomodulatory effects of individual and combined mycotoxins on J774A.1 macrophage cells.

Presentations and posters

Loftus, J.H., Loscher, C.E., and O’Kennedy, R. (30th January, 2015). Mycotoxins: Effects and Analysis. The Annual School of Biotechnology Research Day, Dublin, Ireland (Oral presentation).

Loftus, J.H., Loscher, C.E., and O’Kennedy, R. (1st–3rd June, 2015). Design of a novel microfluidics platform for mycotoxin food contaminant determination. 37th Mycotoxin Workshop, Bratislava, Slovakia (Poster).

Loftus, J.H., Loscher, C.E., and O’Kennedy, R. (11th June, 2015). Investigation into the immunosuppressive effects and detection of Mycotoxins. safefood Biotoxins Knowledge Network and the Irish Society of Toxicology Annual Conference, Belfast, Northern Ireland (Poster).

Loftus, J.H., Loscher, C.E., and O’Kennedy R. (29th January, 2016). A long time ago in a field far, far away... (Star Wars themed project presentation). The Annual School of Biotechnology Research Day, Dublin, Ireland (Oral presentation).

Loftus, J.H., Loscher, C.E., and O’Kennedy, R. (6th–9th June, 2016). Design of a novel microfluidics platform for mycotoxin food contaminant determination. 9th conference of The World Mycotoxin Forum & XIVth IUPAC International Symposium on Mycotoxins, Winnipeg, Canada (Oral Presentation and Poster).

Educational and outreach work

BE433: Immunology and Immunoanalysis is a module in Dublin City University (DCU) aimed at providing a detailed understanding of the theory and applications of advanced aspects of immunology with a focus on the advantages and limitations of immunoanalytical approaches in clinical, industrial and research situations.

Loftus, J.H., (February, 2015 and 2016) Lecture: Introduction to Biosensors and Biacore. BE433: Immunology and Immunoanalysis, DCU, Dublin.

The Irish European Union Science Olympiad (IrEUSO) is an individual, subject based (biology, chemistry or physics) science competition for students who are sixteen years of age or younger prior to the competition. It is held annually in Dublin City University (DCU). Finalists qualify through the Junior Certificate Examinations in Maths and Science.

Loftus, J.H., (October, 2015, 2016 and 2017) Invigilator and corrector for Biology exam. The Irish European Union Science Olympiad (IrEUSO), DCU, Dublin.

The Aisling Project is an after school initiative in the Ballymun area for children deemed at risk. It provides homework supervision, a hot meal and after school activities to help in children's development. The Aisling Project also provides a safe place for these children and works individually with each child to ensure their developmental needs are being met. As chairperson of the Biological Research Society (BRS), I created a partnership between the School of Biotechnology and the Aisling Project to bring science to the children of Ballymun. Postgrad, postdoc and academic BRS members travelled to the Aisling Project's centre to carry out a number of fun experiments with the children. This has led to a long-term partnership with the School of Biotechnology.

Loftus, J.H., (July, 2017) Organiser and Coordinator of a Biology Outreach Day. The Aisling Project, Ballymun, Dublin.

Abstract

Mycotoxins - An analysis of their immunomodulatory effects and methods for their detection

Jonathan Loftus

Mycotoxins are toxic secondary fungal metabolites which contaminate a variety of food and feed products and pose serious health risks to humans and animals. Exposure to even low concentrations of these toxins can result in chronic diseases, with immunosuppressive and carcinogenic effects being of greatest concern. They are estimated to be found in 25% of the world's food supply and have huge economic consequences globally.

There is a lack of understanding of how mycotoxins interact with the immune system. The purpose of this research was to increase this understanding by examining the cytotoxic and immunomodulatory effects of the mycotoxins patulin, DON, ZEN and T-2 toxin *in vitro*, using the murine macrophage cell line, J774A.1. The results clearly demonstrated that T-2 toxin and ZEN significantly affect cell viability at high concentrations while sub-lethal concentrations of patulin, DON, ZEN and T-2 toxin, alone and in combinations, had a significant effect on host defence functions, through deregulation of IL-6, IL-10, IL-27, IL-12p40, IL-1 β and TNF- α cytokine production, phagocytosis, and the cell surface expression of CD80, CD86, TLR4 and MHCII. The effects of these toxins are dependent on concentrations and combinations. This knowledge should be taken into consideration in the implementation of detection limits, aimed at minimising risks to human and animal health from mycotoxin exposure. A possible solution to this was explored through the use of a novel microfluidic technology, Lab-in-a-Trench, which demonstrated the ability to measure the immunomodulatory effects of mycotoxin combinations in 'real-time'.

Increased awareness of the hazards presented by mycotoxins has also led to the need for rapid detection systems. Recombinant antibodies incorporated into sensitive immunoassays offers the ability to satisfy this need. This thesis describes optimisation of immune library production for the mycotoxins patulin, ochratoxin A and aflatoxin M1 using an avian host. Immune libraries were generated and screened for all three targets and a scFv clone capable of binding AFM1 was successfully isolated using phage display technology in a depletion bio-panning process. The incorporation of recombinant antibodies with high sensitivity into rapid and inexpensive detection systems coupled with a novel method of determining immunomodulatory effects of mycotoxin combinations would allow early intervention, thus improving global food safety and providing significant cost savings to the agri-food sector.

Chapter 1: Introduction

1.1 Overview

Mycotoxins are the naturally-occurring toxic secondary metabolites of some fungal species. They are food contaminants which are proven to have detrimental effects on human and animal health. Their immunosuppressive and carcinogenic nature is of particular concern. According to the World Health Organisation (WHO) 25% of the world's food supply is contaminated with mycotoxins (Marroquín-Cardona *et al.*, 2015).

This chapter will introduce mycotoxins by giving a background on their history, classification and structures. The occurrence of mycotoxins across the world will be discussed, with risk management procedures and legislative limits reported. Mycotoxins' negative health effects will be detailed, with a particular focus on how they interact with the immune systems of humans and animals. The current methods of mycotoxin analysis will be examined and their issues will be highlighted. Finally, the structure and function of antibodies will be described with a focus on how recombinant production can aid mycotoxin analysis.

Overall, this thesis is based on research examining how mycotoxins affect the immune system and how improvement to mycotoxin analysis can be achieved through lab-in-a-trench technology and recombinant antibody production.

1.1.1 History of mycotoxins

The name mycotoxin originates from the combination of the Greek word for fungus '*mykes*', and the Latin word '*toxicum*', meaning poison (Turner *et al.*, 2009). It is thought that mycotoxins have been in existence for as long as crops have been grown throughout the world. There are many significant events throughout history to which mycotoxin contamination was attributed. It can be found as far back as the Dead Sea Scrolls, and in historical events such as the plagues of Egypt, St. Anthony's Fire, and the Salem Witchcraft trials. It was not until throughout the early 1900s, however, that there was recognition that some species of fungi were producing "secondary metabolites" during fermentation processes. The potential for harm from these metabolites was realised and this began the work on the area of fungal metabolites (Richard, 2007).

In 1955 Forgacs and Carll described diseases caused by fungal toxins as “mycotoxicosis” but modern mycotoxicology really all started with the discovery of aflatoxins in the 1960s after the mysterious death of thousands of turkey poults in England was attributed to consumption of contaminated Brazilian groundnut meal. Today the word mycotoxin is a name given to any toxin produced by a fungus that is harmful in low concentrations. At present, the total number of mycotoxins in existence is not known but it is estimated that hundreds of thousands could exist (Hawksworth, 1991; Marin *et al.* 2013).

The potent toxicity of these compounds was realised in recent years and there is a growing concern that these toxins are resulting in more and more chronic diseases in both humans and animals due to their presence on food commodities and their ability to enter the food chain (Zain, 2011).

1.2 Classification, sources and chemical properties of mycotoxins

Generally, mycotoxins are classified based on the fungus producing them. However, individual mycotoxins can be produced by a number of different species of fungi and a single species of fungus can produce a range of mycotoxins. Most of the mycotoxins that are considered to be important are produced primarily by three genera of fungi; *Aspergillus*, *Penicillium*, and *Fusarium*. *Claviceps* and *Stachybotrys* also are important producers of mycotoxins. Many types of secondary metabolites have been identified in fungi, however, most of them are not known to cause human or animal disease (CAST, 2003). Regarding health risks, the mycotoxins that are of the greatest importance are; aflatoxins, fusariums, trichothecenes, patulin and ochratoxins (Zain, 2011; Edite Bezerra da Rocha *et al.* 2014). These are the mycotoxins of greatest agro-economic importance.

Aspergillus species are the predominant producers of mycotoxins and are responsible for production of the most potent mycotoxins, the aflatoxins. They are present in all ‘oxygen-rich’ environments as they are aerobic. Corn, cotton, and certain types of nuts are most commonly contaminated. “Ear rot” in corn is caused by *Aspergillus flavus* under suitable environmental conditions. Peanuts are often infected during high temperature and low-moisture stress. *Fusarium* species produce an array of important mycotoxins. Some of the most significant plant pathogens are produced by this genus including T-2 toxin, deoxynivalenol (DON), zearalenone (ZEN), fumonisins (FBs), patulin

and ochratoxins. Blight diseases and ear rot also can be caused by *Fusarium spp.*, targeting foods such as wheat, barley, and oats. *Penicillium spp.* are more typically found post-harvest and contamination is associated with storage of crops. This species is primarily involved in the production of mycotoxins such as ochratoxins and patulin. Ochratoxins are usually formed when storage conditions are poor or during drying of certain commodities for processing, while patulin is a common contaminant of apples and apple juices. Mycotoxins are secondary metabolites with no apparent function in the normal metabolism of fungi. They are produced mainly, although not exclusively, when the fungus reaches maturity.

Table 1.1: Major mycotoxins and their producing fungal species.

Mycotoxin	Producing Species
Aflatoxins	<i>Aspergillus</i>
Trichothecenes	<i>Fausrium</i> and <i>Stachbotrys</i>
Zearalenone	<i>Fausrium</i> and <i>Gibberella</i>
Patulin	<i>Penicillium</i> , <i>Bysochlamis</i> and <i>Aspergillus</i>
Ochratoxins	<i>Aspergillus</i> and <i>Penicillium</i>

Mycotoxins vary greatly in their size and chemical structure. Aflatoxins (~320 Da) are difuranocoumarins whereas the trichothecenes (~250-550 Da) are a group of sesquiterpene epoxides and zearalenone (~318 Da) is a resorcyclic acid lactone. Patulin (~150 Da), a polyketide lactone, is one of the smallest mycotoxins discovered. Most mycotoxins come from simple precursors such polyketides suggesting a complicated synthesis pathway for many of the toxins (Maggon, 1977). While synthesis mechanisms have been determined for several mycotoxins the exact synthesis of all of these compounds is not fully known. Generally most mycotoxins are soluble in highly polar solvents and are primarily highly heat-stable, being able to withstand heating above 100°C.

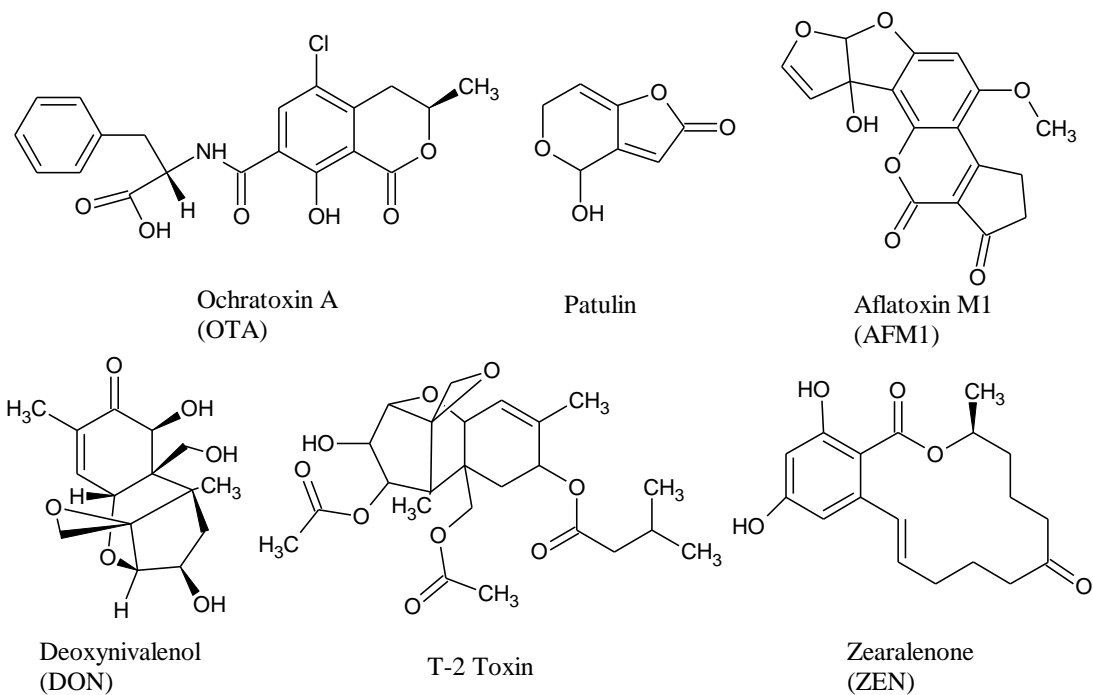


Figure 1.1: Chemical structures of ochratoxin A (OTA), patulin, aflatoxin M1 (AFM1), deoxynivalenol (DON), T-2 toxin and zearalenone (ZEN).

1.3 Mycotoxins, food safety and economic impact

1.3.1 Mycotoxin occurrence and exposure

Mycotoxin contamination can occur at any time during harvest or storage of food. Investigations have shown elevated mycotoxins in foods and feeds from countries throughout the world, but they tend to occur most frequently in areas with a hot and humid climate which are the favourable conditions for the growth of the moulds that produce them. They are not limited to these regions, however, and can also be found in most temperate zones.

Mycotoxin contamination can occur in a variety of plants used as food, including commodities such as cereal grains (barley, corn, rye and wheat), coffee, dairy products, fruits, nuts, peanuts, and spices. Contamination can also arise in animal products, like milk, caused by animals consuming contaminated feeds. However, commodities such as cereal grains are eaten in the greatest quantities, therefore, the mycotoxins present in these foods represent the greatest risk (Cousins *et al.*, 2005). Generally, crops that are stored for more than a few days become a potential target for mould growth and mycotoxin formation. The primary way in which humans

become exposed to mycotoxins is by eating contaminated food such as grain, corn, and other foodstuff or, alternatively, by consuming animals or animal products that have eaten contaminated feed. Mycotoxins are extremely stable compounds so it is easy for them to avoid damage in the digestive system and make their way into the human bloodstream (Stoev, 2015).

Mycotoxins can enter the human and animal food chains through direct or indirect contamination. Indirect contamination is when any ingredient was previously contaminated by a toxigenic fungus, and, even though the fungus is eliminated during the processing, the mycotoxins remain in the final product. Direct contamination occurs when the product, food or feed becomes infected by a toxigenic fungus, with the subsequent formation of mycotoxins. The majority of food and feed products can allow the growth and development of toxigenic fungi during their production, processing, transport and storage.

Humans can also be exposed to the toxins by inhalation. It was found by several studies that workers interacting with mycotoxins regularly have extremely high levels of mycotoxins in their systems due to inhalation (Degen, 2011). The danger of this is highlighted by studies which have demonstrated that AFB1 is mutagenic to mammalian pulmonary tissues to a greater extent than many known respiratory carcinogens (Ball *et al.*, 1995). It was also proven that mycotoxins can be absorbed through the skin. Boonen *et al.* (2012) looked at 6 different mycotoxins and how varying concentrations were absorbed through the dermal layer. It was found that a cancer health risk exists after dermal exposure to AFB1.

Within the last decades, numerous outbreaks of mycotoxicoses have been reported worldwide. In 2004, 125 people died following a major outbreak of aflatoxicosis in the eastern and central provinces of Kenya. Three hundred and seventeen cases were reported, and most were linked to aflatoxin poisoning from contaminated maize. In 2005, more than 75 dogs died in the United States after consuming pet food contaminated with aflatoxins, and hundreds more experienced severe liver problems associated with the intoxication. There have been many reported cases of trichothecene toxicity in farm animals and a few in humans. One of the well-known cases of presumed trichothecene human toxicity occurred in Russia during 1944 in Orenburg, Siberia. Disruption of agriculture caused by World War II resulted in millet,

wheat, and barley being overwintered in the field. Consumption of these commodities resulted in vomiting, skin inflammation, diarrhoea, and multiple haemorrhages, among other symptoms. The causative agent was subsequently identified as alimentary toxic aleukia (ATA) (CAST, 2003).

These outbreaks have been detrimental to health and they have inflicted large costs to economies in both health-related expenses and trade impact. It is difficult to assess the exact worldwide economic impact and, therefore, most reports on economic impact are on a single aspect of mycotoxin exposure or contamination (Hussein and Brasel, 2001). It was estimated that in the US eight South-eastern states lost \$97 million due to aflatoxins in corn during the 1980's with additional \$100 million in production losses at hog farms feeding the contaminated corn (Shane, 1994). Robens and Cardwell (2003) estimated loss due to aflatoxin-contaminated corn and peanuts, as well as fumonisin-contaminated corn and DON-contaminated wheat resulted in losses ranging from \$0.5 million to over \$1.5 billion for the US. It is evident that loss due to mycotoxins may have disastrous monetary impacts not just for the producers but for all of the world population.

1.3.2 Mycotoxin risk management

It is considered almost impossible to prevent some level of mycotoxin contamination and, as previously discussed, due to their chemical properties, mycotoxins are extremely difficult to eradicate. Therefore, great efforts are made to minimise exposure and contamination. Generally these efforts are made at two stages, firstly pre-harvest when crops are still in the field. Specific cultivation practises are implemented to minimise contamination, while sometimes gene-level modifications can be made to crops. Post-harvest measures are implemented during the storage of crops and involve the use of physical, chemical or biological agents for treatment. These treatments must prevent toxicity with no detrimental effects on animals, while also being cost effective (Stoev, 2015). Many mycotoxins can be removed using absorbing agents and some can be destroyed with enzymes or degrading agents but there are issues with how biohazardous these chemical treatments are and most absorbent materials have not yet received EU regulatory approval (Stornetta *et al.*, 2015).

Timely harvesting, cleaning and drying of crops, controlling temperature and moisture during storage, and use of anti-fungal agents along with adoption of the HACCP (Hazard Analysis and Critical Control Points) system can assist in decreasing or eliminating mycotoxins in food and feed. Furthermore, research efforts to understand the genetic and biosynthetic aspects of mycotoxin development may lead to more successful control strategies in grains (Marin *et al.*, 2013).

1.3.3 Legislative limits for mycotoxins

Since the discovery of the mycotoxins in the 1960s, regulations and limits have been put in place in countries all across the world. There are several factors involved in setting limits for mycotoxins. These include: the availability of toxicological data, survey data, knowledge about mycotoxin distribution, and analytical methodology. Economical and political factors such as commercial interests also have significant impact. At least 77 countries now have specific regulations for mycotoxins. Each country or region has its own individual limits for certain mycotoxins. Limits within the EU are described by Commission Regulation (EC) No. 1881/2006 (Table 1.2). Some free trade zones (EU, MERCOSUR) are now attempting harmonisation of the limits and regulations, but it is not likely that worldwide harmonized limits for mycotoxins will be achieved any time soon (Stoev, 2015).

Table 1.2: Maximum levels for mycotoxin contaminants in foodstuffs.

Mycotoxin	Foodstuff	Maximum levels (µg/kg)
AFB1	Groundnuts to be subjected to sorting, or other physical treatment, before human consumption or use as an ingredient in foodstuffs	8
	Nuts to be subjected to sorting, or other physical treatment, before human consumption or use as an ingredient in foodstuffs	5
	Groundnuts and nuts and processed products thereof, intended for direct human consumption or use as an ingredient in foodstuffs	2
	Dried fruit to be subjected to sorting, or other physical treatment, before human consumption or use as an ingredient in foodstuffs	5
	Dried fruit and processed products thereof, intended for direct human consumption or use as an ingredient in foodstuffs	2
	All cereals and all products derived from cereals, including processed cereal products.	2
	Processed cereal-based foods and baby foods for infants and young children	0.10

AFM1	Raw milk, heat-treated milk and milk for the manufacture of milk-based products	0.050
	Infant formulae and follow-on formulae, including infant milk and follow-on milk	0.025
	Dietary foods for special medical purposes intended specifically for infants	0.025
ZEN	Unprocessed cereals other than maize	100
	Unprocessed maize	200
	Cereals intended for direct human consumption, cereal flour, bran as end product marketed for direct human consumption and germ	75
	Maize intended for direct human consumption, maize flour, maize meal, maize grits, maize germ and refined maize oil	200
	Bread (including small bakery wares), pastries, biscuits, cereal snacks and breakfast cereals, excluding maize snacks and maize based breakfast cereals	50
	Processed cereal-based foods (excluding processed maize- based foods) and baby foods for infants and young children	20
	Processed maize-based foods for infants and young children	20
DON	Unprocessed cereals other than durum wheat, oats and maize	1,250
	Unprocessed durum wheat and oats	1,750

	Unprocessed maize	1,750
	Pasta (dry)	750
	Bread (including small bakery wares), pastries, biscuits, cereal snacks and breakfast cereals	500
Patulin	Fruit juices, concentrated fruit juices as reconstituted and fruit nectars	50
	Spirit drinks, cider and other fermented drinks derived from apples or containing apple juice	50
	Solid apple products, including apple compote, apple puree intended for direct consumption	25
	Apple juice and solid apple products, including apple compote and apple puree, for infants and young children	10
	Baby foods other than processed cereal-based foods for infants and young children	10

Table adapted from Commission Regulation (EC) No. 1881/2006 of 19 December 2006 setting maximum levels for certain contaminants in foodstuffs (Annex Section 2).

1.4 Effects of mycotoxins on human and animal health

1.4.1 Mycotoxicosis and toxicological studies for mycotoxins

Mycotoxicosis is the broad term used to describe any poisoning associated with exposure to mycotoxins. Diagnostic features of mycotoxicosis include: non-transmissible disease, no response to drug and antibiotic treatment, seasonal outbreak in specific foods, and fungal activity (Zain, 2011; Marin *et al.*, 2013; Edite Bezerra da

Rocha *et al.*, 2014). Mycotoxins have a broad spectrum of detrimental effects that depend on a large number of factors including; mycotoxin concentration, the class (or combination of classes) and the species affected.

Mycotoxins affect all systems in the body with a wide variety of pathological effects (Table 1.3). A number of mycotoxins produce nephrotoxicity such as aflatoxin B1, citrinin, ochratoxins, fumonisins, and patulin (O'Brien, 2005). Fumonisin B1 and B2 are commonly found on corn and corn products and produce nephrotoxicity in rats and rabbits (Bucci *et al.*, 1998). There are few reports of acute intoxications caused by mycotoxins, however, prolonged exposure to small quantities of mycotoxin may lead to more dangerous effects including growth retardation, birth defects, impaired immunity, decreased disease resistance, and tumour formation in humans and decreased production in farm animals (CAST, 2003). Aflatoxins are also known to be teratogenic, mutagenic and immunosuppressive (Jiang *et al.*, 2005; Bruneau *et al.*, 2012; Yeni *et al.*, 2015). In 2012, Bruneau *et al.* examined the effect of administering toxin mixtures at low concentrations for prolonged periods on macrophages, particularly in relation to cytokine secretion. The investigation observed changes in cytokine secretion and cell surface marker expression in murine macrophages exposed to single aflatoxin isoforms and aflatoxin mixtures. The investigation also showed that the combination of aflatoxin isoforms had a specific effect on cytokine secretion and that depending on the two isoforms used and the cytokine examined, the combinations could abrogate the effect observed in single aflatoxin exposure, or to act synergistically.

Table 1.3: Pathological effects of major mycotoxins.

Mycotoxin	Pathological Effects
Aflatoxins	Hepatotoxicity, bile duct hyperplasia, haemorrhage, carcinogenesis
Trichothecenes	Digestive disorders, haemorrhage, oedema, oral lesions, dermatitis, blood disorders
Zearalenone	Estrogenic effects, atrophy of reproductive organs, abortion
Patulin	Oedema, haemorrhage, capillary damage, paralysis of motor nerves, convulsions, carcinogenesis
Ochratoxins	Nephrotoxicity, porcine nephropathy, liver damage, enteritis, teratogenesis, carcinogenesis, urinary tract tumours

Based on the toxicological data, several mycotoxins including aflatoxins, fumonisins, ochratoxins and trichothecenes have now been designated carcinogens by the International Agency for Research on Cancer (IARC) (IARC, 2002) (Table 1.2). AFB1 is listed as a class 1 carcinogen (carcinogenic to humans) as it is a potent hepatocarcinogen, and aflatoxin exposure has been linked to development of hepatocellular carcinoma (HCC) (Kew, 2003).

Table 1.4: IARC classification of carcinogenic mycotoxins.

IARC Classification	Definition	Mycotoxins
1	Carcinogenic to humans	AFB1
2A	Probably carcinogenic to humans	-
2B	Possibly carcinogenic to humans	AFM1, FBs, OTA
3	Not classifiable as to its carcinogenicity to humans	DON, T-2/HT-2, ZEN, Patulin
4	Probably not carcinogenic to humans	-

1.4.2 Mycotoxins and the immune system

Immunosuppression is viewed as one of the most significant effects of mycotoxin exposure and it has a major economic impact. Studies have already highlighted the immunosuppressive nature of several mycotoxins such as aflatoxins, trichothecenes, ochratoxin A and zearalenone (Edite Bezerra da Rocha *et al.*, 2014; Jia *et al.*, 2014). These mycotoxins can cause a variety of immune-related changes, including thymic aplasia and inhibition of phagocytosis by macrophages, delayed cutaneous hypersensitivity, lymphocyte proliferation and leukocyte migration. The involvement of specific mycotoxins in infectious diseases depends on the agent of disease, the toxin dose and constitution, the animal species, and the sensitivity of the test employed (Richard, 1991). One of the most consistent features of the effects of mycotoxins, particularly aflatoxins, on immunity is the decrease of cell mediated immunity. Aflatoxins have been shown to affect the production of cytokines important in relation to certain immune processes by a number of cell types. While aflatoxins are not notable in impacting antibody production, they have an important effect on levels of nonspecific humoral factors such as complement, interferon, and some bactericidal serum components (CAST, 2003).

Generally studies on mycotoxin immunosuppression involve *in vitro* analysis or animal models. Increased susceptibility to yeast infections, pasteurellosis, and salmonellosis was demonstrated in poultry. Some mycotoxins, such as the aflatoxins and zearalenone, can move transplacentally in swine, immunocompromising neonatal piglets (Marin *et al.*, 2014). Chicken embryos can exhibit depressed immune responses when exposed to aflatoxin B1. Trichothecenes generally decrease serum protein levels. The trichothecenes usually decrease phagocytosis and delayed hypersensitivity; exceptions do occur, as was found with delayed hypersensitivity where small amounts of T-2 toxin were given to mice subcutaneously and in phagocytosis by macrophages if T-2 toxin is given prior to immunisation (Richard, 1991).

It is evident that mycotoxins form complex interactions with human and animal immune systems but much more research is needed in this area to elucidate the exact mechanisms, particularly around the interactions of multiple mycotoxins. *In vitro* studies have shown that mycotoxin combinations can act additively, synergistically and even in some cases antagonistically (Bruneau *et al.*, 2012).

1.4.2.1 Inflammatory response

The inflammatory response to an infection, as part of innate immunity, involves the triggering of physiological responses, including fever, pain, redness and swelling and a build-up of white blood cells at the site of infection (White, 1999; Akira *et al.*, 2006). This response will recruit effector cells and chemical factors of the innate immune system to the site of infection from local blood vessels. A local environment is formed, which promotes the migration of white blood cells to the site of infection, the destruction of the invasive agents and the repair of the damaged tissue. Acute inflammation is initiated by certain cells present in all tissues of the body, known as mononuclear phagocytes, or macrophages.

Macrophages (M \emptyset) are key effector innate immune cells that play a fundamental role in tissue homeostasis, pathogen clearance, wound healing and resolution of inflammation. M \emptyset are prodigious phagocytic immune cells that perform several different functions throughout the innate and adaptive immune response. They are present in lymphoid and non-lymphoid tissues and their primary role is to recognise, engulf and kill invading pathogens. M \emptyset express numerous pattern recognition receptors (PRRs) such as toll-like receptors (TLRs) which enable them to recognise

pathogen-associated molecular patterns (PAMPs) resulting in phagocytosis and the initiation of intracellular signalling pathways, leading to the production of inflammatory mediators such as cytokines and chemokines (Gordon, 2005).

Cells of the immune system are continuously sending and receiving messages. Cytokines are small protein molecules, usually less than 30 kDa in size, secreted by T-cells and macrophages (Stow *et al.*, 2009). Cytokines are pleiotropic or multi-functional and the specific response elicited by a given cytokine is dependent upon the cellular context, the environment and the cell's state of maturation. Cytokines frequently function in a redundant manner, in that multiple cytokines can produce the same physiological response. Furthermore, individual cytokines can be produced simultaneously and act synergistically. The response elicited by a cytokine or group of cytokines can have an expansive effect, in that one signal can trigger a cascade of cytokine signalling events. Cytokines usually operate in a targeted fashion, operate over short distances and have short life-spans (Sullivan *et al.*, 1991). The overall result of successful cytokine signalling is the rapid activation and recruitment of the appropriate cells of the immune system in response to a pathogenic agent. There are five families of cytokines and cytokine receptors including: the Toll/IL-1 family, the tumor necrosis factor (TNF) family, the haematopoietic receptors, the interferon receptors and the chemokine receptors (Dinarello, 2000). MØ are capable of initiating an adaptive immune response by presenting antigen to CD4+ T-cells *via* major histocompatibility class (MHC) II molecules. Phagocytosis is a fundamental process that is involved in the clearance of cellular debris from tissue remodelling and apoptosis and without this process the host would not survive (Janeway *et al.*, 2008). MØ activation is dependent on the type of pathogen encountered or the environment in which the macrophage resides. Classical activation is associated with increased expression of the antigen presentation receptor, MHCII and also the co-stimulatory marker, CD86 (Martinez, Helming and Gordon, 2009). Although MØ are vital components of host defence their activation must be firmly controlled as overproduction of pro-inflammatory cytokines can lead to host-tissue damage resulting in autoimmune diseases (Szekanecz and Koch, 2007; Zhang and Mosser, 2008).

1.5 Mycotoxin detection methods

1.5.1 Analytical techniques

The variety in the structures and isoforms of mycotoxins means it is not currently possible to use one standard technique for their analysis. In 2009, Turner *et al.* reviewed and compared some of most commonly employed methods and found there was no one favourable method but that choice usually depended on: (a) the mycotoxin(s) being analysed and, (b) the matrix being used.

To provide quantitative measurement of mycotoxins, analytical approaches based on the chromatographic properties of toxins have been established. Historically, Thin Layer Chromatography (TLC) was the most commonly used separation technique in mycotoxin, and specifically aflatoxin, determination. TLC is a good preliminary screening technique for mycotoxins and is still used. However, it lacks sensitivity and is not ideal for on-site analyses.

Advances in the area of chromatography have led to a progression from TLC to more sophisticated methods based around liquid chromatographic (LC) separation coupled to detection methods such mass spectrometry (MS) (LC-MS), fluorometric detection (FD) (HPLC-FLD) or ultra-violet detection (UVD) (HPLC-UVD) (Turner *et al.*, 2009; Turner *et al.*, 2015). These LC-based techniques allow higher throughput and offer greater sensitivity, selectivity and more flexibility. They are now considered the gold standard for mycotoxin detection by the AOAC allowing high throughput multi-toxin analysis.

1.5.2 Immunological techniques

Currently, immunoassay is a widely utilised tool for the analysis of mycotoxins. It is a valuable analytical technique based on molecular recognition between antibody and antigen that allows for detection with high sensitivity and specificity. These assays are used for the quantification of target molecules in many applications (Han *et al.*, 2013). Enzyme-linked immunosorbent assay (ELISA) is one of the most commonly used immunoassay formats as it is an inexpensive, colour-based test where the outputs may be assessed by absorbance determination. It is extremely useful for detecting haptens (low molecular weight molecules) such as mycotoxins that lend themselves well to competitive immunoassay detection. To achieve this, a conjugated form of the toxin is pre-coated onto multi-well plates, a mixture of toxin to be detected and detection

antibody are added to the plate. The free toxin (from the sample being analysed) and conjugated toxin compete for antibody binding, excess antibody is washed away and a labelled secondary antibody is added to detect bound anti-toxin antibody. Following addition of the substrate the absorbance of the product generated is determined. In a competitive immunoassay the intensity of the colour is inversely proportional to the concentration of free-toxin present.

Recently, lateral flow devices and ELISA kits have also been developed for a number of different mycotoxins. In general, lateral flow systems only consist of one-step method where instrumentation and reagents are not needed. Sample is placed on a sample pad and results are viewed by eye after several minutes, making them a useful on-site screening tool. ELISA test kits consist of the required reagents and materials. These kits are useful tools for screening but also allow some quantification. Many of these immunoassay test strips and kits are now commercially available for the analysis of the most common mycotoxins and are validated by organisations such as the AOAC. These kits can be used in the field but do not offer the same levels of sensitivity and high throughput analysis compared to lab-based methods.

1.5.3 Limitations of current techniques

Chromatographic analytical techniques and immunoassay analysis offer suitable sensitive methods for determining mycotoxin contamination within a laboratory, but there are many limitations to these techniques.

TLC has now generally been replaced by more sophisticated methods. The main issue with these chromatographic methods is they are time-consuming, costly and require skilled personnel to operate. These techniques also require rigorous sample clean up and pre-treatment, and for GC analysis there is often a need for derivatisation of non-volatile mycotoxins. Often mycotoxins can be lost or altered during these procedures leading to inaccurate results.

Immunoassay techniques lend themselves to being considerably more user-friendly and cost-effective, but ELISAs often still require lengthy analysis times and so like chromatographic methods they have significant limitations for implementation as rapid user-friendly 'on-site' testing platforms. This indicates a current need for new

cost-effective, highly sensitive, portable methods of analysis for mycotoxins to bring analysis from the lab to the field.

1.6 Novel mycotoxin binders

1.6.1 Antibodies

A large variety of binding ligands such as synthetic polymers, antibodies and aptamers have been developed in the past for mycotoxins detection. Antibodies are globular protein called immunoglobulins (IgGs). IgGs are natural biological scaffolds with structurally variable antigen binding domains, which are used by the immune system of higher organisms to mount a humoral immune response. They are the key bio-recognition elements of the immune response. IgGs are large glycoprotein structures with a characteristic 'Y' shape. More than 10^8 different antibodies can be in circulation in a body at any one time (Nelson, 2010).

Gene rearrangement is used in the production of a primary repertoire of antibodies. Antigens trigger a clonal expansion of naïve B-lymphocytes that express a cognate antibody of low affinity. The genes in the B-cell undergo rapid mutation achieving specific affinity maturation. This clonal expansion and affinity maturation generates immunoglobulins with highly evolved molecular recognition properties (Conroy *et al.*, 2009).

An IgG antibody consists of two heavy chains and two light chains, which are covalently linked by disulfide bonds. In addition to an inter-chain disulfide bond, an IgG has two intra-chain disulfide bonds. Each light chain has an N-terminal variable domain (V_L) and a constant domain (C_L). Each heavy chain is composed of an N-terminal variable domain (V_H), three constant domains (C_{H1} - C_{H3}) and a hinge region. In chickens, immunoglobulin Y (IgY) is the functional equivalent to IgG. IgYs are also composed of two light and two heavy chains (Figure 1.3). IgY and IgG mainly differ in the heavy chains, with the IgY being larger than in IgG. The light chains in IgY are slightly smaller than the light chains of an IgG. An IgY is less sterically flexible than its IgG counterpart. IgY does not bind to Protein A, Protein G, or to cellular Fc receptors and cannot activate the complement system.

The V_H and V_L chain form the antigen-binding site of the molecule. The sequence and structural variation in the variable domains is generally restricted to three short

hypervariable loops, known as complementary determining regions (CDRs). The variable domain also consists of a framework region, which is highly conserved. The combination of amino acid residues in the CDRs determines the antibodies ability to recognise a specific antigenic determinant (Murphy *et al.*, 2006).

The smallest fragment of the whole antibody practically used is the Fv which comprises of the V_H and V_L domains that are associated via a disulphide bond. Stability problems at lower concentrations were overcome by incorporating a flexible peptide linker into the Fv fragment resulting in a single chain Fv (scFv) (Figure 1.3). One of the main advantages of the scFv fragment is that it is essentially a minimal version of an IgG molecule and despite its reduced size, the fragment still retains the full activity, specificity and stability of a full immunoglobulin molecule. When used in immunoassay formats the reduced size of the scFv fragment allows for more densely packed coating of the fragment's binding regions (CDRs) thus giving higher potential assay sensitivities. Additionally, due to the removal of the entire immunoglobulin Fc region there is reduced likelihood of observing interference from secondary antibodies (Borrebaeck, 2000).

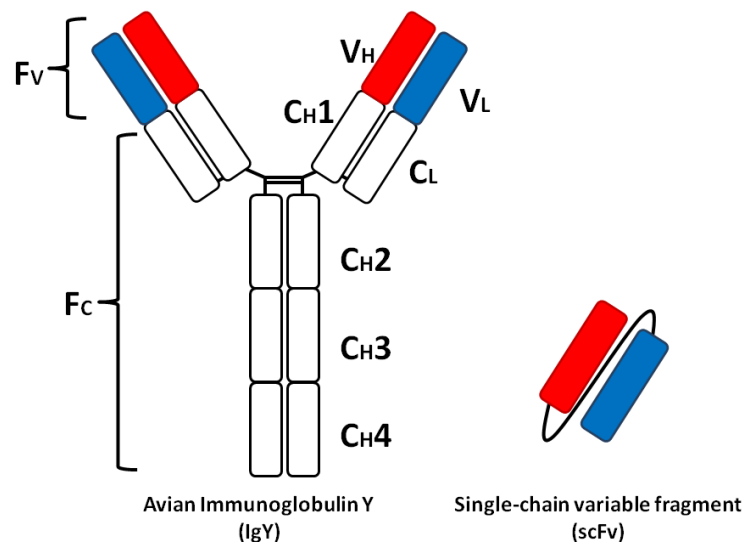


Figure 1.2: Immunoglobulin formats. Structure of intact immunoglobulin Y (IgY) molecule made up of a heavy and a light chain consisting of variable and constant regions. A single chain Fv (scFv) is an antibody fragment made of a variable heavy and variable light chain joined by a linker.

1.6.2 Recombinant antibody production

Recombinant antibodies can be sensitive and specific for their target molecules, and can be produced relatively easily and cheaply. Generation involves amplifying the variable genes from the cDNA of the lymphocytes of an immunised host. Phage display and bio-panning against a target of interest have been widely utilised for the detection of a range of structurally diverse antigens, including haptens, cell surface markers, and proteins. Three types of libraries may be used as sources of antibody pools; synthetic, naïve and immune. Synthetic and naïve antibody libraries are non-immune sources, derived from natural, rearranged V genes. Naïve libraries, consisting of the variable region repertoires can be generated from collections of variable genes from the messenger RNA (mRNA) of B-cells of non-immunised host donors, isolated from peripheral blood lymphocytes, tonsils, bone marrow and spleen cells.

Immune libraries are constructed from RNA isolated from splenocytes or the bone marrow of an animal host immunised with an antigen that generates an immune response. Antibody fragments isolated from immune libraries will generally be highly specific and have a high affinity, due to natural affinity maturation in the host. The RNA is converted into complementary DNA (cDNA), which in turn serves as a template for the amplification of variable heavy (V_H) and variable light (V_L) gene sequences. These are fused through an overlapping-extension splicing PCR reaction and subsequently cloned into a suitable phage or phagemid vector. The introduction of this construct into suppressor strains of *Escherichia coli* (*E. coli*) by electroporation, in conjunction with the packaging of phage particles *via* the addition of helper phage (a process referred to as rescuing), allows the encoded antibody structure to be 'presented' on the exterior of a bacteriophage particle. In the phage display technique, the scFv fragments encoded by the antibody library are expressed on the surface of the phage molecule. In this way, specific antibodies can be selected for using biopanning (Barbas *et al.*, 1992).

1.6.3 Phage Display Technology

Phage display is currently the most widespread method used for the display and selection of large collections of antibodies, and for the engineering of selected antibodies (Ma and O'Kennedy, 2017). The principle of phage display was first introduced in 1985 by George Smith (Smith, 1985). Phage display is a molecular

diversity technique that employs non-lytic filamentous bacteriophage fd/M13 to display ligands on the surface of their phage coat. *E. coli* containing the F conjugative plasmid are a natural host for replication of this phage family. Initially, complete phage vectors or bacteriophage, which carried all the genetic information required for the phage life-cycle, were used as the display vector. Now, small plasmid vector or phagemids, which contain the appropriate packaging signal and cloning sites, have become a more popular type of vector for display. Phagemids have high transformation efficiencies, making them ideal for generating large antibody repertoires. When using phage to display antibody fragments, phagemids usually consist of the DNA encoding a scFv, fused to the gene encoding a phage coat protein (pIII or pVIII) (Figure 1.4).

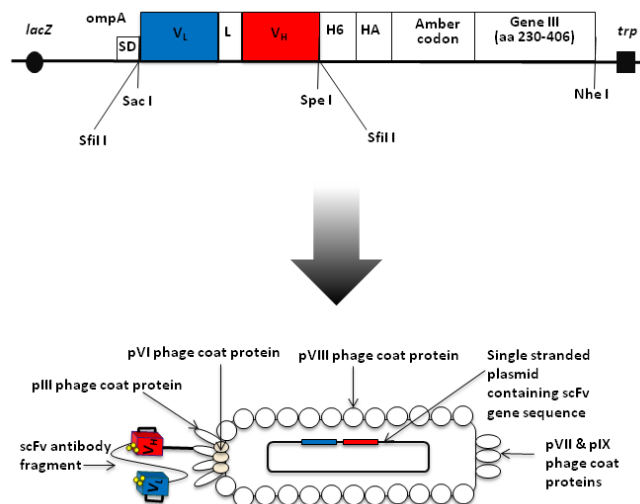


Figure 1.3: pComb phagemid vector and filamentous phage structure. The *lacZ* promoter allows for the expression of the heavy and the light chains of the antibody. The Shine Dalgarno (SD) is a ribosome-binding sequence that initiates protein synthesis. The leader sequence *ompA* directs the expression of the antibody and fusion gene III protein coat. The amber codon is present between the 3' *SfiI* restriction site and the 5' end of the gene III which permits the soluble protein expression in non-suppressor strains of bacteria. The *SfiI* sites allows for directional cloning of the protein for phage display. The six-histidine tag allows for purification and the HA tag can be used for detection using an anti-HA antibody. The terminator *trp* provides transcription termination. PIII, PVIII, PVII and PIX are the proteins of the phage coat. The scFv is displayed on the PIII/PVII.

Other vector features include an antibiotic resistance marker, an origin of replication, a promoter region and an affinity tag to aid in purification. Helper phage, such as M13K07 or VCSM13, are also required to supply all necessary structural proteins for correct packaging of the phage particle. The lacZ promoter is the most common promoter used to control expression. Expression may be suppressed by the addition of the catabolic repressor, glucose, or induced by addition of isopropyl- β -D-1-thiogalactopyranoside (IPTG). Upon induction, the scFv-coat fusion β -isopropylprotein is incorporated into new phage particles that are assembled in the bacterium and displayed on their surface, while the genetic information encoding the scFv remains within the phage particle (Barbas *et al.*, 2004) (Figure 1.4).

Phage display has been successfully employed to isolate antibody fragments specific for small molecules (Sheedy *et al.*, 2007). Small molecules alone do not have the molecular mass required to elicit an immune response and hence, must be conjugated to larger carrier proteins (Fodey *et al.*, 2007). Various carrier proteins, including bovine serum albumin (BSA), ovalbumin (OVA), keyhole limpet hemocyanin (KLH) and thyroglobulin (THY), are commonly used for this purpose. Regardless of the type of molecule, a carrier must be highly immunogenic, have the required solubility properties, be non-toxic *in vivo* and possess suitable functional groups for coupling to the hapten (Hermanson, 2005). Conjugation is a crucial step in antibody production, as the specificity of the resultant antibodies is dependent on the hapten used to produce them. The choice of method is governed by the functional groups available on both the hapten and the carrier and the orientation of the hapten desired, for presentation to the immune system.

1.6.4 Biopanning of phage display libraries

Biopanning is an affinity selection technique which relies on subjecting a library of antibodies on filamentous phage to bind to a specific target (immobilized on a solid support or in solution). This process enriches analyte-specific clones, by incubation with the target molecule in consecutive rounds, with increasing stringency. Unbound phage are washed away and specific phage are eluted by changing the binding conditions, either by pH elution, enzymatic cleavage or incubation with excess antigen. Specific phage are then amplified in *E. coli*. This selection process is outlined in Figure 1.5. In practice, several rounds of selection (approximately 3-5) are necessary, as the

binding of non-specific phage limits the enrichment that can be achieved in one single cycle (Azzazy and Highsmith, 2002).

Using the pComb vector series, specific phage can then be solubly expressed by infection into a non-suppressor *E. coli* strain such as Top10F, which allows the scFv to be secreted independently of the phage particle. Screening of the enriched library is then performed by analysing single colonies in a monoclonal ELISA to determine the specificity of each isolated clone.

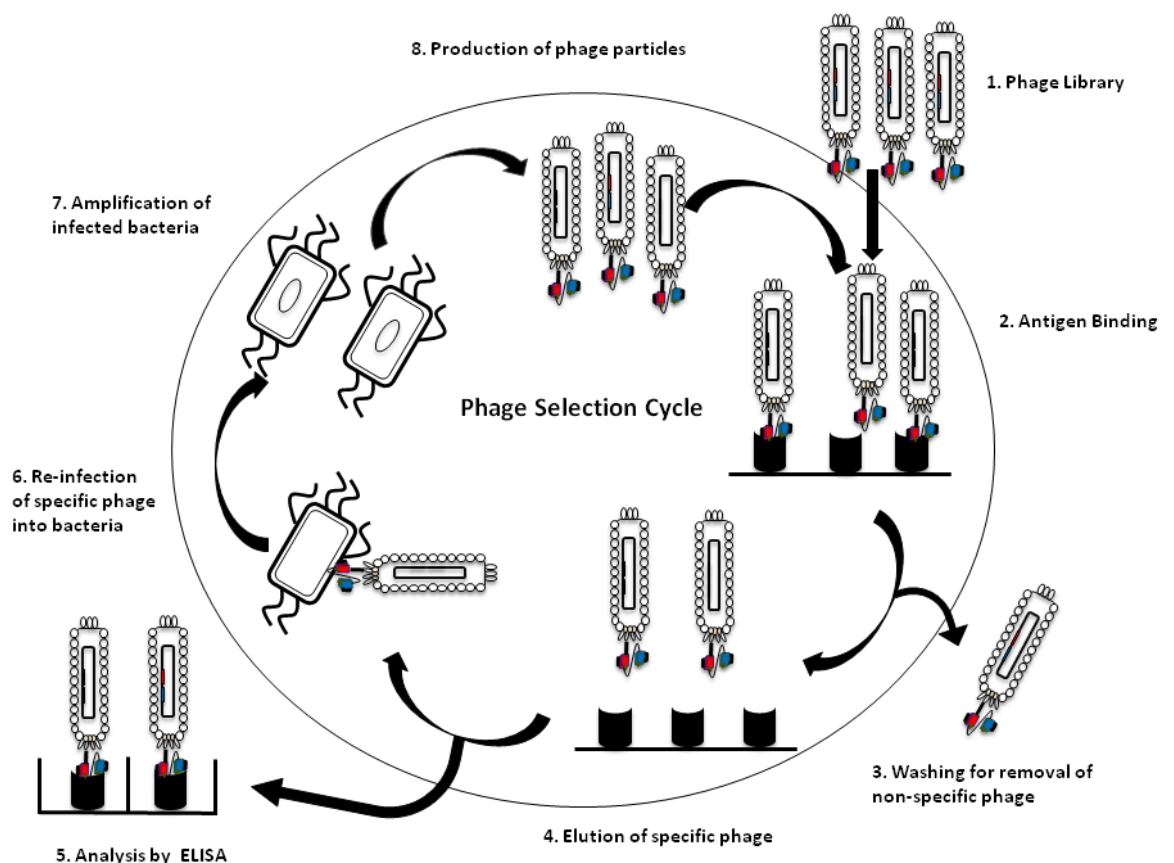


Figure 1.4: Biopanning of a scFv library using phage display technology. (1) Construction of the phage library. (2) Binding of the phage to the target antigen immobilised on an immunotube. (3) Removal of unbound phage by washing. (4) Recovery of antigen-specific phage. (5) Analysis of antigen-specific phage by ELISA; (6) Re-infection of specific-phage into *E. coli*. (7) Amplification of antigen-specific phage. (8) Production of enriched phage particles against the target.

1.7 Analysis of multiple mycotoxin contamination

The detrimental health effects of mycotoxins has been described and the need for rapid analysis tools highlighted but it is important to note that most toxin-producing fungi are capable of producing multiple mycotoxins concurrently (Bottalico, 1998). Furthermore, food and feed can be contaminated with various fungal species at the same time (Grenier and Oswald, 2011). Co-contaminated commodities might provoke adverse effects despite the concentrations of individual mycotoxins not exceeding legislative limits (Streit *et al.*, 2013). Additive and synergistic interactions have been highlighted for various combinations of mycotoxins. Therefore, it would be ideal to be able to not only quantify mycotoxins in a sample, but also account for the effects of their combinations. The novel microfluidic technology, Lab-in-a-Trench (LiaT), offers the ability to provide such analyses. The LiaT platform is a two layer polydimethylsiloxane (PDMS) system containing channels, trenches and reservoirs. The microfluidic trench allows capture and 'real-time' analysis of single cells. The application of this technology for mycotoxin analysis is described in Chapter 5 of this thesis.

1.8 Thesis Aims

Food-contaminating mycotoxins are a serious global health issue. There is a lack of understanding of how these adulterants interact with the immune system. While mycotoxins have been shown to modulate certain immune functions, their specific mechanisms of action remain unknown. Specifically, this work aims to elucidate mechanism involved in the effects of the mycotoxins patulin, DON, ZEN, and T-2 toxin on the murine macrophage cell line, J774A.1, in response to LPS. This research looks to examine the possible mechanisms of toxin-mediated modulation of macrophage function by first observing their effects to provide an important insight into the mechanisms by which mycotoxins modulate the host immune response to exert their immunomodulatory activity. To achieve this, varying concentrations these mycotoxins, alone and in combinations, will be examined *in vitro* for their effects on the cell viability, cytokine production and cell surface marker expression of the murine macrophage cells.

Furthermore, the need for a rapid analysis tool for complete mycotoxin determination has been highlighted. Therefore, this project aims to generate recombinant antibodies to target the mycotoxins patulin, ochratoxin A and aflatoxin M1 through generation and screening of avian immune libraries. Incorporating these novel recombinant antibodies into an immunoassay would allow for rapid and sensitive detection of the mycotoxins. This project will carry out immunisation campaigns using mycotoxin conjugates, optimise the production of immune libraries and screen these libraries for high-affinity scFv antibody fragments capable of binding their mycotoxin targets.

Moreover, this project aims to utilise the insight gained from basic research to give novel diagnostic applications of mycotoxins analysis through the novel Lab-in-a-Trench (LiaT) microfluidic technology. Information gained from *in vitro* studies will be used to determine the suitability of a platform such as LiaT for 'real-time' analysis of the immunomodulatory effects of mycotoxins.

Ultimately, this research will contribute to efforts in taking mycotoxin analysis from the lab to the field. This project aims to not only to shed light on the how mycotoxins interact with the immune system, but to also to use this information in their analysis by designing a way of monitoring the effects of multiple mycotoxins in a sample on immune cells, while also quantifying these toxins using recombinant antibodies.

Chapter 2: Materials and Methods

2.1 Materials

2.1.1 General reagents

Reagent	Supplier
dNTPs	Medical Supply Company Ltd.,
GoTaq® DNA Polymerase	Damastown, Mulhuddart,
MgCl₂	Dublin 15,
MyTaq™ Red Mix	Ireland.
1kb DNA ladder	
Sodium Chloride (NaCl)	Sigma-Aldrich Ireland,
Sodium phosphate dibasic (Na₂HPO₄)	Vale Road, Arklow,
Sodium phosphate monobasic (NaH₂PO₄)	Wicklow,
	Ireland.
Tween 20	
Tris base	
Bovine serum albumin (BSA)	
PCR primers	Integrated DNA Technologies, Interleuvenlaan 12A, Leuven, Belgium.
Agarose	Fisher Scientific Ireland,
Molecular grade water	Suite 3 Plaza 212,
Precept tablets	Blanchardstown Corporate Park 2, Ballycoolin, Dublin 15, Ireland.

Trizol	Bio-Sciences,
RNaseZap™	Charlemont Terrace, Crofton Road,
3M Sodium acetate	Dun Laoghaire, Co. Dublin,
SYBR® Safe DNA gel stain	Ireland.
Glycogen	
SYBR® Safe	
M13K07 Helper Phage	
Bacteriological Agar	Cruinn Diagnostics Ltd.,
Tryptone Powder	Hume Centre,
Yeast Extract	Parkwest Business Park,
	Nangor Road,
	Dublin 12,
	Ireland.
Restriction digest enzymes	New England Biolabs,
	Hitchin,
	Hertfordshire,
	SG4 0TY,
	England.
HyperLadder™ 1Kb	Bioline USA Inc,
HyperLadder™ Plus 1Kb	305 Constitution Drive,
	Taunton,
	MA 02780,
	USA.

Virkon	Lennox Laboratory Supplies Ltd, John F. Kennedy Drive, Naas Road, Dublin 12, D12 FP79, Ireland.
SureBlue™ TMB Microwell peroxidase substrate	Insight Biotechnology Ltd., PO Box 520, Wembley, Middlesex, HA9 7YN, United Kingdom.
Antartic Phosphatase Buffer Antartic Phosphatase Enzyme T4 DNA Ligase	Brennan and Company, Unit 61, Birch Ave, Stillorgan Industrial Park, Stillorgan, Co. Dublin, Ireland.
3,3',5,5'-tetramethyl-benzidine (TMB)	Insight Biotech, Unit G7, Wembley Commercial Centre, East Lane, Wembley, Middlesex, HA9 7XX, UK.

2.1.2 Buffer and Media preparation

The constituents of each buffer and medium are dissolved in 990 mL distilled and deionised water and adjusted to a final pH of 7.4 (unless otherwise stated). The solutions are made up to a final volume of 1 L. All components were analytical grade.

Buffer	Components
Phosphate-buffered saline (PBS) (1X) 150 mM	NaCl (5.84 g/L) Na ₂ HPO ₄ (4.72 g/L) NaH ₂ PO ₄ (2.64 g/L)
PBS tween 20 (PBST)	NaCl (5.84 g/L) Na ₂ HPO ₄ (4.72 g/L) NaH ₂ PO ₄ (2.64 g/L) Tween 20 (0.05 %, v/v)
Tris-buffered saline (TBS) (1X) 150 mM	Tris base (6.05 g/L) NaCl (8.76 g/L)
Tris-acetate-EDTA (TAE) (pH 8.0)	Tris base (10.8 g/L) Boric acid (5.5 g/L) 0.5 M EDTA (40 mL)
FACS buffer	FBS (2 % , v/v) NaN ₃ (0.05 %, w/v) in 1X PBS
Wash buffer	Tween 20 (0.05 %, v/v); in 1X PBS
Reagent diluent I	BSA (1 %, w/v); in 1X PBS

Reagent diluent II	BSA (0.1 %, w/v) Tween 20 (0.05, % v/v); in 1X TBS
10X SDS-PAGE Electrophoresis buffer	50 mM Tris (pH 8.3) 196 mM Glycine SDS (0.1 %, w/v)
SDS sample loading buffer	Glycerol (25 %, v/v) SDS (2 %, w/v) 14.4 mM β - Mercaptoethanol Bromophenol Blue (0.1 %, w/v)
Transfer buffer	Methanol (20 %, v/v) 1X Electrophoresis Buffer
Lysis buffer	50 mM NaH ₂ PO ₄ 300 mM NaCl 10 mM Imidazole pH 8.0
Wash buffer A	1X PBS 150 mM NaCl 20 mM Imidazole pH 8.0
IMAC Elution buffer	300 mM Imidazole pH 8.0

Media	Components
Luria Bertani Broth (LB) medium	Tryptone 10 g/L Yeast Extract 5 g/L NaCl 5 g/L
Super Broth (SB) medium	MOPS 10 g/L Tryptone 30 g/L Yeast Extract 20 g/L

Solid medium was made by the addition of 15 g/L bacteriological agar to the aforementioned formulations.

2.1.3 Commercial antibodies, antigens and mycotoxins

Reagent	Supplier
Peroxidase-labelled rabbit anti-Chicken IgY (IgG) (whole molecule)	Sigma-Aldrich Ireland, Vale Road, Arklow, Wicklow, Ireland.
Peroxidase-labelled rat anti-HA (human Influenza virus hemagglutinin) antibody	
Aflatoxin M1-BSA	
Deoxynivalenol	
Patulin	
T-2 toxin	
Zearalenone	
Lipopolysaccharide (LPS) <i>E. coli</i>, serotype R515	Enzo Life Sciences Inc., 10 Executive Boulevard, Farmingdale, NY 11735, USA.

Patulin-HG-KLH	Abcam,
Patulin-HS-BSA	330 Cambridge Science Park,
Peroxidase-labelled mouse anti-M13 antibody	Cambridge, CB4 0FL, UK.
FITC-labelled anti-mouse TLR4/MD-2 complex (MTS510)	Thermo Fisher Scientific Inc., 3747 N Meridian Rd,
PE-labelled anti-mouse MHC II (I-A/I-E) (m5/114.15.2)	Rockford, IL USA.
FITC-labelled anti-mouse CD86 (B7-2) (GL1)	BD Biosciences, 1 Becton Drive, Franklin Lakes, New
PE-labelled anti-mouse CD80 (16-10A1)	Jersey, 07417, USA.

2.1.4 Commercial kits

Kit	Supplier
Superscript III first strand synthesis system	Bio-Sciences, Charlemont Terrace, Crofton Rd, Dun Laoghaire, Co. Dublin, Ireland.
CellTiter 96® Aqueous One Solution	Thermo Fisher Scientific Inc., 3747 N Meridian Rd, Rockford, IL USA.
Nucleospin Gel and PCR clean up kit NucleoSpin® Plasmid mini prep kit NucleoSpin® Xtra midi plasmid kit	Fisher Scientific Ireland Ltd., Suite 3, Plaza 212, Blanchardstown Corporate Park 2, Ballycoolin, Dublin 15, Ireland.

DuoSet ELISA kits	R&D Systems, Inc., 614 McKinley Place NE, Minneapolis, MN 55413, USA.
--------------------------	--

2.1.5 Cell culture materials

Material	Supplier
Dulbecco's Modified Eagle's Medium (DMEM)	Invitrogen Corporation, 5791 Van Allen Way, Carlsbad, CA 92008, USA.
Fetal Bovine Serum (FBS)	Carlsbad, CA 92008, USA.
DPBS (1X) without calcium and magnesium	USA.
Penicillin-Streptomycin solution	
Tissue culture flasks (T-25 cm² and T-75 cm²)	Sarstedt , Sinnottstown Lane, Drinagh, Co. Wexford, Ireland.
Tissue culture plates (96-well and 6-well)	
Dimethyl sulphoxide (DMSO)	Sigma-Aldrich Ireland, Vale Road, Arklow, Wicklow, Ireland.
Trypan blue (0.4 %, v/v)	
1M HEPES solution	
MYCOZAP™ PLUS-PR	Brennan and Company, Unit 61, Birch Ave, Stillorgan Industrial Park, Stillorgan, Co. Dublin, Ireland.

2.1.6 Equipment

Equipment	Supplier
Eppendorf™ Centrifuge 5810 R with swing-bucket rotor (A-4-62) and fixed angle rotor (F-45-30-11)	Eppendorf AG, Barkhausenweg 1, 22339 Hamburg, Germany.
Biofuge Pico microcentrifuge	Heraeus Instruments Inc., 111-a Corporate Boulevard, South Plainfield, New Jersey, USA.
Sigma 2K15 Centrifuge	Sigma Laborzentrifugen GmbH, 37507 Osterode am Harz, Germany.
Safire™ II plate reader	Tecan™ Group Ltd. Seestrasse 103, CH-8708 Männedorf, Switzerland.
pH Metre (Orion 3 star) Mettler Model-PJ300 Pierce™ G2 Fast Blotter	Medical Supply Company Ltd, Damastown, Mulhuddart, Dublin 15, Ireland.
Water bath (Y6 model)	Grant Instruments Ltd., 29 Stratton Roa, Shepreth, Royston, Herts SG8 6PZ, UK.

MSC-Advantage Laminar Flow Cabinet	Thermo Electron Corporation,
Thermo Scientific Hybaid PX2 Thermal Cycler	81 Wyman Street, Waltham, Massachusetts (MA), 02454, USA.
Bio-Rad Horizontal gel electrophoresis system	Bio-Rad Laboratories, Inc.,
Bio-Rad Gel Doc™ EZ Imager	2000 Alfred Nobel Drive, Hercules, California 94547, USA.
Nanodrop™ ND-1000	NanoDrop Technologies, Inc.,
	3411 Silverside Rd 100BC, Wilmington, DE19810-4803, USA.
Biometra T-Gradient Thermocycler	Anachem Ltd.,
	Charles St., Luton, Bedfordshire, UK.
Mini-PROTEAN® Tetra Cell	Fannin House,
	South County Business Park, Leopardstown, Dublin 18, Ireland.
FACSAria™ I Flow Cytometer	BD Biosciences,
	1 Becton Drive, Franklin Lakes, New Jersey, 07417, USA.

Bio-Rad Gene Pulser Xcell	Alpha Technologies,
Bio-Rad PowerPac™ Basic	The Leinster Technology Centre,
DNA Gel Apparatus Bio-Rad	Blessington Industrial Estate,
(Wide-Mini-Sub® Cell GT)	Blessington, Co.Wicklow, Ireland.
DarkReader® Transilluminator	Clare Chemical Research, 995 Railroad Ave, Unit E, Dolores, CO 81323 USA.
VAPOUR-Line^{eco} 50 Autoclave	VWR International Ltd., Orion Business Park, North West Business Park, Ballycoolin, Dublin, Ireland.
Thermo Forma Series II 3110 water-jacketed CO₂ incubator	Fisher Scientific Ireland, Suite 3, Plaza 212, Blanchardstown Corporate Park 2, Ballycoolin, Dublin 15, Ireland.
Ohaus Pioneer 210g x 1mg Balance	Lennox, John F. Kennedy Drive, Naas Road, Dublin 12, Ireland.

Branson Digital Sonifier®

ABG Scientific Ltd.,
Dublin Industrial Estate,
Glasnevin,
Dublin 9,
Ireland.

Homogeniser Ultra Turrax

Janke & Kunkel IKA-Werk Ultra-
Turrax,
Staufen,
79129,
Germany.

**New Brunswick Scientific-Excella®
Incubator Shaker Type E24**

Mason Technologies,
Greenville Hall,

**Olympus IX81 motorized inverted
microscope with an attached**

228 South Circular Road,
Dublin 8,

Hamamatsu ORCA - ER digital camera

Ireland.

2.2 Methods

2.2.1 Cell culture

2.2.1.1 Culture of cell line

The murine macrophage cell line J774A.1 was obtained from the European Collection of Cell Cultures (ECACC; Salisbury, UK). The cells were cultured in Dulbecco's Modified Eagle's Medium (DMEM) (Invitrogen, UK) supplemented with 10 % (v/v) foetal bovine serum (FBS) (Invitrogen, UK), 50 U penicillin and 50 µg streptomycin (Invitrogen, UK). The semi-adherent cell line, J774A.1, was subcultured by dislodging the cells from the surface of the flask using a cell scraper (Sarstedt, Ireland). Cells were recovered by centrifugation in a Sigma 2K15 centrifuge (Sigma Laborzentrifugen, Germany) at 400 g for 5 minutes, diluted in fresh medium and then transferred to a sterile 75 cm² tissue culture flasks for further growth. All cultures were maintained in a 37°C, in a 5 % CO₂ humidified atmosphere. All work was carried out in a MSC-Advantage laminar flow cabinet (Thermo, USA) to ensure safety and sterility.

2.2.1.2 Long-term storage of cell line

Cells were prepared by aliquoting into 1 mL cryovials at a concentration of 5-10 x 10⁶ cells/mL in freeze medium. Freeze medium consisted of 95 % (v/v) DMEM and 5 % (v/v) dimethyl sulfoxide (DMSO) (Sigma-Aldrich, Ireland). Once aliquoted, the vials were immediately transferred to a Nalgene® Mr Frosty and placed in a -80°C freezer for slow freezing. Once frozen, the vials were transferred to liquid nitrogen for long-term storage.

2.2.1.3 Resuscitation of frozen cell line stocks

One aliquot of cells was thawed when new cultures were required. Ten mL of DMEM was pre-warmed to 37°C in a 25 cm² sterile tissue culture flask. The cryovial was warmed briefly at room temperature before thawing in a 37°C water bath. The contents of the vial were slowly transferred to the pre-warmed medium, which was then placed in the incubator. Cell growth was monitored by examining the cells, under a Nikon® Diaphot inverted microscope (Nikon, USA). After 72-96 hours, the regular subculture routine was initiated to ensure that the optimal cell concentration and conditions were maintained.

2.2.1.4 Cell counting

Cells were counted and their viability assessed using trypan blue exclusion. Trypan blue is negatively charged, so it is excluded from viable cells. Therefore, only the cells with damaged cell membranes (i.e. dead cells) will stain blue. Cell suspension (100 μ L) was mixed with 150 μ L PBS and 250 μ L trypan blue solution (0.4 %, v/v) (Sigma-Aldrich, Ireland). After \sim 2 minutes cells were applied to a haemocytometer and examined using a Nikon[®] Diaphot inverted microscope (Nikon, USA). Cells inside the central grid were counted. A viable cell count was determined using the following formula: Cell/mL = $N \times 5 \times 10^4$ where, N = average cell number counted, 5 = dilution factor and 10^4 = constant.

2.2.1.5 Cell authentication and mycoplasma testing

Cell line authentication and mycoplasma testing for the J774A.1 cell line were carried out by DDC Medical using their DNA collection card kit.

2.2.2 Effects of mycotoxin exposure on murine macrophage cell line

2.2.2.1 Mycotoxin treatments

For cell culture analysis, all required toxin dilutions were prepared in sterile PBS. The mycotoxins were dissolved in methanol to ensure the final concentration of solvent exposed to cells was always less than 0.1 % (v/v) methanol. In all experiments, a control assay was prepared, in which cells were exposed to the equivalent vehicle concentration to that used in the mycotoxin treatment.

2.2.2.2 Analysis of effect of individual mycotoxins on cell viability (MTS assay) in the J774A.1 murine macrophage cell line

The CellTiter 96[®] Aqueous One Solution (Pierce, UK) is a colorimetric method for determining the number of viable cells in a sample. It contains an MTS tetrazolium compound (Owen's reagent) which is bio-reduced by cells into a soluble coloured formazan product. The quantity of formazan product is measured at an absorbance reading of 490 nm and is directly proportional to the number of living cells in the culture medium. J774A.1 cells were plated in a 96-well plate with 100 μ L per well at a concentration of 1×10^6 cells/mL (previously determined as optimal seeding concentration for 24 hours analysis). Mycotoxins were then added at increasing concentrations (10 – 100,000 pg/mL) 1 hour prior to stimulation with LPS (100 ng/mL).

Cells alone, vehicle and 10 % (v/v) DMSO controls were also used. Twenty four hours after the addition of LPS (allowing determination of mycotoxin effects only, without need to replenish media for cell health), 20 µL of the CellTiter 96® Aqueous One Solution was added to each well of the 96-well plate. The plates were incubated for 4 hours at 37°C in 5 % CO₂ and absorbance read at 490 nm. The cell viability of each sample was calculated by treating the absorbance of the cells alone control as 100 % and comparing the remaining samples to this and expressing results as percentage viability. DMSO (10 %, v/v) was used as a positive control of cytotoxicity. Data was analysed using Prism Software (GraphPad Software, Inc.).

2.2.2.3 Analysis of effects of individual mycotoxins on cytokine (IL-6, IL-10, IL-27, IL-12p40, IL-1β and TNF-α) release in the J774A.1 murine macrophage cell line

Two hundred and fifty µL of a J774A.1 cell suspension at a concentration of 1 x 10⁶ cells/mL (previously determined as optimal seeding concentration for 24 hours analysis) was added to each well of a NUNC™96 well tissue culture plate. The mycotoxins (patulin, ZEN, DON and T-2 toxin) were added in increasing concentrations (0.001 – 100 pg/mL), with and without 100 ng/mL LPS, to induce an inflammatory response. Cells were incubated with an equivalent methanol concentration, as a vehicle control. The plates were placed in a 37°C incubator, in 5 % CO₂. After 24 hour incubations (allowing determination of mycotoxin effects only, without need to replenish media for cell health) , the cell supernatants were harvested and dispensed into sterile 96 well tissue culture plates and stored at -20°C until required. All experiments were performed in triplicate.

IL-6, IL-10, IL-27, IL-12p40, IL-1β and TNF-α DuoSet ELISAs were performed according to the manufacturer's instructions (R&D Systems Ltd). Each sample and standard was assayed in triplicate for each of the cytokines indicated. Data was analysed using Prism Software (GraphPad Software, Inc.).

2.2.2.4 Analysis of effects of mycotoxin combinations on cytokine (IL-6, IL-10, IL-12p40 and TNF-α) release in the J774A.1 murine macrophage cell line

Two hundred and fifty µL of a J774A.1 cell suspension at a concentration of 1 x 10⁶ cells/mL was added to each well of a NUNC™96 well tissue culture plate. The mycotoxin combinations were added, along with each individual mycotoxin in the

combination, with and without 100 ng/mL LPS, to induce an inflammatory response. Cells were incubated with an equivalent methanol concentration, as a vehicle control. The plates were placed in a 37°C incubator, in 5 % CO₂, for 24 hours. After 24 hours incubations, the cell supernatants were harvested and aliquoted into sterile 96 well tissue culture plates and stored at -20°C until required. All experiments were performed in triplicate.

IL-6, IL-10, IL-12p40 and TNF- α DuoSet ELISAs were performed according to the manufacturer's instructions (R&D Systems Ltd). Each sample and standard was assayed in triplicate for each of the cytokines indicated. Data was analysed using Prism Software (GraphPad Software, Inc.).

2.2.2.5 Statistical analysis

Data was pooled and mean values \pm 3SE was calculated. A one-way analysis of variance (ANOVA) was performed. If the ANOVA table was significant (*P < 0.05; ** P < 0.01; *** P < 0.001), post-hoc analysis was performed using Newman-Keuls Multiple Comparison Test to evaluate the differences between sample groups.

2.2.2.6 Analysis of effects of mycotoxin combinations on cell surface marker (CD80, CD86, TLR4 and MHCII) expression in the J774A.1 murine macrophage cell line using flow cytometry

Two millilitres of a J774A.1 cell suspension at a concentration of 1×10^6 cells/mL was added to each well of a NUNC™ 6 well tissue culture plate. The mycotoxin combinations were added, along with each individual mycotoxin in the combination, with and without 100 ng/mL LPS, to induce an inflammatory response. Cells were incubated with an equivalent methanol concentration, as a vehicle control. The plates were placed in a 37°C incubator, with 5 % CO₂. After 24 hours incubations, cells were labelled to determine cell surface expression of CD80, CD86, TLR4 and MHCII. For this, cells were scraped from the bottom of the well and collected in a 15 mL tube. Non-specific binding was blocked by addition of an equal volume of foetal bovine serum (FBS) for 15 minutes at room temperature to prevent the nonspecific binding of antibodies. Samples were centrifuged for 5 minutes at 400 g. Supernatant was discarded and the cells are washed once in 2 mL FACS buffer (See Section 2.1.2). The cell pellet was resuspended in 2 mL FACS buffer and 200 μ L of cell suspension was added to a 96 well round bottomed plate. The plate was centrifuged at 805 g for 5

minutes, in an Eppendorf 5018R centrifuge. The supernatant was discarded and the pellets were resuspended in 100 μ L of appropriate antibody solution. The plate was incubated at 4°C for 30 minutes. At the end of incubation time, the cells were pelleted, as previously described, and washed 3 times in 200 μ L FACS buffer. The stained cells were transferred to a labelled FACS tube and stored at 4°C protected from light prior to analysis. A minimum of 10,000 events were acquired for each sample on a FACSAria™ flow cytometer (BD Biosciences). Data was analysed using FlowJo software (Treestar).

2.2.2.7 Analysis of effects of mycotoxin combinations on phagocytosis in the J774A.1 murine macrophage cell line using flow cytometry

Mycotoxin treatment was carried out as in Section 2.2.2.6. To assess phagocytosis, J774A.1 macrophages were incubated with 1 μ m fluorescent latex beads (Sigma-Aldrich), at a concentration of 20 beads per cell, for 1 hour at 37°C. Cells were then washed with 2 % (v/v) FBS and the uptake of beads (λ_{ex} ~470 nm; λ_{em} ~505 nm) was measured by flow cytometry on a FACSAria™ flow cytometer. Data was analysed using FlowJo software (Treestar).

2.2.2.8 Analysis of effects of mycotoxin combinations on cell surface marker (CD80 and CD86) expression from the J774A.1 murine macrophage cell line using Lab-in-a-Trench

Cell surface expression of CD80 and CD86 on J774A.1 cells was assessed in real-time using the microfluidic technology, Lab-in-a-Trench (LiaT). LiaT is a microfluidic platform previously developed by Dimov *et al.* (2010). The microfluidic trench structure allows efficient capture and retention of cells or particles through gravity-based sedimentation. The laminar flow conditions assure a vanishing flow field throughout the trench, thus permanently retaining particles and minimising hydrodynamic stress. Furthermore, its small depth of 150 μ m allows continuous loading, mixing and refreshment of reagents by mere diffusion from a controlled flow through the supply channel on the top of the trench. The chips were designed by Prof. Jens Ducreé's Research Group in DCU and supplied by Dr Damien King and Ms Albina Julius.

The LiaT platform (Figure 2.1) is a two layer polydimethylsiloxane (PDMS) system whereby a lower PDMS panel holds structures (channels and trenches), while an upper panel has reservoirs. PDMS (Dow Corning) was mixed with curing agent in a ratio of 5 :

1 for the trenches and 20 : 1 for the lid, followed by degassing for 30 minutes under vacuum. Degassed PDMS was then poured on the appropriate silicon masters and partially cured for 4 hours at room temperature under vacuum. Inlet holes (diameter: 1 mm) were then punched in the lid structure. The two PDMS layers containing the channels and reservoirs were then aligned, bonded and cured at 70°C for 24 hours. Gravity driven flow was implemented by fitting a vertically aligned, standard pipette tip in the inlet hole of the LiaT chip and loading it with input fluid.

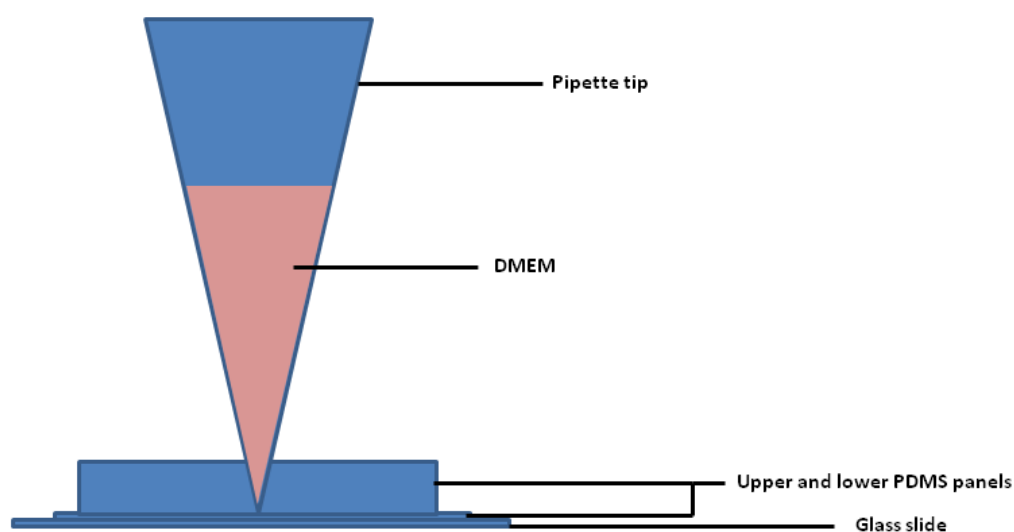


Figure 2.1: Structure of the Lab-in-a-Trench platform. The chip is composed of lower PDMS panel containing channels and trenches and an upper PDMS panel containing reservoirs, supported on a glass slide. A pipette tip is used as a liquid reservoir for cell and reagent addition.

The fabricated LiaT was O₂-plasma-treated for 5 minutes. The channels and trenches were immediately primed with DMEM (Invitrogen, UK) supplemented with 10 % (v/v) foetal bovine serum (FBS) (Invitrogen, UK), 50 U penicillin, 50 µg streptomycin (Invitrogen, UK), 1X MYCOZAP™ PLUS-PR (Brennan and Co., Ireland) and 10 mM HEPES (Sigma-Aldrich, Ireland). Each inlet was then loaded with J774A.1 cells which were captured in the trenches (Figure 2.2). The J774A.1 murine macrophage cells were cultured on and off chip using DMEM. For the on-chip cell culture and stimulation experiments the entire device was incubated at 37°C in an inverted fluorescence microscope (Olympus IX81) fitted with an incubation chamber (Solent Scientific, UK).

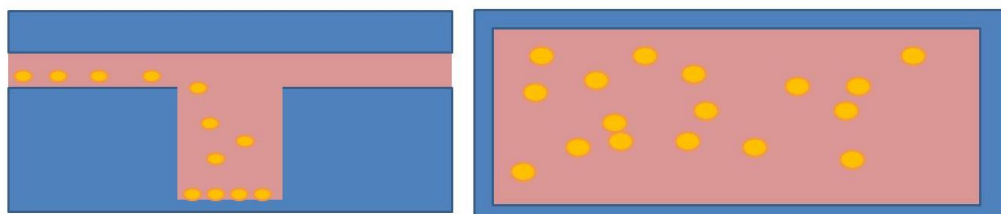


Figure 2.2: Cell capture in the Lab-in-a-Trench platform (side aspect left and top aspect right). Cells are captured in the microfluidic trench, allowing for single cell analysis using brightfield and fluorescent microscopy.

Mycotoxin exposure, cell surface marker labelling and LPS stimulation on the macrophages was performed on-chip by adding the relevant reagents to the perfusion culture medium, and maintaining a constant perfusion flow velocity at the chamber inlet. For the real-time staining of the CD80 and CD86 surface markers, FITC-labelled anti-CD86 and PE-labelled anti-CD80 antibodies were used. The J774A.1 cells were captured (approximately 20 – 40), exposed to controls (1X PBS and methanol vehicle) or mycotoxins, individually and in combination, for 1 hour, probed with the anti-CD80 and anti-CD86 antibodies then stimulated with LPS (200 ng/mL). Bright field, and FITC and PE fluorescent images were acquired by mounting the chip on an inverted fluorescence microscope (Olympus IX81) and imaging at time points. Data was analysed using ImageJ software. The steps in the process are detailed in Figure 2.3 below.

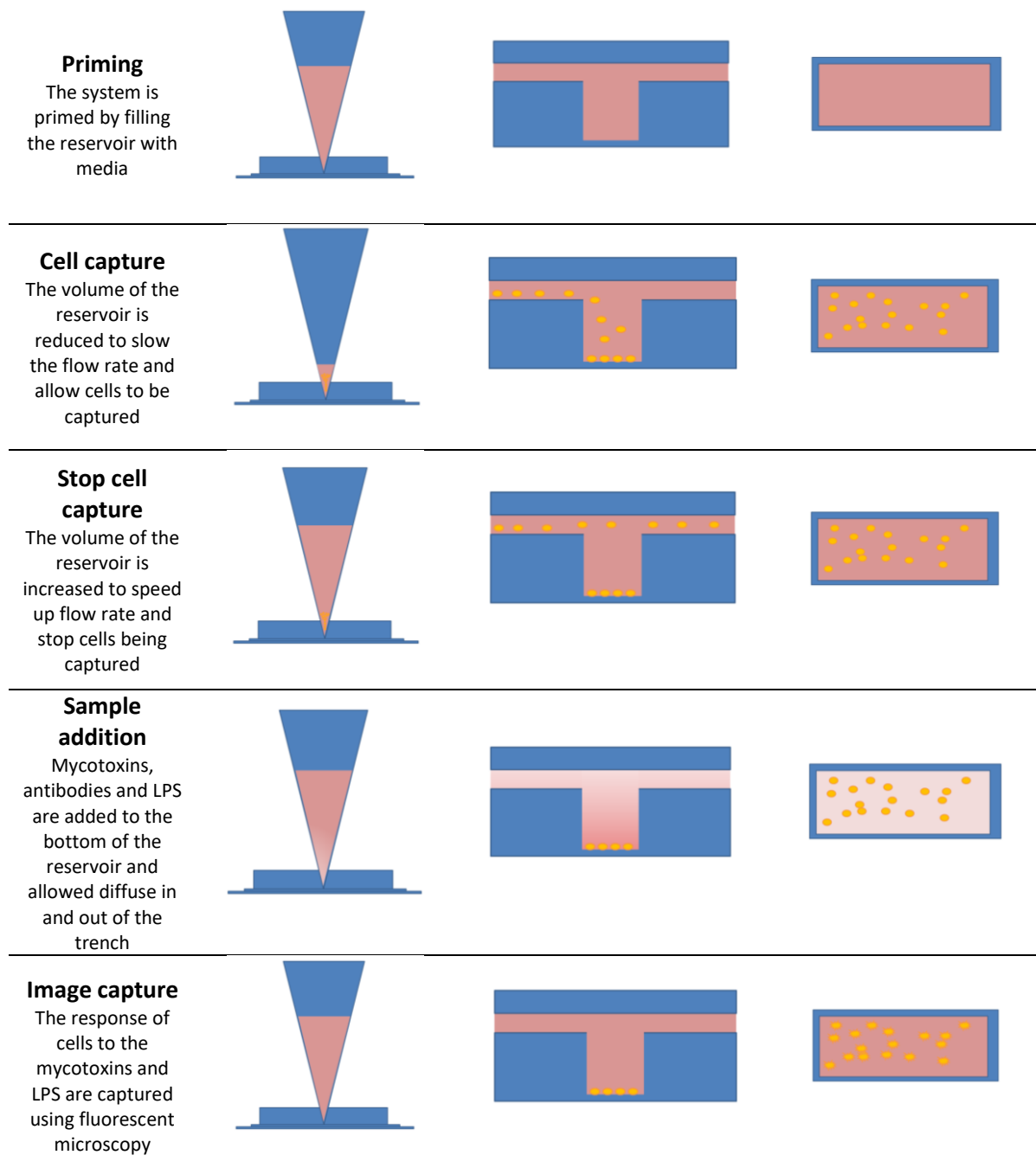


Figure 2.3: Process for opto-microfluidic monitoring of cell expression dynamics. Cells are captured in a microfluidic Lab-in-a-Trench device and recorded using brightfield and fluorescent microscopy. Concentration kinetics are quantified in real-time for cells in the trench.

2.2.3 Generation of an avian immune library for Aflatoxin M1, Patulin and Ochratoxin A

2.2.3.1 Immunisation of a leghorn chicken with AFM1-BSA and Patulin-HG-KLH

Prior to immunisation, a pre-bleed was taken from two female Leghorn chickens. The immunogens, AFM1-BSA (Sigma-Aldrich, Ireland) and Patulin-HG-KLH (Abcam, UK), were prepared in a final volume of 1 mL in a 1:1 ratio with Freund's complete adjuvant (Sigma-Aldrich, Ireland) for the primary immunisation and Freund's incomplete adjuvant (Sigma-Aldrich, Ireland) for subsequent immunisations.

The immunogen was vortexed for 1 hour at 4°C before immunisation to create a stable emulsion. One mL of the emulsion was administered to the chicken subcutaneously over four sites (250 µL each). For the primary immunisation, the animal was injected with 100 µg AFM1-BSA and Patulin-HG-KLH and for subsequent boosts, 75 µg of each was used. A period of three weeks was left between each immunisation. A bleed was taken 1 week after the each boost to determine the level of immune response.

2.2.3.2 Serum titre of AFM1-BSA and Patulin-HG-KLH-immunised chickens by ELISA

In order to determine an immune response against AFM1 and patulin, a bleeds were taken, left to coagulate and centrifuged in a Biofuge Pico microcentrifuge (Heraeus, USA) at 18,514 g for 20 minutes to harvest serum. For patulin, a NUNC™ 96 well plate was coated with 10 µg/mL Patulin-HG-KLH, 10 µg/mL Patulin-HS-BSA, 10 µg/mL KLH and 10 µg/mL BSA, for 1 hour at 37°C. The plate was washed 3 times with PBS (150 mM, pH 7.4) and wells were blocked with 4 % (w/v) Milk Marvel/PBS (150 mM, pH 7.4) solution, 200 µL per well at 37°C for 1 hour. Following blocking, the plate was washed three times with PBST (150 mM, pH 7.4) and three times with PBS (150 mM, pH 7.4). The immune serum was serially diluted from 10⁻¹ to 10⁻⁷ in 1 % (w/v) Milk Marvel/ 0.01 % (v/v) Tween 20/PBS (150 mM, pH 7.4) and added to the plate. This was incubated for 1 hour at 37°C; following this it was washed as above. A secondary HRP-labelled anti-Chicken IgY (IgG) antibody (100 µL) produced in rabbit (Sigma Aldrich, Ireland) at a 1/2,000 dilution in a 1 % (w/v) Milk Marvel/PBS (150 mM, pH 7.4) solution was added to each well. The plate was incubated at 37°C for 1 hour.

Following incubation, the plate was washed as above and 100 μ L of 3, 3', 5, 5' tetramethylbenzidine (TMB) substrate solution (Insight Biotech, UK) was added to each well. The plate was then incubated for approximately 20 minutes under tinfoil to allow for colour development after which the reaction was stopped by addition of 50 μ L of 10 % (v/v) HCl. The absorbance was then determined at 450 nm with a Tecan™ Safire II plate reader (Tecan™, UK).

For AFM1 the serum titre was carried out as above with the additional step of incubating the serum dilutions with 5 % (w/v) BSA /PBS (150 mM, pH 7.4) for 30 minutes at room temperature in order to deplete out the BSA-specific antibodies in the serum.

2.2.3.3 Phenol-chloroform extraction of RNA

When satisfactory immune responses were achieved the chickens were euthanised and spleens harvested. Ice-cold Trizol reagent (30 mL) (Invitrogen, Bio-Sciences) was immediately added to the spleens in 50mL RNase-free tubes and the samples were homogenised for ~1 minute using an IKA T-18 Ultra Turrax homogenizer (Sigma-Aldrich, Ireland). The samples were allowed to stand for 5 minutes at room temperature to allow for the total dissociation of nucleoprotein complexes, while maintaining the integrity of the RNA, before centrifuging at 2,500 g in an Eppendorf 5810R centrifuge (bucket rotor A-4-62) for 20 minutes at 4°C. The supernatant was carefully removed and transferred to a polypropylene tube which had been pre-treated with RNaseZap and rinsed with 'RNase free' MG-water prior to use. MG-chloroform (6 mL) was added and the samples were vortexed for 15 seconds. This resulted in the separation of the homogenised spleen preparation into an upper aqueous phase (containing RNA) and a lower organic phase (containing DNA and protein). This was incubated at room temperature for 15 minutes before centrifugation (fixed angle, pre-cooled Sorval SS34 rotor) at 17,500 g for 20 minutes at 4°C.

The centrifugation produced 3 layers; a lower red phenol/chloroform phase, a protein interphase and a colourless liquid-upper phase with the RNA. The upper aqueous layer was very carefully removed and transferred to a polycarbonate tube. Molecular grade (MG)-isopropanol (15 mL) was added, vortexed for 15 seconds and incubated at room temperature for 10 minutes. The isopropanol precipitated the RNA from solution. The

samples were centrifuged in a polypropylene tube (fixed angle, pre-cooled Sorval SS34 rotor) for 25 minutes at 4°C and an RNA pellet was formed. The supernatant was carefully removed and 30 mL of 75 % (v/v) MG-ethanol was added.

The samples were centrifuged in an Eppendorf 5018R centrifuge (Eppendorf AG, Germany) at 17,000 g for 20 minutes at 4°C and the supernatant was again removed. The pellet was air dried and 500 µL of 'RNase-free' water was used to gently re-suspend the pellet. The samples were stored on ice before immediately proceeding with cDNA synthesis. The spleen RNA samples were quantified using a Nanodrop™ spectrophotometer.

2.2.3.4 cDNA synthesis by reverse transcription

For cDNA synthesis, a Superscript III First Strand Synthesis System for RT-PCR (Invitrogen, UK) kit was used. A total of 5 µg RNA is required for each reaction. Two mixtures are prepared; mixture 1 and mixture 2, which each containing a 20X reaction mixture.

The preparation of each mixture is outlined:

Mixture 1	20X Reaction
RNA	To give 20 x 5 µg
Oligo-(dT)₂₀ (50 µM)	20 µL
dNTPs (10 mM)	20 µL
MG H₂O	Up to 200 µL

Mixture 2	20X Reaction
10X RT Buffer	40 µL
MgCl₂ (25 mM)	80 µL
DTT (0.1 M)	40 µL
RNase OUT (40 U/µL)	20 µL
Superscript III RT (200 U/µL)	20 µL

Mixture 1 was divided into eight 25 μ L aliquots and mixed by vortexing before Stage 1 on the Thermocycler was run, as described below. The tubes were placed on ice for 1 minute, 25 μ L Mixture 2 was added and Stage 2 of the program was carried out. RNase H was added at a volume of 1 μ L RNase H per 10 μ L of reaction mixture. The purpose of RNase H was to digest template RNA from the RNA:cDNA hybrid mix following cDNA synthesis. After RNase H addition, Stage 3 of the program is followed. Following synthesis, the reaction mixture was aliquoted and stored at -80°C . cDNA synthesis was carried out using a PX2 thermal cycler (Thermo Electron Corporation, USA) using the following PCR program:

Stage	Temperature	Time
1	65 $^{\circ}\text{C}$	5 minutes
		Pause
2	50 $^{\circ}\text{C}$	50 minutes
	85 $^{\circ}\text{C}$	5 minutes
		Pause
3	37 $^{\circ}\text{C}$	20 minutes
	4 $^{\circ}\text{C}$	Hold

2.2.3.5 Amplification of antibody variable domain sequences using PCR

Spleen cDNA obtained from reverse transcription was used in the first round of polymerase chain reaction (PCR) to amplify the variable heavy and variable light chain genes. The primers were obtained from Integrated DNA Technologies. pComb3XSS series primer sequences were obtained from Barbas *et al.* (2001). To amplify the V gene rearrangements from the immunised chicken, one V_H amplification and one V_L amplification was performed. The following PCR primers were used:

V_H Primers

CSCVHo-F (sense) 5' GGT CAG TCC TCT AGA TCT TCC GCC GTG ACG TTG GAC GAG 3'

CSCG-B (reverse) 5' CTG GCC GGC CTG GCC ACT AGT GGA GGA GAC GAT GAC TTC
GGT CC 3'

V_L Primers

CSCVK (sense) 5' GTG GCC CAG GCG GCC CTG ACT CAG CCG TCC TCG GTG TC 3'

CKJo-B (reverse) 5' GGA AGA TCT AGA GGA CTG ACC TAG GAC GGT CAG G 3'

The PCR program was set up:

Stage	Temperature	Time	No. of cycles
1	94°C	10 minutes	1
2	94°C	15 seconds	
	56°C	30 seconds	30
	72°C	60 seconds	
3	72°C	10 minutes	1
	4°C	Hold	

The PCR reaction mixtures were prepared:

Component	Volume
V _H /V _L Sense Primer	0.5 µL
V _H /V _L Reverse Primer	0.5 µL
cDNA	1 µL
MyTaq™ Red Mix	25 µL
MG H ₂ O	23 µL

To optimise MgCl₂ concentration the PCR reaction mixture was prepared:

Component	Volume
GoTaq Buffer (5x)	10 µL
V _H /V _L Sense Primer	0.5 µL
V _H /V _L Reverse Primer	0.5 µL
MgCl ₂	2/4/6 µL
cDNA	1 µL
dNTP	1 µL
MG H ₂ O	34.75/32.75/30.75 µL
GoTaq® Polymerase	0.25 µL

The reaction was repeated in large-scale, using optimised conditions for both V_H and V_L fragments. The products were ethanol-precipitated by adding a 0.1X volume of 3M sodium acetate (pH 5.2), a 10X volume of 100 % (v/v) ice-cold ethanol and 1 µL glycogen, and stored at -20°C overnight. The following day, the DNA was harvested by centrifuging in a Biofuge Pico microcentrifuge (Heraeus, USA) at 18,514 g for 30 minutes. Subsequently, the ethanol supernatant was decanted and the pellet was washed with 70 % (v/v) ethanol and centrifuged in a Biofuge Pico microcentrifuge (Heraeus, USA) for 10 minutes (18,514 g) at 4°C. The pellet was allowed to air-dry briefly and then gently dissolved in 5 µL of molecular grade H₂O. This product was gel purified from a 1 % (w/v) agarose gel, using a Nucleospin Gel and PCR clean up kit (Section 2.2.3.8).

2.2.3.6 SOE-PCR optimisation

The purified V_H and V_L fragments were used for SOE-PCR. The following overlap PCR primers were used:

CSC-F (sense) 5' GAG GAG GAG GAG GAG GAG GTG GCC CAG GCG GCC CTG ACT CAG 3'

CSC-B (reverse) 5' GAG GAG GAG GAG GAG GAG GAG CTG GCC GGC CTG GCC ACT AGT
GGA GG 3'

The PCR gradient program was set up to optimise the annealing temperature of the reaction:

Stage	Temperature	Time	No. of cycles
1	94°C	2 minutes	1
2	94°C	15 seconds	
	58°C – 75°C	30 seconds	30
	72°C	2 minutes	
3	72°C	10 minutes	1
	4°C	Hold	

The PCR reaction mixtures were prepared:

Component	Volume
Sense primer CSC-F	0.5 µL
Reverse primer CSC-B	0.5 µL
V _H	Equivalent to 100 ng
V _L	Equivalent to 100 ng
MyTaq™ Red Mix	25 µL
MG H ₂ O	Up to 50 µL

The approximately 750 bp fragment from this reaction was ethanol-precipitated and purified on a 1 % (w/v) agarose gel, using a Nucleospin Gel and PCR clean up kit (Section 2.2.3.8).

2.2.3.7 Agarose gel electrophoresis

A 1 % (w/v) agarose gel was prepared by adding 0.5 g of agarose to 50 mL of Tris-Acetate-EDTA (TAE) buffer and heating to 100°C for 2-3 minutes. When the agarose was dissolved and partially cooled, 5 µL of SYBR®Safe DNA gel stain (Invitrogen, Bio-sciences) was added and poured into a prepared gel mould. A 1kb DNA molecular weight ladder (Invitrogen, Bio-sciences) was loaded along with samples for size quantification. The gel was run at a voltage of 90V for approximately 45 minutes, viewed and imaged using the Bio-Rad Gel Doc™ EZ Imager.

2.2.3.8 DNA agarose gel purification

All the DNA samples were gel-purified using the Nucleospin Gel and PCR clean up kit. DNA was electrophoresed on a 1 % (w/v) agarose gel. The gel was visualised using a Darkreader transilluminator (Clare Chemical Research) and the required bands were excised from the gel with a sterile, sharp scalpel. The manufacturer's protocol was followed with the exception of elution using MG H₂O instead of elution buffer. Concentrations were obtained by measuring the absorbance at 260nm using the Nanodrop™ and samples were stored at -20°C.

2.2.3.9 Digestion of scFv insert and pComb3XSS vector using SfiI

The *SfiI* restriction enzyme allows for unidirectional cloning of the scFv fragment library into the pComb3XSS vector (Figure 2.4). The enzyme recognises 8 bases which are interrupted by 5 random nucleotides (5' ggccnnnnnggcc 3'), thus eliminating internal digestion in antibody sequences.

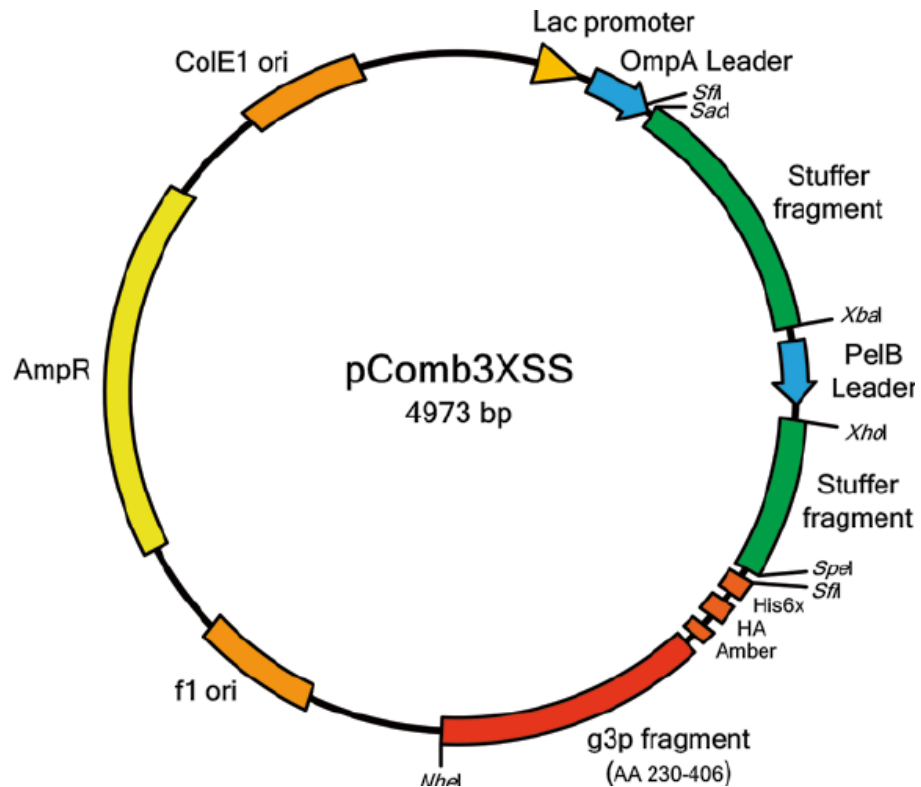


Figure 2.4: Details of the pComb3X phagemid vector. The cloning site contains an *SfiI* cassette for cloning. The *SfiI* sites have different internal pentamer sequences allowing the directional cloning of full Fab, scFv, peptide and other proteins for phage display. Alternatively, the *SacI* and *SpeI* sites can also be used for directional cloning. The *OmpA* leader sequence facilitates the transport of the fusion protein to the periplasm. The site also contains a histidine (His6x) tag and a hemagglutinin (HA) tag, which can be used for the purification and detection of recombinant proteins. The amber stop codon (Amber) is used to turn off expression of the p3 fusion protein. Recombinant protein can be produced without sub-cloning, by switching to a non-suppressor strain of *E. coli*. There are two stuffer fragments: a 1,200 bp stuffer in the Fab light chain cloning region bordered by *SacI* and *XbaI* restriction sites and a 300 bp stuffer in the Fab heavy chain cloning region bordered by *XhoI* and *SpeI* restriction sites. The 1,600 bp double stuffer sequence (both stuffer fragments plus the PelB leader sequence) can be removed by *SfiI* (or *SacI* and *SpeI*) digest so that genes of interest can be cloned (Levisson *et al.*, 2014).

Digests of the scFv insert (SOE product) and pComb3XSS vector were prepared as follow:

Component	Volume
SOE product	Equivalent to 10 µg
10X Buffer	5 µL
<i>Sfi</i> I (6 U/ µg)	160 U
MG H₂O	Up to 50 µL

Component	Volume
pCom3xSS vector	Equivalent to 20 µg
10X Buffer	5 µL
<i>Sfi</i> I (16 U/ µg)	120 U
MG H₂O	Up to 50 µL

Digestions were incubated for 5 hours at 50°C and the enzyme was de-activated for 5 minutes at 65°C. Both digests were separated by electrophoresis on a 1 % (w/v) agarose gel and purified.

2.2.3.10 Treatment of pComb3XSS vector with antarctic phosphatase

In order to prevent pComb3XSS vector re-ligation without insert, the digested vector was treated with Antarctic phosphatase. Antarctic phosphatase (AP) causes the removal of 5' phosphate groups from DNA. Since DNA fragments treated with AP lack the 5' phosphate group needed by ligase, they cannot self-ligate. This would potentially decrease vector background in cloning. The reaction was prepared as follows:

Component	Volume
Restricted pComb3XSS vector	50 μ L
10X Buffer	4.5 μ L
Antarctic phosphatase	1 μ L

The reaction was incubated for 20 minutes at 37°C and the enzyme was deactivated for 5 minutes at 70°C.

2.2.3.11 Ligation of SOE insert into pComb3XSS vector

The restricted scFv fragment library was ligated into the pComb3XSS vector in a 2:1 (insert:vector) ratio under the conditions below and incubated overnight at room temperature before being ethanol precipitated.

Component	Volume
Digested pComb3XSS vector	Equivalent to 1.4 μ g
Digested SOE insert	Equivalent to 700 ng
10X Ligase buffer	5 μ L
T4 DNA Ligase (400 U/ μ L)	2.5 μ L
MG H ₂ O	Up to 50 μ L

2.2.3.12 Library transformation and rescue of chicken scFv-displaying phage

Electrocompetent *E.coli* XL1-Blue cells (Stratagene) were thawed on ice. The ethanol-precipitated library ligations (10 μ L) were added to 100 μ L of the XL1-Blue cells. This was stored on ice for 1 minute. Electrocuvettes (Bio-Rad®) were pre-chilled prior to transformations. The ligation:cell mixture was electroporated at 2.5 kV, 25 μ F and 200 Ω using a Bio-Rad® electrophorator. The electro-cuvette was washed with 1 mL pre-warmed SOC media and transferred to 50 mL tubes, containing 3 mL SOC media. This was followed by incubation for 1 hour at 37°C in an orbital shaker. Serial dilutions of the transformed library were prepared, from 10⁻¹ to 10⁻⁸ and 100 μ L was plated onto LB agar plates, containing carbenicillin (100 μ g/mL), which were incubated at 37°C overnight. The titre was calculated using the following equation:

Estimated library titre = (No. of colonies x culture vol. x total ligation vol.) / (Plating vol. x ligation vol.)

The remaining culture of rescued cells was then spun down for 10 minutes at 4,000 g (Sigma Laborzentrifugen 2K15). The supernatant was discarded and the pellet resuspended in 400 μ L of SB. This was plated onto LB agar plates, containing carbenicillin (100 μ g/mL), which were incubated at 37°C overnight.

The following day, these stock plates were scraped using 1 mL of SB per plate and placed in a 50 mL tube. This stock culture was spun down for 10 minutes at 4,000 g (Sigma Laborzentrifugen 2K15). The pellet was resuspended in 1 mL of SB. Five-hundred μ L of the resuspended pellet was added to SB in a baffled conical flask (volume details in table 2.1 below) supplemented with 100 μ g/mL carbenicillin. The remaining 500 μ L of resuspended pellet was mixed with 500 μ L of 50 % (v/v) glycerol and stored at -80°C. The culture was grown at 37°C and 220 rpm until an OD600 of 0.6 was reached. Helper phage M13K07 (volume details in table 2.1 below) was then added to the culture and incubated stationary at 37°C for 30 minutes. The culture was then incubated at 37°C and 220 rpm for 1 hour. Kanamycin was added to a final concentration of 60 μ g/mL and the culture was incubated overnight at 30°C and 220 rpm.

Three 50 mL tubes containing 10 mL SB with 5 μ g/mL tetracycline were each inoculated with one colony of XL1-Blue *E. coli* cells and grown overnight at 37°C and 220 rpm.

An immunotube was coated with 1 mL of a given concentration of mycotoxin conjugate (the concentration of mycotoxin conjugate was reduced in each round of panning, as described in table 2.1 below) and stored overnight at 4°C.

Table 2.1: Bio-panning conditions

Panning Round	Coating Concentration	Culture Volume	Phage Volume
1	100 µg/mL	200 mL	400 µL
2	50 µg/mL	100 mL	200 µL
3	25 µg/mL	100 mL	200 µL
4	12.5 µg/mL	100 mL	200 µL

2.2.3.13 Enrichment of chicken phage library by bio-panning

The phage library (section 2.2.3.12) was centrifuged at 10,414 g for 20 minutes. The phage supernatant was transferred to 85 mL Nalgene® centrifuge tubes and PEG (4 %, w/v) and NaCl (3 %, w/v) added. The tubes were shaken for 10 minutes at 37°C to dissolve the PEG and NaCl, after which the tubes were placed on ice at 4°C for 1 hour. The mycotoxin-coated immunotube (Section 2.2.3.12) was blocked with 5 % (w/v) BSA/PBS (150 mM, pH 7.4) for 1 hour at 37°C. One of the 50 mL tubes containing XL1-Blue *E. coli* cells (Section 2.2.3.12) was subculture into a number of dilutions of 20 mL SB with 5 µg/mL tetracycline and grown at 37°C and 220 rpm.

Subsequently, the phage were precipitated by centrifuging at 10,414 g (brake off) for 20 minutes at 4°C. The supernatant was discarded and the resulting pellet dried on tissue. The pellet was re-suspended thoroughly in 2 mL of 1 % (w/v) BSA/PBS (150 mM, pH 7.4) and transferred to a 2 mL micro-centrifuge tube as the Input. The blocked immunotube was washed three times with PBS / 0.05 % (v/v) Tween 20 and three times with PBS. The phage library Input (1 mL) was added to immunotube and incubated, rotating, for 2 hours at room temperature. The unbound phage were then carefully removed and the immunotube was washed. One mL of 10 mg/mL trypsin, prepared in PBS (150 mM, pH 7.4) was added in the immunotube for 15 minutes rotating at room temperature, followed by vigorous pipetting and transferred to a 2 mL micro-centrifuge tube as the Output.

Twenty-five µL of the rescued phage Input was added to 225 µL of XL-1 Blue *E. coli* cells at OD 600 0.6. From this, serial dilutions down to 10⁻⁹ were made. Additionally, 25 µL of the eluted phage output was added to 225 µL of XL-1 Blue *E. coli* cells. From this, serial dilutions down to 10⁻⁶ were made. Five hundred µL of the remaining output was

re-infected into 3 mL of electrocompetent XL-1 Blue *E. coli* cells at an OD600 of 0.6. The phage-infected cells and titres were incubated for 30 minutes at 37°C. The serial dilutions were plated out on LB plates containing 100 µg/mL carbenicillin and incubated overnight, while inverted, at 37°C.

The phage-infected 3 mL culture was then centrifuged for 10 minutes at 4,000 g (Sigma Laborzentrifugen 2K15). The supernatant was discarded and the pellet resuspended in 400 µL of SB. This was plated out 100 µL / plate supplemented with 100 µg/mL carbenicillin and incubated overnight at 37°C. The following day the stock plates were scraped and centrifuged as before. Five-hundred µL was used then in the next round of panning and the remaining stored as a glycerol stock at -80°C.

2.2.3.14 Polyclonal phage ELISA

A Nunc MaxiSorp™ 96-well plate was coated with 100 µL/well of 2 µg/mL of mycotoxin conjugate diluted in PBS and incubated at overnight at 4°C. The plate was washed 3 times with PBS / PBS-T (0.05 % ,v/v) and blocked with 200 µL/well PBS containing 5 % (w/v) Milk Marvel for 1 hour at 37°C. Rescued phage inputs from each round of panning were added to the plate in triplicate (100 µL/well) and incubated for 1 hour at 37°C then washed as before. HRP-labelled anti-M13 rat secondary antibody in PBS-T (0.05 % (v/v)) with 1 % (w/v) Milk Marvel at a 1 in 2,000 dilution was added to each well (100 µL) and incubated for 1 hour at 37°C. The plate was washed as before. One hundred µL/well of TMB substrate was added to the plate and was developed for 20 minutes with gentle agitation. The reaction was stopped using 10 % (v/v) HCl (50 µL/well) and the absorbance was read at 450 nm on the Tecan Safire2™ platereader.

2.2.3.15 Colony-pick PCR

Colonies were randomly picked from each round of panning and were analysed using a colony pick-PCR to determine if the scFv insert was incorporated into the vector. The PCR conditions were set up as follows:

Component	Volume
Sense primer CSC-F	0.5 µL
Reverse primer CSC-B	0.5 µL
Single colony	1
MyTaq™ Red Mix	25 µL
MG H ₂ O	Up to 50 µL

Stage	Temperature	Time	No. of cycles
1	94°C	2 minutes	1
2	94°C	15 seconds	
	68°C	30 seconds	30
	72°C	2 minutes	
3	72°C	10 minutes	1
	4°C	Hold	

2.2.3.16 Direct monoclonal ELISA of solubly-expressed scFv fragments

Clones were selected from panning rounds and grown overnight in individual wells in a 96-well plates containing 200 µL of SB (supplemented with 100 µg/mL carbenicillin) at 220 rpm and 37°C. The following day, this plate was sub-cultured into a 96 deep-well plate containing 1 mL SB (supplemented with 100 µg/mL carbenicillin, 1X 505 and 1 mM MgSO₄). Glycerol stocks were made of the overnight plate by the addition of 20 % (v/v) glycerol and placed at -80°C for long-term storage. The sub-cultured plates were incubated at 37°C and 220 rpm for 6 hours before the addition of 1 mM IPTG to induce expression. The plates were incubated at 30°C and 220 rpm overnight. The following day, the deep-well subcultured plates were placed at -80°C for 30 minutes until fully frozen. The samples were thawed for 1 hour at 37°C. This free-thaw procedure was repeated 3 times. The deep-well plates were centrifuged at 3,220 g (Eppendorf™ Centrifuge with fixed angle rotor (F-45-30-11)) for 20 minutes at 4°C.

A Nunc MaxiSorp™ 96-well plate was coated with 100 µL/well of 2 µg/mL mycotoxin conjugate and incubated overnight at 4°C. The plate was washed 3 times with PBS/PBST (0.05 %,v/v) and blocked with 200 µL/well PBS containing 5 % (w/v) Milk

Marvel for 1 hour at 37°C. The plate was washed as before. The lysate was added to the plate at 200 µL/well and was incubated for 1 hour at 37°C. The plate was washed as before. PBST (0.05 % ,v/v) with 1 % (w/v) Milk Marvel containing a 1 in 2,000 dilution of HRP-labelled anti-HA rat antibody was added at 100 µL/well and incubated for 1 hour at 37°C. The plate was washed as before. One hundred µL/well of TMB substrate was added and developed for 20 minutes with gentle agitation. The reaction was then stopped by the addition of 50 µL/well 10 % (v/v) HCl and the absorbance was read at 450 nm on the Tecan Safire2™ platereader.

2.2.3.17 Analysis of scFv clones by direct and competition ELISA

Fresh 'scFv-rich' lysate was prepared, as described in Section 2.2.3.16. A Nunc MaxiSorp™ 96-well plate was coated overnight at 4°C with 2 µg/mL mycotoxin conjugate. The plate was blocked with 5 % (w/v) Milk Marvel-PBS (150 mM, pH 7.4) solution (200 µL per well) for 1 hour at 37°C. For direct binding analysis, the scFv-enriched lysate from each clone was serially diluted and added (100 µL / well) to the plate before incubation at 37°C for 1 hour. For competition analysis, the lysate was incubated on the coated-plate with varying concentrations of free mycotoxin for 1 hour at 37°C (100 µL per well). The scFv ability to bind free mycotoxin was then determined by comparison of the absorbance response (A) to A₀. The A₀ represents the absorbance of the same lysate without free toxin. The captured avian scFv was detected using an anti-HA monoclonal antibody (HRP-labelled). After each stage, the ELISA plate was washed three times with PBST (150 mM, pH 7.4) and three times with PBS (150 mM, pH 7.4). Binding was detected using TMB substrate, stopped with 10 % (v/v) HCl and measured at 450 nm with the Tecan Safire2™ platereader.

2.2.3.18 Expression optimisation of scFv clones

A culture of a selected clone was grown in 10 mL SB media, containing 100 µg/mL carbenicillin, by inoculating a single colony from a stock plate and growing overnight at 37°C in an orbital shaker. Five hundred µL of this overnight culture was then inoculated into four flasks with 100 mL fresh SB media containing 100 µg/mL carbenicillin, 1X 505 and 1 mM MgSO₄. The sub-cultured clones were incubated at 37°C in an orbital incubator until an OD₆₀₀ of approximately 0.6 was reached. Two of the cultures were then induced by addition of IPTG to a final concentration of 1 mM. One was incubated at 30°C and the other at 37°C in an orbital shaker overnight. IPTG was not added to

the other two flasks and, as before, one was incubated at 30°C and the other at 37°C in an orbital shaker overnight. The overnight-expressed cultures were transferred into sterile 50 mL tubes and centrifuged at 3,220 g for 30 minutes (Eppendorf 3810R), to pellet the bacterial cells. The supernatant was discarded and the excess media removed by inversion of the 50 mL tube onto a paper towel. The cell pellet was thoroughly resuspended in 5 mL of lysis buffer and put on ice. The sample was kept on ice and sonicated at an amplitude of 40 % for 6 second pulses for 3 minutes using a microtip Vibra Cell™ sonicator. The cell extract was centrifuged (Herlme Microlitre centrifuge Z 233 M-2) at 15,000 g for 20 minutes at 4°C, in order to remove cell debris. The lysate supernatant was then passed through a 0.2 µM filter to remove any residual cell debris. The expressed clones were analysed using ELISA, SDS-PAGE and western blotting.

2.2.3.19 scFv purification using immobilised metal affinity chromatography

Purification of scFv fragments using immobilised metal affinity chromatography (IMAC) was carried out using Ni⁺-NTA agarose resin (Novagen). Two mL of Ni⁺-NTA agarose resin was added to a 20 mL column and allowed to settle for 10 minutes. The column was equilibrated using 4 mL of lysis buffer. The filtered lysate was passed through the column. The 'flow-through' was collected and passed through the column twice more. A 100 µL sample of this flow-through was kept for analysis on SDS-PAGE gel. The column was washed twice with 8 mL wash buffer to remove any loosely bound nonspecific proteins. The wash fractions were collected for SDS-PAGE analysis. The protein was eluted with 10 mL of elution buffer and twenty 0.5 mL fractions were collected in 1.5 mL tubes. The protein concentration of each fraction was measured at 280 nm using the Nanodrop™ ND-1000. The fractions containing a sufficient quantity of protein were pooled and thoroughly buffer exchanged against 20mL filter-sterilised PBS (150 mM, pH 7.4) using a 5 kDa molecular weight 'cut-off' Vivaspin™ 6 column (AGB). The buffer exchanged scFv was again quantified using the Nanodrop™ ND-1000, aliquoted and stored at -20°C.

2.2.3.20 scFv purification analysis by SDS-PAGE and western blotting

The purified scFv fragments were analysed for their purity and to verify correct molecular weight by separation on a 12.5 % (w/v) SDS-PAGE gel, using a Bio-rad® gel electrophoresis apparatus (Bio-Rad®). The separation gel was prepared, cast between

two clean glass plates and left to polymerise. After the gel had polymerised, a stacking gel was prepared, poured and wells were formed using a plastic comb, for loading of protein samples. The samples were prepared by addition of appropriate volumes of 4X loading dye and deionised water and heated (to facilitate protein denaturation) for 5 minutes at 95°C. Each protein sample was added into each well in a total volume of 20 µL. The gels were placed in an electrophoresis apparatus and submerged in 1X electrophoresis buffer. The gel was run at 120 V until the tracker dye had reached the bottom of the gel, taking approximately 1 hour. The gels were taken out and stained using Instant Blue for 1 hour until the protein band is clearly visible. Western blot analysis was also carried out to confirm the results obtained by SDS-PAGE. SDS-PAGE gels were prepared, as outlined above, loading 20 µL protein per well. Six sheets of Whatman® Gel Blot paper (Sigma) and one sheet of 3 mm Protran BA 85 Nitrocellulose membrane (Carl Stuart Ltd.) were cut to the same dimensions as the SDS-PAGE gel and soaked in ice-cold transfer buffer for 30 minutes. The SDS-PAGE gel was also soaked in transfer buffer. Three layers of the soaked blotting paper were placed between the electrodes of the Pierce™ G2 Fast Blotter. The nitrocellulose membrane was placed over the blotting paper, followed by the SDS-PAGE gel containing the resolved proteins to be transferred. The gel was sandwiched by placing three more sheets of blotting paper on top. Any air bubbles were removed by carefully rolling each of the layers. Proteins were transferred from the gel to the nitrocellulose by applying 25 V for 7 minutes. The nitrocellulose membrane was blocked with 20 mL of 5 % (w/v) Milk Marvel/PBS solution (150 mM, pH 7.4) for 1 hour at room temperature with gentle agitation. The blocked membrane was washed 3 times with PBST (150 mM, pH 7.4) and three times with PBS (150 mM, pH 7.4), followed by incubation with 20 mL of 1 % (w/v) milk/PBST solution containing a rat monoclonal anti-HA-HRP-labelled antibody (1/2,000), for 1 hour at room temperature with gentle agitation. The membrane was then washed 3 times with PBST (150 mM, pH 7.4) and three times with PBS (150 mM, pH 7.4). The membrane was developed by the addition of TMB substrate for western blotting (Sigma Aldrich, Ireland). Once sufficient colour development had occurred, the reaction was stopped by repeatedly washing with distilled water.

2.2.4 Synthesis of Pautlin-Hemisuccinate-Bovine Serum Albumin (Patulin-HS-BSA) Conjugate

In order to screen the patulin-biased avian immune library, an alternative patulin-protein conjugate to the immunogen (Patulin-HG-KLH) needed to be synthesised.

Firstly, the patulin derivative Pautlin-Hemisuccinate (Patulin-HS) was made. Patulin (2 mg) and succinyl chloride (10 μ L) were dissolved in 200 μ L of tetrahydrofuran. Then, 4-N,N-dimethylaminopyridine (10 mg) was added and the solution was stirred for 1 hour at room temperature. The solvent was removed and the product was partitioned between chloroform (1 mL x 3) and 1M HCl (300 μ L). The organic layer was dried and evaporated to leave the Pautlin-HS product.

After this, the Patulin-HS derivative was conjugated to BSA. Patulin-HS (1 mg), ethanol (20 % v/v), EDC (10 mg) and BSA (1 mg) were stirred at room temperature for 30 minutes. EDC (30 mg) was added and the solution was incubated at room temperature overnight. The following day, the solution was buffer exchanged with PBS (150 mM, pH 7.4).

2.2.5 Ethical authorisation for animal experimentation

Ethical approval for the use of chickens in antibody generation experiments is covered by licence number B100/2705 issued by the Department of Health and Children allowing the injection of avian, murine or lapine hosts for the purpose of generating antibodies.

2.2.6 Safety precautions and protocols for handling mycotoxin material and waste

All mycotoxins used are highly toxic and hazardous substances. Therefore, for all experiments involving these compounds, the correct protocols for their safe storage, handling and disposal were carried out, in accordance with approval from the DCU Safety Committee and the Environmental Protection Agency (EPA). All cell culture work was carried out in a designated toxin laminar flow hood. All ELISA experiments were also carried out in a designated toxin fume hood. Toxin-containing liquid waste, including coating, blocking, washing, assay and cell culture media solutions were decanted into designated glassware containing 10 % (v/v) sodium hypochlorite.

**Chapter 3: Effect of individual
mycotoxin exposure on
murine macrophage viability
and cytokine production**

3.1 Introduction

The work described in this chapter is focused on how naturally-occurring fungal toxins may affect the functions of macrophages, specifically secretion of cytokines by these cells. The individual immunomodulatory effects of the mycotoxins; patulin, DON, ZEN and T-2 toxin, were also analysed on the basis of their ability to modulate immune function in response to LPS, a bacterial cell wall component. This work lays the foundations of gaining a greater understanding of how mycotoxins exert their toxic effects to suppress the immune system in humans and animals.

The J774A.1 murine macrophage cell line was utilised in the course of this research. The J774A.1 cell line originated from cultured murine lymphoblastoid cells (Snyderman *et al.*, 1977). The behaviour of the J774A.1 murine model mimics the physiological behaviour of a macrophage *in vivo*, making it an ideal candidate to study the effects of these toxins *in vitro*.

3.1.1 Mycotoxins as immunomodulatory agents

Mycotoxins, as secondary metabolites of fungi that grow on various food stuffs and feeds, have the potential to elicit a wide variety of toxicological effects, including immune-suppression and immune-stimulation. Exposure to sub-lethal doses of many mycotoxins has the potential to either stimulate or suppress immune functions, such as lymphocyte proliferation, cell-mediated immunity and humoral immunity, depending on concentration and exposure time (Edite Bezerra da Rocha *et al.*, 2014).

Production of cytokines by monocytes and macrophages in response to inflammatory stimuli and microbial products is well established (Bendtzen *et al.*, 1988). Several studies have shown that aflatoxins can affect macrophages, both *in vitro* and *in vivo*. Numerous animal studies have demonstrated that aflatoxins have immunosuppressive activity. Poultry (chickens and turkeys), pigs and lambs in particular, are susceptible to aflatoxin-induced immunosuppression (Devegowda and Murthy, 2005). Furthermore, cell-mediated immunity is affected by aflatoxin exposure. Murine macrophages exposed to aflatoxins both *in vivo* and *in vitro* have exhibited decreased cytokine secretion. Other macrophage functions, such as release of reactive intermediates and phagocytosis are decreased in macrophages exposed to AFB1 (Liu *et al.*, 2002). Although the immunomodulatory effects of the aflatoxins have been demonstrated

previously, the exact mechanisms by which these compounds exert their immunomodulatory effects is still unknown.

Mycotoxins can induce cellular depletion in lymphoid organs, cause alterations in T-cell and B-cell function, suppress antibody responses, suppress NK cell activity, decrease delayed-type hypersensitivity responses, and increase susceptibility to infectious disease. T-2 toxin was implicated as a developmental immunotoxicant, which targets fetal lymphocyte progenitors (Holladay *et al.*, 2002). The dose, the route of administration, and the species type, are all critical factors in the immunotoxicity of mycotoxins (Al-Anati and Petzinger, 2006). The effects of mycotoxins on the human immune system have not yet been fully characterised but concerns have arisen in areas, such as West Africa, where widespread aflatoxin contamination has resulted in 99% of children in some areas possessing aflatoxin–albumin adducts in their blood (Gong *et al.*, 2003).

The effect of the tricothecene group on immune function has shown that the mechanism of impairment is related to inhibition of protein synthesis. Interestingly, high doses of tricothecenes induce lymphocyte apoptosis along with immune suppression. In contrast, low dose tricothecene promotes expression of a diverse array of cytokines including IL-1, IL-2, IL-5, and IL-6. Tricothecenes also activate mitogen-activated protein kinases (MAPK's) *in vivo* and *in vitro*, via the ribotoxic stress response (Zhou *et al.*, 2003; Pestka *et al.*, 2004). Pestka and Zhou (2006) showed that pre-exposure with LPS sensitised murine RAW264.7 macrophages and peritoneal murine macrophages to the pro-inflammatory effects of DON. Prolonged consumption of DON by mice was shown to induce elevation of IgA and IgA immune complex formation (Pestka, 2003).

ZEN has been shown to be immunotoxic (Luongo *et al.*, 2008), but its role in inflammation is not yet fully understood. ZEN has been shown to be both a suppressor and inducer of the production of inflammatory cytokines (Salah-Abbès *et al.*, 2008; Marin *et al.*, 2011). Several alterations of immunological parameters were found associated with ZEN concentrations in mice (Abbès *et al.*, 2013) and *in vitro* (Murata *et al.*, 2003). Jia *et al.* (2014) examined the toxic effects of ZEN on oxidative stress, inflammatory cytokines, biochemical and pathological changes in the kidney of pregnant rats to explore the possible mechanism in ZEN induced kidney damage. They

found that ZEN caused kidney damage to pregnant rats and the TLR4-mediated inflammatory reactions signal pathway was one of the mechanisms of ZEN mediated toxicity in kidney.

3.1.2 Chapter aims

The purpose of this chapter was to study the effect of individual mycotoxins on the immune response to infection, using the J774A.1 murine macrophage cell line as a model for host defence. This data provides a preliminary insight into the potential mechanisms by which, individually, mycotoxins modulate the host immune response to exert immunotoxicity and immunomodulatory activity.

Firstly, analysis of the cytotoxic effect of patulin, DON, ZEN and T-2 toxin on J774A.1 murine macrophages was examined to determine at what concentrations, if any, these toxins affect cell viability. Using the information gathered from this, a range of concentrations that are not cytotoxic to the cells could be chosen and used to examine the production of a number of pro- and anti- inflammatory cytokines, after mycotoxin exposure. A range of concentrations for each individual toxin was used to determine the dosage-range effect of these mycotoxins on the secretion of key cytokines in response to bacterial infection.

3.2 Results

3.2.1 Analysis of mycotoxin exposure on J774A.1 murine macrophage viability using MTS assay

3.2.1.1 J774A.1 macrophage viability after exposure to patulin, zearalenone, deoxynivalenol and T-2 toxin with LPS challenge

The CellTiter 96® Aqueous One Solution (Pierce, UK) is a colorimetric method for determining the number of viable cells in a sample. It contains an MTS tetrazolium compound (Owen's reagent) which is bio-reduced by cells into a soluble coloured formazan product. The quantity of formazan product is measured at an absorbance reading of 450 nm and is directly proportional to the number of living cells in the culture medium. The growth rate of the J774A.1 murine macrophage cell line, in the presence of patulin, DON, ZEN and T-2 toxin in concentrations ranging from 10 to 100,000 pg/mL was assessed using this MTS assay (Section 3.2.2.2). A graph was plotted, which compared the percentage viability of the control groups (cells not exposed to toxins), with that of the toxin-treated cells. The inflammatory processes in the macrophage are activated by the endotoxin, LPS. Therefore, LPS was included in the MTS analysis, to analyse the effect of toxin exposure on macrophage viability. LPS is a potent stimulator of the 'toll-like' receptor 4 (TLR4) pathway in the immune response to infection,. Each treatment was carried out in triplicate and mean values \pm 3SEM were calculated. A one-way analysis of variance (ANOVA) was performed. Post-hoc analysis was performed using Dunnett's two-tailed test to evaluate the differences between treatment and control groups.

The results indicate that patulin and DON have no cytotoxic effect on J774A.1 macrophages at any of the chosen concentrations (Figures 3.1 and 3.2). Patulin, however, appears to increase the proliferation ($P < 0.05$) of the cells at the highest concentration (100,000 pg/mL). For ZEN, there is a significant ($P < 0.05$) decrease in the percentage viability at a concentration of 100,000 pg/mL, which is cytotoxic without LPS stimulation (Figure 3.3). T-2 toxin (Figure 3.4) appears to have an effect on cell viability across all concentrations, however, a significant cytotoxic effect only becomes apparent at 100,000 pg/mL ($P < 0.01$) for unstimulated cells and at 10,000 pg/mL ($P < 0.05$) and 100,000 pg/mL ($P < 0.01$) for LPS-stimulated cells. All experiments show no effect of the vehicle control on cell viability with and without LPS stimulation.

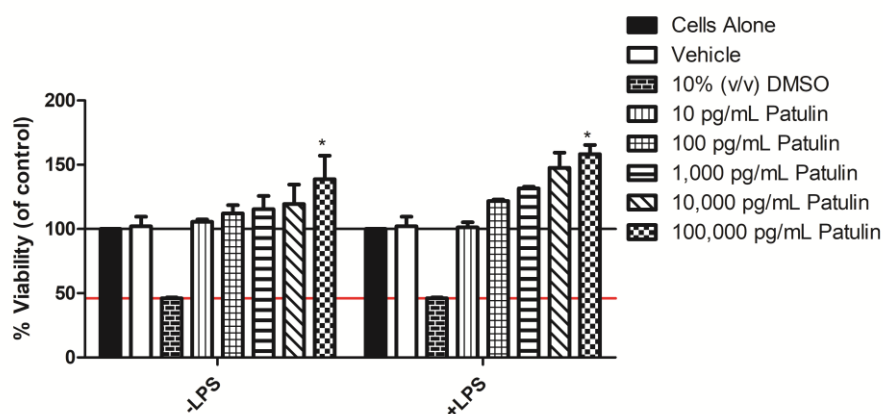


Figure 3.1: MTS assay to analyse the effect of **patulin** on the J774A.1 macrophage cell line. J774A.1 cells were treated for 24 hours with patulin, ranging in concentration from 10 to 100,000 pg/mL, with and without LPS (100 ng/mL) stimulation. DMSO (10% v/v) was included as a positive control of cytotoxicity. Results indicate a mean % viability (of cells alone control) from three independent experiments and error bars represent mean \pm 3SEM (standard error of mean) (n=3). Significance: P < 0.05*; P < 0.01**; P < 0.001*** as illustrated, all relative to cells not exposed to toxin.

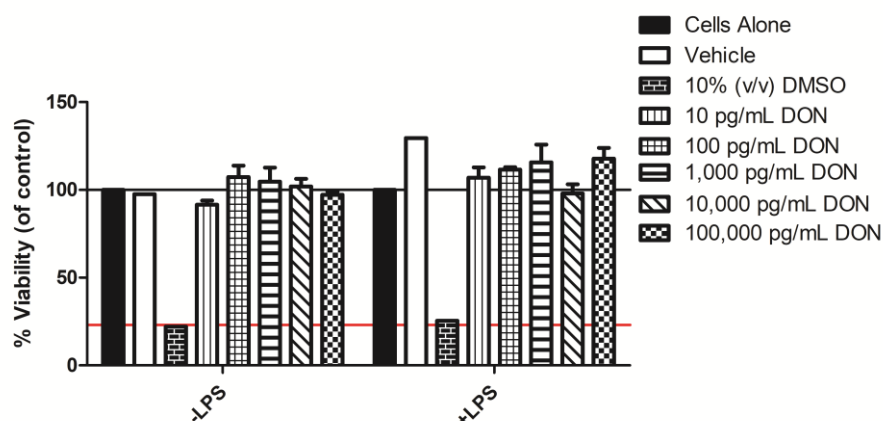


Figure 3.2: MTS assay to analyse the effect of **DON** on the J774A.1 macrophage cell line. J774A.1 cells were treated for 24 hours with DON, ranging in concentration from 10 to 100,000 pg/mL, with and without LPS (100 ng/mL) stimulation. DMSO (10% v/v) was included as a positive control of cytotoxicity. Results indicate a mean % viability (of cells alone control) from three independent experiments and error bars represent mean \pm 3SEM (standard error of mean) (n=3). Significance: P < 0.05*; P < 0.01**; P < 0.001*** as illustrated, all relative to cells not exposed to toxin.

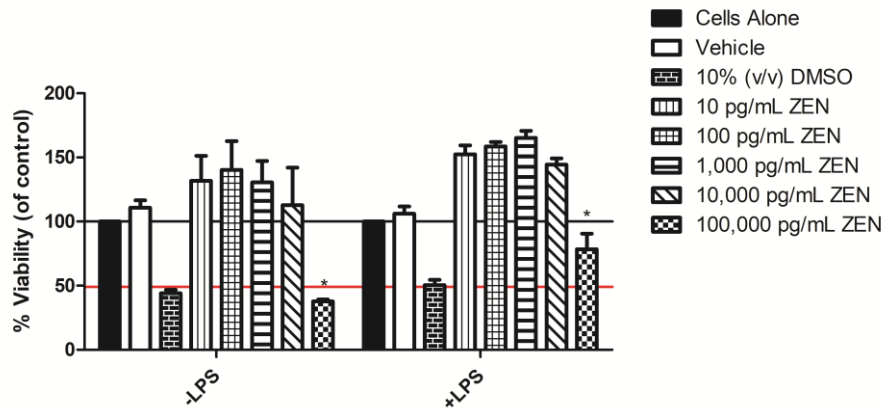


Figure 3.3: MTS assay to analyse the effect of **ZEN** on the J774A.1 macrophage cell line. J774A.1 cells were treated for 24 hours with ZEN, ranging in concentration from 10 to 100,000 pg/mL, with and without LPS (100 ng/mL) stimulation. DMSO (10% v/v) was included as a positive control of cytotoxicity. Results indicate a mean % viability (of cells alone control) from three independent experiments and error bars represent mean \pm 3SEM (standard error of mean) (n=3). Significance: P < 0.05*; P < 0.01**; P < 0.001*** as illustrated, all relative to cells not exposed to toxin.

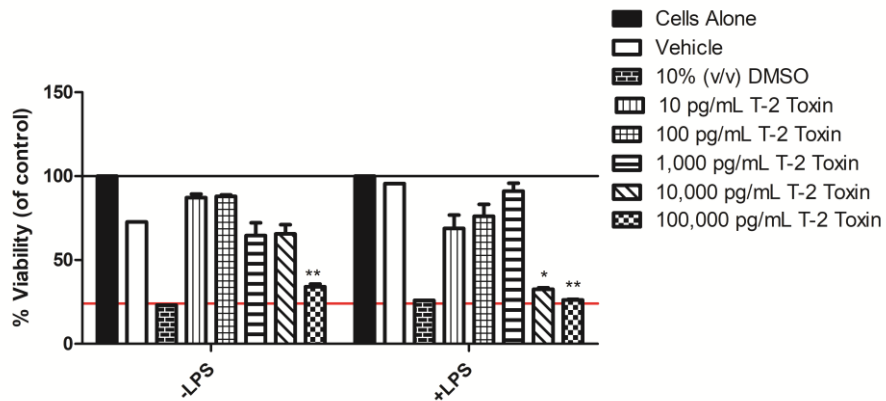


Figure 3.4: MTS assay to analyse the effect of **T-2 toxin** on the J774A.1 macrophage cell line. J774A.1 cells were treated for 24 hours with T-2 toxin, ranging in concentration from 10 to 100,000 pg/mL, with and without LPS (100 ng/mL) stimulation. DMSO (10% v/v) was included as a positive control of cytotoxicity. Results indicate a mean % viability (of cells alone control) from three independent experiments and error bars represent mean \pm 3SEM (standard error of mean) (n=3). Significance: P < 0.05*; P < 0.01**; P < 0.001*** as illustrated, all relative to the cells not exposed to toxin.

3.2.2 Analysis of mycotoxin exposure on J774A.1 murine macrophage cytokine production

3.2.2.1 J774A.1 macrophage cytokine production after exposure to patulin, zearalenone, deoxynivalenol and T-2 toxin with LPS challenge

DuoSet ELISA kits (R&D systems) were used to quantify the levels of cytokines (IL-6, IL-10, IL-27, IL-12p40, IL-1 β and TNF- α) in the supernatants of J774A.1 macrophage cells treated with patulin, DON, ZEN and T-2 toxin in increasing concentrations from 0.001 to 100 pg/mL (concentrations below legislative limits that do not effect cell viability) for 24 hours with and without LPS (100 ng/mL) stimulation (Section 2.2.2.3). Samples were carried out in triplicate and mean values \pm SEM was calculated. A one-way analysis of variance (ANOVA) was performed. Post-hoc analysis was performed using Dunnett's two-tailed test to evaluate the differences between treatment and control groups

The results for patulin (Figure 3.5) (Table 3.1) show that there is a significant ($P < 0.001$) increase in the production of IL-6 at 10 pg/mL patulin without LPS stimulation, however significant suppression is observed at 0.1 pg/mL ($P < 0.01$) and 1 pg/mL ($P < 0.05$). The production of IL-10 is increased significantly at 1 pg/mL ($P < 0.01$), 10 pg/mL ($P < 0.001$) and 100 pg/mL ($P < 0.05$) without LPS stimulation, and at 0.1 – 10 pg/mL ($P < 0.01$) following LPS treatment. IL-27 levels are up significantly at 1 pg/mL (-LPS) ($P < 0.01$) and 0.001 pg/mL (+LPS) ($P < 0.05$), however the vehicle control also shows a significant increase following LPS stimulation ($P < 0.05$). An increase in IL-12p40 is observed at 10 pg/mL ($P < 0.001$) and 100 pg/mL ($P < 0.01$) without LPS stimulation and also 10 pg/mL and 100 pg/mL ($P < 0.001$) with LPS stimulation. IL-1 β levels were increased significantly at 10 pg/mL patulin ($P < 0.001$) both with and without LPS stimulation. TNF- α was increased at 10 pg/mL patulin (-LPS) ($P < 0.001$) and (+LPS) ($P < 0.05$), however its levels were decreased at 0.001 pg/mL and 0.1 pg/mL ($P < 0.05$).

DON (Figure 3.6) (Table 3.2) causes a significant increase in IL-6 production at 1 pg/mL ($P < 0.01$) and at 10 pg/mL ($P < 0.001$) without LPS, and at 10 pg/mL ($P < 0.05$) with LPS. Levels of IL-10 are increased significantly without LPS stimulation at 0.1 pg/mL ($P < 0.01$), 1 pg/mL ($P < 0.001$), 10 pg/mL ($P < 0.001$) and 100 pg/mL ($P < 0.05$) but only increased for 10 pg/mL ($P < 0.001$) with LPS stimulation. IL-27, IL-12 p40 and IL-1 β are all significantly increased ($P < 0.001$) at 10 pg/mL both + and - LPS, while IL-12p40 is

decreased ($P < 0.05$) by 0.001 pg/mL DON following LPS stimulation. TNF- α is significantly increased at 0.1 pg/mL ($P < 0.05$), 1 pg/mL ($P < 0.01$) and 10 pg/mL ($P < 0.001$) without LPS, but only up for 10 pg/mL ($P < 0.001$) with LPS.

The results for ZEN (Figure 3.7) (Table 3.3) show that IL-6 is significantly increased ($P < 0.001$) by 0.1 – 100 pg/mL ZEN with no LPS stimulation. However, no significant changes are observed for IL-6 following LPS treatment. IL-10 was significantly increased by 10 pg/mL ($P < 0.001$) before LPS treatment and by 0.01 pg/mL ($P < 0.05$), 0.1 pg/mL ($P < 0.01$) and 1 pg/mL ($P < 0.01$) after LPS treatment. There is a significant increase in the levels of IL-12p40 at 1 pg/mL ($P < 0.001$) and 10 pg/mL ($P < 0.001$) (-LPS) and 10 pg/mL ($P < 0.001$) (-LPS). 10 pg/mL ZEN also caused a significant increase in the production IL-1 β -LPS ($P < 0.01$) +LPS ($P < 0.001$). TNF- α was significantly increased 0.1 pg/mL ($P < 0.05$), 1 pg/mL ($P < 0.05$) and 10 pg/mL ($P < 0.001$) without LPS stimulation and 1 pg/mL ($P < 0.05$) and 10 pg/mL ($P < 0.001$) with LPS treatment.

T-2 toxin (Figure 3.8) (Table 3.4) exposure resulted in a significant increase in IL-6 production at 0.1 pg/mL ($P < 0.05$) 1 pg/mL ($P < 0.01$) and 10 pg/mL ($P < 0.001$) (-LPS). However, significant suppression of IL-6 was observed at 0.001 pg/mL ($P < 0.001$), 0.01 pg/mL ($P < 0.001$), 0.1 pg/mL ($P < 0.01$), 1 pg/mL ($P < 0.05$) and 100 pg/mL ($P < 0.01$) following LPS stimulation. IL-10 levels were increased ($P < 0.001$) by 10 pg/mL T-2 without LPS but significant decrease was seen by 0.001 pg/mL ($P < 0.05$), 0.01 pg/mL ($P < 0.001$) and 100 pg/mL ($P < 0.05$). Following LPS stimulation an increase ($P < 0.01$) of IL-10 was only seen at 10 pg/mL T-2 toxin. IL-27 was increased by 10 pg/mL with ($P < 0.001$) and without ($P < 0.01$) LPS stimulation, however it was significantly suppressed by 0.001 pg/mL ($P < 0.01$) and 100 pg/mL ($P < 0.001$) after LPS treatment. IL-12p40 levels were increased at 10 pg/mL ($P < 0.01$) (-LPS), and 1 pg/mL ($P < 0.05$) and 10 pg/mL ($P < 0.001$) (+LPS). 10 pg/mL of T-2 toxin also caused a significant increase in the production of IL-1 β both +LPS ($P < 0.05$) and -LPS ($P < 0.001$). TNF- α production was significantly increased by 1 pg/mL ($P < 0.05$) and 10 pg/mL ($P < 0.001$) both with and without LPS stimulation. However, LPS stimulated cells also showed a significant decrease in TNF- α at 0.01 pg/mL ($P < 0.05$) and 1 pg/mL ($P < 0.05$) T-2 toxin.

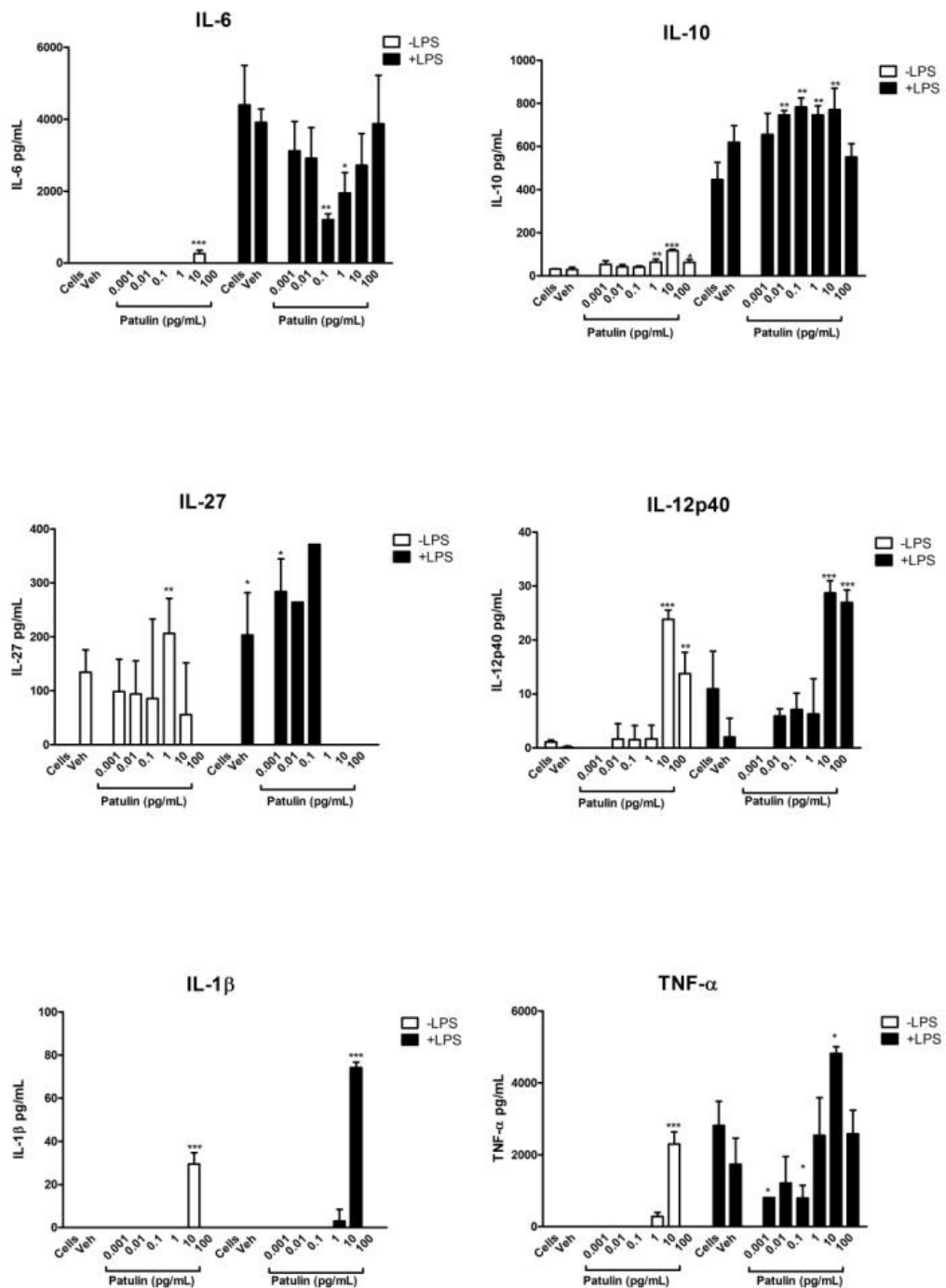


Figure 3.5: Production of IL-6, IL-10, IL-27, IL-12p40, IL-1 β and TNF- α in the supernatants of J774A.1 murine macrophage cells, cultured for 24 hours in the presence of **patulin** ranging in concentration from 0.001 to 100 pg/mL, with and without LPS (100 ng/mL) stimulation. The toxin treatment alone is represented by the white bars (\square) and the toxin treatment with LPS challenge is represented by the black bars (\blacksquare). Data was expressed as the mean for each experiment (n=3), with error bars indicating \pm 3SEM. Significance: P < 0.05*; P < 0.01**; P < 0.001*** as illustrated, all relative to the cells not exposed to toxin.

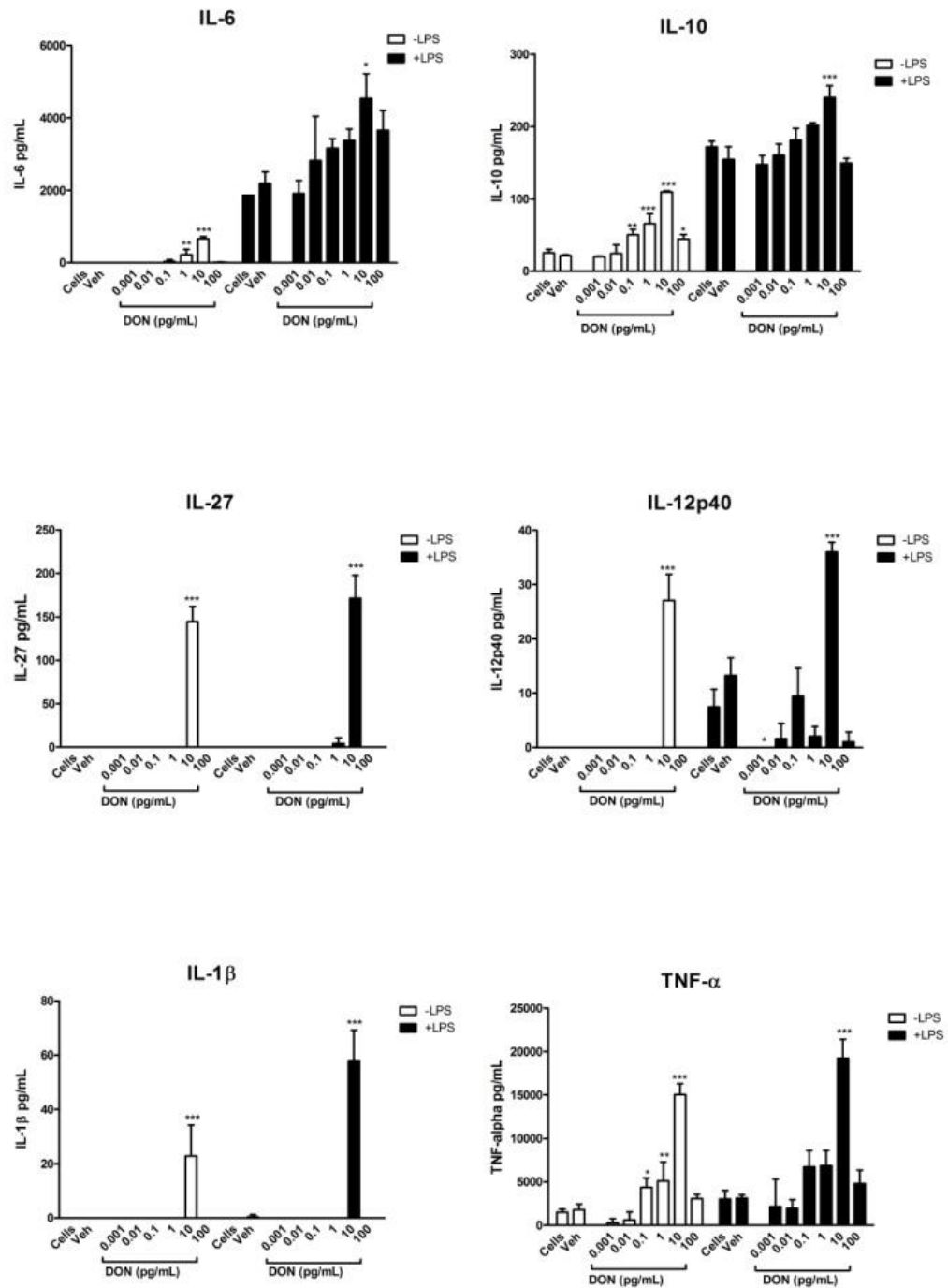


Figure 3.6: Production of IL-6, IL-10, IL-27, IL-12p40, IL-1β and TNF-α in the supernatants of J774A.1 murine macrophage cells, cultured for 24 hours in the presence of **DON** ranging in concentration from 0.001 to 100 pg/mL, with and without LPS (100 ng/mL) stimulation. The toxin treatment alone is represented by the white bars (□) and the toxin treatment with LPS challenge is represented by the black bars (■). Data was expressed as the mean for each experiment (n=3), with error bars indicating ± 3SEM. Significance: P < 0.05*; P < 0.01**; P < 0.001*** as illustrated, all relative to the cells not exposed to toxin.

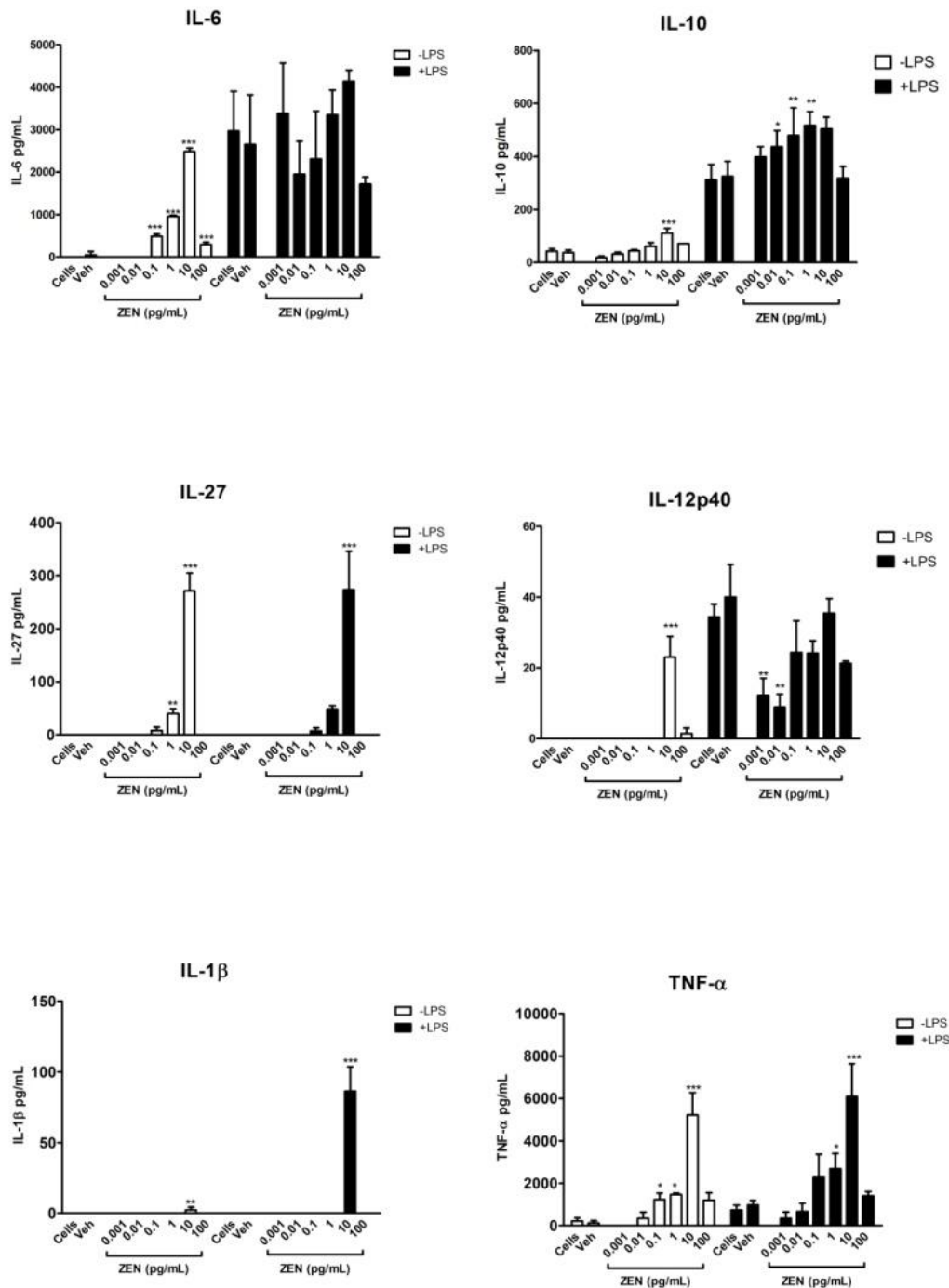


Figure 3.7: Production of IL-6, IL-10, IL-27, IL-12p40, IL-1β and TNF-α in the supernatants of J774A.1 murine macrophage cells, cultured for 24 hours in the presence of ZEN ranging in concentration from 0.001 to 100 pg/mL, with and without LPS (100 ng/mL) stimulation. The toxin treatment alone is represented by the white bars (□) and the toxin treatment with LPS challenge is represented by the black bars (■). Data was expressed as the mean for each experiment (n=3), with error bars indicating ± 3SEM. Significance: P < 0.05*; P < 0.01**; P < 0.001*** as illustrated, all relative to the cells not exposed to toxin.

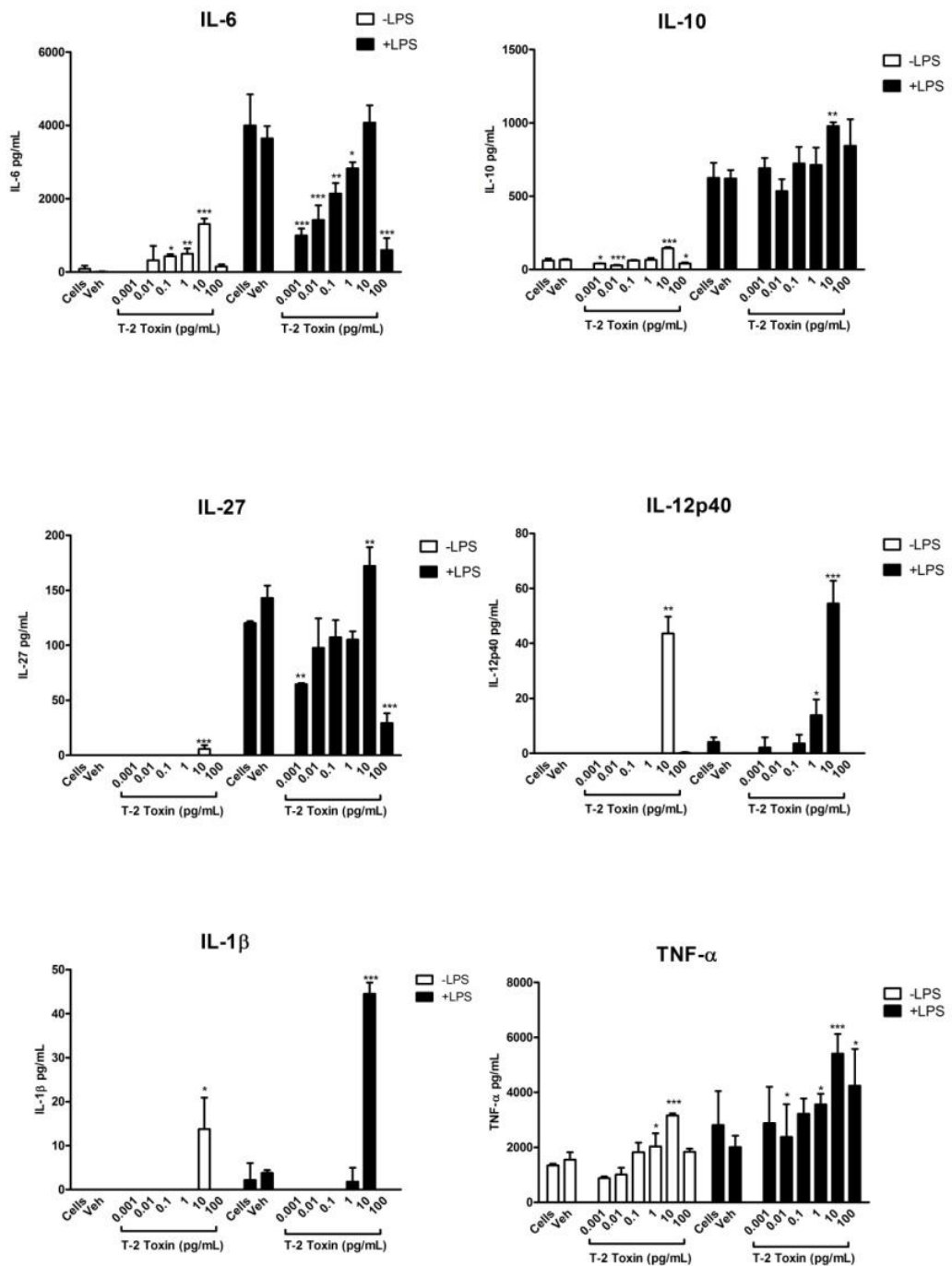


Figure 3.8: Production of IL-6, IL-10, IL-27, IL-12p40, IL-1β and TNF-α in the supernatants of J774A.1 murine macrophage cells, cultured for 24 hours in the presence of **T-2 toxin** ranging in concentration from 0.001 to 100 pg/mL, with and without LPS (100 ng/mL) stimulation. The toxin treatment alone is represented by the white bars (□) and the toxin treatment with LPS challenge is represented by the black bars (■). Data was expressed as the mean for each experiment (n=3), with error bars indicating ± 3SEM. Significance: P < 0.05*; P < 0.01**; P < 0.001*** as illustrated, all relative to the cells not exposed to toxin.

Table 3.1: The effect of increasing concentrations of **patulin** (0.001 – 100 pg/mL) on the production levels of cytokines from J774A.1 macrophages with and without LPS (100 ng/mL) treatment. Significance represented by: no change –, increase P < 0.05↑; P < 0.01↑↑; P < 0.001↑↑↑, decrease P < 0.05↓; P < 0.01↓↓; P < 0.001↓↓↓, compared to control cells.

Patulin (pg/mL)	IL-6	IL-10	IL-27	IL-12p40	IL-1β	TNF-α
0.001	–	–	–	–	–	–
0.01	–	–	–	–	–	–
0.1	–	–	–	–	–	–
1	–	↑↑	↑↑	–	–	–
10	↑↑↑	↑↑↑	–	↑↑↑	↑↑↑	↑↑↑
100	–	↑	–	↑↑	–	–
Patulin (pg/mL) + LPS (100 ng/mL)						
0.001	–	–	↑	–	–	↓
0.01	–	↑↑	–	–	–	–
0.1	↓↓↓	↑↑	–	–	–	↓
1	↓	↑↑	–	–	–	–
10	–	↑↑	–	↑↑↑	↑↑↑	↑
100	–	–	–	↑↑↑	–	–

Table 3.2: The effect of increasing concentrations of **DON** (0.001 – 100 pg/mL) on the production levels of cytokine from J774A.1 macrophages with and without LPS (100 ng/mL) treatment. Significance represented by: no change –, increase P < 0.05↑; P < 0.01↑↑; P < 0.001↑↑↑, decrease P < 0.05↓; P < 0.01↓↓; P < 0.001↓↓↓, compared to control cells.

DON (pg/mL)	IL-6	IL-10	IL-27	IL-12p40	IL-1β	TNF-α
0.001	–	–	–	–	–	–
0.01	–	–	–	–	–	–
0.1	–	↑↑	–	–	–	↑
1	↑↑	↑↑↑	–	–	–	↑↑
10	↑↑↑	↑↑↑	↑↑↑	↑↑↑	↑↑↑	↑↑↑
100	–	↑	–	–	–	–

DON (pg/mL) + LPS (100 ng/mL)	IL-6	IL-10	IL-27	IL-12p40	IL-1β	TNF-α
0.001	–	–	–	↓	–	–
0.01	–	–	–	–	–	–
0.1	–	–	–	–	–	–
1	–	–	–	–	–	–
10	↑	↑↑↑	↑↑↑	↑↑↑	↑↑↑	↑↑↑
100	–	–	–	–	–	–

Table 3.3: The effect of increasing concentrations of **ZEN** (0.001 – 100 pg/mL) on the production levels of cytokines from J774A.1 macrophages with and without LPS (100 ng/mL) treatment. Significance represented by: no change –, increase P < 0.05↑; P < 0.01↑↑; P < 0.001↑↑↑, decrease P < 0.05↓; P < 0.01↓↓; P < 0.001↓↓↓, compared to control cells.

ZEN (pg/mL)	IL-6	IL-10	IL-27	IL-12p40	IL-1β	TNF-α
0.001	–	–	–	–	–	–
0.01	–	–	–	–	–	–
0.1	↑↑↑	–	–	–	–	↑
1	↑↑↑	–	↑↑	–	–	↑
10	↑↑↑	↑↑↑	↑↑↑	↑↑↑	↑↑↑	↑↑↑
100	↑↑↑	–	–	–	–	–
ZEN (pg/mL) + LPS (100 ng/mL)						
0.001	–	–	–	–	–	–
0.01	–	↑	–	↓↓	–	–
0.1	–	↑↑	–	↓↓	–	–
1	–	↑↑	–	–	–	↑
10	–	–	↑↑↑	–	↑↑↑	↑↑↑
100	–	–	–	–	–	–

Table 3.4: The effect of increasing concentrations of **T-2 toxin** (0.001 – 100 pg/mL) on the production levels of cytokines from J774A.1 macrophages with and without LPS (100 ng/mL) treatment. Significance represented by: no change –, increase $P < 0.05$ ↑; $P < 0.01$ ↑↑; $P < 0.001$ ↑↑↑, decrease $P < 0.05$ ↓; $P < 0.01$ ↓↓; $P < 0.001$ ↓↓↓, compared to control cells.

T-2 toxin (pg/mL)	IL-6	IL-10	IL-27	IL-12p40	IL-1β	TNF-α
0.001	–	↓	–	–	–	–
0.01	–	↓↓↓	–	–	–	–
0.1	↑	–	–	–	–	–
1	↑↑	–	–	–	–	↑
10	↑↑↑	↑↑↑	↑↑↑	↑↑	↑↑	↑↑↑
100	–	↓	–	–	–	–
T-2 toxin (pg/mL) + LPS (100 ng/mL)						
0.001	↓↓↓	–	↓↓	–	–	↓
0.01	↓↓↓	–	–	–	–	↓
0.1	↓↓	–	–	–	–	–
1	↓	–	–	↑	–	↑
10	–	↑↑	↑↑	↑↑↑	↑↑↑	↑↑↑↑
100	↓↓↓	–	↓↓↓	–	–	↑

3.3 Discussion

Under normal healthy conditions, the immune system defends the host against pathogenic infections. However, certain environmental factors, including toxins, can alter the activation and function of the immune response, leading to autoimmunity, hypersensitivity or immunosuppression. A functioning immune system is essential for survival as it defends the body against infection from foreign agents. Currently our understanding of the biological processes underlying immune system dysfunction in the context of mycotoxins is incomplete.

Immunotoxicology is the study of undesired effects resulting from the interactions of xenobiotics, including toxins, with the immune system. There is evidence that certain xenobiotics cause immune suppression. It is clear that there are a vast number of cellular and molecular targets for xenobiotics that act as immunosuppressants (Grinyó *et al.*, 2012). Xenobiotics, such as toxins, may interfere with receptor-ligand binding at the cell surface or with the cascade of signalling events that leads to transcription of genes responsible for generating and regulating the appropriate immune responses.

One of the major adverse consequences of immunosuppression is that host resistance against microbial pathogens is impaired, leading to infection. Moreover, immunostimulation and immunosuppression can occur with the same xenobiotic depending on the exposure conditions, including dosage and time. Such experimental observations have given rise to the term 'immunomodulation' which accounts for this dual effect. It is important to stress that any deregulation of immune cell homeostasis can result in serious consequences for immune functions, increasing the susceptibility to infections and cancer, as well as favouring the development of autoimmune diseases. Therefore, any significant change in the functionality of immune cells must be considered as a hazard (Marin *et al.*, 2013).

The effect of various mycotoxins on the immune system has been widely investigated (Ubagai *et al.*, 2008; Alassane-Kpembé *et al.*, 2013; Clarke *et al.*, 2014; Solhaug *et al.*, 2015) but there is a lack of understanding of the exact mechanisms behind the interactions involved. The effects of individual toxins can vary depending on concentration, time and other environmental factors. Significantly, little is known about the effect of administering toxins alone and in combinations at low concentrations.

The aim of this research is to characterise the individual affects of patulin, DON, ZEN and T-2 toxin in order to improve our understanding of the individual mechanisms of mycotoxin immunomodulation.

Firstly, the effect of each of these mycotoxins on the viability of J774A.1 murine macrophages was examined. An understanding of this is crucial for two main reasons; primarily to assess if these toxins are cytotoxic to macrophage cells at concentrations below the legislative limits, and secondly to determine which concentrations to use for further investigations in order to prevent results being affected by cytotoxicity.

The result of this investigation showed that patulin and DON did not display cytotoxic effects on the macrophage cells at any of the chosen concentrations; this is not unexpected given that the highest concentration (100,000 pg/mL) is below the legislative limits for these toxins which are in the region of 10 – 50 µg/kg for patulin and 500 – 1,750 µg/kg for DON. ZEN, however, begins to have an effect on cell viability at 100,000 pg/mL and even appears to be cytotoxic without LPS stimulation at this concentration. This is potentially worrying when the legislative limit allows up to 200 µg/kg of ZEN in some foodstuffs. Most interestingly, T-2 toxin appears to affect the viability of the J774A.1 cells at all concentrations, although it only becomes significantly cytotoxic at 10,000 pg/mL, but again this is concerning when levels of up to 1,000 µg/kg T-2 toxin are allowed in some foods (CAST, 2003).

The implication of this result is that for further investigations concentrations that have been shown not to cause cytotoxicity must be used to avoid the results being affected due to cell death. This means that for experiments on cytokine secretion a maximum of 100 pg/mL of each toxin will be used. Furthermore, this investigation highlights potential issues with legislative limits of mycotoxins. Although it is difficult to relate consumption levels to bioavailable toxin at a cellular level, it is clear that even at these low levels toxins can affect cell viability significantly. This is the first report of the cytotoxic effects of patulin, DON, ZEN and T-2 toxin on J774A.1 murine macrophages. Other studies such as Clarke *et al.* (2014) examined the cytotoxicity of AFB1, FB1 and OTA on Caco-2, MDBK and RAW264.7 cell lines. They also found these toxins to be cytotoxic, but at much higher concentrations to that used in this study. Hymery *et al.* (2014) found that the mycotoxin cyclopiazonic acid was toxic to the human cell lines; CD34+, monocytes, THP-1 and Caco-2.

From the cytokine production study, it was clear mycotoxins have varying effects on the secretion of IL-6, IL-10, IL-27, IL-12p40, IL-1 β and TNF- α , which was dependent on toxin dosage and exposure to LPS stimulation. These results demonstrate that different mycotoxins can have similar or vastly differing effects on macrophage function and cytokine secretion.

For example, across each toxin the 10 pg/mL concentration appears to cause an increase in the pro-inflammatory response with large increases in the secretion of IL-27, IL-12p40, IL-1 β and TNF α . DON also induced an overall pro-inflammatory response at higher concentrations. However, some of the toxins exhibited suppression of pro-inflammatory cytokines at lower concentrations. Patulin and T-2 toxin both caused a significant decrease in the production of the key pro-inflammatory cytokines IL-6 and TNF- α at low concentrations following LPS stimulation. DON and ZEN exposure resulted in a decrease in the levels of IL-12p40 after LPS stimulation. These results demonstrate a dose-dependent effect on the modulation of cytokine secretion.

These results are significant due to importance of these cytokines in homeostasis and clearance of infections pathogens. IL-27 is an IL-12-related cytokine that can promote both anti- and pro-inflammatory immune responses. IL-27 induces mRNA and surface expression of class II MHC in macrophages. In addition, IL-27 enhances expression of co-stimulatory molecules CD80 and CD86. The pro-inflammatory role of IL-27 is mediated in part through increased expression of key molecules involved in the class II and class I MHC pathways (Feng *et al.*, 2008). Alterations to IL-27 levels, as demonstrated by DON, ZEN and T-2 toxin, can interfere with this response and reduce ability to clear infection. The actions of the cytokine, IL-6, are highly pleiotropic. In adults IL-6 functions as a major mediator of inflammatory responses as well as inducing the synthesis of acute phase proteins by the liver following infection or injury. Based on *in vitro* and *in vivo* studies IL-6 also has important functions in regulating the development of multiple lineages of hemopoietic cells. It may also be an inflammatory mediator in the central nervous system. IL-6 dictates the transition from acute to chronic inflammation by changing the nature of leucocyte infiltrate (from polymorphonuclear neutrophils to monocyte/macrophages). In addition, IL-6 exerts stimulatory effects on T- and B-cells, thus favouring chronic inflammatory response (Gabay, 2006). Deregulation of this cytokine, seen with patulin and T-2 toxin, may lead

to an inability to activate an inflammatory response needed for infection clearance. IL-12 is a key cytokine that links innate and adaptive immunity as it targets DCs, T-cells and NK cells. IL-12 has pleiotropic functions, with a fundamental function to differentiate naïve T-cells into a Th1 phenotype. In addition, it has an essential role in maintaining the balance between Th1 and Th2 responses *in vivo* (Brahmachari and Pahan, 2008; Caprioli *et al.*, 2011). IL-12 has been linked to autoimmune diseases such as RA, IBD and MS. Expression of IL-12p40 is enhanced in inflamed colonic tissue from patients with IBD (Ng, *et al.* 2010). IL-12 is also a potent inducer of IFN- γ , which directs the induction of classically activated macrophage by inactivating feedback inhibitory mechanisms, such as those mediated by IL-10 (Trinchieri, 2003). IL-12p40 can promote the migration of bacterially-stimulated dendritic cells. It is associated with several pathogenic inflammatory responses such as silicosis, graft rejection and asthma but it is also protective in a mycobacterial model. Alterations to production levels of this cytokine can affect both protective and pathogenic immune responses (Cooper and Khader, 2006). Furthermore, IL-12 causes the up-regulation of MHCII, CD80 and CD86 expression on APC (Bettelli and Kuchroo, 2005). IL-12p40 production is affected by all mycotoxins examined here, which could lead to detrimental effects in an inflammatory response.

The significance of modulation of these cytokines cannot be understated. There have been numerous reported studies of their importance in preventing infection. Suppression of IL-6 has been observed to increase enterovirus A71 lethality in mice (Wang *et al.*, 2017). It was shown that infection of IL-12p40-deficient mice with *M. tuberculosis* resulted in uncontrolled growth of the bacteria in all target organs. Livonesi *et al.* (2008) demonstrated that deficiency of the IL-12p40 subunit determines severe paracoccidioidomycosis in mice and their findings suggested that the IL-12p40 subunit mediates resistance in paracoccidioidomycosis by inducing IFN- γ production and a Th1 immune response. IL-12 was also seen to be essential for a protective Th1 response in mice infected with *Cryptococcus neoformans* (Decken *et al.*, 1998) and plays a role in modulating respiratory syncytial virus-induced airway inflammation distinct from that of viral clearance (Wang *et al.*, 2004). Similarly, IL-27 limits pathology during parainfluenza virus infection by regulating the quality of CD4⁺ T cell responses (Muallem *et al.*, 2017) and also mediates susceptibility to visceral leishmaniasis by

suppressing the IL-17-Neutrophil Response (Quirino *et al.* 2016). These studies highlight the modulation of cytokines can lead to disease progression due to failure of immune function.

This is the first report of the effect of patulin, DON, ZEN and T-2 toxin on cytokine secretion from J774A.1 murine macrophages. Other studies have shown how mycotoxins can interact with immune function in a similar way. Jia *et al.* (2014) showed that ZEN increased mRNA and protein expression of TLR4 and inflammatory cytokines in kidney cells in dose-dependent manner. Their results indicated that TLR4-mediated inflammatory reactions signal pathway was one of the mechanisms of ZEN mediated toxicity in the kidney. Capasso *et al.* (2015) demonstrated that low doses of DON used alone have scarce toxic effects, while induce cytotoxicity and inflammation when used in combination with particulate matter.

The results from this investigation demonstrate that although these compounds come from similar sources, due to the differences in structure, they exert variable effects on cytokine production. Overall, the results indicate that individually patulin, DON, ZEN and T-2 toxin have the ability to modulate the typical inflammatory response of macrophages to LPS stimulus. In particular, these toxins affected the secretion of cytokines that are critical for the normal host responses to infection. From this research, it is clear that these mycotoxins have the ability to cause macrophage dysfunction. Some of the molecular processes of toxicity are still not fully understood. However, this report has provided data that will be further developed to shed light on the mechanisms by which mycotoxins inhibit macrophage functions and, therefore, host defence functions, through deregulation of cytokine profiles.

Chapter 4: Effect of mycotoxin combinations on murine macrophage cytokine production

4.1 Introduction

The work detailed in this chapter looks at the effects that mycotoxin combinations have on cytokine production from J774A.1 murine macrophages. The concentration-dependent immunomodulatory effects of the mycotoxins; patulin, DON, ZEN and T-2 toxin, were highlighted in chapter 3. The data from chapter 3 highlighted several mycotoxin concentrations which, in this chapter, are combined and further examined to determine if these combinations differ significantly from their individual effects. This will provide further understanding of how mycotoxin combinations exert their immunomodulatory effects.

Immunomodulation is now seen as one of the most important aspects in the field of mycotoxicology. There are now a large number of studies demonstrating the immunosuppression caused by major mycotoxins including aflatoxins, trichothecenes, ochratoxin A and zearalenone (Ferrante *et al.*, 2002; Sharma *et al.*, 2004; Ferrante *et al.*, 2008; Ubagai *et al.*, 2008; Marzocco *et al.*, 2009). Many of these studies include stimulation using lipopolysaccharide (LPS), a component of Gram-negative bacterial cell walls. Macrophage exposure to LPS results in the production of pro-inflammatory cytokines, such as IL-12p40, TNF- α and IL-6 followed by the production of anti-inflammatory cytokines, including IL-10, for immune response regulation (Bruneau *et al.*, 2012). Changes to secretion levels of these cytokines can lead to serious health problems.

4.1.1 Co-occurrence of multiple mycotoxins

It is important to note that most toxin-producing fungi are capable of producing multiple mycotoxins concurrently (Bottalico, 1998). Furthermore, food and feed can be contaminated with various fungal species at the same time (Grenier and Oswald, 2011). Co-contaminated commodities might provoke adverse effects despite the concentrations of individual mycotoxins not exceeding legislative limits (Streit *et al.*, 2013). Additive and synergistic interactions have been highlighted for various combinations of mycotoxins, such as OTA, citrinin, AFB1, DON, FB1 and ZEN, (Klaric *et al.*, 2008; Grenier and Oswald, 2011; Halbin *et al.*, 2013; Lei *et al.*, 2013). Clarke *et al.* (2014) examined the toxic effect of AFB1, FB1 and OTA on the cell viability of three cell lines (Caco-2, MDBK and RAW264.7). Individual toxicity showed that OTA was the most cytotoxic mycotoxin in all three lines. Binary combinations were cytotoxic to the MDBK

cell line, whilst all effects observed were classified as being additive. Tertiary combinations of the toxins at the EU regulatory limits were not found to exhibit measurable cytotoxicity in MDBK, Caco-2 or RAW264.7 cells. However, when the concentrations were increased above the legal limits cytotoxicity was observed with up to 26% reduction in cell viability and synergistic effects were evident with regard to impairment of mitochondrial integrity.

Despite the fact that humans and animals alike can be exposed to a range of mycotoxins simultaneously, most toxicological studies have only taken into account the effects of exposure to a single mycotoxin. Very limited data is available on the combined toxic effects or the 'cocktail effect' of exposure to mycotoxins. Thus, the ability to accurately assess the risks to health of combined mycotoxin exposure is currently inadequate.

4.1.2 Chapter aims

The goal of this chapter was to continue the study of the effect mycotoxins on the immune response, using the J774A.1 murine macrophages. This data provides an insight into the potential mechanisms by which mycotoxin combinations modulate immune response through cytokine production levels

In total, fifty eight combinations were chosen based on the data from chapter 3's cytokine analysis. The ultimate aim of this chapter is to determine if sub-lethal combinations of mycotoxins modulate cytokine production from J774A.1 murine macrophage cells, and to determine if this modulation differs from the individual effects observed previously.

4.2 Results

4.2.1 Analysis of multiple mycotoxin exposure on J774A.1 murine macrophage cytokine production

DuoSet ELISA kits (R&D systems) were used to quantify the levels of cytokines (IL-6, IL-10, IL-12p40 and TNF- α) in the supernatants of J774A.1 macrophage cells treated with 58 different combinations of patulin, DON, ZEN and T-2 toxin in ranging in concentrations from 0.001 to 100 pg/mL for 24 hours with and without LPS (100 ng/mL) stimulation. The instances in which combinations showed significance compared to individual mycotoxins are described below. None of the concentrations and combinations used affected the viability of the cells as determined using an MTS assay.

4.2.1.1 J774A.1 macrophage cytokine production after exposure to deoxynivalenol and T-2 toxin with LPS challenge

An individual dose of 1 pg/mL T-2 Toxin was observed to increase the production of the pro-inflammatory cytokines IL-12p40 and TNF- α following LPS stimulation, while 0.1 pg/mL DON had no significant effect on the levels of these cytokines. The combination of these mycotoxins resulted in a significant suppression of this stimulation. This was also observed in experiments without LPS treatment for IL-12p40.

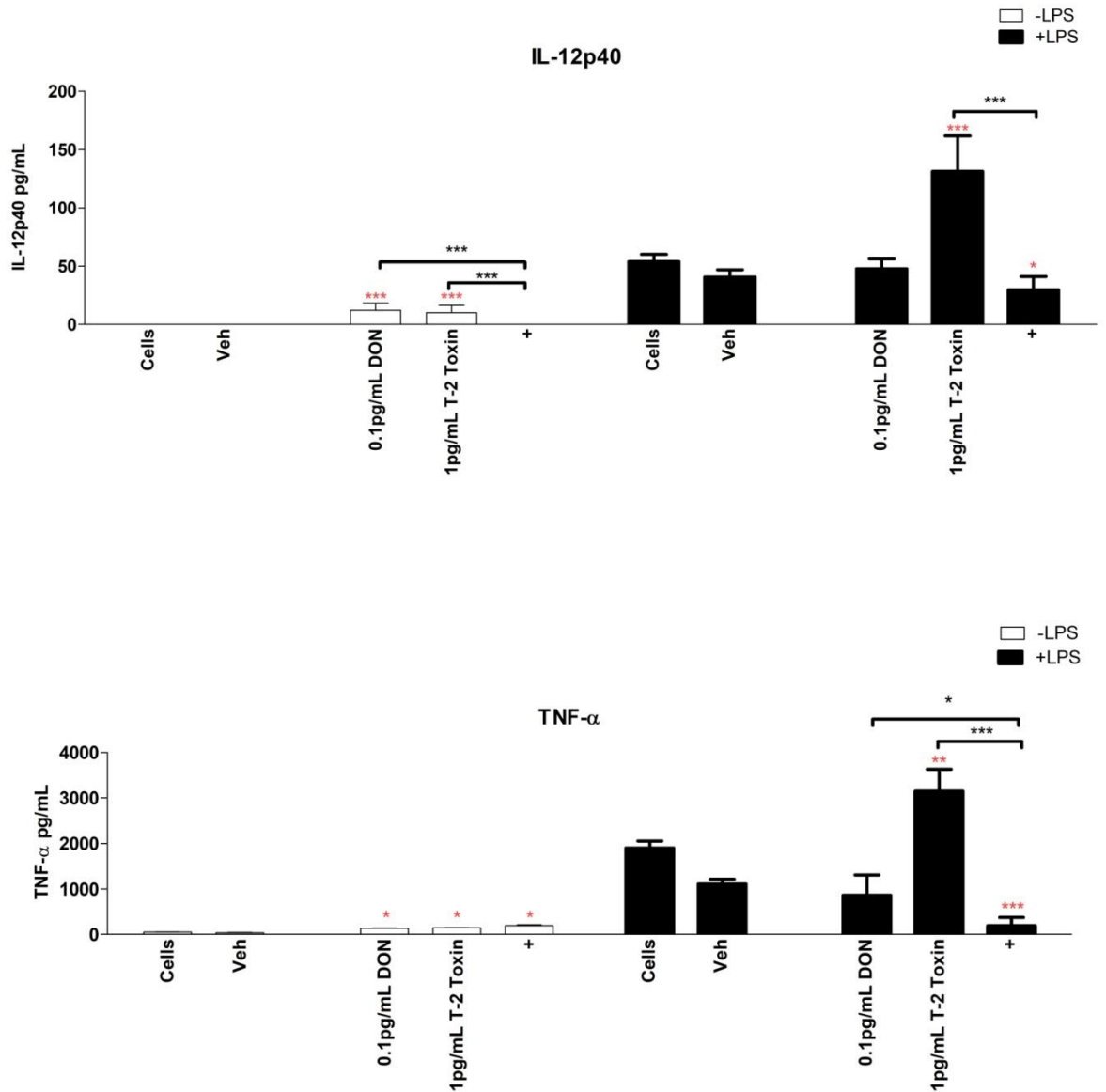


Figure 4.1: Production of IL-12p40 and TNF- α in the supernatants of J774A.1 murine macrophage cells, cultured for 24 hours in the presence of **DON**, **T-2 Toxin** or their combination (+), with and without LPS (100 ng/mL). The mycotoxin treatment alone is represented by white bars (\square) and mycotoxin treatment following LPS stimulation is represented by black bars (\blacksquare). Data are expressed as mean (n=3), with error bars indicating \pm 3SEM. Significance in red: P < 0.05*; P < 0.01**; P < 0.001*** relative to cells not exposed to mycotoxins. Significance in black: P < 0.05*; P < 0.01**; P < 0.001*** relative to individual mycotoxins

4.2.1.2 J774A.1 macrophage cytokine production after exposure to patulin and deoxynivalenol with LPS challenge

Treatment with patulin (0.001 pg/mL, 1 pg/mL, 100 pg/mL) and DON (0.01 pg/mL, 0.1 pg/mL) all resulted in the suppression of IL-6 following treatment with LPS. This suppression was maintained with the combination of 0.001 pg/mL patulin and 0.01 pg/mL DON, however, the combination of 1 pg/mL patulin and 0.1 pg/mL DON caused a large increase in the production of this cytokine. Subsequently, when the concentration of patulin was increased to 100 pg/L the combination had no significant effect compared to the controls. Prior to LPS stimulation, IL-12p40 levels were increased by 100 pg/mL patulin and 0.1 pg/mL DON, but their combination resulted in no increase. Following LPS treatment patulin was seen to increase IL-12p40 while DON suppressed its production but again their combination showed no significant difference from the controls.

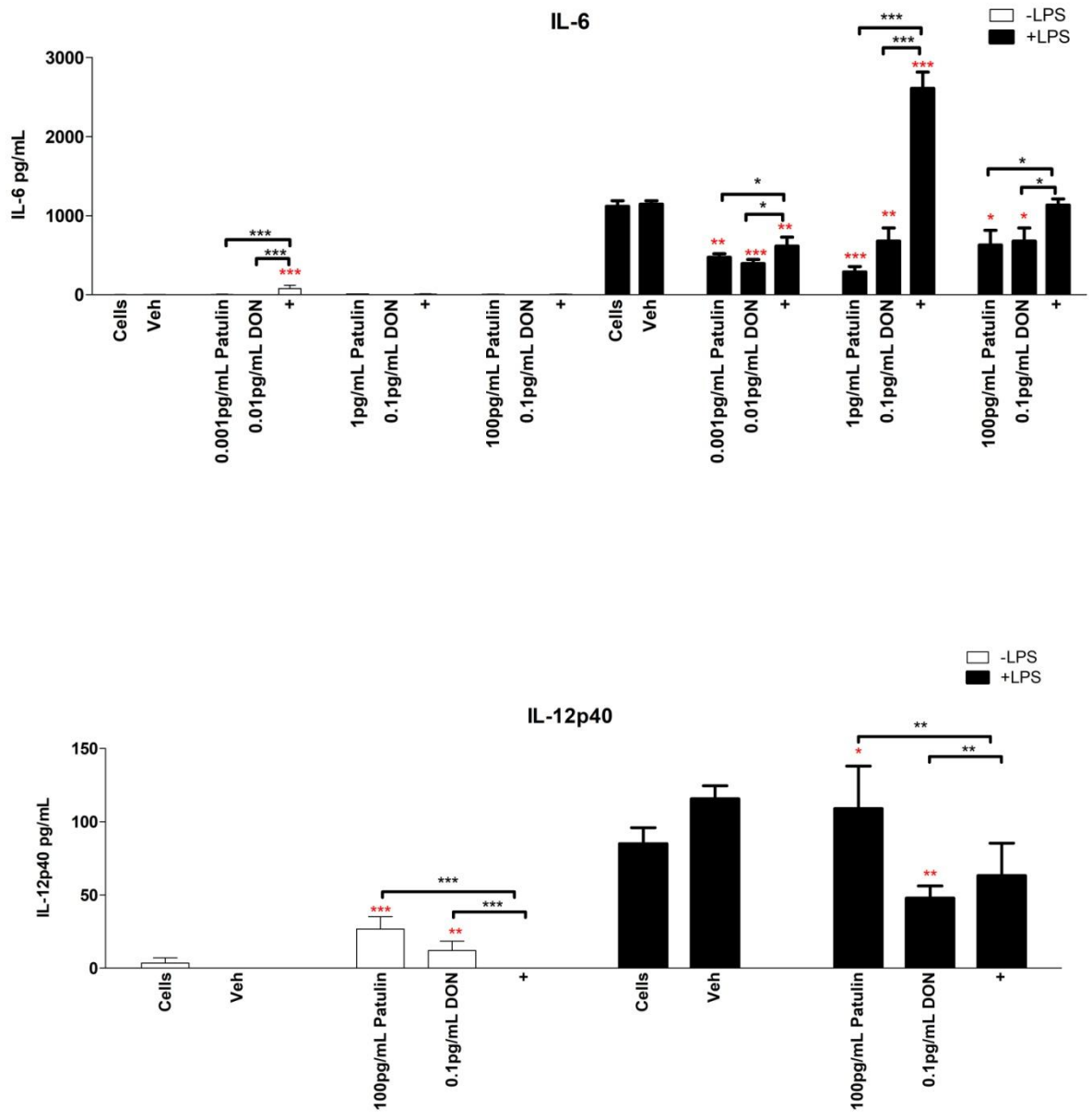


Figure 4.2: Production of IL-6 and IL-12p40 in the supernatants of J774A.1 murine macrophage cells, cultured for 24 hours in the presence of **Patulin**, **DON** or their combination (+), with and without LPS (100 ng/mL). The mycotoxin treatment alone is represented by white bars (□) and mycotoxin treatment following LPS stimulation is represented by black bars (■). Data are expressed as mean (n=3), with error bars indicating ± 3SEM. Significance in red: P < 0.05*; P < 0.01**; P < 0.001*** relative to cells not exposed to mycotoxins. Significance in black: P < 0.05*; P < 0.01**; P < 0.001*** relative to individual mycotoxins.

4.2.1.3 J774A.1 macrophage cytokine production after exposure to zearalenone and deoxynivalenol with LPS challenge

Individually, 1 pg/mL DON and 100 pg/mL ZEN significantly increased the levels of IL-6 without stimulation but their combination did not cause any increase. Following LPS stimulation suppression of IL-6 is observed by the individual toxins and their combination. Interestingly, combinations of DON and ZEN showed several significant effects on TNF- α production. Suppression of this cytokine is observed following exposure to individual doses of DON (0.01 pg/mL, 0.1 pg/mL, 0.001 pg/mL) and ZEN (100 pg/mL, 0.001 pg/mL) without LPS activation, but the combinations resulted in either increased production or a return to basal levels when compared to control cells. After treatment with LPS, these individual concentrations did not have a significant effect on TNF- α production compared to controls but their combinations resulted in a large suppression of the cytokine.

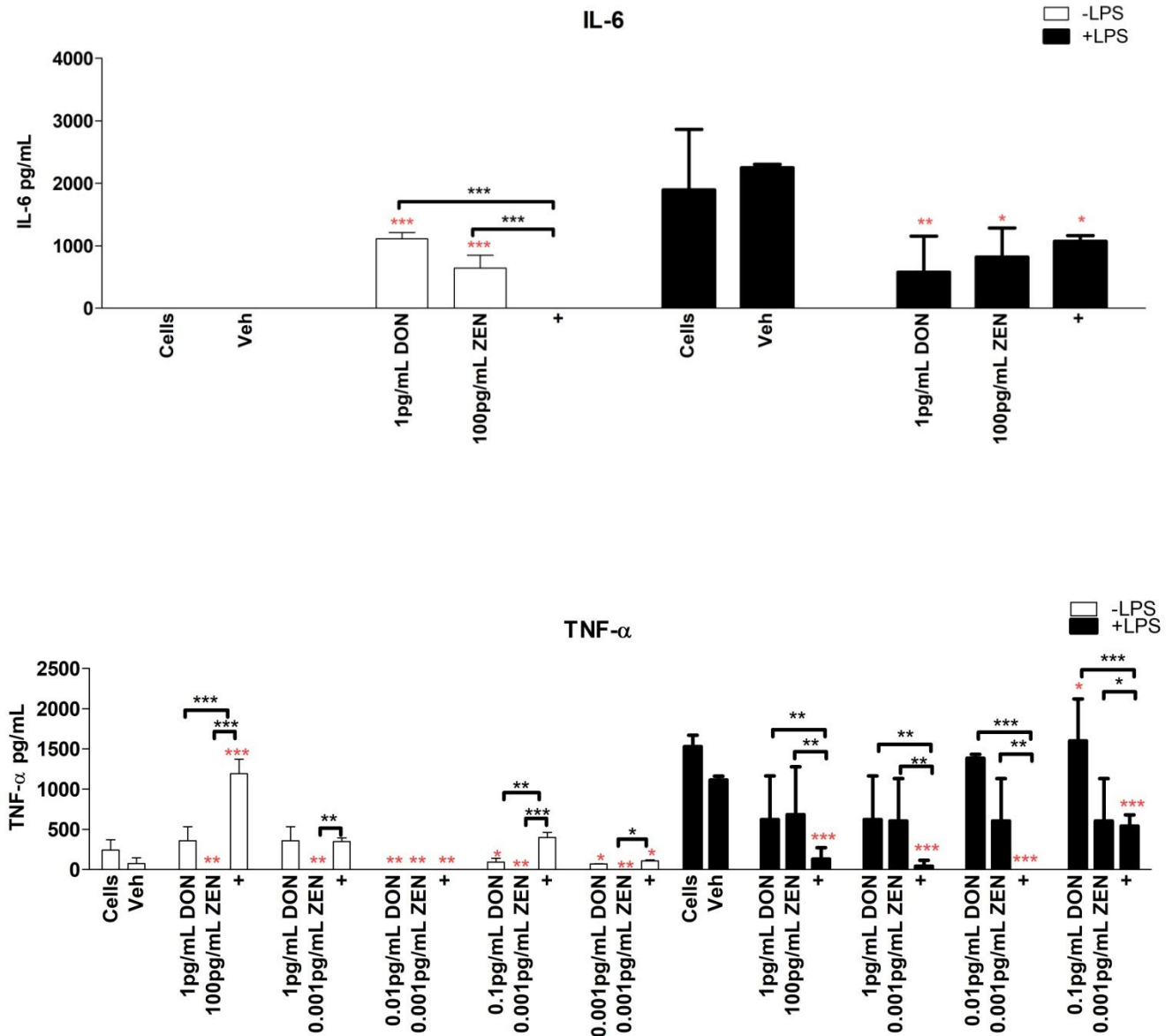


Figure 4.3: Production of IL-6 and TNF- α in the supernatants of J774A.1 murine macrophage cells, cultured for 24 hours in the presence of **DON**, **ZEN** or their combination (+), with and without LPS (100 ng/mL). The mycotoxin treatment alone is represented by white bars (\square) and mycotoxin treatment following LPS stimulation is represented by black bars (\blacksquare). Combinations are represented by the plus symbol (+). Data are expressed as mean (n=3), with error bars indicating \pm 3SEM. Significance in **red**: P < 0.05*; P < 0.01**; P < 0.001*** relative to cells not exposed to mycotoxins. Significance in **black**: P < 0.05*; P < 0.01**; P < 0.001*** relative to individual mycotoxins.

4.2.1.4 J774A.1 macrophage cytokine production after exposure to zearalenone and T-2 toxin with LPS challenge

IL-6 levels are significantly altered by ZEN and T-2 toxin, individually and in combination. An increase in IL-6 production was seen following exposure to all combinations of these mycotoxins without LPS stimulation, despite individual concentrations of T-2 toxin not showing any affect on IL-6 production compared to control cells. Following stimulation with LPS, suppression of IL-6 was caused by all individual concentrations of ZEN and T-2 toxin but their combinations showed an even more dramatic suppression, indicating a possible additive effect of these mycotoxins. TNF- α levels were unaffected by 0.01 pg/mL ZEN and 0.01 pg/mL T-2 toxin both with and without LPS stimulation, but the combination of these concentrations resulted in increased TNF- α production (- LPS) and a reduction in TNF- α secretion (+ LPS).

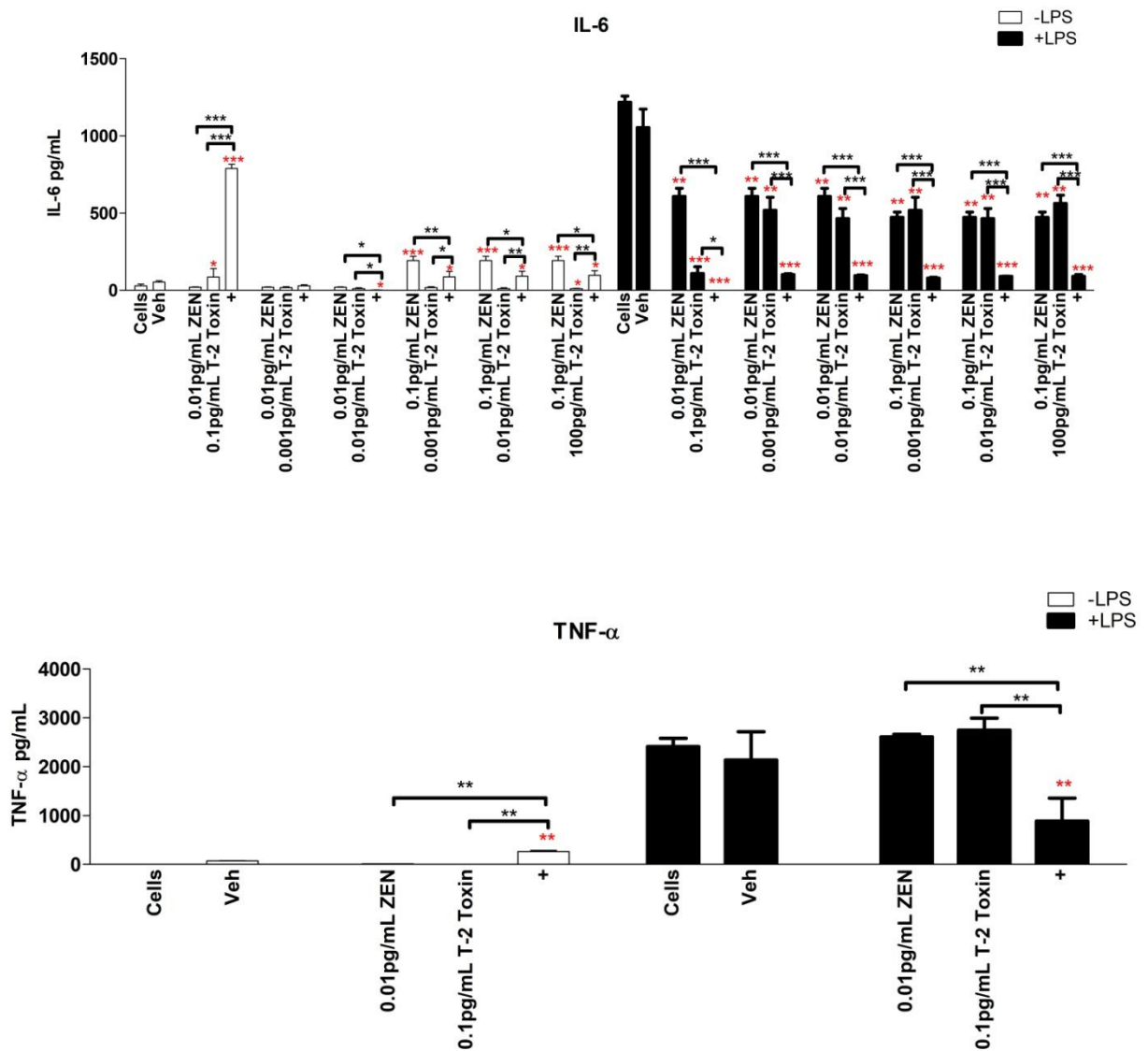


Figure 4.4: Production of IL-6 and TNF- α in the supernatants of J774A.1 murine macrophage cells, cultured for 24 hours in the presence of **ZEN**, **T-2 Toxin** or their combination (+), with and without LPS (100 ng/mL). The mycotoxin treatment alone is represented by white bars (\square) and mycotoxin treatment following LPS stimulation is represented by black bars (\blacksquare). Combinations are represented by the plus symbol (+). Data expressed as mean (n=3), with error bars indicating \pm 3SEM. Significance in **red**: P < 0.05*; P < 0.01**; P < 0.001*** relative to cells not exposed to mycotoxins. Significance in **black**: P < 0.05*; P < 0.01**; P < 0.001*** relative to individual mycotoxins.

4.2.1.5 J774A.1 macrophage cytokine production after exposure to patulin and T-2 toxin with LPS challenge

Following LPS stimulation, individual concentrations of patulin and T-2 toxin do not show significant difference to the controls but their combinations caused a large reduction in the secretion of IL-6. Suppression of IL-12p40 is also observed by some of these combinations after LPS activation. Conversely, TNF- α production is suppressed by the individual concentrations but their combination drives an increase in the production of the pro-inflammatory cytokine. The anti-inflammatory cytokine, IL-10, is significantly increased by the combination of 0.1 pg/mL patulin and 0.001 pg/mL T-2 toxin despite T-2 toxin showing some suppression of this cytokine individually and patulin having no effect compare to the control.

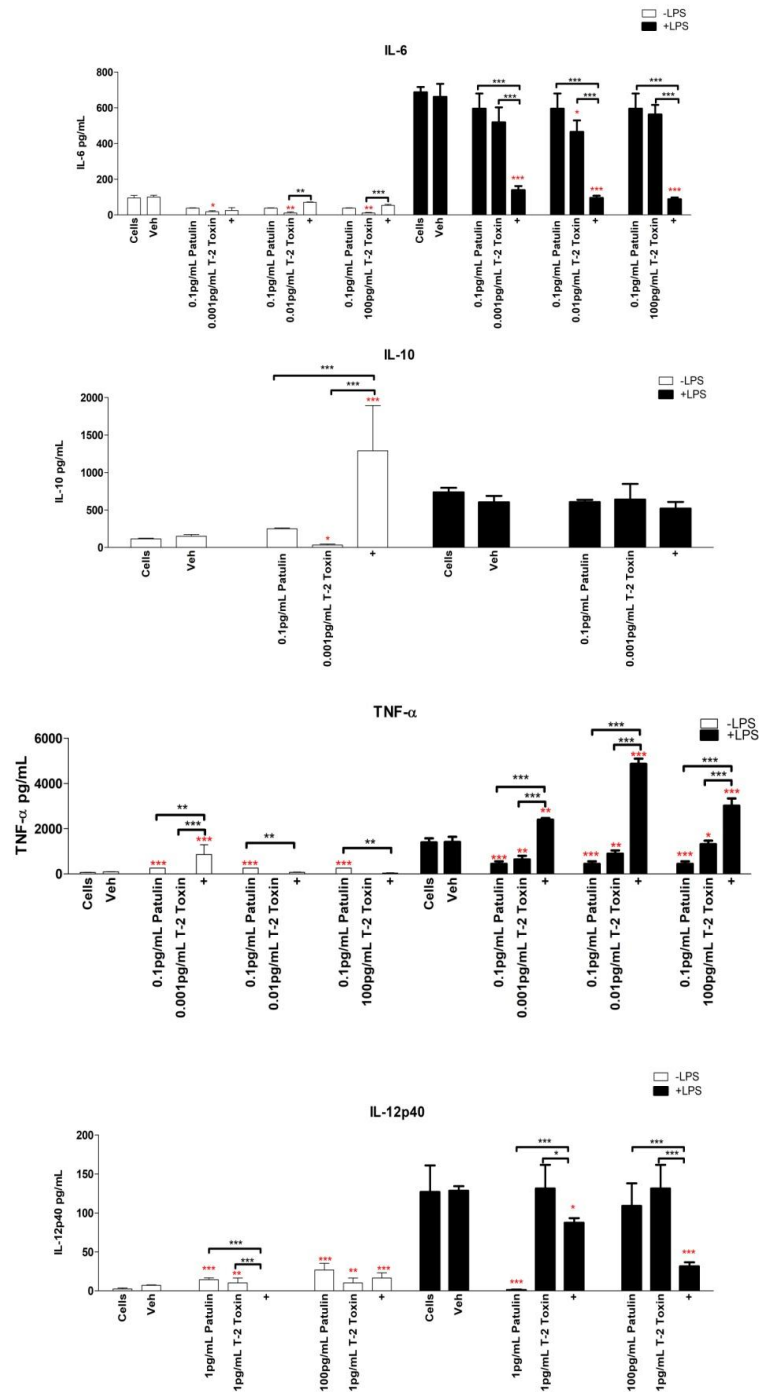


Figure 4.5: Production of IL-6, IL-10, IL-12p40 and TNF- α in the supernatants of J774A.1 murine macrophage cells, cultured for 24 hours in the presence of **Patulin**, **T-2 Toxin** or their combination (+), with and without LPS (100 ng/mL). The mycotoxin treatment alone is represented by white bars (\square) and mycotoxin treatment following LPS stimulation is represented by black bars (\blacksquare). Combinations are represented by the plus symbol (+). Data are expressed as mean (n=3), with error bars indicating \pm 3SEM. Significance in red: P < 0.05*; P < 0.01**; P < 0.001*** relative to cells not exposed to mycotoxins. Significance in black: P < 0.05*; P < 0.01**; P < 0.001*** relative to individual mycotoxins.

4.2.1.6 J774A.1 macrophage cytokine production after exposure to patulin and zearalenone with LPS challenge

The production of IL-6 is suppressed by individual concentrations and combinations of patulin and ZEN with LPS, except for 10 pg/mL patulin and its combination with 1 pg/mL ZEN which shows no significant change. After LPS stimulation, a suppression of the production of IL-6 is observed following exposure to 0.1 pg/mL, 0.01 pg/mL patulin and 1 pg/mL ZEN but suppression is not observed in any combinations where either no change or an increased production of IL-6 is seen. TNF- α production is increased by 10 pg/mL of patulin as well as its combination with 1 pg/mL ZEN however on its own, ZEN has no significant effect following LPS activation. Individually, patulin and ZEN do not affect the levels of IL-10 without LPS stimulation but their combination results in some suppression of the cytokine. After LPS, significant a increase of IL-10 is observed by 10 pg/mL patulin, 1 pg/mL ZEN and their combination.

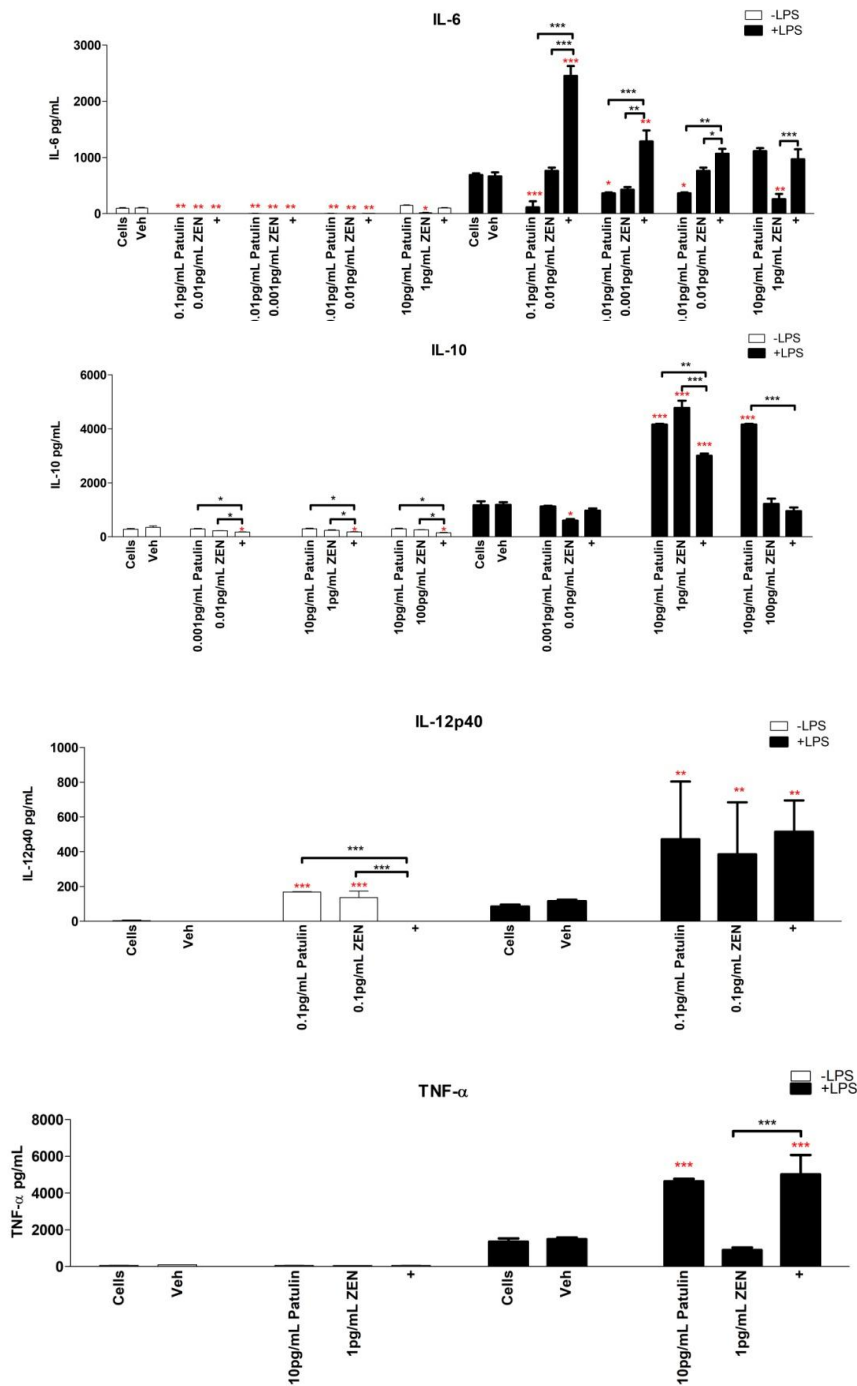


Figure 4.6: Production of IL-6, IL-10, IL-12p40 and TNF- α in the supernatants of J774A.1 murine macrophage cells, cultured for 24 hours in the presence of **Patulin**, **ZEN** or their combination (+), with and without LPS (100 ng/mL). The mycotoxin treatment alone is represented by white bars (\square) and mycotoxin treatment following LPS stimulation is represented by black bars (\blacksquare). Combinations are represented by the plus symbol (+). Data are expressed as mean (n=3), with error bars indicating \pm 3SEM. Significance in **red**: P < 0.05*; P < 0.01**; P < 0.001*** relative to cells not exposed to mycotoxins. Significance in **black**: P < 0.05*; P < 0.01**; P < 0.001*** relative to individual mycotoxins.

4.3 Discussion

Mycotoxin contamination is so common that exposure to low levels of multiple toxins is almost unavoidable. It is crucial to understand how low concentrations of multiple mycotoxins interact with the immune systems of humans and animals. A healthy and functioning immune system defends against a variety of pathogenic infections. Therefore, it is important to decipher the processes by which environmental factors, such as mycotoxins, cause dysfunction to the immune system. Mycotoxins' ability to modulate the immune system is well documented (Bianco *et al.*, 2012; Alassane-Kpembé *et al.*, 2013; Clarke *et al.*, 2014; Solhaug *et al.*, 2015), but there is still a lack of understanding of how multiple mycotoxins interact with each other and the immune system. It is evident that the effects of mycotoxins can vary depending on concentration, combination, exposure time as well as other environmental factors.

The aim of this study was to build on previous work (Loftus *et al.*, 2016) which critically analysed the effects of patulin, DON, ZEN and T-2 toxin in order to investigate how binary combinations of these mycotoxins differ from their individual effects. The data described here can hopefully help improve understanding of the mechanisms of multiple mycotoxin immunomodulation. From our previous study, it was observed that while mycotoxins are not cytotoxic at very low concentrations they can still cause immune dysfunction. The cytokine production data displayed here clearly indicates that these mycotoxins, alone and in combinations, have varying effects on the production levels of IL-6, IL-10, IL-12p40 and TNF- α , which are dependent on mycotoxin concentration, combination and exposure to LPS. Depending on the dosage and combination, it is possible for mycotoxins to be immunostimulatory or immunosuppressive.

Exposure of macrophages to patulin, DON, ZEN and T-2 toxin resulted in a concentration and combination-dependent modulation of cytokine secretion. For example, exposure to individual concentrations of DON and ZEN had no significant effect on the secretion levels of TNF- α following LPS stimulation, however, in all cases the combination of these toxins resulted in a largely significant suppression of TNF- α production. A similar effect was observed with the combination of ZEN and T-2 toxin, with each of these toxins having no effect on TNF- α but their combination caused suppression after LPS activation. While the individual concentrations of ZEN and T-2

toxin did result in suppression of IL-6, their combination produced a much greater suppression of the cytokine's secretion level. Possibly the most interesting result arose from the combination of patulin and T-2 toxin. Here, the individual concentrations had no effect on IL-6 production after LPS activation but showed suppression when combined, and one of the combinations also significantly increased the production of IL-10 without LPS stimulation. However, the individual concentrations of patulin and ZEN suppressed the production of TNF- α , yet their combination drove the over-production of this cytokine. Overall, examples of these mycotoxins working additively, synergistically and agnostically were observed. The nature of these combinatory effects is dependent on the mycotoxins involved, and their concentrations. In some cases, such as combinations of patulin and T-2 toxin, the combined effect is additive. Others, like ZEN and T-2 toxin, produce synergistic effects while, sometimes, even agnostic effects are observed as was seen for combinations of patulin and ZEN.

The result of this could have consequences on how macrophages maintain function and respond to infection. Studies have shown that over-activation of macrophages plays a major role in mediating chronic mucosal inflammation which has been seen in patients with ulcerative colitis and Crohn's disease (Xavier and Podolsky, 2007). Furthermore, aggravated macrophage activation results in extensive tissue damage associated with autoimmune diseases such as rheumatoid arthritis (Feldmann and Maini, 2008) and with infection, such as schistosmiasis (Wynn *et al.*, 2004).

A large suppression of TNF- α is seen with combinations of DON and ZEN. TNF- α is a pro-inflammatory cytokine that plays a pivotal role in regulating the inflammatory response in diseases such as RA. Although it is controversial whether TNF- α genes are associated with RA susceptibility, they are well known to mediate RA pathogenesis (Vasanthi *et al.*, 2007). The activities of TNF- α are mediated by two receptors, TNF-R1 (p55) and TNF-R2 (p75) (Peschon *et al.*, 1998). TNFR1 is constitutively expressed in most tissue, whereas TNFR2 is usually found in cells of the immune system (Wajant *et al.*, 2003). Although their mechanisms have not been completely elucidated, it seems that they have opposing effects. The pro-inflammatory and apoptotic pathways of TNF- α are largely mediated through TNFR1, while TNFR2 has been shown to mediate signals that promote proliferation and tissue repair (Bradley, 2008). Suppression of this cytokine will prevent these processes from occurring and have significant effects on

the health of a host. TNF- α is produced by activated monocytes, macrophages and lymphocytes in response to a number of different pathogens including viruses, bacteria and parasites. TNF- α acts with other cytokines to generate a competent cell-mediated immune response to intracellular pathogens such as *M. tuberculosis*, *Listeria* spp. and *Histoplasma* spp. The importance of TNF- α in the host response against tuberculosis has been well demonstrated in animal models (Johnston and Conly, 2006).

Rather interestingly, modulation of IL-10 is observed with combinations of patulin, T-2 Toxin and ZEN. IL-10 an important mediator of immunosuppression following traumatic injury, it also is beneficial with regard to its ability to counter-regulate the early inflammatory response under such conditions (Schneider *et al.*, 2004). It is a cytokine with potent anti-inflammatory properties that plays a central role in limiting host immune response to pathogens, thereby preventing damage to the host and maintaining normal tissue homeostasis. Dysregulation of IL-10 is associated with enhanced immunopathology in response to infection as well as increased risk for development of many autoimmune diseases (Iyer and Cheng, 2012). Importantly, IL-10 down-regulates the production of pro-inflammatory cytokines including IL-1, IL-6, IL-12 and TNF- α . IL-10 can also act directly on CD4 T-cells, inhibiting proliferation and production of IL-2, IFN- γ and IL-4. Indeed, suppression of IL-10 leads to the overproduction of cytokines and the development of chronic diseases. Primarily, an increase in IL-10 can inhibit Th1 cell differentiation or direct cells to a regulatory response (Asadullah *et al.*, 2003). Further to its effects on cytokine production, IL-10 can also modulate surface marker expression by inhibiting the complete maturation of DC by down-regulating the expression of CD80 and CD86 (de Jong *et al.*, 2005) and the ability to prevent the peptide-MHCII complexes translocating to the DC plasma membrane (Banchereau *et al.*, 2000) all of which lead to impaired T helper cell responses. The effects of these toxins on IL-10 could, therefore, potentially result in overproduction of pro-inflammatory cytokines and the development of chronic diseases.

IL-10 has emerged as a key immunoregulator during infection with viruses, bacteria, and fungi by ameliorating the excessive Th1 and CD8+ T cell responses (typified by overproduction of IFN- γ and TNF- α) that are responsible for much of the

immunopathology associated with infections. Ablation of IL-10 signaling results in the onset of severe, often fatal immunopathology in a number of infections including *T. gondii*, malaria, and *Trypanosoma cruzi*. Excessive, or mistimed, IL-10 production can also inhibit the pro-inflammatory response to *Plasmodium spp.*, *Leishmania spp.*, *T. cruzi*, *Mycobacterium spp.*, and lymphocytic choriomeningitis virus to the extent that pathogens escape immune control, resulting in either fulminant and rapidly fatal or chronic non-healing infections. There is a direct correlation between inappropriate IL-10 production and disease severity (Couper *et al.*, 2008). Redford *et al.* (2011) investigated the role of IL-10 in immune regulation during *M. tuberculosis* (Mtb) infection and found the protective immune response to Mtb infection, which prevents progression to active disease, may be attributed to the finite balance between pro-inflammatory and immunoregulatory mechanisms. IL-10 represents one such regulatory mechanism that Mtb could be exploiting in order to establish a chronic infection.

Published studies on the effect of these mycotoxins on immune regulation, particularly cytokine secretion, are not numerous. Jia *et al.* (2014) showed that ZEN increased mRNA and protein expression of TLR4 and inflammatory cytokines in kidney in dose-dependent manner. Their results indicated that TLR4-mediated inflammatory reactions signal pathway was one of the mechanisms of ZEN-mediated toxicity in the kidney. This dose-dependant response can also be seen with the mycotoxin examined in our previous study (Loftus *et al.*, 2016) and in the data presented above. Kankkunen *et al.* (2014) demonstrated that trichothecene-induced IL-1 β secretion is dependent on NLRP3 inflammasome in human primary macrophages and concluded that roridin A, a fungal trichothecene mycotoxin, acts as a microbial danger signal that triggers activation of the NLRP3 inflammasome through P2X7R and Src tyrosine kinase signaling-dependent pathways in human primary macrophages. Gaining greater insight into how mycotoxins interact with these early-responders of the immune system is crucial to understanding the significance of their immunomodulatory properties.

Capasso *et al.* (2015) examined the synergistic inflammatory effect of PM10 with mycotoxin deoxynivalenol on human lung epithelial cells and showed that low doses of PM and DON used alone have scarce toxic effects, while they induce cytotoxicity and inflammation when used in combination. This, similar to the data presented here,

indicates that examining individual effects of mycotoxins is not sufficient and their combinations can result in drastically differing effects. Oh *et al.* (2015) examined the effect of the *Penicillium* mycotoxins citrinin, ochratoxin A, patulin, mycophenolic acid and penicillic acid on the cytokine gene expression, reactive oxygen species production, and phagocytosis of bovine macrophage function. They found that exposure to sub-lethal concentrations of toxins can affect macrophage function, which could affect immunoregulation and innate disease resistance to pathogens, similar to this study. Thus, it is clear that there is a plethora of pathways associated with cell signaling that can be modulated by mycotoxins and that this modulation can occur at sub-lethal concentrations.

The studies described, along with our own, highlight the importance of understanding how mycotoxins, particularly at sub-lethal concentrations, interact with the immune systems of humans and animals, but much more work is needed in this field to fully comprehend their modulatory abilities.

Chapter 5: Effect of mycotoxin combinations on murine macrophage phagocytosis and cell surface marker expression

5.1 Introduction

The work described in this chapter examines the effects that mycotoxins, alone and in combinations, have on phagocytosis and cell surface marker expression of J774A.1 murine macrophages. The concentration-dependent immunomodulatory effects of the mycotoxins; patulin, DON, ZEN and T-2 toxin, were highlighted in chapter 3. This work laid the foundation for chapter 4 in which combinations of these mycotoxins were shown to modulate cytokine secretion. The data from chapter 4 highlighted several mycotoxin combinations which, in this chapter, are examined further to determine whether these combinations also exert effects on phagocytosis and key cell surface marker expression. This allows for an even further understanding of how mycotoxin combinations exert their immunomodulatory effects.

As previously discussed, it is important to note that most toxin-producing fungi are capable of producing multiple mycotoxins concurrently (Bottalico, 1998). Furthermore, food and feed can be contaminated with various fungal species at the same time (Grenier and Oswald, 2011). Co-contaminated commodities might provoke adverse effects despite the concentrations of individual mycotoxins not exceeding legislative limits (Streit *et al.*, 2013). Additive and synergistic interactions have been highlighted for various combinations of mycotoxins, such as OTA, citrinin, AFB1, DON, FB1 and ZEN, (Klaric *et al.*, 2008; Grenier and Oswald, 2011; Halbin *et al.*, 2013; Lei *et al.*, 2013). Clarke *et al.* (2014) examined the toxic effect of AFB1, FB1 and OTA on the cell viability of three cell lines (Caco-2, MDBK and RAW264.7). Individual toxicity showed that OTA was the most cytotoxic mycotoxin in all three lines. Binary combinations were cytotoxic to the MDBK cell line, whilst all effects observed were classified as being additive. Tertiary combinations of the toxins at the EU regulatory limits were not found to exhibit measurable cytotoxicity in MDBK, Caco-2 or RAW264.7 cells. However, when the concentrations were increased above the legal limits cytotoxicity was observed with up to 26% reduction in cell viability and synergistic effects were evident with regard to impairment of mitochondrial integrity.

Despite the fact that humans and animals alike can be exposed to a range of mycotoxins simultaneously, most toxicological studies have only taken into account the effects of exposure to a single mycotoxin. Very limited data is available on the combined toxic effects or the 'cocktail effect' of exposure to mycotoxins. Thus, the

ability to accurately assess the risks to health of combined mycotoxin exposure is currently inadequate.

5.1.1 Phagocytosis

Phagocytosis is the first step in triggering host defence and inflammation, it is required for the removal of the enormous numbers of senescent cells that die every day, and it is needed for embryonic development, tissue remodelling, and infection clearance (Aderem, 2003). Together with monocytes and dendritic cells, macrophages make up the mononuclear phagocyte network and play an important role in tissue homeostasis. Macrophages are often referred to as “professional phagocytes” in so far as one of their key roles in the body is to phagocytose pathogens and cell debris initiating the innate immune response, which in turn orchestrates the adaptive response (Aderem and Underhill, 1999). Any disruption to the ability of a macrophage to phagocytose could have detrimental effects to an organism. For this reason, we thought it pertinent to assess the phagocytotic ability of macrophages after exposure to sub-lethal doses of mycotoxins. Thus far, this study has focused on the effect of mycotoxins on cytokine secretion, but it is also important to determine if this is how mycotoxins affect the ability of the macrophage to carry out other important functions.

There is limited data on the effect of mycotoxins on macrophage phagocytosis. Niyo *et al.* (1988) examined the effects of T-2 mycotoxin ingestion on phagocytosis of *Aspergillus fumigatus conidia* by rabbit alveolar macrophages and found phagocytosis was significantly reduced in cultures that used serum from rabbits treated with 0.5 mg of T-2/kg/day and alveolar macrophages from untreated rabbits or rabbits treated with T-2. There was little reduction in phagocytosis when alveolar macrophages from rabbits treated with T-2 and normal serum were used. More recently, Liu *et al.* (2002) showed that fumonisin B1 and aflatoxin B1 were immunotoxic to swine alveolar macrophages by examining phagocytosis. Ultimately, a better understanding of mycotoxins’ interaction with this process is needed.

5.1.2 Cell surface makers

Pattern recognition receptors (PRRs) are cell surface markers found on a variety of immune cells used for cell recognition and signalling purposes. Because macrophages must be selective of the cells and materials they phagocytose, they use these PRRs and costimulatory signals, including toll-like receptors (TLRs), Cluster of differentiations

(CDs) and major histocompatibility complexes (MHCs), to recognise signals associated with invading pathogens, foreign substances and dead or dying cells. Modulation of cell surface makers' expression levels can result in inhibition of macrophage function and a suppression of activity.

Several studies have examined the ability of mycotoxins to modulate cell surface maker expression. Bruneau *et al.* (2012) found aflatoxin exposure affected expression levels of key cell surface markers involved in the inflammatory response. In their study, Toll-like receptor 2 (TLR2) and Cluster of Differentiation 14 (CD14) expression levels decreased significantly, but Toll-like receptor 4 (TLR4) expression was unaffected. Previous investigations have shown that AFB1 pre-treatment, followed by LPS stimulation, decreases CD14 expression in murine peritoneal macrophages. However, CD14 expression was unaffected in cells that were pre-treated with AFB1, but not challenged with LPS (Moon and Pyo, 2000). Traditionally levels of these makers are measured using flow cytometry, as in this study, however, there are some emerging methods capable of quantifying these cell surface makers in 'real-time' as described in this investigation.

5.1.3 Lab-in-a-Trench

Lab-in-a-Trench (LiaT) is a microfluidic platform previously developed by Dimov *et al.* (2010). The LiaT platform is a two layer polydimethylsiloxane (PDMS) system whereby a lower PDMS panel holds structures (channel and trenches), while an upper panel has reservoirs. The microfluidic trench structure allows efficient capture and retention of cells through gravity-based sedimentation. The laminar flow conditions assure a vanishing flow field throughout the trench, thus permanently retaining particles and minimizing hydrodynamic stress. Furthermore, its small depth of 150 μm allows continuous loading, mixing and refreshment of reagents by mere diffusion from a controlled flow through the supply channel on the top of the trench. This makes LiaT an ideal candidate for the analysis of cell surface makers on macrophage cells. This method provides an alternative to traditional flow cytometry for 'real-time' single cells analysis in a smaller, simple and more robust format.

5.1.4 Chapter aims

The purpose of the research described in this chapter was to continue the study of the effect mycotoxins on the immune response to infection, using the J774A.1 murine macrophage cell line as a model for host defence. This data provides an insight into the potential mechanisms by which mycotoxins, alone and in combination, modulate the immune responses *via* effects on phagocytosis and cell surface marker expression.

In total, six mycotoxin combinations were chosen based on the data from chapter 4's cytokine analysis. Combinations showing modulation of cytokine that differed significantly from the individual effects were selected to determine if these effects were also observed for phagocytosis and cell surface marker expression. Firstly, analysis of the effect of these patulin, DON, ZEN and T-2 toxin combinations on J774A.1 murine macrophage phagocytosis was examined using flow cytometry to determine if these toxins directly inhibit macrophage function. Then, the same combinations were used to examine the effect on the expression levels of the key cell surface markers, CD80, CD86, MHCII and TLR4 using flow cytometry while concurrently using the LiaT platform to investigate if it is possible to observe the same effects in 'real-time' using this microfluidic technology.

The ultimate aim of this chapter is to determine if sublethal combinations of mycotoxins modulate phagocytosis and cell surface marker expression, and if this can be analysed in 'real-time' using a rapid, cost-effective method such as LiaT.

5.2 Results

5.2.1 Analysis of multiple mycotoxin exposure on J774A.1 murine macrophage phagocytosis using flow cytometry

5.2.1.1 J774A.1 macrophage phagocytosis after exposure to patulin, zearalenone, deoxynivalenol and T-2 toxin with LPS challenge

Phagocytosis and clearance of pathogens is a hallmark of macrophage function and critical to host defence. Therefore, the effect of mycotoxin exposure on macrophages' ability to phagocytose was investigated.

J774A.1 murine macrophage cells were cultured for 24 hours in the presence of patulin, DON, ZEN and T-2 Toxin, with and without LPS (100 ng/mL) stimulation, followed by incubation with 1 µm FITC-labelled latex beads for 1 hour. Cells were then washed and the uptake of beads was measured by flow cytometry. Cells that took up the beads showed green fluorescence which can be measured with the FITC channel of the flow cytometer and expressed as a percentage of phagocytosing cells. In total, six mycotoxin combinations consisting of ten individual mycotoxins were analysed. The results shown below are the most interesting and illuminating results from the data analysed.

The results show that 0.001 pg/mL ZEN and 0.1 pg/mL DON increased phagocytosis after LPS stimulation. Phagocytosis was decreased by 0.01 pg/mL ZEN, 0.1 pg/mL DON and 100 pg/mL T-2 Toxin without LPS challenge. The combinations of 0.01 pg/mL DON and 0.001 pg/mL ZEN showed an increase in phagocytosis without LPS, while the combinations of 0.1 pg/mL patulin and 0.001 pg/mL ZEN increased phagocytosis after LPS activation. Any individual mycotoxin concentrations not displayed below did not have a significant effect on phagocytosis compared to the controls.

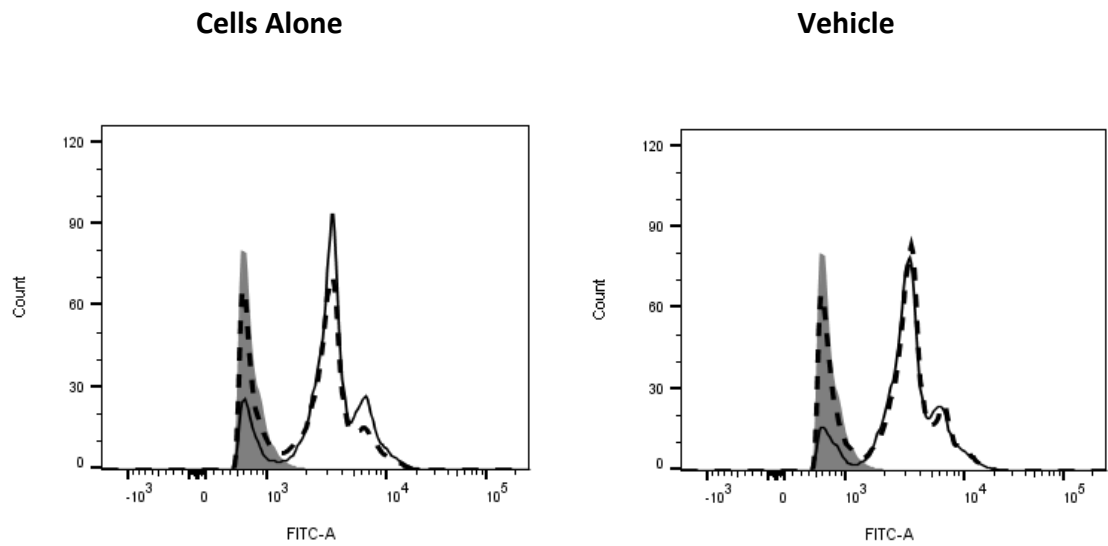


Figure 5.1: Controls for the effect of mycotoxin exposure on phagocytosis. J774A.1 murine macrophage cells cultured for 24 hours with and without LPS (100 ng/mL) stimulation, followed by incubation with 1 μ m FITC-labelled latex beads for 1 hour. Cells were washed and analysed by flow cytometry for uptake of beads. The toxin treatment alone is represented by the solid lines and the toxin treatment with LPS challenge is represented by the dashed lines. Unstained cells are represented by the filled grey histogram.

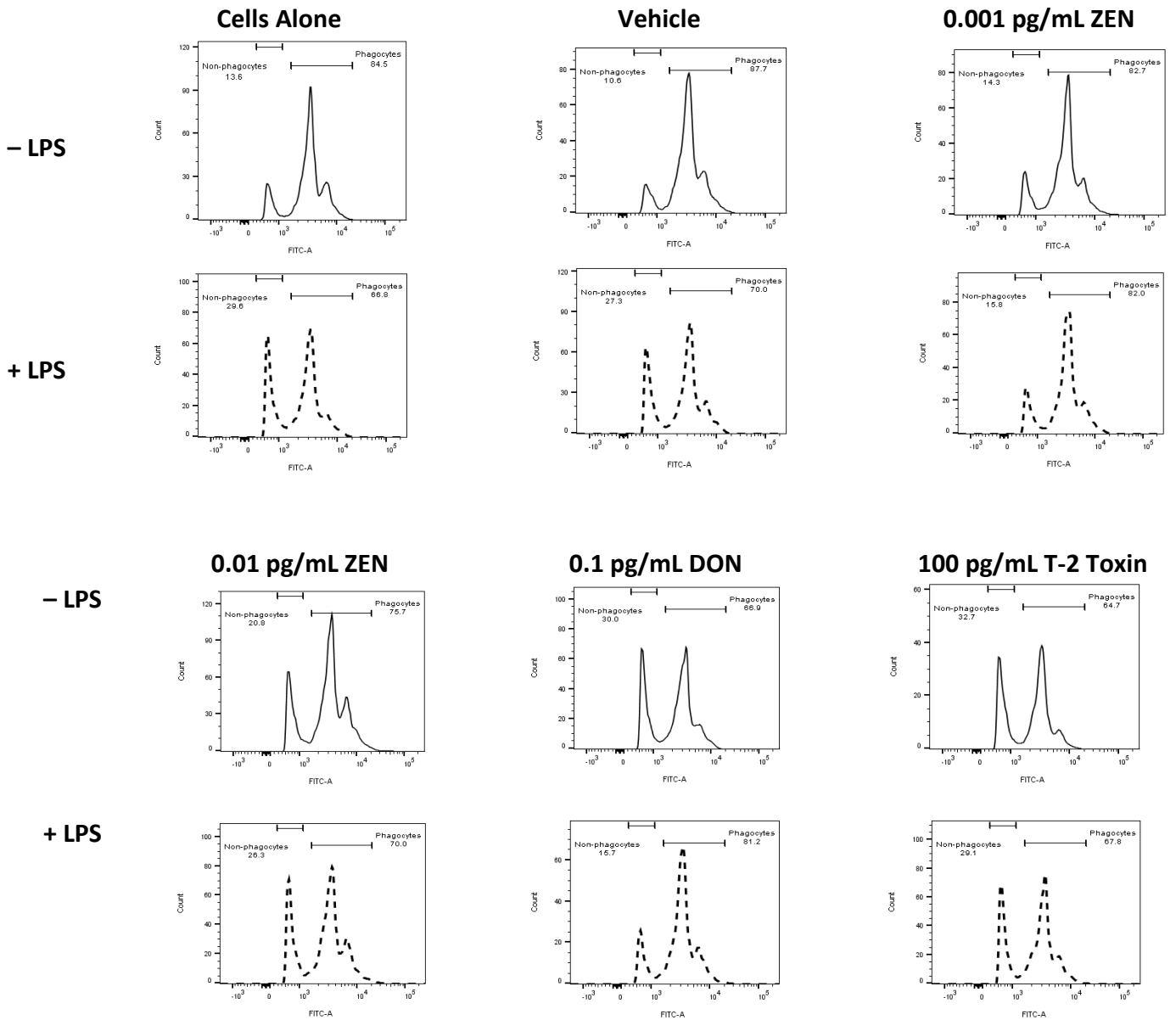


Figure 5.2: The effect of mycotoxin exposure on phagocytosis. J774A.1 murine macrophage cells, cultured for 24 hours in the presence of **patulin, DON, ZEN and T-2 Toxin**, with and without LPS (100 ng/mL) stimulation, followed by incubation with 1 μ m FITC-labelled latex beads for 1 hour. Cells were washed and analysed by flow cytometry for uptake of beads. The toxin treatment alone is represented by the solid lines and the toxin treatment with LPS challenge is represented by the dashed lines. Gates on histograms show percentage of cells that contain beads (phagocytes) or do not contain beads (non-phagocytes).

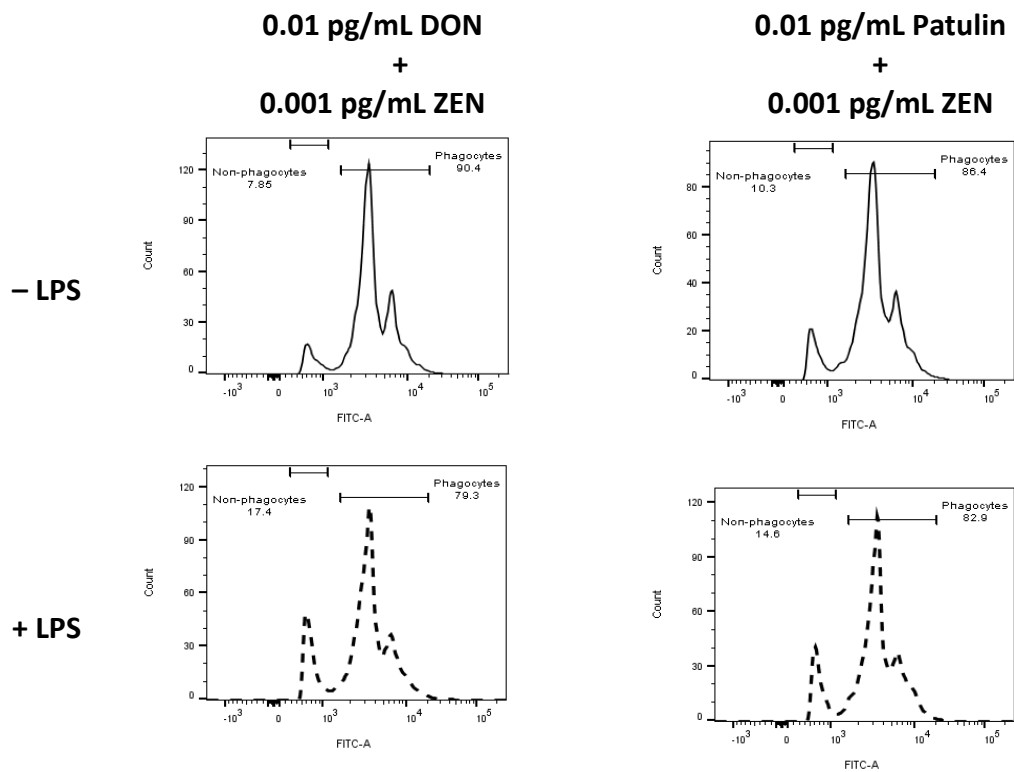


Figure 5.3: The effect of mycotoxin exposure on phagocytosis. J774A.1 murine macrophage cells, cultured for 24 hours in the presence of **patulin, DON and ZEN** combinations, with and without LPS (100 ng/mL) stimulation, followed by incubation with 1 μ m FITC-labelled latex beads for 1 hour. Cells were washed and analysed by flow cytometry for uptake of beads. The toxin treatment alone is represented by the solid lines and the toxin treatment with LPS challenge is represented by the dashed lines. Gates on histograms show percentage of cells that contain beads (phagocytes) or do not contain beads (non-phagocytes).

5.2.2 Analysis of multiple mycotoxin exposure on J774A.1 murine macrophage cell surface marker expression using flow cytometry

5.2.2.1 J774A.1 macrophage cell surface marker expression after exposure to patulin, zearalenone, deoxynivalenol and T-2 toxin with LPS challenge

Since cell surface markers play such a crucial role in the initiation of an inflammatory response, the effect of mycotoxin exposure on the expression of CD80, CD86, MCHII and TLR4 on the J774A.1 murine macrophage cells was investigated using flow cytometry. The results are displayed below and summarised in Table 5.1. Data was analysed using mean fluorescence intensity (MFI) values. MFI is defined as the arithmetic mean of the data, in which the linear scaled fluorescence was averaged and the result is weighted by outliers at the high end of the distribution. The MFI of each sample was compared and presented as relative to the cells alone control. In total, six mycotoxin combinations consisting of ten individual mycotoxins were analysed. The results shown below are the most interesting results from the data analysed.

Controls include cells alone and cells exposed to the vehicle control (equivalent to the highest concentration of methanol in the mycotoxin samples). Isotype controls were previously performed for these cells and antibodies with no interference observed and, therefore, were not carried out in this study. The results show that 0.01 pg/mL ZEN causes an increased expression of MHCII, TLR4, CD80 and CD80 without LPS but after LPS activation the levels of all of these cell surface markers are decreased by this concentration. MHCII and CD80 levels are increased when exposed to 0.1pg/mL DON without LPS but a reduction in CD80 levels is seen after LPS stimulations compared to controls. Patulin appears to show suppression in the levels of CD80 and CD80 at a number of concentrations (0.01, 0.1 and 1 pg/mL) both with and without LPS activation. Combinations of these patulin concentrations with DON, ZEN and T-2 show significant effects on the expression levels of all four surface makers. Any individual mycotoxin concentrations not displayed below did not have a significant effect on the expression levels compared to the controls.

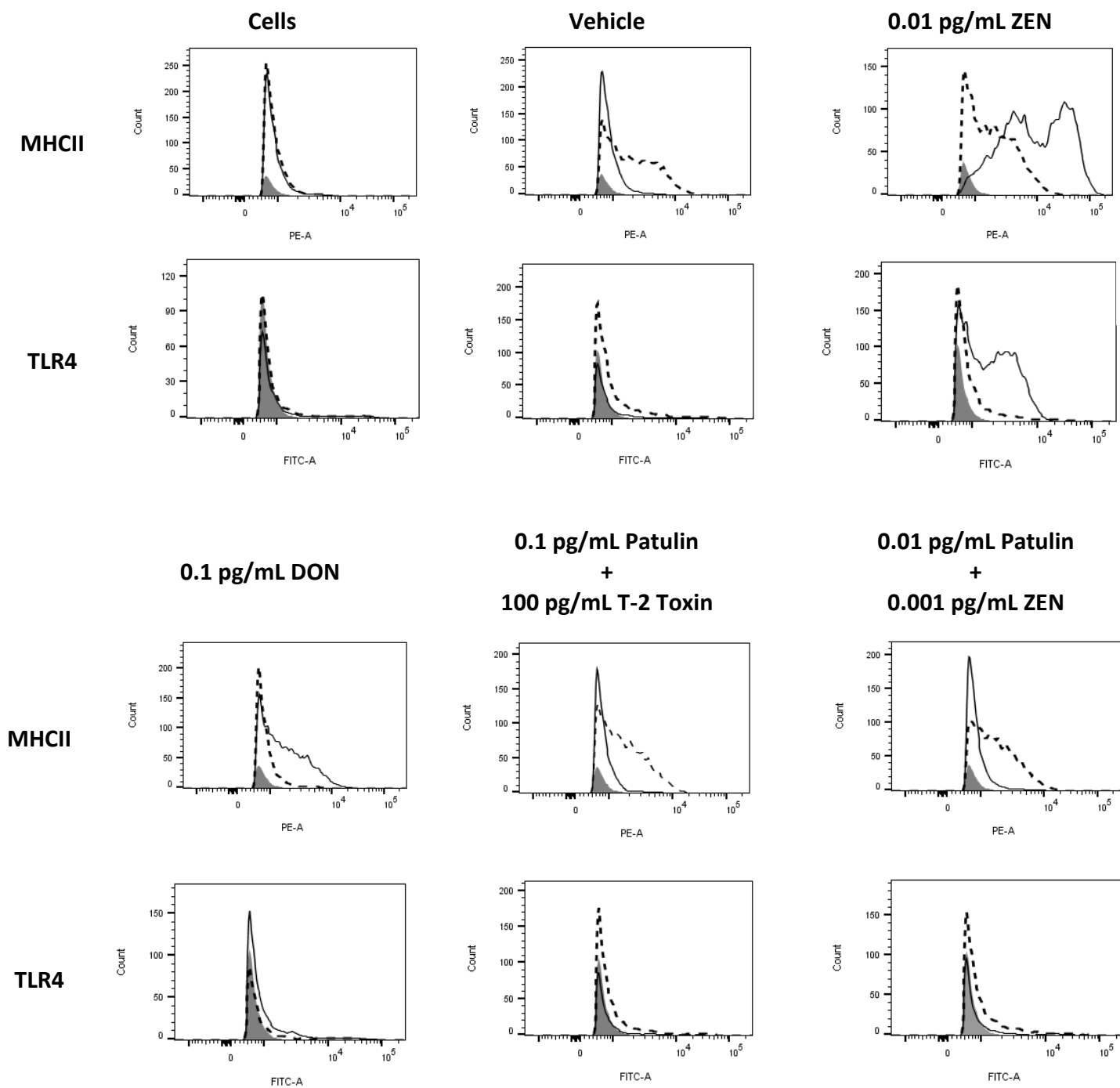


Figure 5.4: Expression of MHCII and TLR4 on the surface of J774A.1 murine macrophage cells, cultured for 24 hours in the presence of **patulin, DON, ZEN and T-2 Toxin**, with and without LPS (100 ng/mL) stimulation. The toxin treatment alone is represented by the solid lines and the toxin treatment with LPS challenge is represented by the dashed lines. Unstained cells are represented by the filled grey histogram.

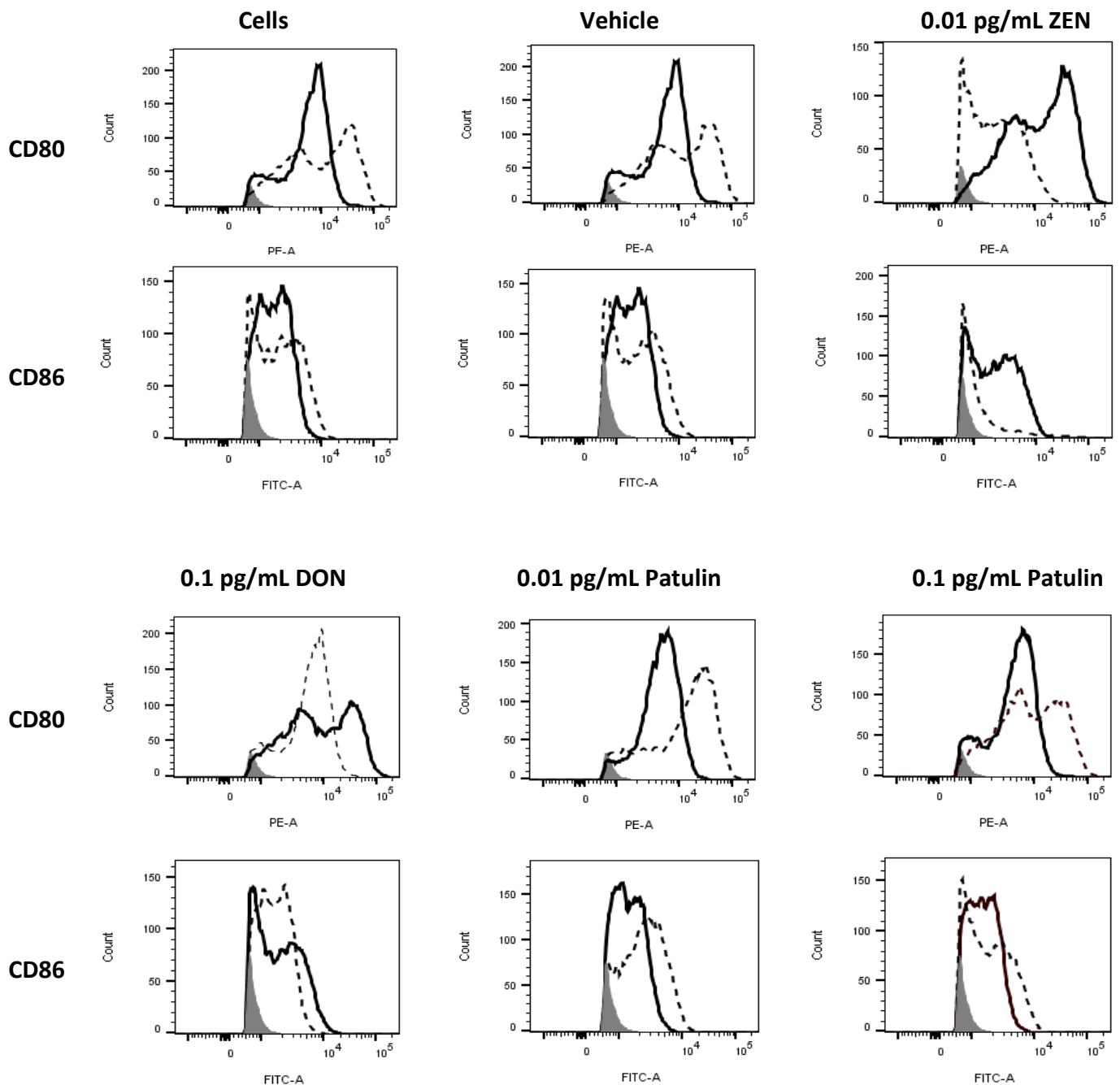


Figure 5.5: Expression of CD80 and CD86 on the surface of J774A.1 murine macrophage cells, cultured for 24 hours in the presence of **patulin, DON, ZEN and T-2 Toxin**, with and without LPS (100 ng/mL) stimulation. The toxin treatment alone is represented by the solid lines and the toxin treatment with LPS challenge is represented by the dashed lines. Unstained cells are represented by the filled grey histogram.

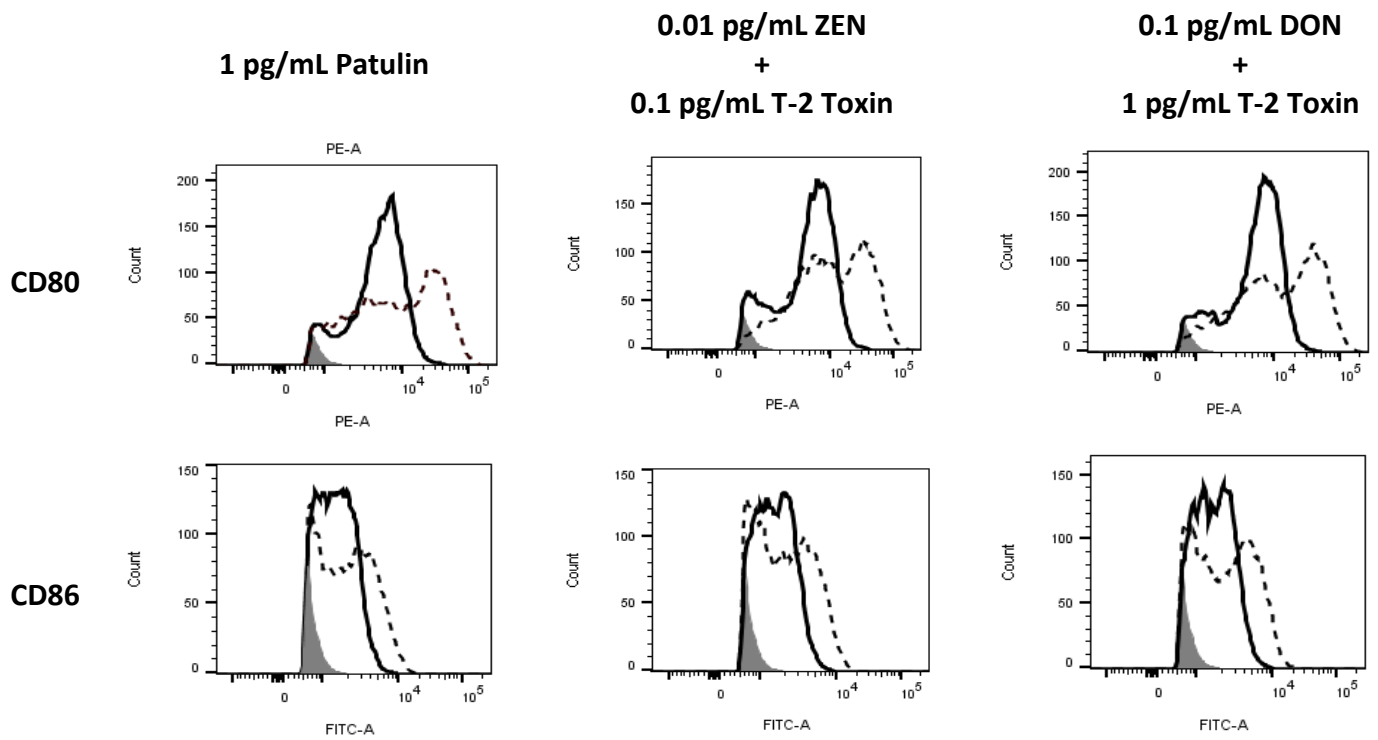


Figure 5.6: Expression of CD80 and CD86 on the surface of J774A.1 murine macrophage cells, cultured for 24 hours in the presence of **patulin, DON, ZEN and T-2 Toxin**, with and without LPS (100 ng/mL) stimulation. The toxin treatment alone is represented by the solid lines and the toxin treatment with LPS challenge is represented by the dashed lines. Unstained cells are represented by the filled grey histogram.

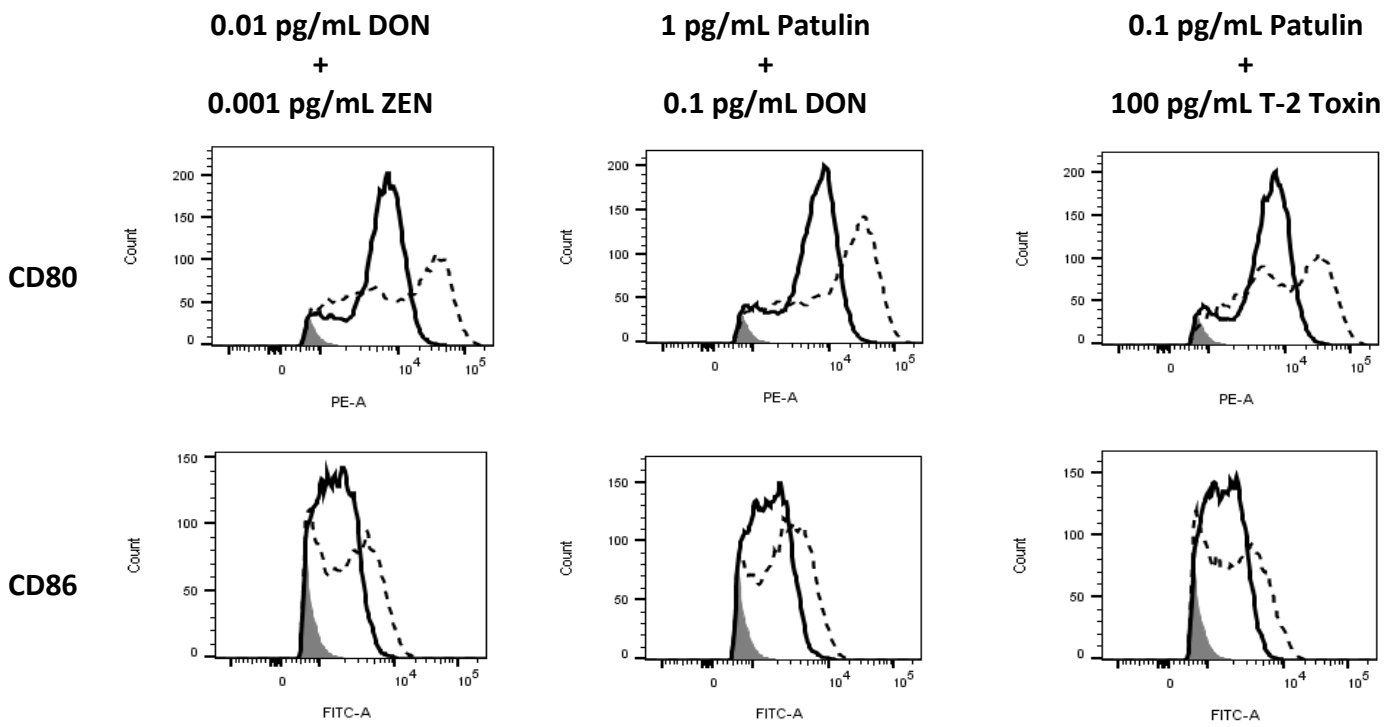


Figure 5.7: Expression of CD80 and CD86 on the surface of J774A.1 murine macrophage cells, cultured for 24 hours in the presence of **patulin, DON, ZEN and T-2 Toxin**, with and without LPS (100 ng/mL) stimulation. The toxin treatment alone is represented by the solid lines and the toxin treatment with LPS challenge is represented by the dashed lines. Unstained cells are represented by the filled grey histogram.

Table 5.1: Expression of CD80, CD86, MHCII and TLR4 on the surface of J774A.1 murine macrophage cells, cultured for 24 hours in the presence of **patulin, DON, ZEN and T-2 Toxin**, with and without LPS (100 ng/mL) stimulation. Cells were stained with anti-CD86 antibody, labelled with FITC, anti-CD80 antibody, labelled with PE, anti-MHCII antibody, labelled with PE and anti-TLR4 antibody, labelled with FITC. Samples were analysed using a FACSAria™ flow cytometer (BD) and FlowJo software (Treestar). Data is represented as the difference in mean fluorescence intensity (MFI), compared to the control cells.

Treatment	CD80	+LPS	CD86	+LPS	TLR4	+LPS	MHCII	+LPS
Vehicle	29	53.1	35.4	48.3	50.8	60.1	33	75.5
0.01 pg/mL ZEN	57.1	6.19	48.3	15.6	85.1	58.6	97.4	74.2
0.1 pg/mL DON	47.2	26.9	43.4	31.2	55.1	51	71	30.8
0.01 pg/mL Patulin	15.3	64.9	24.7	57.7				
0.1 pg/mL Patulin	16.5	46.5	26.1	41.1				
1 pg/mL Patulin	16.5	48.6	25.9	47.3				
0.01 pg/mL ZEN + 0.1 pg/mL T-2 Toxin	20.8	53.8	30.1	47				
0.1 pg/mL DON + 1 pg/mL T-2 Toxin	28.1	55.9	33.9	52.4				
0.01 pg/mL DON + 0.001 pg/mL ZEN	23.4	49.5	30.5	50.8				
1 pg/mL Patulin + 0.1 pg/mL DON	27.5	61.5	33.8	58.2				
0.1 pg/mL Patulin + 100 pg/mL T-2 Toxin	22.6	49.6	30.2	48.6	11.6	55.7	27.6	73.5
0.01 pg/mL Patulin + 0.001 pg/mL ZEN					28.8	59.2	45.4	75.7

5.2.3 Analysis of multiple mycotoxin exposure on J774A.1 murine macrophage cell surface marker expression using Lab-in-a-Trench

5.2.3.1 J774A.1 macrophage cell surface marker expression after exposure to patulin, zearalenone, deoxynivalenol and T-2 toxin with LPS challenge

Opto-microfluidic monitoring of CD80 and CD86 expression dynamics on J774A.1 murine macrophage cells was carried out using LiaT technology. Cells (20 – 40) were captured in a microfluidic LiaT device and stimulated with LPS (200 ng/mL). The CD80 and CD86 expression was visualized with PE-labelled anti-CD80 and FITC-labelled anti-CD86 antibodies. The laminar flow conditions assure a vanishing flow field throughout the trench, thus permanently retaining particles and minimizing hydrodynamic stress. Furthermore, its small depth of 150 μm allows continuous loading, mixing and refreshment of reagents by mere diffusion from a controlled flow through the supply channel on the top of the trench. Brightfield, FTIC and PE fluorescent images were acquired by mounting the chip on an inverted fluorescence microscope (Olympus IX81) and imaging at time points. Concentration kinetics for CD80 and CD86 were quantified in real-time for cells in the trench. Data for 20 individual cells was analysed using ImageJ software.

The analysis showed that many of the effects observed in the flow cytometry analysis of CD80 and CD86 was also observed in the LiaT data. For example, suppression of CD80 by 0.01 $\mu\text{g/mL}$ ZEN and 0.1 $\mu\text{g/mL}$ DON or the dramatic effects of 0.01 $\mu\text{g/mL}$ and 0.1 $\mu\text{g/mL}$ patulin on CD86 expression levels. The data also allows a direct comparison of the effects of individual mycotoxins versus their combinations. The data from this investigation demonstrates the ability of the LiaT platform to successfully determine the levels of surface makers in 'real-time' and in response to mycotoxin exposure and LPS stimulation.

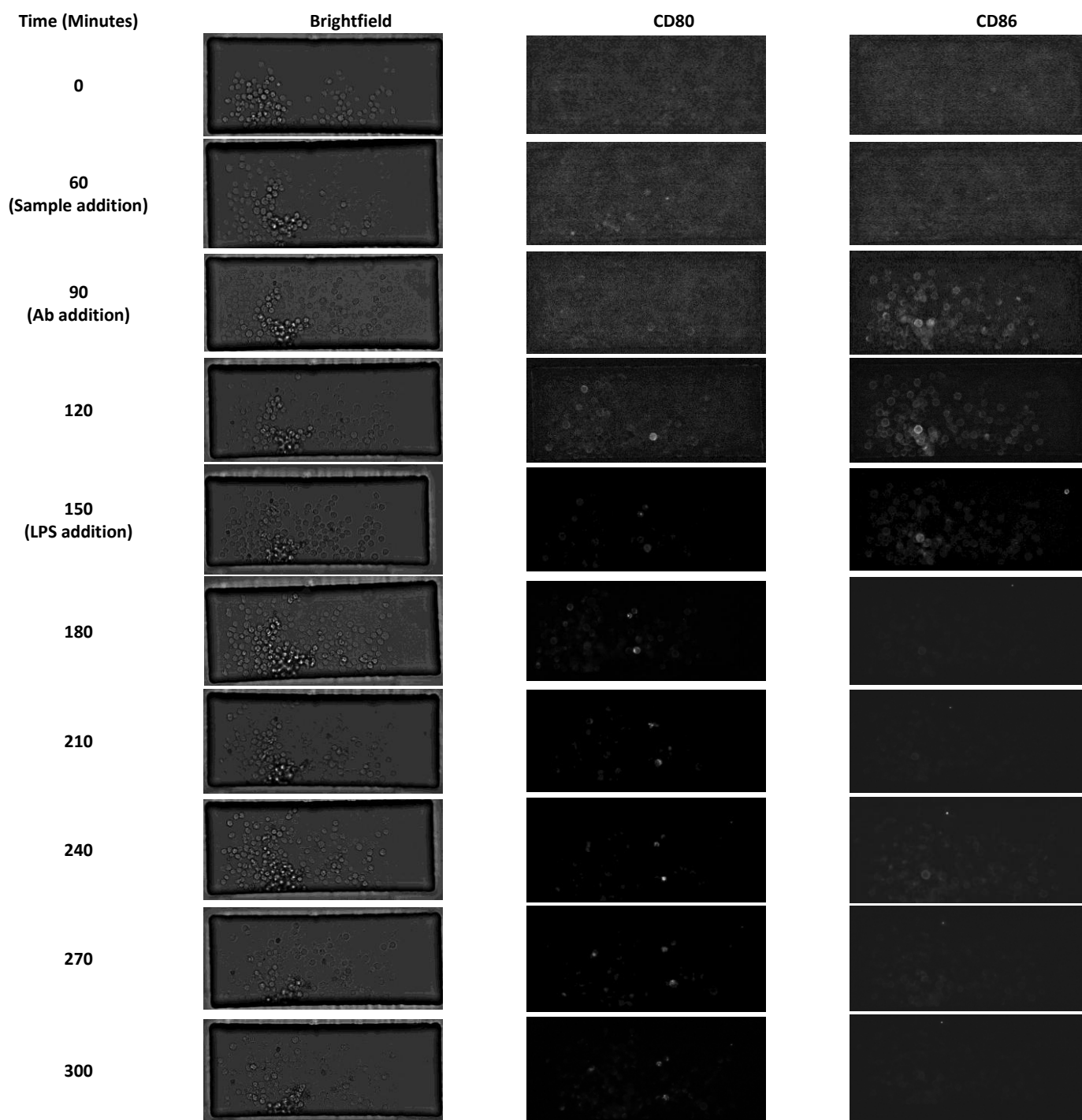


Figure 5.8: Opto-microfluidic monitoring of CD80 and CD86 expression dynamics on J774A.1 murine macrophage cells. Cells (20 – 40) were captured in a microfluidic Lab-in-a-Trench device and stimulated with LPS (200 ng/mL). The CD80 and CD86 expression was visualized with PE-labelled anti-CD80 and FITC-labelled anti-CD86 antibodies and recorded using brightfield and fluorescent microscopy. Concentration kinetics for CD80 and CD86 were quantified in real-time for cells in the trench.

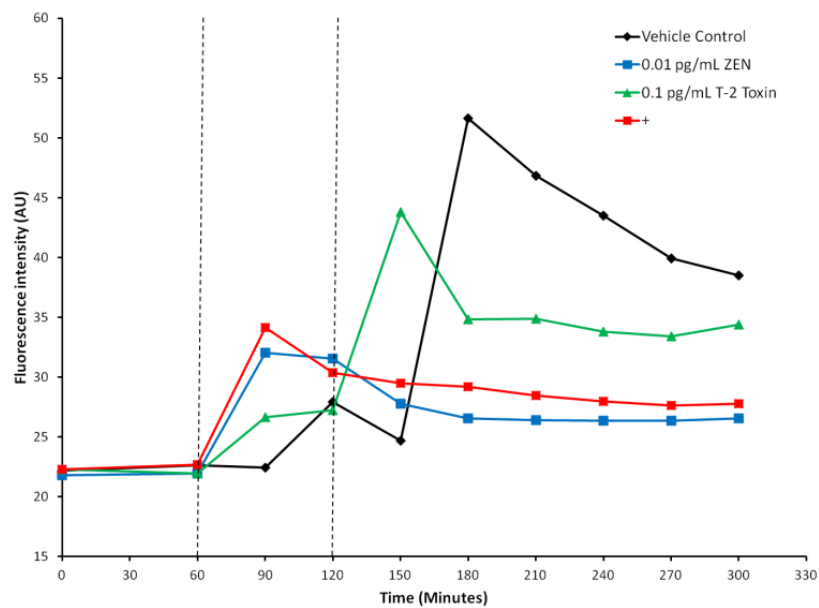


Figure 5.9: ‘Real-time’ monitoring for **CD80** expression on the surface of J774A.1 murine macrophage cells captured in a microfluidic Lab-in-a-Trench device, exposed to **ZEN and T-2 Toxin** (first dashed line) then stimulated with 200 ng/mL LPS (second dashed line). Mycotoxin combinations are represented by the plus symbol (+).

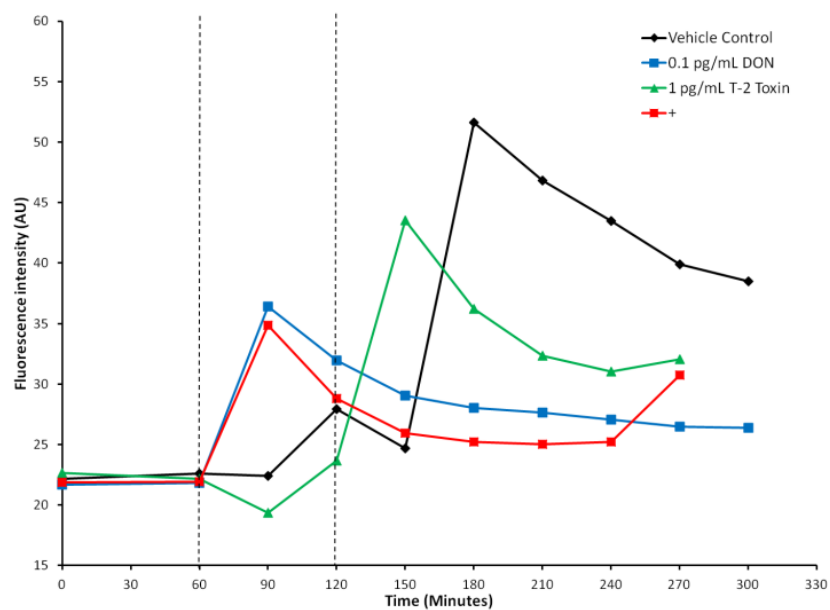


Figure 5.10: ‘Real-time’ monitoring for **CD80** expression on the surface of J774A.1 murine macrophage cells captured in a microfluidic Lab-in-a-Trench device, exposed to **DON and T-2 Toxin** (first dashed line) then stimulated with 200 ng/mL LPS (second dashed line). Mycotoxin combinations are represented by the plus symbol (+).

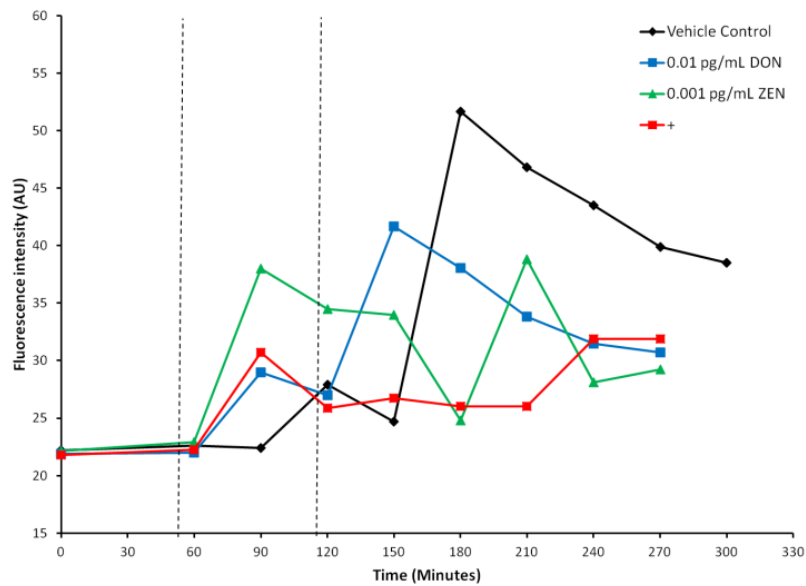


Figure 5.11: ‘Real-time’ monitoring for **CD80** expression on the surface of J774A.1 murine macrophage cells captured in a microfluidic Lab-in-a-Trench device, exposed to **DON and ZEN** (first dashed line) then stimulated with 200 ng/mL LPS (second dashed line). Mycotoxin combinations are represented by the plus symbol (+).

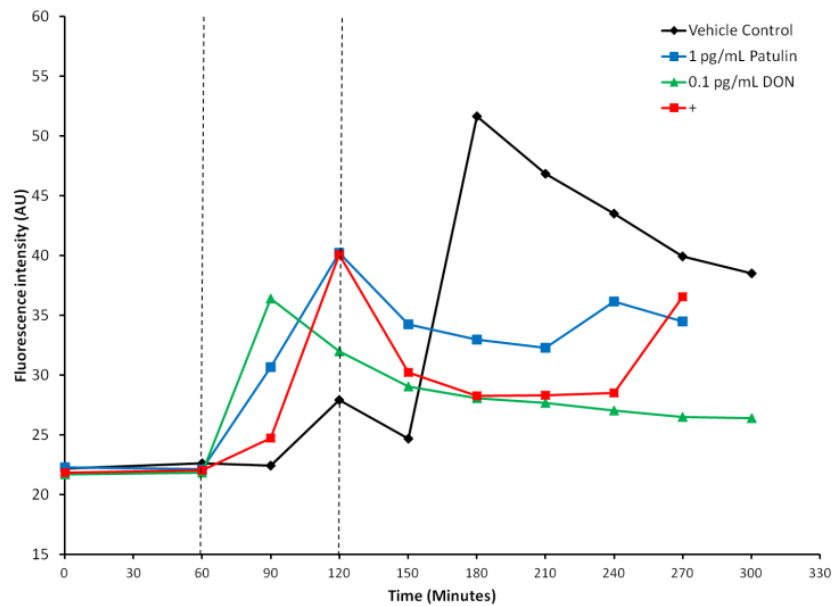


Figure 5.12: ‘Real-time’ monitoring for **CD80** expression on the surface of J774A.1 murine macrophage cells captured in a microfluidic Lab-in-a-Trench device, exposed to **patulin and DON** (first dashed line) then stimulated with 200 ng/mL LPS (second dashed line). Mycotoxin combinations are represented by the plus symbol (+).

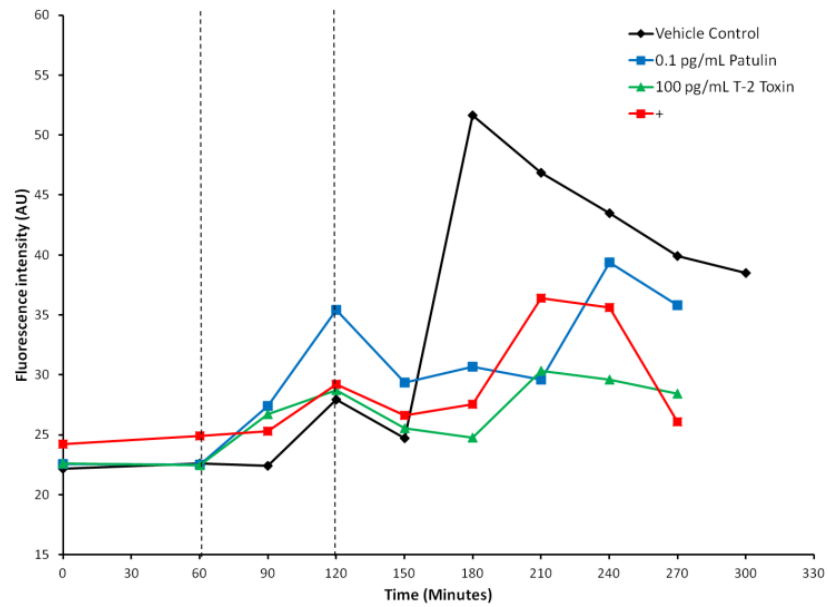


Figure 5.13: ‘Real-time’ monitoring for **CD80** expression on the surface of J774A.1 murine macrophage cells captured in a microfluidic Lab-in-a-Trench device, exposed to **patulin and T-2 Toxin** (first dashed line) then stimulated with 200 ng/mL LPS (second dashed line). Mycotoxin combinations are represented by the plus symbol (+).

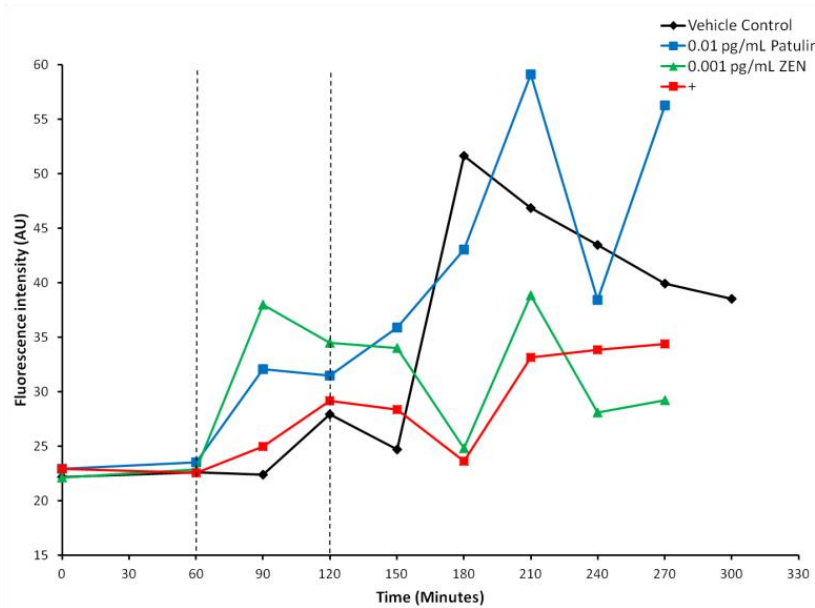


Figure 5.14: ‘Real-time’ monitoring for **CD80** expression on the surface of J774A.1 murine macrophage cells captured in a microfluidic Lab-in-a-Trench device, exposed to **patulin and ZEN** (first dashed line) then stimulated with 200 ng/mL LPS (second dashed line). Mycotoxin combinations are represented by the plus symbol (+).

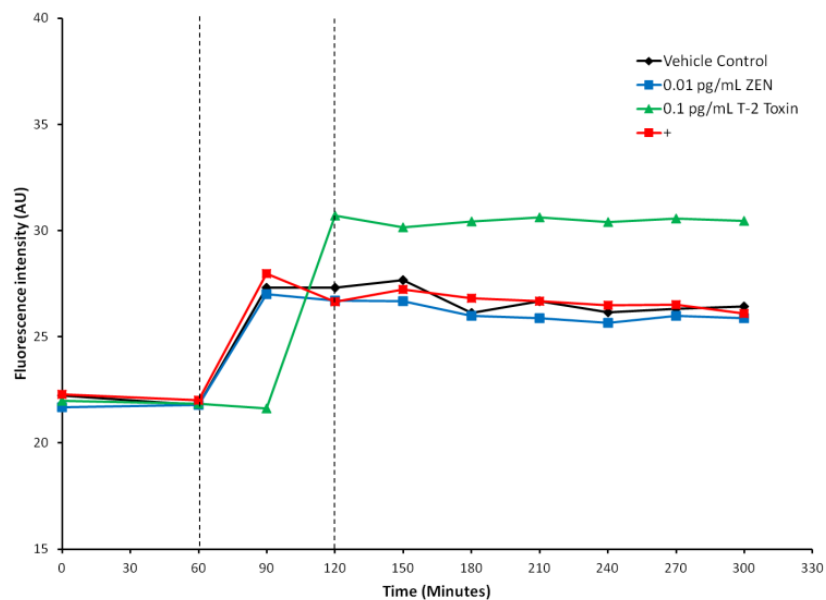


Figure 5.15: ‘Real-time’ monitoring for **CD86** expression on the surface of J774A.1 murine macrophage cells captured in a microfluidic Lab-in-a-Trench device, exposed to **ZEN and T-2 Toxin** (first dashed line) then stimulated with 200 ng/mL LPS (second dashed line). Mycotoxin combinations are represented by the plus symbol (+).

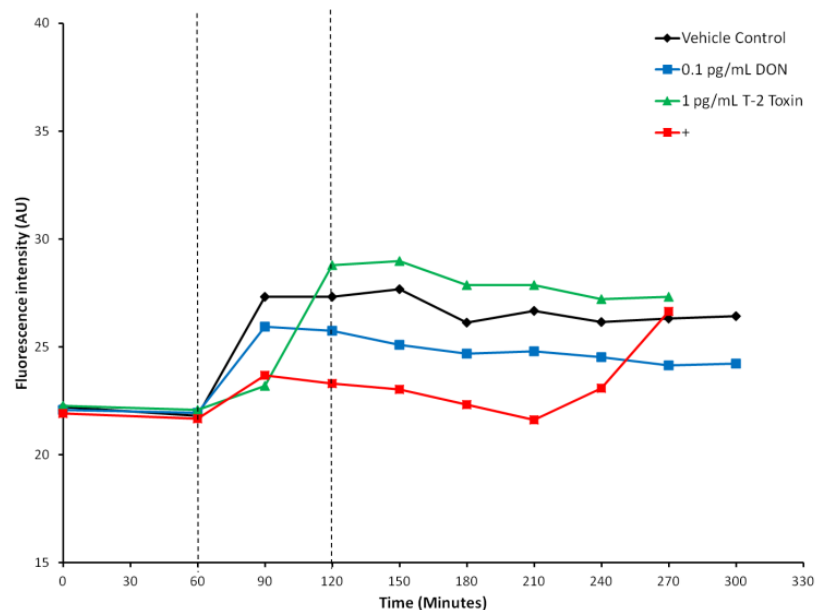


Figure 5.16: ‘Real-time’ monitoring for **CD86** expression on the surface of J774A.1 murine macrophage cells captured in a microfluidic Lab-in-a-Trench device, exposed to **DON and T-2 Toxin** (first dashed line) then stimulated with 200 ng/mL LPS (second dashed line). Mycotoxin combinations are represented by the plus symbol (+).

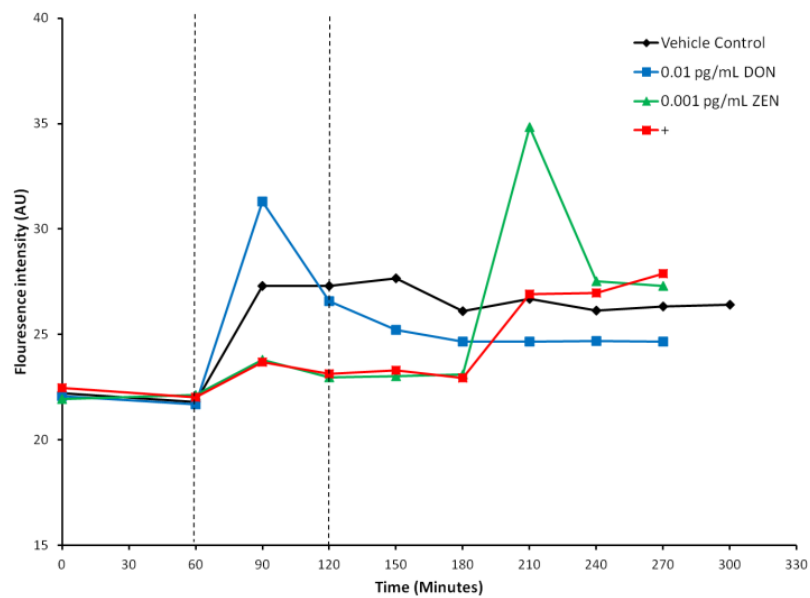


Figure 5.17: ‘Real-time’ monitoring for **CD86** expression on the surface of J774A.1 murine macrophage cells captured in a microfluidic Lab-in-a-Trench device, exposed to **DON and ZEN** (first dashed line) then stimulated with 200 ng/mL LPS (second dashed line). Mycotoxin combinations are represented by the plus symbol (+).

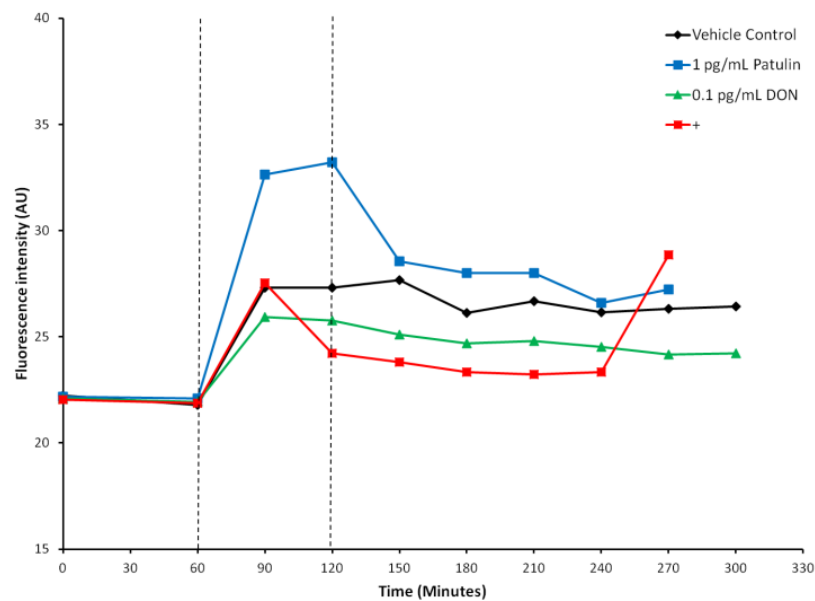


Figure 5.18: ‘Real-time’ monitoring for **CD86** expression on the surface of J774A.1 murine macrophage cells captured in a microfluidic Lab-in-a-Trench device, exposed to **patulin and DON** (first dashed line) then stimulated with 200 ng/mL LPS (second dashed line). Mycotoxin combinations are represented by the plus symbol (+).

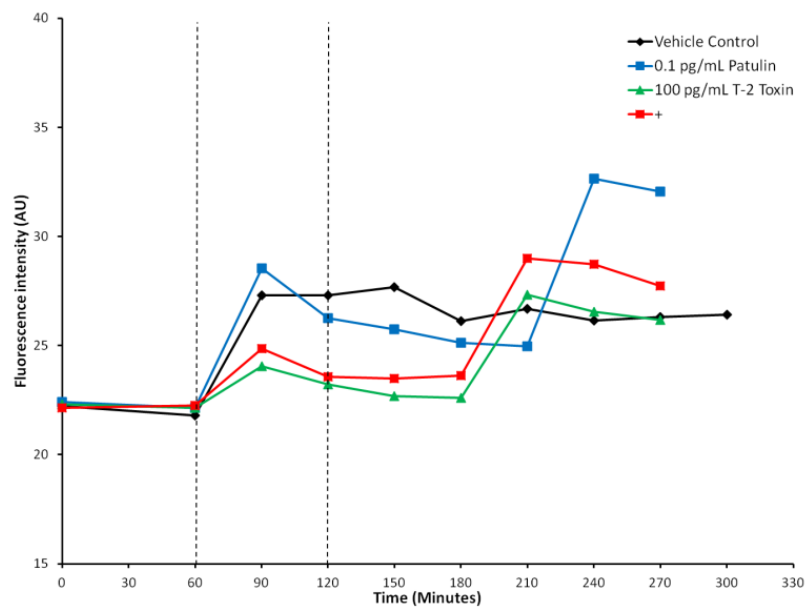


Figure 5.19: ‘Real-time’ monitoring for **CD86** expression on the surface of J774A.1 murine macrophage cells captured in a microfluidic Lab-in-a-Trench device, exposed to **patulin and T-2 Toxin** (first dashed line) then stimulated with 200 ng/mL LPS (second dashed line). Mycotoxin combinations are represented by the plus symbol (+).

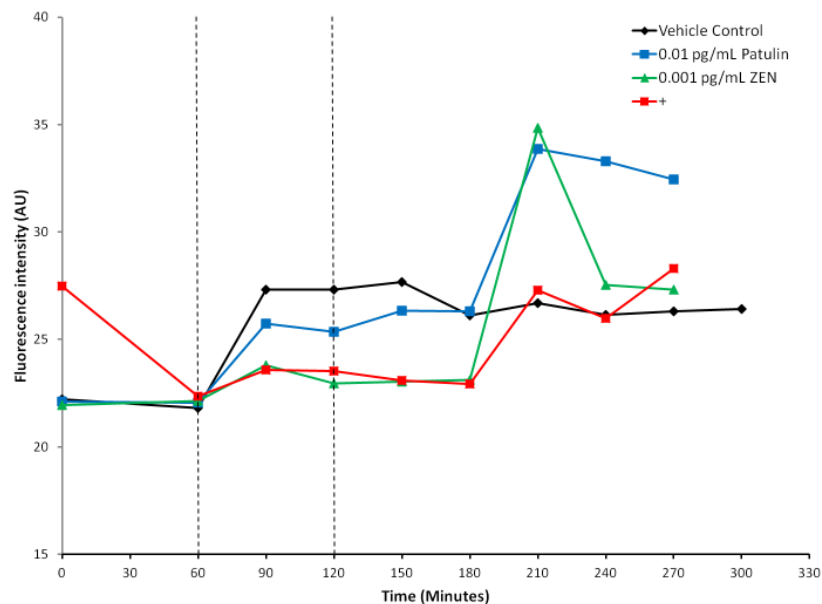


Figure 5.20: ‘Real-time’ monitoring for **CD86** expression on the surface of J774A.1 murine macrophage cells captured in a microfluidic Lab-in-a-Trench device, exposed to **patulin and ZEN** (first dashed line) then stimulated with 200 ng/mL LPS (second dashed line). Mycotoxin combinations are represented by the plus symbol (+).

5.3 Discussion

As previously discussed, contamination of food and feed with multiple mycotoxins is common and exposure to low concentrations these of these toxins cannot be avoided. Understanding how these low concentrations of multiple mycotoxins interact with each other and the immune system must now be a priority. The ability to monitor and quantify the “cocktail effect” of multiple contaminants in a sample is moving from desirable to necessary. Therefore, it is important to understand just how these low concentrations of multiple mycotoxins exactly interact with the immune systems of humans and animals and, furthermore, design methods capable of measuring these effects in a rapid and cost-effective manner.

Firstly, the aim of this study was to build on the work of chapter 3 and chapter 4. Chapter 3 demonstrated the dose-dependent modulation of cytokine secretion by individual mycotoxins. Chapter 4 then used this information to show how binary combinations of these mycotoxins can differ significantly from their individual effects with relation to their effect on cytokine expression levels. The cell surface marker data displayed in this chapter supports this data and demonstrates that these mycotoxins, alone and in combinations, have varying effects on the expression levels of the key cell surface markers CD80, CD86, MHCII and TLR4, as well as on phagocytosis. These effects are dependent on mycotoxin concentration, combination and exposure to LPS. Once again, it is apparent that these mycotoxins can be immunostimulatory or immunosuppressive depending on the concentration and combinations.

For example, 0.1 pg/mL DON increased phagocytosis after LPS stimulation but this was decreased without LPS challenge. The combinations of 0.01 pg/mL DON and 0.001 pg/mL ZEN showed an increase in phagocytosis without LPS, while the combinations of 0.1 pg/mL patulin and 0.001 pg/mL ZEN increased phagocytosis after LPS activation. Phagocytosis is a vital role of all macrophages and is fundamental in the ingestion and clearing of pathogens (Aderem, 2003). Numerous diseases have resulted from a decrease in the ability of macrophages to phagocytose (Allen and Aderem, 1996). Phagocytosis is crucial in the host in controlling infection and it has been well documented that a reduction in phagocytosis can cause increased susceptibility to infection (Morran *et al.*, 2009).

ZEN (0.01pg/mL) caused an increased expression of MHCII, TLR4, CD80 and CD80 without LPS but after LPS activation the levels of all of these cell surface markers are decreased by this concentration. MHCII and CD80 levels are increased when exposed to 0.1 pg/mL DON without LPS but a reduction in CD80 levels is seen after LPS stimulations compared to controls. Patulin appears to show suppression in the levels of CD80 and CD80 at a number of concentrations (0.01, 0.1 and 1 pg/mL) both with and without LPS activation. Combinations of these patulin concentrations with DON, ZEN and T-2 show significant effects on the expression levels of all four surface makers. Overall, examples of these mycotoxins working additively, synergistically and agnostically were observed depending on the concentrations and combinations. TLRs sense invasion of pathogens by detecting microbial components that are conserved among micro-organisms thus triggering the activation of innate immunity. They are considered a link between innate and adaptive immunity due to their promotion of pro-inflammatory cytokine production, surface maker expression and activation of T cells. On engagement with ligands, TLRs recruit specific adaptor molecules that propagate downstream signalling (McCoy *et al.*, 2008). Roles for TLRs have emerged in sepsis (Lorenz *et al.*, 2002), RA (Seibl *et al.*, 2003), asthma (Eder *et al.*, 2004) and atherosclerosis (Kiechl *et al.*, 2003). TLR4 is key player of the inflammatory process due to both infectious and non-infectious stimuli. In several pathological conditions TLR4 engagement contributes to disease resolution; however, when TLR4 activation pathways are poorly regulated as demonstrated here, it can contribute to disease progression (Molteni *et al.*, 2016). Ryan *et al.* (2011) investigated the role of TLR4 in *Clostridium difficile* infection and the recognition of surface layer proteins (SLPs), and indicated that SLPs isolated from *C. difficile* can activate innate and adaptive immunity and that these effects are mediated by TLR4, with TLR4 having a functional role in experimental *C. difficile* infection.

The main function of MHCII is to present processed antigens, which are derived primarily from exogenous sources, to CD4(+) T-lymphocytes. MHCII molecules thereby are critical for the initiation of the antigen-specific immune response. Besides antigen presentation, growing evidence is showing that ligation of MHCII molecules also activates intracellular signalling pathways, frequently leading to apoptosis (Holling *et al.*, 2004). The consequences are almost always deleterious to a pathogen as

macrophages and B cells are activated to produce antibodies that eliminate or neutralise pathogens. Thus, there is strong selective pressure in favour of any pathogen that has the ability to escape presentation by an MHC molecule. Many infections have been shown to reduce MHCII expression to avoid protective immune response such as *Chlamydia trachomatis* (Zhong *et al.*, 1999) and listerial infection (Schüller *et al.*, 2008). Abnormal expression of MHCII, shown in this data, can be linked to the development of autoimmune and infectious diseases (Guardiola and Maffei, 1993). The susceptibility of mice deficient in the MHCII transactivator to infection with *M. tuberculosis* has been demonstrated (Repique *et al.*, 2003).

The interaction of surface markers CD80 and CD86 with T cells plays a major role in the activation and expansion of all effector and regulatory Th cell subsets (Lu *et al.*, 1997). Over-expression of these surface markers has been reported in the inflamed tissue of patients with RA and IBD (Maerten *et al.*, 2003). The engagement of CD80 and CD86 on APCs with CD28 on T cells initiates T cell proliferation and differentiation and also cytokine production. CD80 and CD86 play important pathogenic roles in T-cell responses. Up-regulation of CD80 and loss of constitutive CD86 expression on monocytes was associated with higher severity of illness and inflammation (Nolan *et al.*, 2009). CD80 and CD86 activation also synergizes with TLR-4 signalling to produce IL-27 and IL-10. Dysregulation of CD80 and CD86 expression has been observed in autoimmune disorders and cancer, and may also influence the development of immune responses including production of cytokines in response to stimulation with LPS. In 2003, Miyahira *et al.* examined the contribution of CD28-CD80/CD86 co-stimulatory pathway to protection from *Trypanosoma cruzi* infection and their results demonstrate a critical contribution of the CD28-CD80/CD86 co-stimulatory pathway not only to natural protection against primary *T. cruzi* infection but also to DNA vaccine-induced protective immunity to Chagas' disease.

Interestingly, throughout this thesis, ZEN has been shown to modulate several key cytokines and cell surface markers. It has been long known that ZEN is capable of binding oestrogen receptors. Oestrogen has been shown to be a major regulator of wound repair that can reverse age-related impaired wound healing in human and animal models, characterised by a dampened inflammatory response and increased matrix deposited at the wound site. Macrophage migration inhibitory factor (MIF) is a

candidate pro-inflammatory cytokine involved in the hormonal regulation of inflammation. Ashcroft *et al.* (2003), demonstrated that MIF is up-regulated in a distinct spatial and temporal pattern during wound healing and its expression is markedly elevated in wounds of oestrogen-deficient mice as compared with intact animals. Conversely, research on age-related impaired wound healing suggests that the decline in sex steroid hormones with age may have a substantial influence on the inflammatory response *in vivo*. Topical and systemic oestrogen treatments have shown an increased rate of healing by reducing inflammation, however, the underlying mechanisms are little understood. Routley and Ashcroft (2009), suggest that with the reduction of steroid hormones macrophages are activated in a classical manner, promoting inflammation, whereas oestrogen or progesterone are contributing toward macrophage activation in an alternative manner, driving wound repair, angiogenesis, and remodelling. It is possible that ZEN can replicate the effect demonstrated by oestrogen and therefore alter hormone-related immune function.

There have been some published reports on the effect of mycotoxins on cell surface marker expression and phagocytosis. Liu *et al.* (2002) showed that fumonisin B1 and aflatoxin B1 had significant effects on the phagocytosis of swine alveolar macrophages. Oh *et al.* (2015) examined the effect of the *Penicillium* mycotoxins citrinin, ochratoxin A, patulin, mycophenolic acid and penicillic acid on phagocytosis of bovine macrophage function. They found that exposure to sub-lethal concentrations of toxins can affect macrophage function, similar to this study. PAT and PA, for example, significantly decreased the percentage phagocytosis of MAP at concentrations of 5.0 μM , and 15.6 μM , respectively, while OTA significantly increased the percentage phagocytosis of MAP at concentrations of 6.3 μM and 12.5 μM .

In 2000, Moon and Pyo showed that AFB1 pre-treatment, followed by LPS stimulation, decreased expression of the CD14 surface marker in murine peritoneal macrophages. However, CD14 expression was unaffected in cells that were pre-treated with AFB1, but not challenged with LPS. These differences in effects with and without LPS challenge are also seen throughout the data in this and previous chapters. Mycotoxins appear to exert different effects depending on the presence of the bacterial cell wall component. Müller *et al.* (2003) examined the immunomodulatory effects of ochratoxin A and some of its metabolites on the human monocyte/macrophage line

THP-1. They found that phagocytic behaviour and cell surface markers were largely suppressed by these mycotoxins at concentrations between 10 and 1000 ng/mL, and, in individual cases it was already occurring at 1 ng/mL. These concentrations are higher than the one used in this study but support the ability of these toxins to exert significant effects at low concentrations. Bruneau *et al.* (2012) found aflatoxin exposure affected expression levels of key cell surface markers involved in the inflammatory response. In their study, TLR2 and CD14 expression levels decreased significantly, but TLR4 expression was unaffected. Their study also highlighted the potential additive and synergistic effects that are observed in the data presented here. In 2014 Hymery *et al.* performed *in vitro* studies on the cytotoxicity and immunotoxicity of the mycotoxin cyclopiazonic acid (CPA) on human cells (CD34+, monocytes, THP-1 and Caco-2). The CPA effect on macrophage differentiation was examined at non-cytotoxic concentrations and it was found that the monocyte differentiation process was markedly disturbed in the presence of CPA. After 6 days of culture, CD71 expression was downregulated, while the expression of CD14 and CD11a did not change.

It is evident that mycotoxins, alone and in combinations, possess the ability to disrupt the signaling and functional ability of macrophages even at sub-lethal concentrations. The studies described above, along with the data in this chapter, highlight the importance of understanding how mycotoxins, particularly at sub-lethal concentrations, interact with the immune systems of humans and animals. Evidence has been presented to show that even if a mycotoxin does not have an effect alone its combination with another can produce detrimental results. This has significant consequences for food safety monitoring. We must be able to account for the combinatory effects of multiple adulterants in contaminated food samples.

The data obtained from LiaT is also largely significant in this respect. Many of the effects observed in the flow cytometry analysis of CD80 and CD86 were also observed in LiaT analysis. The data also allows a direct comparison of the effects of individual mycotoxins versus their combinations. Some effects observed in the flow cytometry analysis, such as the suppression of CD86 by patulin and T-2 toxin following LPS stimulation, were not replicated in LiaT results but, overall, the ability of LiaT to complete with traditional flow cytometry methods was shown. This successfully

demonstrates the ability to measure the effects of multiple mycotoxins in a sample in 'real-time'. At present, there are no methods of doing this available. Currently, methods of mycotoxin analysis are based on the measurement of single mycotoxins in samples and do not take into account the "cocktail effect" of multiple contaminants in a sample. The LiaT offers a simple and robust method to measure potential additive and synergistic effects of multiple mycotoxins in 'real-time'. This analysis is not limited to mycotoxins analysis and has the potential to be used for any adulterants in a sample. The future of food analysis will require much more than simple individual quantification and a technology like LiaT can offer a novel strategy to develop more sophisticated testing that can provide more meaningful data for food safety analysis.

**Chapter 6: Generation of avian
recombinant antibody
libraries to the mycotoxins;
patulin, ochratoxin A and
aflatoxin M1**

6.1 Introduction

Mycotoxins are a major global food safety issue. It is estimated that 200,000 people are added to the global food demand daily and by the year 2050, the world population will surpass 9 billion (UNEP, 2013). Since the health of human populations is largely determined by the condition of food-producing ecosystems, pressures placed on supply may directly impact both the quantity and quality of available food. Populations residing in developing countries and rural areas are generally dependent on locally-produced foods and face issues related to food security and food quality. Increasing demand along with climate change underscores the importance of the role of mycotoxins in the changing environment. Susceptible populations, such as rural residents dependent on staple crops prone to mold contamination, and the economically disadvantaged, who may be forced to consume lower quality foodstuffs may be disproportionately affected by global climate change and resultant heightened exposure to mycotoxins (Marroquín-Cardona *et al.*, 2014). Children may be particularly vulnerable to the effects of mycotoxins. In the case of mycotoxins, there is increased interest on the relationship between mycotoxin exposure (mainly aflatoxins, fumonisins and DON) and growth retardation due to under-nutrition in children under five and *in utero*. The global burden of disease attributable to under-nutrition in children is massive; in 2000 the World Health Organization estimated underweight accounted for 3.7 million deaths and approximately 138 million disability-adjusted years (DALYs) in children under the age of five (Williams *et al.*, 2004). Ultimately, these concerns have led to the introduction of limits for mycotoxins across the world. In order to monitor and enforce these limits a number of methodologies are employed for food analysis.

6.1.1 Detection methodologies for mycotoxins

Liquid chromatographic methods are the cornerstone of mycotoxin analysis, with the key AOAC methods centred on LC separation coupled with MS detection. It is accepted that LC-MS and LC-fluorescence are the gold standard against which all other methods are compared (Yeni *et al.*, 2014). There is significant focus on the further development of HPLC protocols and related techniques (Turnder *et al.*, 2015). TLC and GC analyses are often considered to be less practical, or to have insufficient sensitivity compared with LC methods. However, they still have uses in certain situations (Welke *et al.*, 2009; Rodríguez-Carrasco *et al.*, 2012; Caputo *et al.*, 2014). Chromatographic

techniques will always be the gold standard against which all other techniques are compared. The extreme sensitivity and flexibility observed in published analyses (Turner *et al.*, 2015), as highlighted by the ability to detect multiple analytes (sometimes over 50) at ppb levels in complex samples, cannot be matched. However, LC methods will always suffer from lack of portability, cost and other practical issues. Hence, there is significant focus on developing analytical methodologies, such as biosensors and other immunological techniques, as these are often designed to measure directly at the site of requirement with minimal preparation.

The ability to generate highly specific antibodies is now well established and has proven hugely beneficial for mycotoxin analysis (Daly *et al.*, 2000; Dunne *et al.*, 2005; Edupuganti *et al.*, 2013). Immunochemical detection methods vary from simple lateral flow immunoassays and ELISAs to highly sophisticated immunosensors. Many ELISA kits for mycotoxin detection have been successfully commercialised in the past two decades (Turner *et al.*, 2015; Bahadır and Sezgentürk, 2015). The portability of a test and opportunity for application in situations of minimal use (i.e. a customer requiring a single screening test instead of purchasing expensive analytical equipment) has meant that ELISA methodologies are still popular. However, while ELISA formats are known to be reliable and excellent for screening, the method is time consuming and requires multiple steps and specialist plate readers. If one wishes to gain more information beyond simple screening it is not suitable for field testing. Therefore, the integration of suitable molecular recognition elements, such as antibodies, directly with transduction systems is favoured for portable, non-laboratory-based analysis.

The field of biosensors is rapidly growing. Advances in fabrication techniques, decreased cost, increased sensitivity of transducers, and the desire to bring analyses out of the lab have led to significant interest in the development of such sensors (Wang *et al.*, 2014). Mycotoxins provide excellent targets for such studies, from both the academic and commercial viewpoints. The development of analytical methods that would class as biosensors is now beginning to outweigh the chromatographic development significantly (Marroquín-Cardona *et al.*, 2014). In order to compete with the gold standard LC methods, antibodies that can detect mycotoxins with high sensitivity below the legislated limits are required for incorporation on to these biosensor devices.

6.1.2 Chapter aims

The aim of the research described in this chapter was to generate avian immune libraries for the isolation of recombinant antibody fragments to target the mycotoxins patulin, ochratoxin A and Aflatoxin M1. There has been great difficulty in producing an antibody to target patulin due to its small size (~150 Da), whereas antibodies targeting AFM1 have often suffered issues with matrix effects and cross-reactivity. Therefore, antibodies are required that can detect these mycotoxins with high sensitivity and specificity below the limits of detection required by legislation.

This chapter describes the immunisation of avian hosts with mycotoxin conjugates, RNA extraction and cDNA synthesis. The successful optimisation of antibody variable regions and the joining of these regions by SOE-PCR will be detailed. Finally, the digestion of this SOE product and ligation into a vector followed by transformation into competent cells for antibody library production will be described.

The screening of these libraries by bio-panning, using phage display technology, to isolate clones capable of binding the mycotoxin targets is outlined. These scFv can be used in immunoassay formats to detect OTA, AFM1 and patulin in food samples with high sensitivity.

6.2 Results

6.2.1 Production of an avian recombinant scFv library for aflatoxin M1 and patulin

6.2.1.1 Avian immune response generation to mycotoxin conjugates

An immune response was generated in avian hosts by immunisation with mycotoxin conjugates (Sigma-Aldrich, Ireland). Prior to the euthanasia of the immunised chicken, a serum titre was performed to determine whether a sufficient immune response was generated. In order to characterise the true response to the toxin, an alternative coating conjugate was utilised. As an alternative coating conjugate was not available for AFM1, a depletion step was added to remove BSA-specific antibodies, as BSA was the carrier used in the original immunisations.

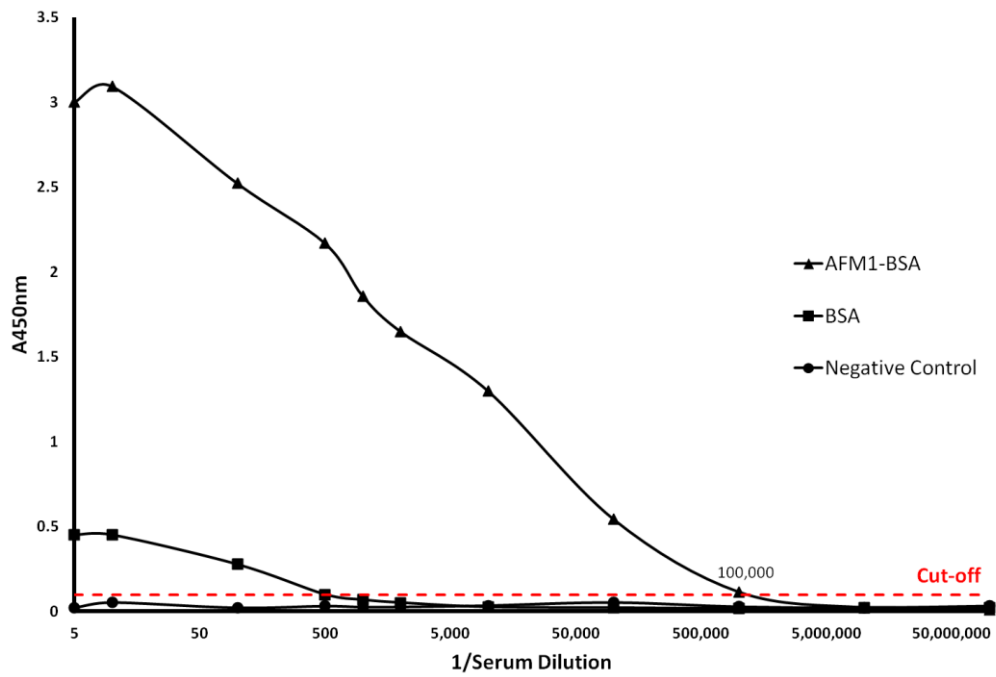


Figure 6.1: Serum titre of an **AFM1-BSA** immunised chicken determined by indirect ELISA. Following depletion with BSA, doubling dilutions of serum were added to an ELISA plate coated with 10 µg/mL AFM1-BSA conjugate. Binding was detected with an anti-chicken (IgY) antibody, conjugated to horseradish peroxidase (HRP). The ELISA was developed with TMB substrate and the absorbance was measured at 450 nm, using a Tecan™ Safire II plate reader. The x-axis represents absorbance at 450 nm, the y-axis is the log of doubling dilutions of serum, and the red dashed line (---) is the cut-off, equivalent to 3SD of the negative control.

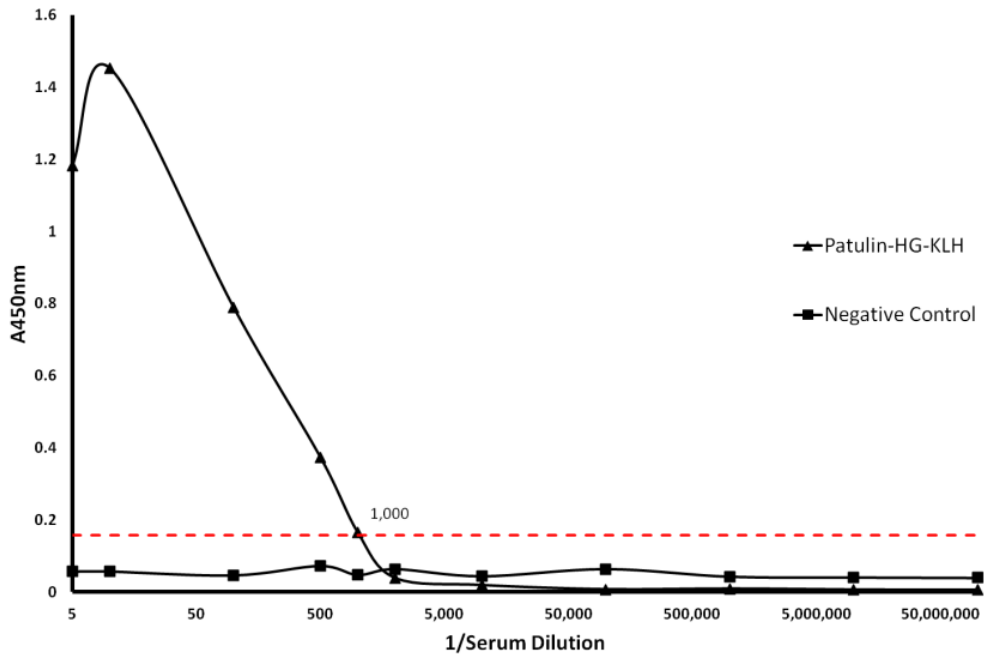


Figure 6.2: Serum titre of a **patulin-HG-KLH** immunised chicken determined by indirect ELISA. Following depletion with BSA, doubling dilutions of serum was added to an ELISA plate coated with 10 µg/mL patulin-HS-BSA conjugate. Binding was detected with an anti-chicken (IgY) antibody, conjugated to horseradish peroxidase (HRP). The ELISA was developed with TMB substrate and the absorbance was measured at 450 nm, using a Tecan™ Safire II plate reader. The x-axis represents absorbance at 450 nm, the y-axis is the log of doubling dilutions of serum, and the red dashed line (---) is the cut-off, equivalent to 3SD of the negative control.

A clear immune response was generated in the chickens by administering boosts with 100 µg initially, followed by 75 µg of the mycotoxin conjugates, at three weekly intervals. The titre was approximately 1/100,000 for AFM1 (Figure 4.1) and 1/1,000 for patulin (Figure 4.2).

6.2.1.2 Extraction of RNA and reverse transcription to cDNA

RNA was extracted from the spleen of the immunised animal and complementary DNA (cDNA) was synthesised using the First Strand® cDNA Synthesis Kit. The total concentration of RNA was 9.9 µg/µL for AFM1 and 9.4 µg/µL for patulin. The total concentration of cDNA was 1.3 µg/µL for AFM1 and 3.6 µg/µL for patulin.

6.2.1.3 Amplification of avian heavy and light chains and PCR optimisation

The long linker primers, CSCVHo-F and CSCG-B (Barbas *et al.*, 2001) were used to amplify V_H segments from the avian cDNA, as long linker scFv fragments have less tendency to dimerise and cause avidity effects. The sense primer has a sequence tail, which corresponds to the linker sequence that is used in the overlap extension PCR. The reverse primer has a sequence tail, containing an *SfiI* restriction site. This tail is recognised by the reverse extension primer used in the second-round PCR. The CSCVK sense primer is combined with the CKJo-B reverse primer to amplify V_L gene segments from the avian cDNA. CSCVK has a 5' sequence tail that contains an *SfiI* site and is recognised by the sense extension primer in the second-round PCR. The reverse primer has a linker sequence tail that is used in the overlap extension.

For cDNA obtained from the AFM1-immunised spleen, a 400 bp product was amplified for the V_H reactions and a 350 bp amplicon was generated for the V_L reactions. The PCR products were evaluated on 1 % (w/v) agarose gel (Figure 6.3). A large-scale PCR amplification (10X reaction) was performed, using the same conditions, and the products were purified by gel extraction.

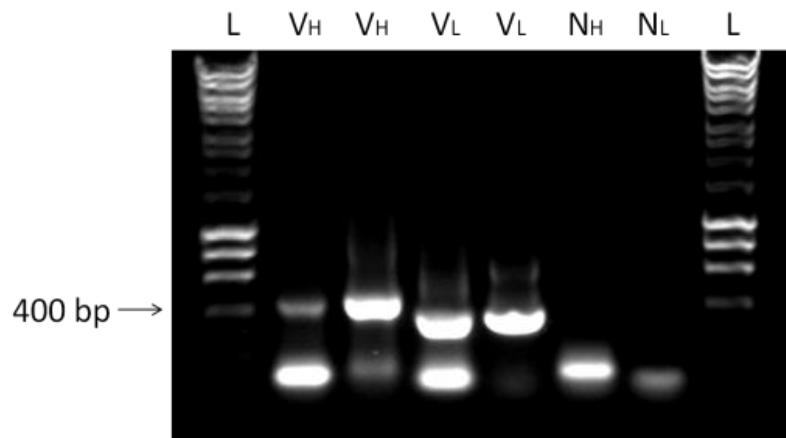


Figure 6.3: First round PCR amplifications in duplicate of V_H and V_L using cDNA from an AFM1-immunised chicken. N_H and N_L represent the respective negative controls (no template) and L is a 1 kb DNA ladder (Bioline).

cDNA, isolated by Dr Edwina Stack from an Ochratoxin A-BSA immunised avian host (Titre: 1/40,000), was obtained from -80°C stocks and used as a template. A 400 bp product was amplified for the V_H reactions and a 350 bp amplicon was generated for the V_L reactions. The PCR products were evaluated on 1 % (w/v) agarose gel (Figure 6.4). A large-scale PCR amplification (10X reaction) was performed, using the same conditions, and the products were purified by gel extraction.

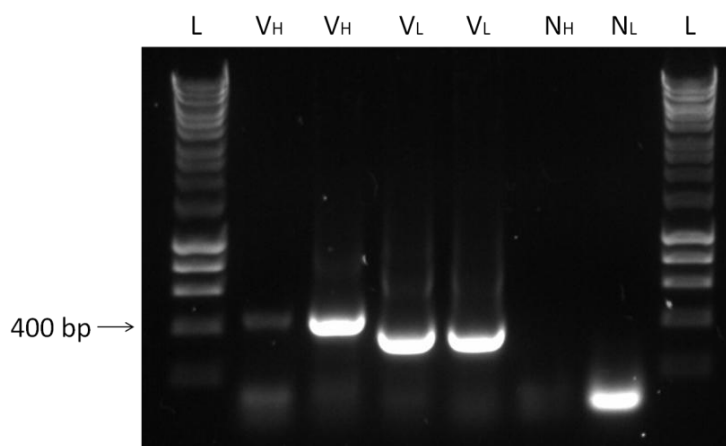


Figure 6.4: First round PCR amplifications in duplicate of V_H and V_L using cDNA from an OTA-immunised chicken. N_H and N_L represent the respective negative controls (no template) and L is a 1 kb DNA ladder (Bioline).

For cDNA obtained from the patulin-immunised spleen, a 350 bp product was amplified for the V_L reactions but no V_H amplification was achieved. The process was repeated and PCR products were evaluated on 1 % (w/v) agarose gel (Figure 6.5). A large-scale PCR amplification (10X reaction) of V_L was performed, using the same conditions, and the product was purified by gel extraction. It was decided to try a different polymerase for V_H amplification.

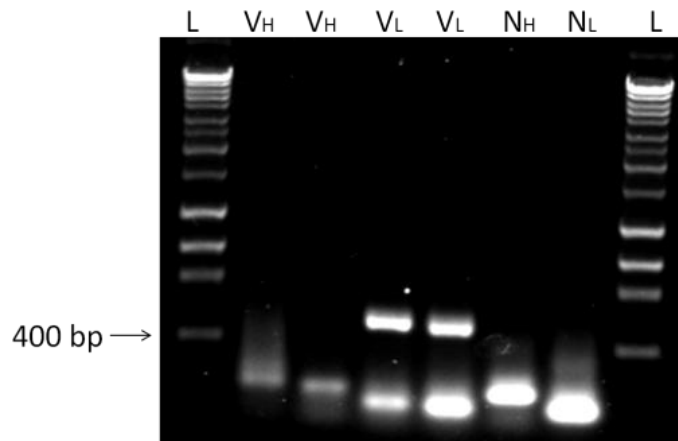


Figure 6.5: First round PCR amplifications in duplicate of V_H and V_L using cDNA from a patulin-immunised chicken. N_H and N_L represent the respective negative controls (no template) and L is a 1 kb DNA ladder (Bioline).

In order to amplify the V_H GoTaq[®] polymerase was used. It was necessary to optimise the MgCl₂ concentration for this reaction. A 400 pb product was amplified and visualised on a 1 % (w/v) agarose gel (Figure 6.6). The concentration of MgCl₂ did not appear to have a significant effect on the amplification, but 3 mM was chosen as the optimal concentration as it produced the cleanest amplification. A large-scale PCR amplification (10X reaction) was performed, using the optimised conditions, and the products were purified by gel extraction.

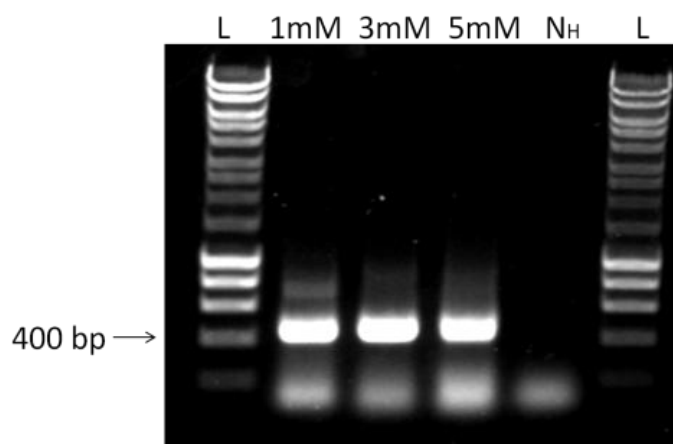


Figure 6.6: Optimisation of $MgCl_2$ concentration for V_H amplification was prepared with 1 mM, 3 mM and 5 mM $MgCl_2$. N_H represents the negative control (no template) and L is a 1 kb DNA ladder (Bioline). 3 mM was chosen as the optimal concentration.

6.2.1.4 SOE-PCR optimisation of variable heavy and light chains from the avian library

Following purification of the V_H and V_L chains by gel extraction, SOE-PCRs were carried out. SOE-PCRs were performed using the extension primers CSC-F and CSC-R. This process joined the V_L and V_H regions, using the sequence tails introduced in the first round of PCR, to create a serine-glycine linker sequence. This second round of PCR produced a 750 bp product.

Initially a problem arose as no SOE product was obtained for AFM1 after visualisation on a 1 % (w/v) agarose gel (Figure 6.7). It was thought that the annealing temperature for the reaction needed to be optimised.

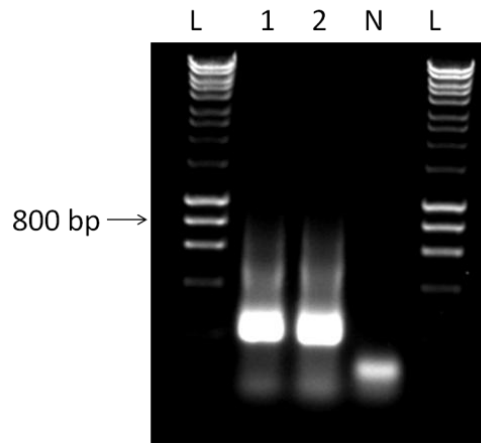


Figure 6.7: SOE amplification of SOE-PCR product in duplicate (1-2) for AFM1. No product is seen at the expected molecular weight of this fragment, 750 bp. A negative control (no template) (N) was included, and L represents a 1 kb DNA ladder (Bioline).

In an attempt to amplify the SOE product, a gradient PCR was set up to optimise the annealing temperature of the SOE-PCR. No SOE product was obtained at any temperature after visualisation on a 1 % (w/v) agarose gel (Figure 6.8). It was decided to repeat the reaction using fresh reagents.

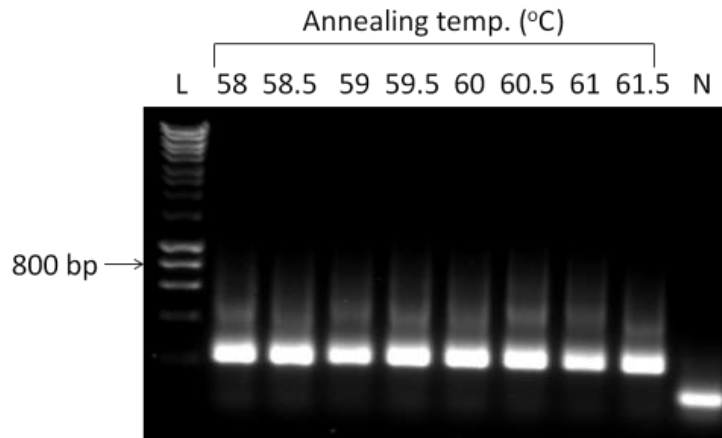


Figure 6.8: Gradient SOE for AFM1 to optimise annealing temperature. Temperatures from 58°C – 61.5°C were used. No product is seen at the expected 750 bp for any of the annealing temperatures. A negative control (no template) (N) was included, and L represents a 1 kb DNA ladder (Bioline).

The gradient PCR was repeated with fresh reagents in order to optimise the annealing temperature of the SOE-PCR. SOE product was obtained at 750 bp after visualisation on a 1 % (w/v) agarose gel (Figure 6.9). 60.5°C was chosen as the optimal annealing temperature as it produced the best amplification. A large-scale PCR amplification (10X

reaction) was performed, using the optimised conditions, and the products were purified by gel extraction.

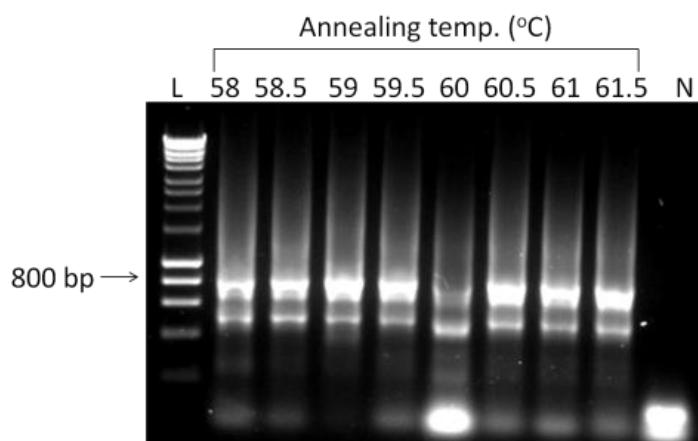


Figure 6.9: Gradient SOE for AFM1 to optimise annealing temperature. Temperatures from 58°C – 61.5°C were used. SOE product is evident at 750 bp. 60.5°C was chosen as the optimal annealing temperature. A negative control (no template) (N) was included, and L represents a 1 kb DNA ladder (Bioline).

In order to amplify the SOE product for patulin, a gradient PCR was also set up to optimise the annealing temperature of this SOE-PCR. Following several attempts a faint SOE product was obtained at 750 bp, along with several non-specific bands, after visualisation on a 1 % (w/v) agarose gel (Figure 6.10). These non-specific bands were subsequently removed through gel purification following large-scale (10X) amplification.

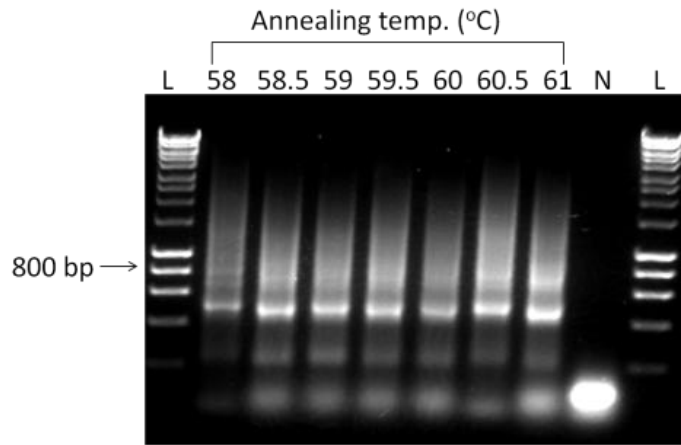


Figure 6.10: Gradient SOE for patulin to optimise annealing temperature. Temperatures from 58°C – 61°C were used. SOE product is evident at 750 bp. 61°C was chosen as the optimal annealing temperature. A negative control (no template) (N) was included, and L represents a 1 kb DNA ladder (Bioline).

In order to try and improve the specificity of the SOE-PCR the PCR enhancers betaine and DMSO were investigated to determine their effect, if any, on the reaction. Reactions with 1 M betaine, 5 % (v/v) DMSO, both enhancers, and no enhancers were performed and compared. After visualisation on a 1 % (w/v) agarose gel (Figure 6.11) it was determined that no PCR additive produced the best yield of SOE product so it was decided that they would not be used in further reactions.

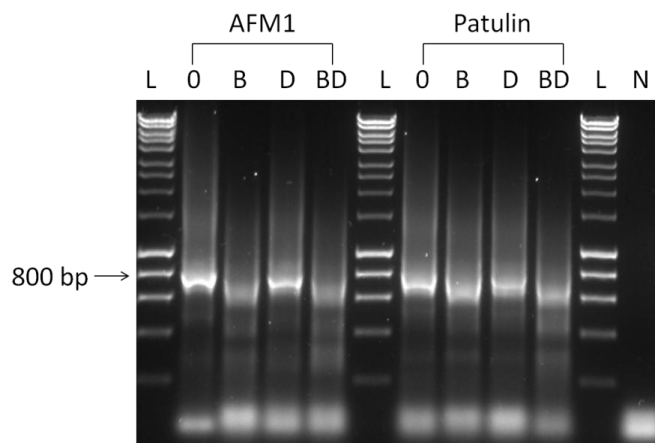


Figure 6.11: PCR enhancer optimisation for patulin and AFM1 SOE-PCR. PCR without enhancer is represented by 0, betaine (1 M) is represented by B, DMSO (5 % v/v) by D and the mixture of both enhancers by BD. N represents the negative control (no template) and L is a 1 kb DNA ladder (Bioline).

For the OTA SOE-PCR, it was decided to investigate if the use of a high fidelity polymerase could improve the specificity and yield of the reaction. SOE-PCRs were carried out using MyTaq™ Red Mix (Bioline) and high fidelity Platinum® PCR SuperMix (Thermo Fisher). A gradient PCR was run to determine the optimal annealing temperature for each of these polymerases over a broader range than was carried out previously. After visualisation on a 1 % (w/v) agarose gel (Figures 6.12 and 6.13) it was observed that while Platinum® PCR SuperMix produced a more distinct band at the target size, and a slightly more specific reaction overall, and the yield from MyTaq™ Red Mix was much greater.

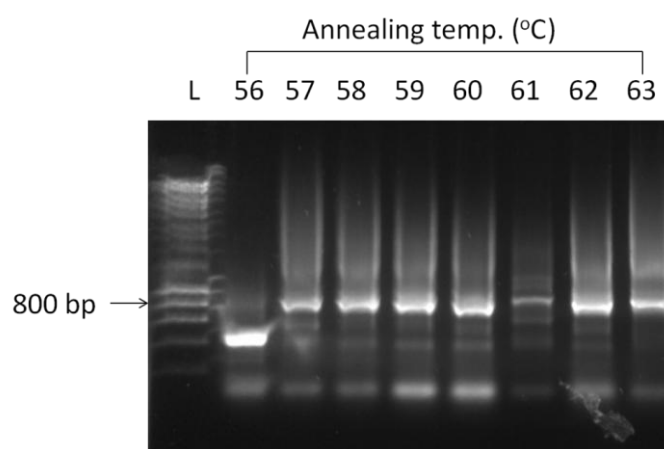


Figure 6.12: Gradient SOE using MyTaq™ Red Mix (Bioline) for OTA to optimise annealing temperature. Temperatures from 56°C – 63°C were used. SOE product is evident at 750 bp. 63°C appears to be the optimal annealing temperature. A negative control (no template) (N) was included, and L represents a 1 kb DNA ladder (Bioline).

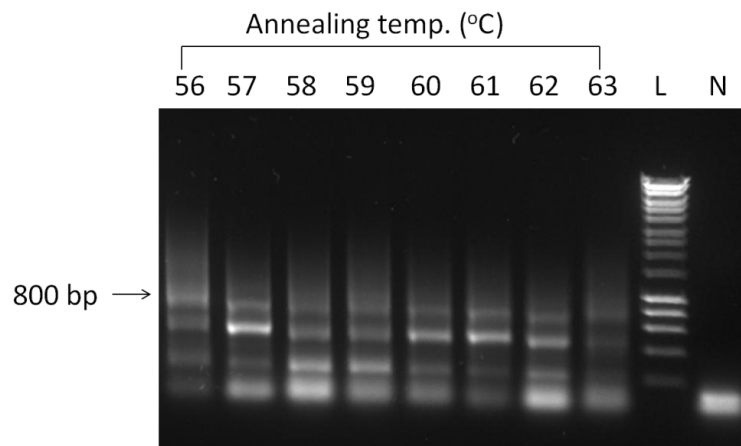


Figure 6.13: Gradient SOE using Platinum® PCR SuperMix (Thermo Fisher) for OTA to optimise annealing temperature. Temperatures from 56°C – 63°C were used. SOE product is evident at 750 bp. The optimal annealing temperature appears to be 61°C. A negative control (no template) (N) was included, and L represents a 1 kb DNA ladder (Bioline).

As the melting temperature (T_m) of the SOE-PCR primers is quite high (~74°C), the use of a two-step PCR was investigated. A two-step PCR can be employed if the T_m of both primers is high enough (usually over 68°C). It involves the annealing and the extension steps being combined into a single step. The reaction was set up in duplicate and compared to a traditional three-step PCR on a 1 % (w/v) agarose gel (Figure 6.14). The specificity of the two-step PCR was not as high as the three-step.

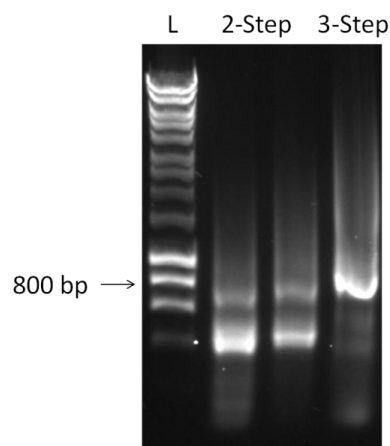


Figure 6.14: Comparison of a two-step and three-step SOE-PCR for OTA. SOE product is evident at 750 bp. L represents a 1 kb DNA ladder (Bioline).

Given that the T_m of the SOE-PCR primers is high the annealing temperature optimisation was repeated for OTA with temperatures ranging from 64°C to 72°C. The

results of the PCRs were visualised on 1 % (w/v) agarose gel (Figure 6.15) and showed that, at these higher annealing temperatures, the reaction is more specific and produces a higher yield. Therefore, a large-scale PCR amplification (10X reaction) was performed, using a 68°C annealing temperature for patulin, OTA and AFM1, and the products were purified by gel extraction.

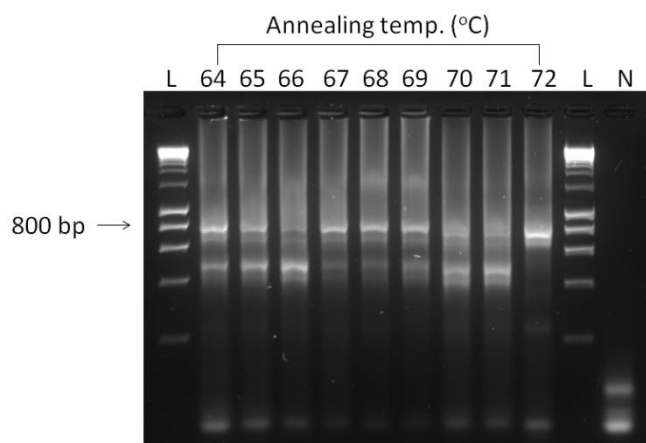


Figure 6.15: Gradient SOE for OTA to optimise annealing temperature. Temperatures from 64°C – 72°C were used. SOE product is evident at 750 bp. 68°C was chosen as the optimal annealing temperature. A negative control (no template) (N) was included, and L represents a 1 kb DNA ladder (Bioline).

6.2.1.5 Digestion of SOE product and ligation into pComb3xSS vector

The SOE products were cloned into a pComb3xSS vector, using the restriction enzyme, *SfiI*. *SfiI* was used for cloning, as the sites at which it cuts are rare in antibody sequences, therefore, the use of this enzyme eliminates the possibility of internal digestion and incorrect sequence lengths. Antarctic phosphatase treatment ensured that self-ligation of the vector did not occur. The digested pComb3xSS vector was run on 0.6 % (w/v) agarose gel (Figure 6.16) and contained undigested vector (~5,000 bp), digested vector (~3,400 bp) and stuffer fragment (~1,600 bp). Due to the high concentration of the vector in the reaction, only partial digestion is achieved and undigested vector remains. The digested product was purified by gel extraction.

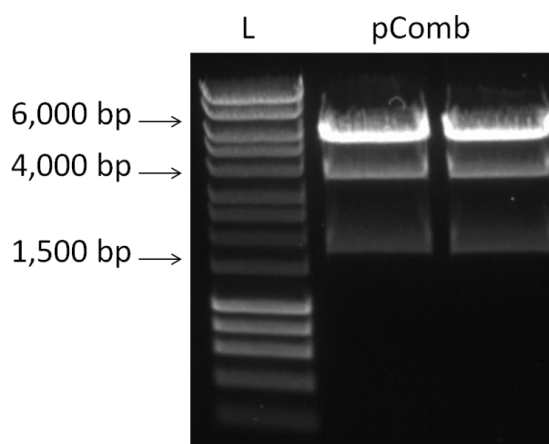


Figure 6.16: *SfiI* digestion of pComb3xSS vector. Digested product is evident at ~3,400 bp. L represents a 1 kb DNA ladder (Bioline).

6.2.1.6 Transformation of pComb3xSS vector in electro-competent E. coli XL1-Blue cells

The ligated products were transformed into electro-competent *E. coli* XL1-Blue cells by electroporation. The efficiency of transformation was determined using colony pick PCR. Ten colonies were picked at random from each library and a PCR was carried out using the optimal conditions for SOE-PCR. The results were visualised on a 1 % (w/v) agarose gel (Figures 6.17 and 6.18) and showed that the patulin, AFM1 and OTA libraries had 6/10, 7/10 and 6/10 colonies with the SOE insert present, respectively. The library sizes were calculated based on the formula described in Section 2.2.3.12 and found to be 8.35×10^5 cfu/mL for patulin, 3.24×10^6 cfu/mL for AFM1 and 2.73×10^6 cfu/mL for OTA.

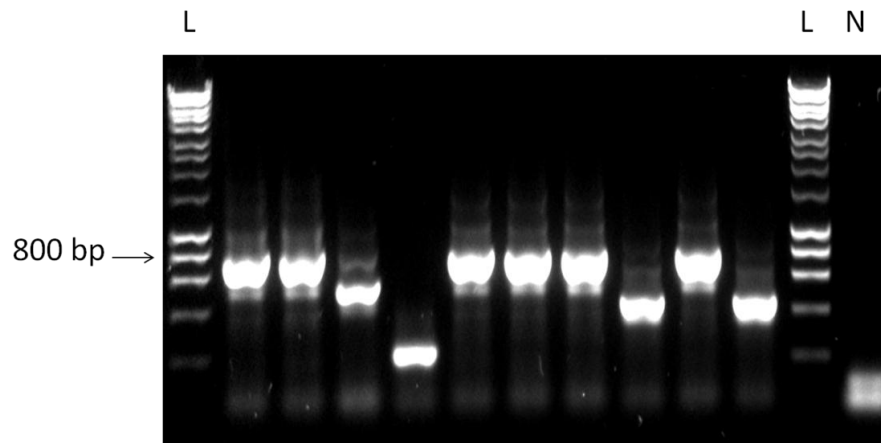


Figure 6.17: PCR insert check for successful cloning of patulin SOE products into the pComb3XSS vector system. Ten colonies were picked at random and incorporated into the PCR. The patulin library had 6/10 colonies with the SOE insert present. A negative control (no template) (N) was included, and L represents a 1 kb DNA ladder (Bioline).

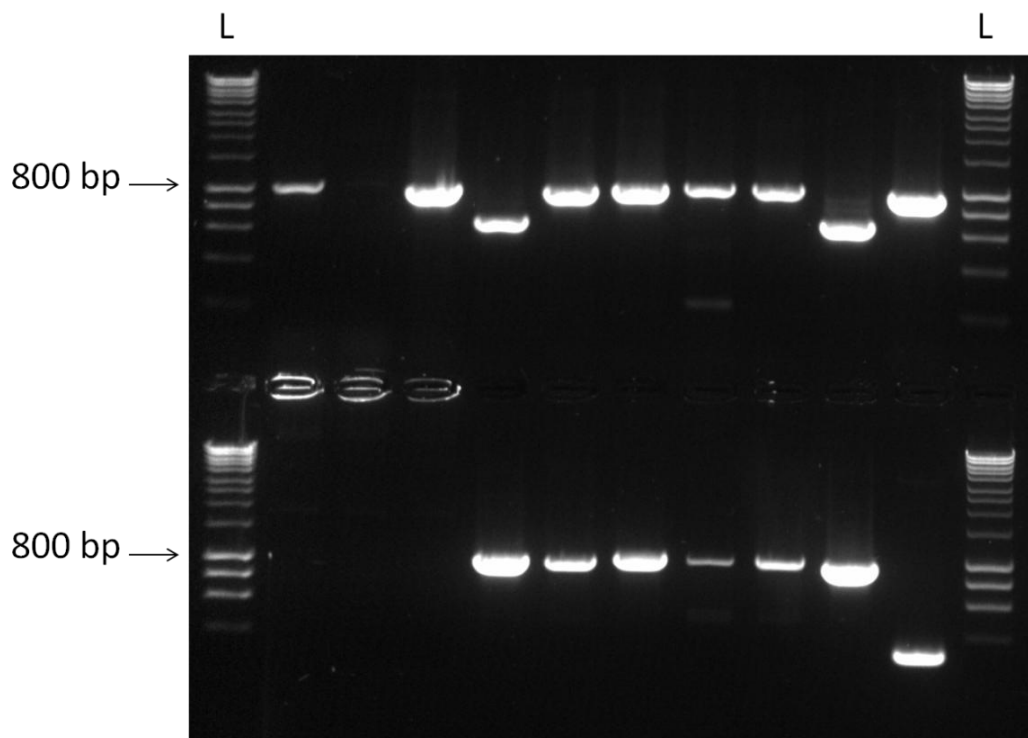


Figure 6.18: PCR insert check for successful cloning of AFM1 (top) and OTA (bottom) SOE products into the pComb3XSS vector system. Ten colonies were picked at random and incorporated into the PCR. The AFM1 and OTA libraries both had 7/10 and 6/10 colonies with the SOE insert present, respectively. A negative control (no template) (N) was included, and L represents a 1 kb DNA ladder (Bioline).

6.3 Discussion

The aim of this research was to generate avian immune antibody libraries to AFM1 and patulin. Two commercial mycotoxin conjugates were purchased and used for immunisation. The spleen, a rich source of antibody-producing B-lymphocytes, was isolated from an avian host, after confirming anti-mycotoxin antibodies were present in the serum by ELISA. The RNA was extracted, using a phenol-chloroform method, and reversed transcribed to cDNA. The variable antibody genes (V_H and V_L) were successfully amplified, using PCR, and joined by SOE-PCR. This will be used to assemble the desired single chain Fv fragments, with a glycine-serine linker. The flexible linker region (20 amino acids) will allow for correct folding of the generated scFv. While being considerably smaller in size compared with a full IgG antibody, scFv fragments consisting of linked antibody heavy and light chains, still retain their specificity and affinity to their cognate antigen.

The difficulty in isolating a recombinant antibody to patulin can be attributed to a number of factors, including ineffective immune response generation, the toxic nature of the immunogen, the size of the hapten and the quality of conjugation. Barbas *et al.* (2001) have specified that ideally recombinant antibody libraries should be built from animals that display a high serum titre to the antigen of interest. A high serum titre reflects a high level of antibody production and, therefore, a high level of specific mRNA for library construction. However, recombinant antibodies have been isolated from immune libraries with titres as low as 1/100 (Burton and Barbas, 1994; Barbas *et al.*, 2001). In this work, considerable difficulty was encountered in generating a response in the patulin-immunised chicken. Despite the poor response to the patulin-conjugate, it was decided to construct a recombinant library from the genetic material of the chicken.

The successful amplification of V_H and V_L was carried out using the cDNA obtained from OTA and AFM1-immunised avian spleens. However, issues occurred when attempting to amplify the V_H region using cDNA from the patulin-immunised host. This issue was overcome through the use of GoTaq[®] polymerase. The concentration of $MgCl_2$ in this PCR was successfully optimised. Mg^{2+} is required for polymerase activity. Without Mg^{2+} bound, the polymerase will not recognize the dNTPs as a substrate and will not work. Mg^{2+} is essential in removing the phosphate groups under DNA elongation.

Furthermore, Mg^{2+} binds to the primers and stabilises dsDNA, thereby influencing annealing and melting temperatures. The Mg^{2+} concentration available in the reaction is dependent on several parameters like dNTP concentration, primer purity and concentration, template DNA purity and concentration, the presence of chelators (e.g. EDTA introduced with the template DNA). Low Mg^{2+} concentrations increase the fidelity but decrease the polymerase activity. High Mg^{2+} concentration promotes fast DNA amplification at the cost of fidelity. Elevated Mg^{2+} concentrations stabilize dsDNA, thereby preventing it from complete denaturation and increasing the melting temperature (Barbas *et al.*, 2001). PCR reactions must also have a free Mg^{2+} concentration in excess of the total dNTP concentration because dNTPs may chelate Mg^{2+} (Rabhi *et al.* 2004).

Following this, the purified V_H and V_L regions were joined by SOE-PCR using the sequence tails introduced in the first round of PCR. Initially no SOE product was amplified for both AFM1 and patulin. However, the use of fresh reagents and optimisation of annealing temperatures for the reactions allowed for the amplification of the SOE-PCR product. The purity and yield of a PCR reaction product depend on several parameters, one of which is the annealing temperature. At both sub- and super-optimal annealing temperatures non-specific products may be formed, and the yield of products is reduced. Optimising the annealing temperatures is crucial step for SOE-PCR. Despite successful amplification of the SOE-PCR product, the yield of this product was low and non-specific amplification still occurred. Therefore, further optimisation of this reaction was required. For SOE-PCRs, the design of primers is constrained by the sequences to be joined and non-optimal primers may result, leading to interior intramolecular annealing. This may cause little or no amplification of products, or nonspecific amplification and smearing (Kelly *et al.*, 1999). Some steps can be taken to further optimise the SOE reaction.

One option is the use of a PCR enhancing agent. A variety of additives and enhancing agents can be included in PCR amplifications to increase yield, specificity and consistency. Agents include: dimethyl sulfoxide (DMSO), N,N,N-trimethylglycine (betaine), formamide, glycerol, polyethylene glycol and tetramethylammonium chloride. These additives have beneficial effects on some PCR amplifications; however, it is not possible to predict which agents might be useful for a particular target.

Generally PCR enhancers work by binding to the DNA at the cytosine residue and changing its conformation, making the DNA more labile for heat denaturation (Chakrabarti and Schutt, 2001). In an attempt to improve the SOE-PCR specificity and yield the effects of betaine and DMSO were investigated. It was determined that neither of these enhancers, nor their combination, produced more specific product so they were not used for further reactions. Similarly, Wurch *et al.* (2000) in their optimisation of overlap extension PCR-based mutagenesis of a GC-rich DNA template found that additives like DMSO, glycerol, betaine and the nucleotide analogue 7-deaza dGTP did not improve the efficiency of the PCR reaction. Another option to improve PCR efficiency is to use a different, high-fidelity, polymerase for the reaction. The fidelity of a DNA polymerase refers to its ability to accurately replicate a template. This relies on a DNA polymerase's ability to read a template strand, select the appropriate nucleoside triphosphate and insert the correct nucleotide. The rate of misincorporation is referred to as the "error rate". Additionally, to effectively discriminate between correct and incorrect nucleotide incorporation, some DNA polymerases possess a 3'→5' exonuclease activity. This activity is called "proofreading" and is used to excise incorrectly incorporated mononucleotides that are then replaced with the correct nucleotide. High-fidelity PCR utilizes DNA polymerases that combine low misincorporation with high proofreading activity to give efficient and specific amplification of the target DNA. Bryksin and Matsumura (2010) found in their investigation on overlap extension PCR cloning to create recombinant plasmids that Phusion DNA polymerase was better suited for overlap extension PCR cloning than the competitors tested due to its superior processivity and fidelity. MyTaq™ Red Mix (Bioline) and Platinum® PCR SuperMix (Thermo Fisher) polymerases were compared. Overall, MyTaq™ Red Mix produced a higher yield of PCR product so this was used for further reactions. Further optimisation of Platinum® PCR SuperMix or other high-fidelity polymerases could be used but the performance of MyTaq™ Red Mix was sufficient for this reaction.

Step-wise methods can be employed to try and circumvent issues with SOE reactions (Kelly *et al.*, 1999; Yingfeng *et al.*, 2005). The advantage of the step-wise method over multistep methods is in the usage of 100 % homologous primers in its first step when the template DNA is more complex. By doing this, it is possible to reduce unwanted interactions between mismatched primers and genomic DNA. In some cases, this can

be the difference between obtaining a final spliced product or not. In PCRs, if the melting temperature (T_m) of both primers is high enough (usually over 68°C), the annealing and the extension steps can be combined into a single step for a two-step PCR. This can sometimes result in a higher efficiency reaction. A comparison was made between a two-step and three-step for the SOE-PCR. While the two-step did produce the desired product it was not as good a yield as the traditional three-step. In general, PCR yields are poor when the reaction conditions are too stringent (primers fail to anneal) or too relaxed (nonspecific priming). Both are manifested by empty lanes in agarose gels, although the latter can also result in smears or undesired bands. The stringency of PCR can be controlled by altering reactant concentrations (primers, template), annealing temperature, buffer ingredients (magnesium, pH, DMSO) or the number of temperature cycles (Bryksin and Matsumura, 2010). Ultimately, optimal conditions were determined by performing further annealing temperature optimisation at higher temperatures. A three-step PCR using MyTaq™ Red Mix with an annealing temperature of 68°C was used for SOE-PCR. The purified SOE products were cloned into a pComb3xSS vector, using the *SfiI* restriction enzyme. *SfiI* was used for cloning as the sites at which it cuts are rare in antibody sequences and, therefore, the use of this enzyme eliminates the possibility of internal digestion and incorrect sequence lengths. Antarctic phosphatase treatment ensured that self-ligation of the vector did not occur. The ligated products were transformed into electro-competent *E. coli* XL1-Blue cells by electroporation. These cells are designed for high-efficiency transformations which are crucial to produce large and diverse scFv immune libraries. The efficiency of transformation was determined using colony pick PCR. Ten colonies were picked at random from each library and a PCR was carried out using the optimal conditions for SOE-PCR. The results showed that the patulin, AFM1 and OTA libraries had 6/10, 7/10 and 6/10 colonies with the SOE insert present, with library sizes of 8.35×10^5 cfu/mL, 3.24×10^6 cfu/mL and 2.73×10^6 cfu/mL, respectively. The transformed avian scFv libraries were sufficient for immune phage-displayed libraries.

Ultimately this work has, following successful immunisation campaigns, optimised the conditions for the PCR amplification of the variable heavy and light chains, their overlap into a scFv, and the production of scFv immune libraries which can now be screened for isolation of clones to target the mycotoxins patulin, OTA and AFM1.

**Chapter 7: Isolation and
characterisation of avian
antibodies to target the
mycotoxins; patulin,
ochratoxin A and aflatoxin M1**

7.1 Introduction

Recombinant antibody technology allows the generation of high affinity antibody fragments from species such as human, rabbit, mouse, chicken and sheep in prokaryotic and eukaryotic expression systems (Daly *et al.*, 2000). Recombinant antibodies can be sensitive and specific for their target molecules, and can be produced relatively easily and cheaply. Generation involves amplifying the variable genes from the cDNA from the lymphocytes of an immunised host. The challenge in recombinant antibody production is in the selection process, when specific antibody fragments are isolated large libraries of non-functional and non-specific antibodies. In the immune system, a diverse collection of antibody binding sites is created by the combinatorial assembly of germline-encoded segments. This produces a repertoire of naive B-cell lymphocytes which, when activated, express antibodies with a unique antigen binding site on their surface (Hoogenboom, 2005). Exposure to antigen promotes somatic hypermutations in the variable genes, allowing subsequent selection of mutations that improve the affinity of the antibody for the antigen. Antibodies can also be isolated from recombinant antibody libraries in the laboratory, using methods for selection that 'mimic' this *in vivo* process. Several display mechanisms, such as phage, yeast and ribosomal display, have been developed for the isolation of specific antibody fragments, which provide an efficient method to select antibodies based on the antigen-binding behaviour of individual clones.

7.1.1 Phage Display

Phage display is a molecular diversity technique that employs non-lytic filamentous bacteriophage fd/M13 to display ligands on the surface of their phage coat. *E. coli* containing the F conjugative plasmid are a natural host for replication of this phage family. Small plasmid vectors or phagemids, which contain the appropriate packaging signal and cloning sites, are used as vectors for display. Phagemids have high transformation efficiencies, making them ideal for generating large antibody repertoires. When using phage to display antibody fragments, phagemids usually consist of the DNA encoding a scFv, fused to the gene encoding a phage coat protein (pIII or pVIII). Other vector features include an antibiotic resistance marker, an origin of replication, a promoter region and an affinity tag to aid in purification. Helper phage, such as M13K07, are also required to supply all necessary structural proteins for correct packaging of the phage particle. The lacZ promoter is the most common

promoter used to control expression. Expression may be suppressed by the addition of the catabolic repressor, glucose, or induced by addition of isopropyl- β -D-1-thiogalactopyranoside (IPTG). Upon induction, the scFv-coat fusion β -isopropylprotein is incorporated into new phage particles that are assembled in the bacterium and displayed on their surface, while the genetic information encoding the scFv remains within the phage particle (Barbas *et al.*, 2004). Phage display has been successfully employed to isolate antibody fragments specific for small molecules. Small molecules alone do not have the molecular mass required to elicit an immune response and hence, must be conjugated to larger carrier protein such as bovine serum albumin (BSA), ovalbumin (OVA), keyhole limpet hemocyanin (KLH) and thyroglobulin (THY). A carrier must be highly immunogenic, have the required solubility properties, be non-toxic *in vivo* and possess suitable functional groups for coupling to the hapten (Hermanson, 2005). Conjugation is a crucial step in antibody production, as the specificity of the resultant antibodies is dependent on the hapten used to produce them.

Biopanning is an affinity selection technique which relies on subjecting a library of antibodies on filamentous phage to bind to a specific target (immobilized on a solid support or in solution). This process enriches analyte-specific clones, by incubation with the target molecule in consecutive rounds, with increasing stringency. Unbound phage are washed away and specific phage are eluted by changing the binding conditions, either by pH elution, enzymatic cleavage or incubation with excess antigen. Specific phage are then amplified in *E. coli*. In practice, several rounds of selection (approximately 3-5) are necessary, as the binding of non-specific phage limits the enrichment that can be achieved in one single cycle (Azzazy and Highsmith, 2002). Using the pComb vector series, specific phage can then be solubly expressed by infection into a non-suppressor *E. coli* strain such as Top10F, which allows the scFv to be secreted independently of the phage particle. Screening of the enriched library is then performed by analysing single colonies in a monoclonal ELISA to determine the specificity of each isolated clone.

7.1.2 Chapter aims

The aim of this chapter was to use phage-display bio-panning to screen the scFv immune libraries generated in chapter 6 in order to attempt to isolate scFv clones capable of binding mycotoxins with high affinity.

This chapter describes the synthesis of a patulin-carrier protein conjugate, testing of this conjugate, biopanning of three scFv immune libraries, isolation of clones from these libraries and characterisation of these clones to analyse their binding abilities. Isolated clones capable of binding these mycotoxins can be used in immunoassay formats to detect OTA, AFM1 and patulin in food samples with high sensitivity.

7.2 Results

7.2.1 Synthesis of Patulin-HS-BSA conjugate

In order to screen the scFv immune library generated against a Patulin-HG-KLH conjugate an alternative to the immunogen needed to be synthesised. Patulin-HS-BSA was synthesised as described in Section 2.2.2.4. The binding ability of the conjugate was analysed by indirect ELISA using a commercial anti-patulin polyclonal antibody (Agrisera). The results (Figure 7.1) show the antibody binding the conjugate at several concentrations and at a higher level than the BSA control. A high response was seen to BSA, possibly due to non-specific binders present in the polyclonal serum but the response to the conjugate was satisfactory and it was used in the bio-panning procedure.

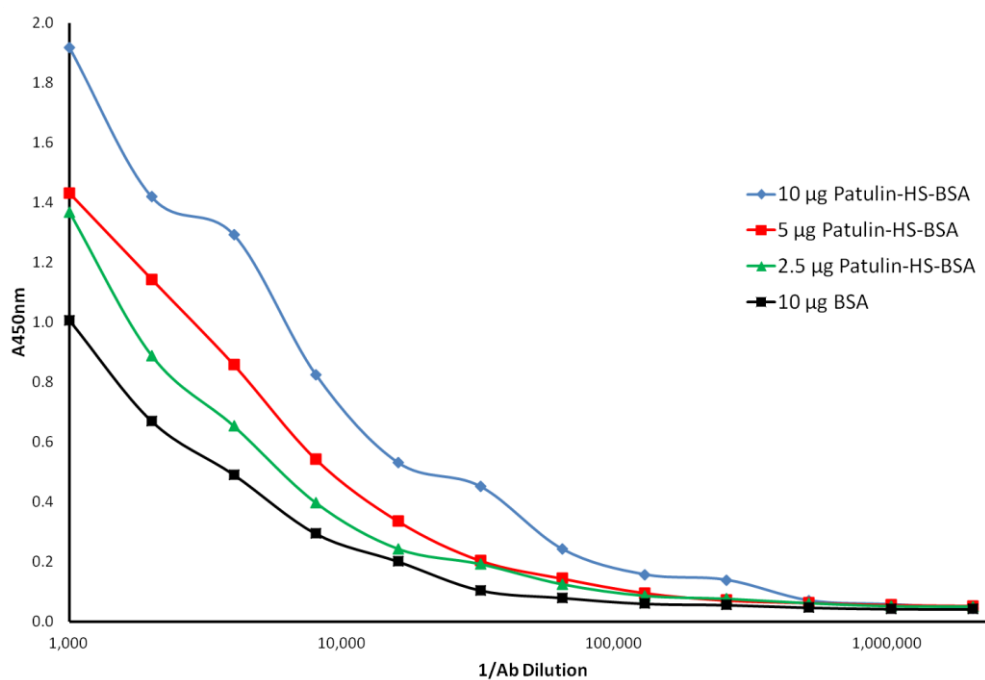


Figure 7.1: Testing of Patulin-HS-BSA conjugate synthesis using direct ELISA. Doubling dilutions of rabbit anti-patulin polyclonal antibody (Agrisera) were added to an ELISA plate coated with the Patulin-HS-BSA conjugate or a BSA control. Binding was detected with a goat anti-rabbit secondary antibody (Agrisera), conjugated to horseradish peroxidase (HRP). The ELISA was developed with TMB substrate and the absorbance was measured at 450 nm, using a Tecan™ Safire II plate reader.

7.2.2 Phage display bio-panning to isolate scFv clones to target patulin, AFM1 and OTA

7.2.2.1 Bio-panning of the immune avian libraries

Rounds of affinity selection through bio-panning were performed on the patulin, OTA and AFM1 scFv immunelibraries using mycotoxin conjugate-coated immunotubes. Enrichment of the library was facilitated by altering the stringency of each consecutive panning step. This was achieved by decreasing the concentration of immobilised antigen on the immunotube and increasing the concentration of the depletion molecule. The panning conditions are outline in Tables 7.1, 7.2 and 7.3.

Table 7.1: Panning conditions employed for each round of the repeated selection for the avian anti-**patulin** scFv library.

Round	[Patulin-HS-BSA coating]	Washes
1	100 µg/mL	3 x PBS-T, 3 x PBS
2	50 µg/mL	3 x PBS-T, 3 x PBS

Table 7.2: Panning conditions employed for each round of the repeated selection for the avian anti-**OTA** scFv library.

Round	[OTA-BSA coating]	[BSA depletion]	Washes
1	100 µg/mL	100 µg/mL	3 x PBS-T, 3 x PBS
2	50 µg/mL	50 µg/mL	3 x PBS-T, 3 x PBS
3	25 µg/mL	No depletion	3 x PBS-T, 3 x PBS

Table 7.3: Panning conditions employed for each round of the repeated selection for the avian anti-**AFM1** scFv library.

Round	[AFM1-BSA coating]	[AFB1-BSA depletion]	Washes
1	100 µg/mL	75 µg/mL	3 x PBS-T, 3 x PBS
2	50 µg/mL	50 µg/mL	3 x PBS-T, 3 x PBS
3	25 µg/mL	100 µg/mL	3 x PBS-T, 3 x PBS

7.2.2.2 Verification of scFv inserts by colony-pick PCR

To ensure that each of the panning rounds contained scFv inserts, a colony-pick PCR was carried out. Colonies were picked at random from plates after each panning round. The colonies were used to amplify the SOE insert from the transformed library using PCR. The extension primers, CSC-F and CSC-B, were used for SOE-PCR amplification and the PCR products analysed on a 1 % (w/v) agarose gel (Figures 7.2, 7.3 and 7.4).

Inserts for patulin were low in round 1 and did not carry into round 2. Round 2 of panning was then repeated but, again, the percentage of inserts was too low. It was thought that issue was potentially caused by a combination of the quality of the immune library and the Patulin-HS-BSA conjugate. The original immune response of the avian host to the commercial Patulin-HG-KLH conjugate was low (Titre: 1 in 1,000) and the conjugate being used to screen the library was synthesised “in-house” as it cannot be sourced commercially so it was unlikely that repeating this process would yield any significantly better results, therefore, work on patulin did not progress any further.

Screening of OTA library showed that inserts were present in all three rounds but reduced after round 2. Panning of round 3 was repeated but as the percentage of inserts was still low a polyclonal phage ELISA was carried out to determine if enrichment had occurred in any rounds.

The bio-panning of the AFM1 show that scFv inserts were presented in all three rounds. As AFM1-BSA conjugate was limited, a polyclonal phage ELISA was carried out after 3 rounds to determine if enrichment had occurred.

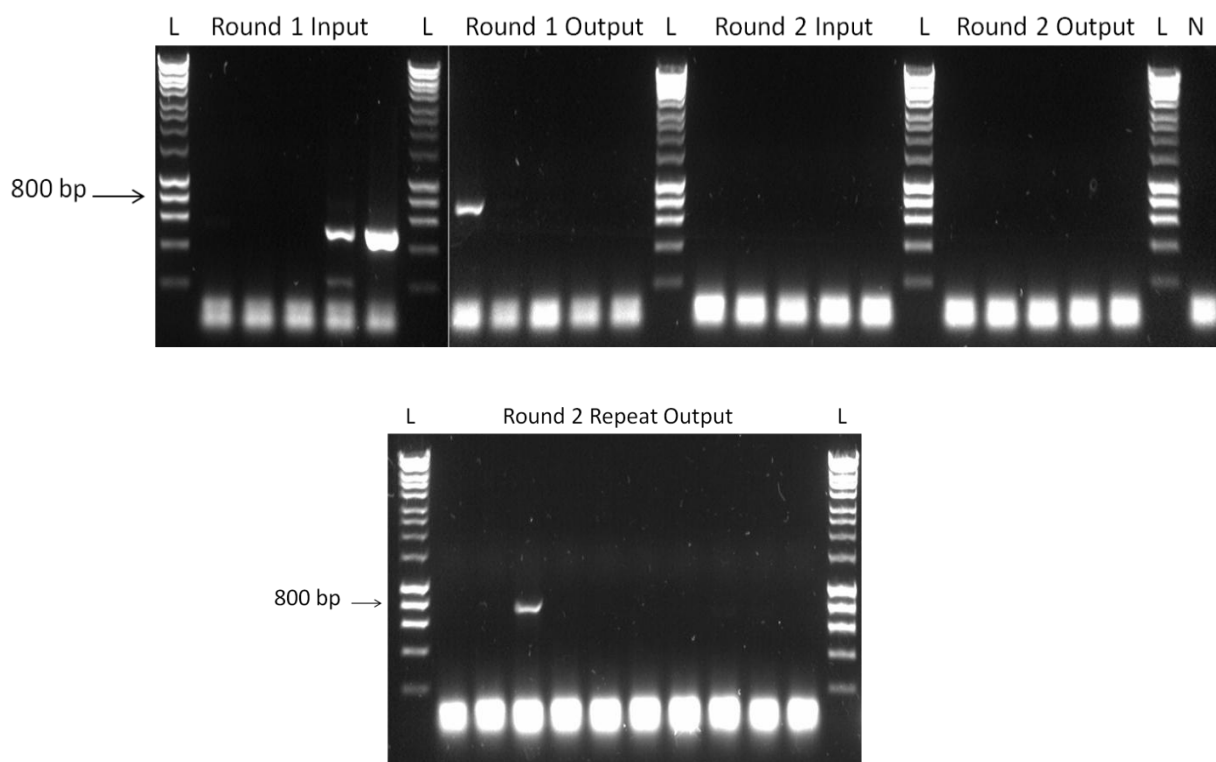


Figure 7.2: PCR insert check for **patulin** panning selection rounds. Colonies were picked at random and incorporated into the PCR. The percentage of colonies containing SOE inserts was low in round 1 and no SOE inserts were carried into round 2 of panning, even after a repeat of the round. A negative control (no template) (N) was included, and L represents a 1 kb DNA ladder (Bioline).

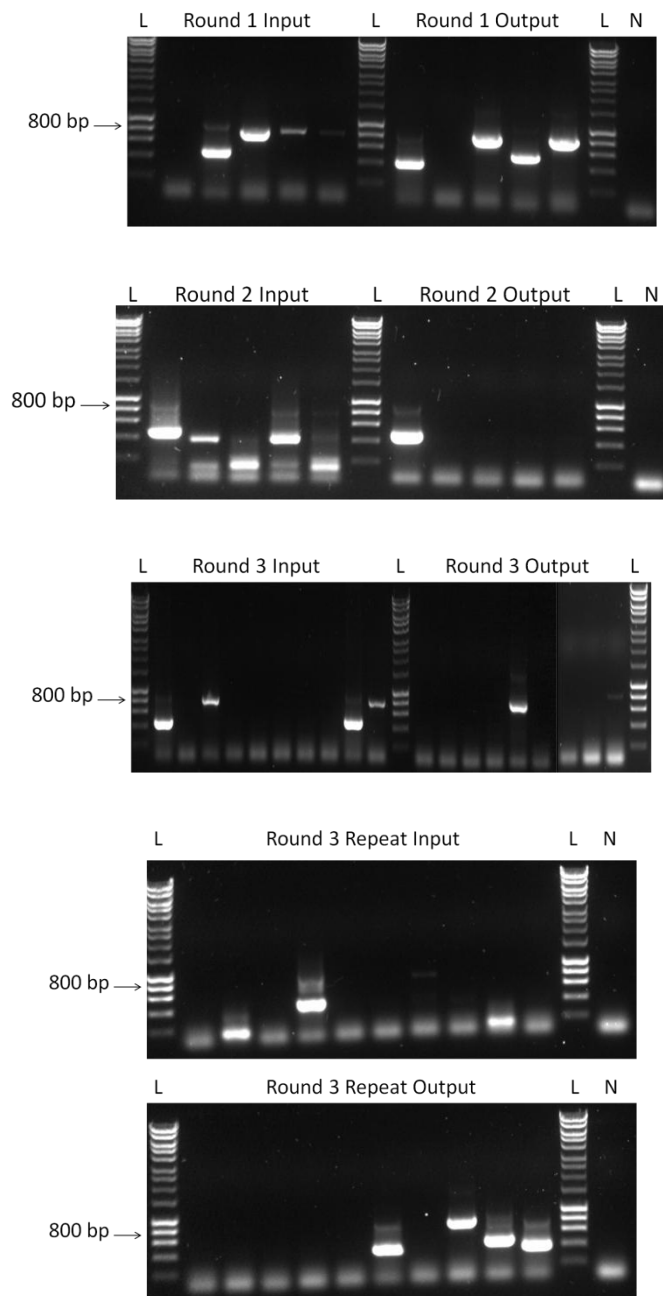


Figure 7.3: PCR insert check for **OTA** panning selection rounds. Colonies were picked at random and incorporated into the PCR. The percentage of colonies containing SOE inserts reduces after round 2. A negative control (no template) (N) was included, and L represents a 1 kb DNA ladder (Bioline).

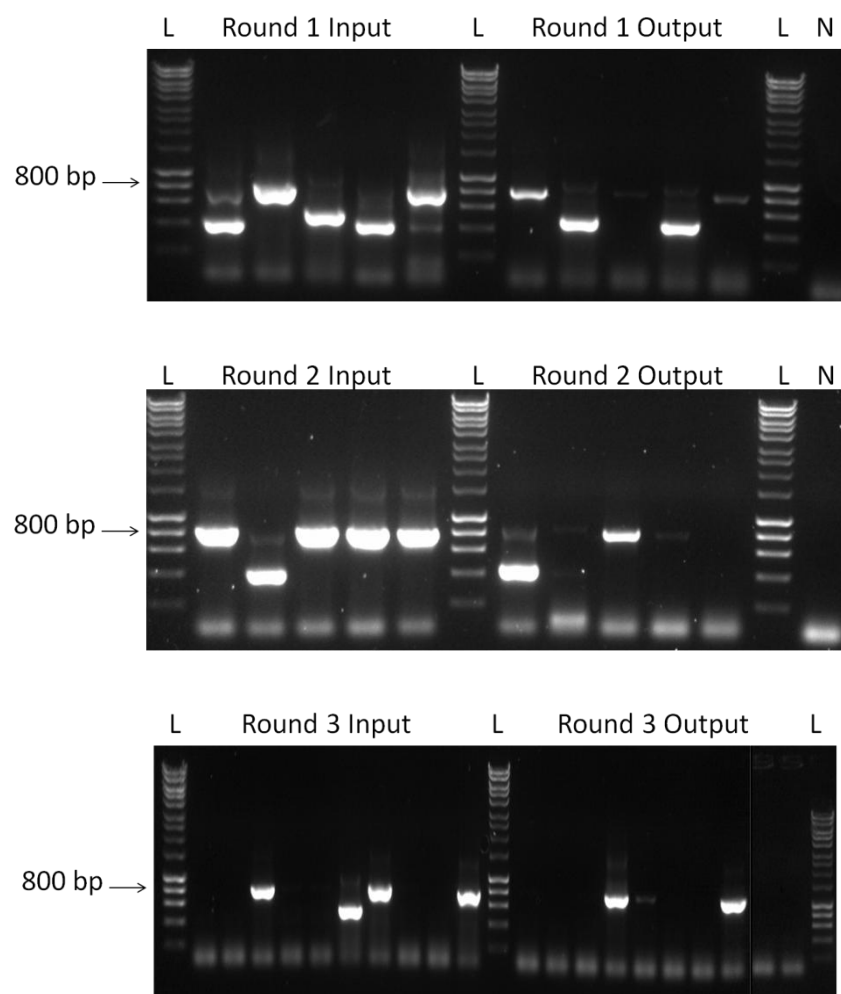


Figure 7.4: PCR insert check for **AFM1** panning selection rounds. Colonies were picked at random and incorporated into the PCR. SOE inserts are present in the inputs and outputs of all three rounds but the percentage of colonies containing inserts reduces in round 3. A negative control (no template) (N) was included, and L represents a 1 kb DNA ladder (Bioline).

7.2.2.3 Polyclonal phage ELISA

The precipitated input phage from each round of panning for AFM1 and OTA was incorporated into a polyclonal phage ELISA to test for enrichment against the mycotoxin-conjugates. Successful enrichment was signified by an increase in absorbance signal after incubating phage with the immobilised conjugates and detecting bound phage with a HRP labelled anti-M13 secondary antibody. The results (Figures 7.2 and 7.3) showed enrichment for round 2 of the AFM1 panning and rounds 2 and 4 of the OTA panning. Clones were then randomly selected from these rounds for monoclonal analysis.

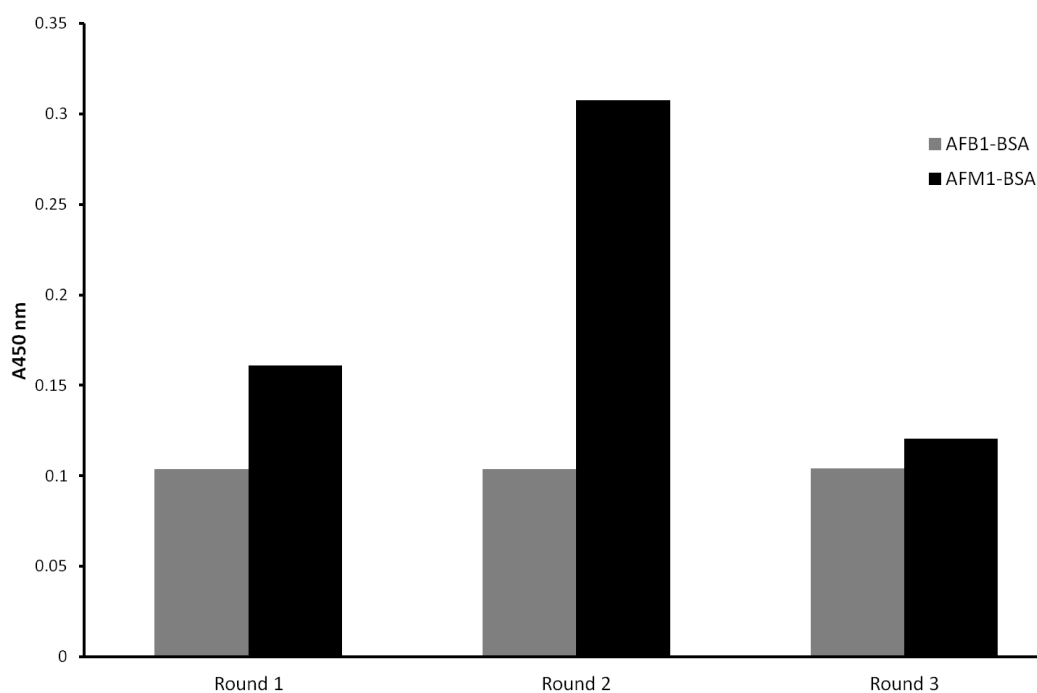


Figure 7.5: Polyclonal phage ELISA screening for anti-AFM1 scFv displayed on phage, following three rounds of panning. Phage pools obtained after each round of panning were tested for binding to the AFM1-BSA conjugate by ELISA. AFB1-BSA was used as a negative control. The scFv-displaying phage were detected using a HRP-conjugated anti-M13 antibody and the absorbance was read at 450 nm using a Tecan Safire™ plate reader following a 20 minute incubation with TMB substrate. The increase in absorbance from round 2 suggested the presence of AFM1-specific scFv-harboring phage within the panned library.

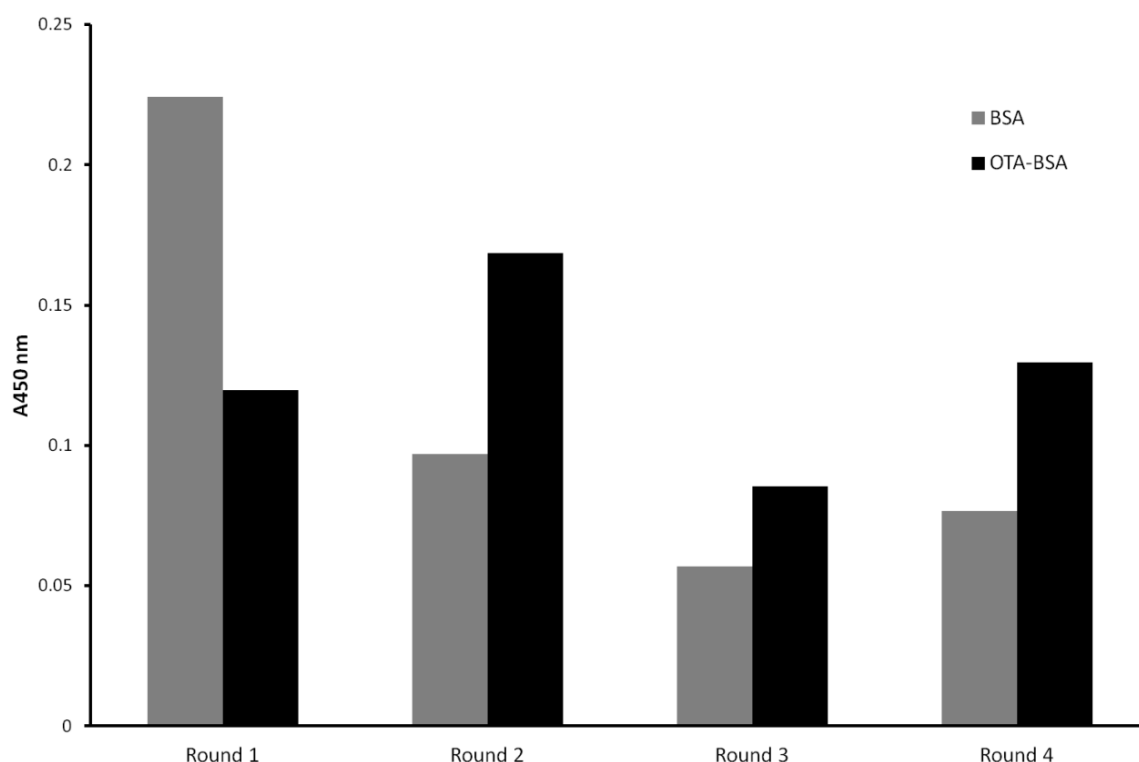


Figure 7.6: Polyclonal phage ELISA screening for anti-OTA scFv displayed on phage, following three rounds of panning. Phage pools obtained after each round of panning were tested for binding to the OTA-BSA conjugate by ELISA. BSA was used as a negative control. The scFv-displaying phage were detected using a HRP-conjugated anti-M13 antibody and the absorbance was read at 450 nm using a Tecan Safire™ plate reader following a 20 minute incubation with TMB substrate. The increase in absorbance from round 2 suggested the presence of OTA-specific scFv-harboring phage within the panned library.

7.2.2.4 Direct monoclonal ELISA of solubly-expressed scFv fragments

To determine whether any OTA and AFM1-binding phage were present, even in low copy number, the libraries were screened by solubly expressing randomly selected scFv. The phage display vector, PComb3XSS, contains an amber stop codon (TAG) between the scFv and the gene III of the phage. When the phage are infected into a non-suppressor *E. coli* strain, which reads the amber stop codon, it facilitates the soluble expression of scFv particles. However, it has been noted that native scFv expression can be achieved without infection into a nonsuppressor strain. Even in suppressor strains such as XL1-Blue, suppression is only 50 % and, after the addition of IPTG, adequate amounts of scFv can be produced (Marks and Bradbury, 2004).

Phage from rounds that showed enrichment were infected into Top10F cells for soluble expression of scFv. Clones (192) were picked from each round and expressed *via* IPTG induction. The scFv were harvested from the cells by performing freeze-thaw procedures for cell lysis. The lysate was then screened for anti-AFM1 and anti-OTA scFv by performing an ELISA (Figure 7.4). Data is not shown for OTA as no scFv capable of binding were observed. The process was repeated for OTA but, again, no clones could be identified so this mycotoxin progressed no further. Nineteen of the clones capable of binding AFM1 but not AFB1 were taken for further characterisation.

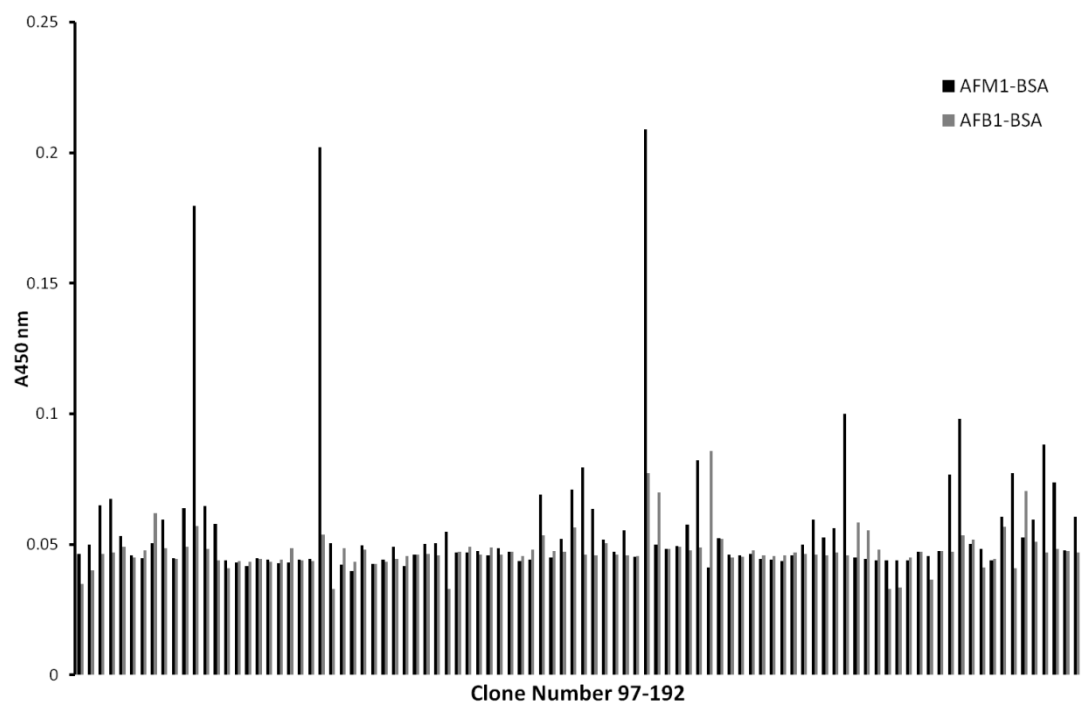
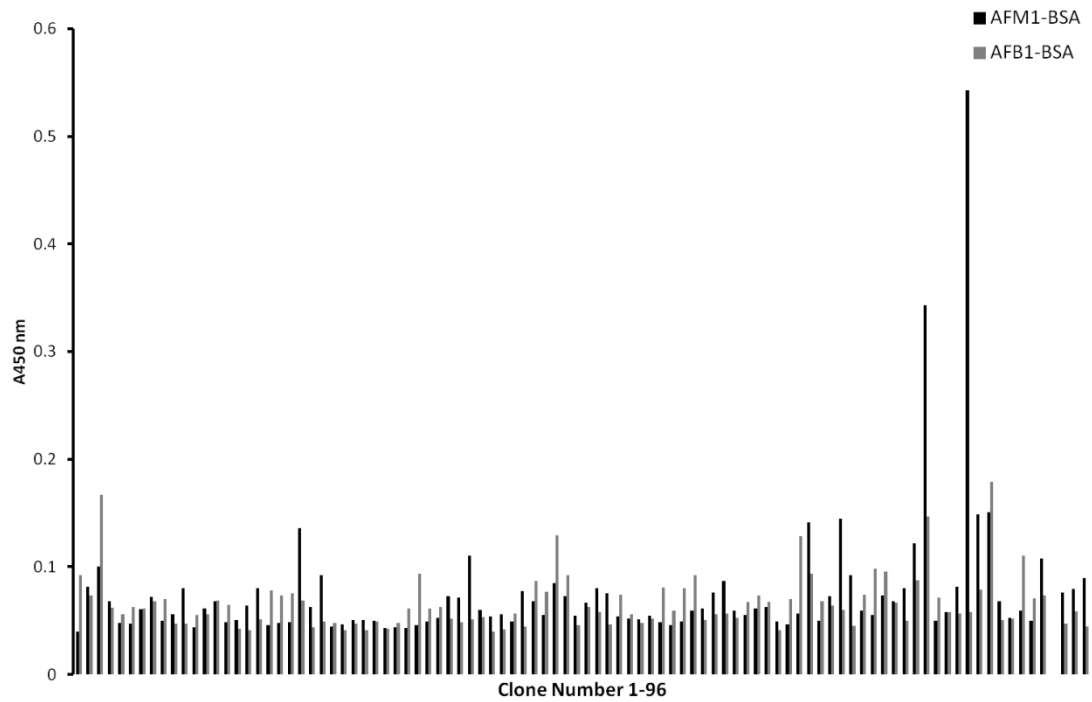


Figure 7.7: Monoclonal ELISA with 192 randomly selected clones from round two of panning. The clones were solubly expressed in Top10F cells. Nunc™ MaxiSorp™ ELISA plates were coated with 2 $\mu\text{g}/\text{mL}$ of AFM1-BSA and AFB1-BSA. ScFv were detected using a HRP-labelled anti-HA antibody. The ELISA was developed with TMB substrate and the absorbance was measured at 450 nm, using a Tecan™ Safire II plate reader. Nineteen clones were selected from this for competitive analysis.

7.2.3 Analysis of scFv clones

7.2.3.1 Analysis of clones using direct and competitive ELISA

The nineteen identified scFv clones were grown overnight and expression was induced by the addition of IPTG. The clones were analysed using competitive ELISA to determine their ability to bind AFM1 and AFB1 in free solution. An ideal clone should be capable of binding AFM1 but not AFB1. The results (Figure 7.5) highlighted 6 clones that potentially fit this criterium and so were chosen for further titration analysis. For this titration analysis, the six identified scFv clones were grown overnight and, once again, expression was induced by the addition of IPTG. Dilutions of the scFv were made to determine the titration profile of the antibodies. The results (Figure 7.6) showed one clone (H1) with a good titration profile. This clone was used for expression optimisation and IMAC purification.



Figure 7.8: Competitive ELISA of 19 scFv clones. A Nunc™ MaxiSorp™ ELISA plate was coated with 2 µg/mL of AFM1-BSA and the cell lysate containing solubly-expressed scFv clones were allowed to compete with 10 µg/mL of free AFM1 and AFB1. Bound antibody was detected with the addition of a HRP-labelled anti-HA antibody. The ELISA was developed with TMB substrate and the absorbance was measured at 450 nm, using a Tecan™ Safire II plate reader. Six clones were selected from this for titration analysis (Clone 3, 6, 8, 11, 12 and 18 from above).

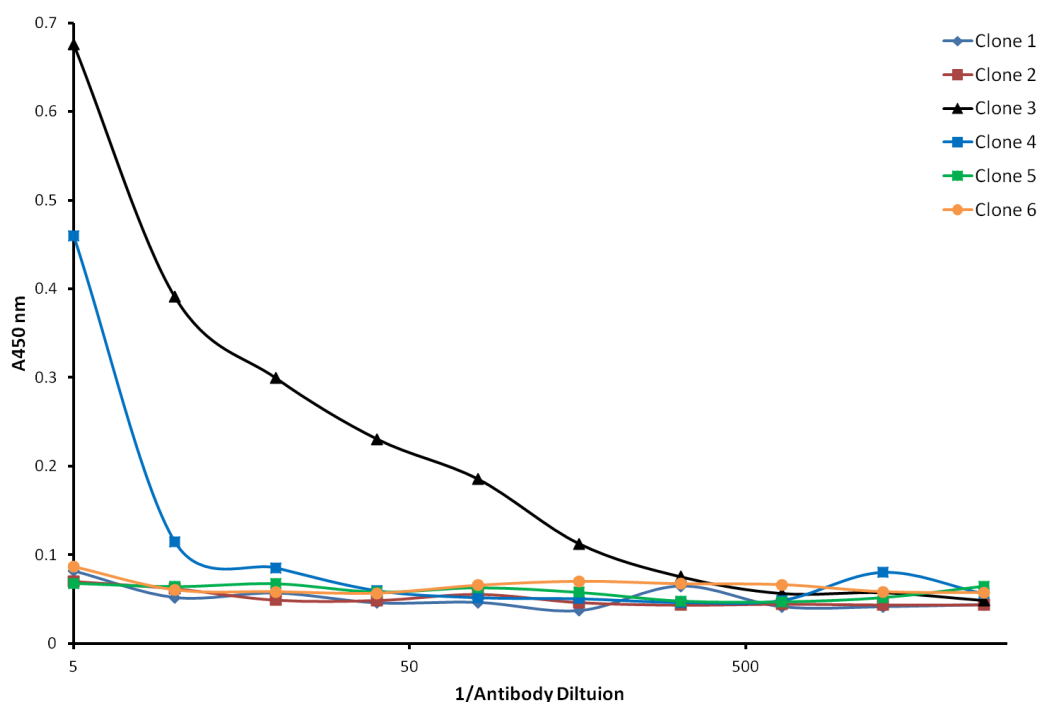


Figure 7.9: Titration analysis of six AFM1-specific clones. An indirect ELISA was performed using 2 $\mu\text{g}/\text{mL}$ of AFM1-BSA. Dilutions of lysate containing the scFv clones were added and detected using HRP-labelled anti-HA antibody. The ELISA was developed with TMB substrate and the absorbance was measured at 450 nm, using a Tecan™ Safire II plate reader. Clone 1 was selected for expression optimisation.

7.2.3.2 Optimisation of scFv expression

In order to try improve the expression level of the H1 scFv clone. An expression optimisation was carried out. Cultures of the clones were grown and expression was induced under different conditions (30°C, 37°C, 30°C + IPTG and 37°C + IPTG) overnight. The scFv were harvested from the cells by performing a sonication procedure for cell lysis. Dilutions of the scFv were made and analysed using ELISA. The results (Figure 7.7) showed that 37°C + IPTG were the optimal conditions for this clone.

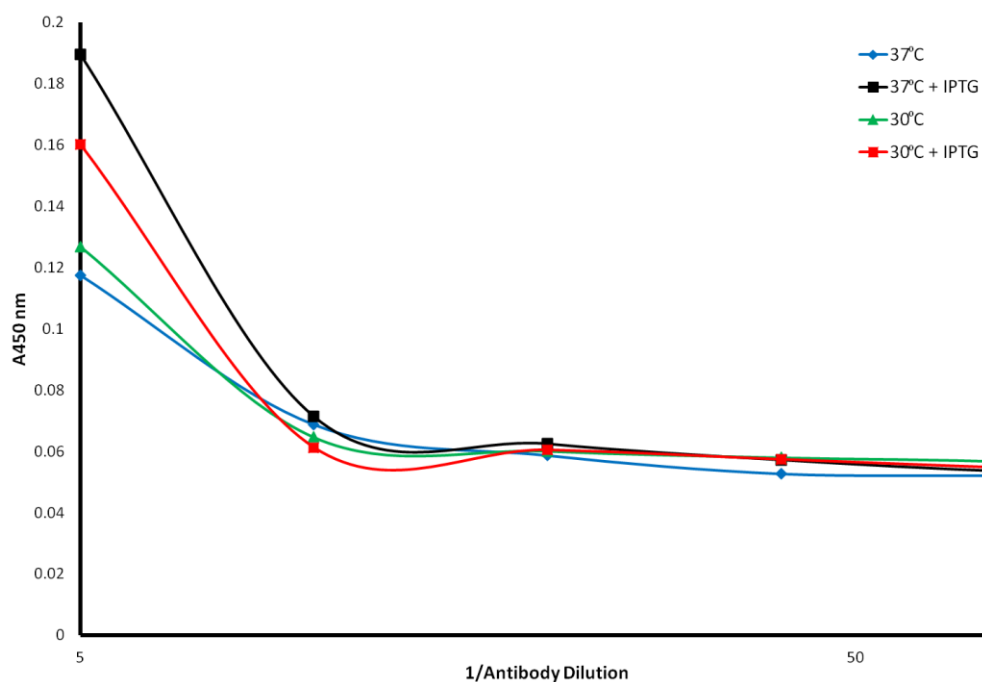


Figure 7.10: Expression optimisation analysis of the AFM1-specific clone, H1. An indirect ELISA was performed using 2 µg/mL of AFM1-BSA. Dilutions of lysate containing the scFv clone, grown under different induction conditions, were added and detected using HRP-labelled anti-HA antibody. The ELISA was developed with TMB substrate and the absorbance was measured at 450 nm, using a Tecan™ Safire II plate reader. Although there is very little difference in the expression profiles, the optimal expression conditions were determined to be 37°C overnight with IPTG induction.

7.2.3.3 IMAC purification of scFv clone and analysis using SDS-PAGE and Western Blotting

Using the optimal expression conditions, a culture of the H1 clone was grown and expression was induced overnight. The scFv were harvested from the cells by performing a sonication procedure for cell lysis. The lysate was purified using Immobilised Metal Affinity Chromatography (IMAC) and the purification was analysed by SDS-PAGE and Western Blotting. The results (Figure 7.8) show that while the scFv appears at approximately 27 kDa in the ‘flow-through’ samples in the SDS-PAGE analysis. However, it does not appear in the elution fraction or western blot. Therefore, the purification was not successful and no further analysis could be completed on the sample. However, it is hoped to further optimise and characterise this antibody in subsequent research projects in our laboratory.

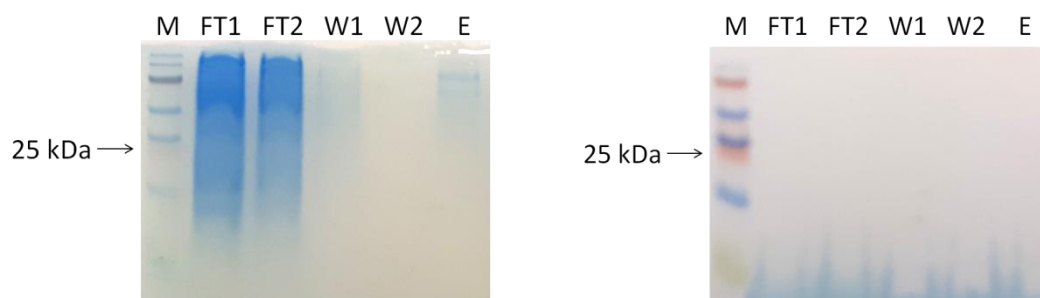


Figure 7.11: SDS-PAGE (left) and Western Blotting (right) analysis of IMAC-purified H1 scFv. M = PageRuler Plus Prestained Protein Ladder; FT1 = Lysate Flow through 1; FT2 = Lysate Flow through 2; W1 = Wash 1; W2 = Wash 2; E = Concentrated eluted purified antibody fractions. A band is visible at approximately 27 kDa, representing the scFv, in the 'flow-through' samples of the SDS-PAGE but not in the wash or elution samples or at all in the Western Blot.

7.3 Discussion

Currently, methods used for mycotoxin analysis are primarily laboratory-based techniques that are costly, time-consuming and require skilled operators. There is a pressing need to move mycotoxin analysis from the lab to the field, for rapid on-site monitoring. This 'point-of-need' analysis must be simple, cost-effective and be able to quantify multiple mycotoxins at the legislative limits. Antibodies offer the characteristics needed to facilitate this move. More specifically, recombinant antibody fragments possess the qualities required for rapid on-site analysis through immunoassay development. Recombinant antibodies can be highly specific having potential for incorporation of tags for functionalisation, immobilisation, purification and detection. They can be expressed in large quantities in bacterial systems. Additionally, they can be further improved using *in vitro* affinity maturation. (Conroy *et al.*, 2009).

Food samples are so often contaminated with multiple mycotoxins (Stoev *et al.*, 2015) and hence a multiplex assay would be preferred. Multiplex immunoassays are possible for mycotoxin detection. Burmistrova *et al.* (2014) designed a membrane-based 'flow-through' immunoassay for rapid non-instrumental multi-detection of OTA, ZEN and fumonisin B1 in cereal grains and silage. The test was based on a direct competitive enzyme immunoassay format performed on a membrane. Multiplexing an immunoassay can, however, be difficult so ideally all the antibodies would be in the same format and isolated from similar hosts, to provide a uniform approach for assay development.

Therefore, the aim of this chapter was to isolate scFv from avian immune libraries to target the mycotoxins patulin, OTA and AFM1 for incorporation into multiplex immunoassays. Development of rapid testing methodologies for these mycotoxins would serve to support existing techniques by providing a rapid warning mechanism for mycotoxin contamination outbreaks.

There are some reported instances in the literature of antibody generation for mycotoxin targets using phage display technology (Hu *et al.*, 2013; Xu *et al.*, 2015; Min *et al.*, 2016) However, there is very limited reporting of high affinity recombinant antibody fragments for AFM1, patulin and OTA, avian hosts being used, or successful patulin immunoassays. Assays for AFM1 have also struggled with cross-reactivity

issues. An avian host was chosen because of its suitability for antibody generation to small-molecular weight targets and because of its unique diversification and gene rearrangement capabilities. A chicken-derived recombinant antibody is also a preferable choice, since it is technically easier to generate than other animal species and displays high specificity and affinity. Chickens preserve their diversity by gene rearrangement and recombination even though they possess only one functional V segment and one functional J segment in the immunoglobulin heavy and light chain loci. The peculiar mechanism of immunoglobulin gene diversification leads to only one set of primers required for each antibody chain, instead of the mixtures needed for amplification of variable gene families from other animals, although previous studies have indicated that chickens produced lower anti-sera avidity than other animals such as rabbit and sheep (Hu *et al.*, 2012)

One of the main challenges to this work, and any mycotoxin analysis, was the availability and efficiency of mycotoxin-protein conjugates. Ideally, mycotoxin conjugates would be commercially available and fully characterised with comprehensive analytical techniques, such as matrix-assisted laser desorption/ionization, with time of flight (MALDI-TOF), before immunisation or screening. This analysis would provide invaluable information regarding molecular mass of the conjugate and hapten incorporation ratios. However, in this project these systems were not available and the large size of the protein carriers would have made any analysis extremely complex and difficult to analyse. Furthermore, not enough conjugate material was available for this type of analysis.

The effect of this was evident during the bio-panning of the patulin-biased immune library. Initially, a poor immune response was achieved from the avian host (Titre: 1 in 1,000). Subsequently, bio-panning was unsuccessful as the scFv inserts were not being carried through each panning round. Antibody generation does not require an excessively large amount of patulin conjugate, however, a combination of factors, including inability to generate effective immune responses and the lack of characterisation capabilities, have made recombinant antibody production unattainable for patulin at this time. Some success has been achieved in the synthesis of quality patulin conjugates, such as the work of de Champdore *et al.* (2007) in their design of a competitive fluorescence assay for the detection of patulin toxin. However,

the facilities and materials available for their work would be difficult to replicate due to limited access to the necessary equipment. This is the first reported attempt to generate an immune recombinant library for patulin using an avian host. If a reliable source of patulin conjugate becomes available in the future, or if a more efficient synthesis process is established, it may be possible to isolate the first novel recombinant antibody to patulin from the existing immune libraries. An alternative solution to this may be the use of a direct hapten coating. Kaur *et al.* (2008) employed a direct hapten coated immunoassay format for the detection herbicides with relative success, although the chemistries involved may prove as complex as conjugations themselves.

Bio-panning was, however, successful for the OTA and AFM1 libraries in that enrichment was observed from panning around. The polyclonal ELISA results suggested the presence of anti-OTA scFv in rounds 2 and 4, yet the monoclonal ELISA results produced no OTA-binding scFv. The phage used for the polyclonal ELISA was possibly too concentrated and a significant amount of non-specific binding may have occurred, leading to a false-positive result. In a library of 10^6 clones, the incidence of OTA-binding clones should be far greater, after four rounds of affinity selection. This may indicate that the library was not sufficiently diverse initially, and many of the clones analysed were multiple copies of the same clone. It may also indicate that the panning conditions at the start of the selection process were too stringent and did not allow for enrichment of all of the clones in the library, hence library diversity was lost too soon.

The monoclonal ELISA for AFM1 successfully identified nineteen clones that were capable of binding AFM1 at a much higher level than AFB1. This is important as it shows the success of the depletion process and will ultimately circumvent issues with cross-reactivity when incorporated into an immunoassay. This is the first reported instance of AFM1 antibody generation by depletion with AFB1. From the nineteen clones identified in the monoclonal analysis, six were found to have the ability to bind AFM1 competitively in free solution. As most mycotoxin immunoassays use competitive formats it is important to include this ability in the screening and characterisation processes. Finally, a single clone (H1) was isolated that demonstrated

a good titration profile and its expression conditions were optimised, an attempt was made to purify this antibody using IMAC but further optimisation is required.

Overall this work has highlighted the difficulty in generating recombinant antibodies to target mycotoxins. This is not overly surprising as haptens that have been shown to exert immunosuppressive effects do not readily lend themselves to being immune targets. From the initial immunisations to the final screening and characterisation, the availability of high quality mycotoxin and conjugates is crucial. This work aimed to isolate antibodies for three mycotoxins but was only successful in one instance, and it was this mycotoxin that had the highest immune response initially and a commercially available mycotoxin conjugate. The anti-AFM1 scFv clone isolated from this work now has the potential to be used in an immunoassay format to detect AFM1. The immune libraries for OTA and patulin still have potential to be screened further to produce high affinity clones.

Furthermore, the affinity of the AFM1 clones isolated in this study could potentially be improved by genetic engineering methods, such as site-directed mutagenesis or affinity maturation. There are reported successes of these methods for anti-mycotoxin antibody improvement. Hu *et al.*, 2015 detailed how an affinity improved single-chain antibody from phage display of a library derived from monoclonal antibodies detects fumonisins by immunoassay at an 82-fold higher binding affinity than its parent mAb. Min *et al.*, (2016) described an affinity improvement by fine tuning of single-chain variable fragment against aflatoxin B1 and achieved 3.2-fold affinity improvement. Therefore, any scFv clones isolated from these immune libraries have the potential to be engineered and customised for a multitude of uses in mycotoxin detection and monitoring.

Chapter 8: Overall Conclusions

8.1 Overall conclusions

The research detailed in this thesis describes an investigation of the immunomodulatory effects of the mycotoxins patulin, DON, ZEN and T-2 toxin on murine macrophage function *in vitro*, using both end-point and novel 'real-time' analysis. A proof-of-concept for a novel method of measuring the effects of multiple mycotoxins in 'real-time' is described. Additionally, the optimisation of recombinant immune library production for the mycotoxins patulin, OTA and AFM1 is detailed, and the isolation and characterisation of single chain antibody fragments from these libraries is described.

Chapters 3, 4 and 5 have contributed to the understanding of some of the biological processes underlying macrophage dysfunction in the presence of the mycotoxins patulin, DON, ZEN and T-2 toxin. One of the key parameters under investigation was the effect of immunomodulation on the macrophage response to microbial pathogens (LPS) and, therefore, host resistance.

Under the threat of infection, activated macrophages produce pro-inflammatory cytokines (TNF- α , IL-1 β , IL-6, IL-27 and IL-12p40) and anti-inflammatory cytokines (IL-10) to regulate the inflammatory response. In Chapter 3, the cytokine profile, following individual mycotoxin exposure, provided vital information regarding the immunotoxic and immunomodulatory nature of these toxins. This is the first report of an investigation into the *in vitro* effects of these toxins on the murine macrophage cell line, J774A.1. It was found that patulin and DON had no effect on the viability of the macrophages in comparison to the control cells, but patulin does appear to increase the proliferation of these cells at high concentrations. However, both ZEN and T-2 toxin are cytotoxic at high concentrations, as the macrophages displayed a significant decrease in viability compared to the control. These effects were replicated when the cells were exposed to toxins and LPS simultaneously. It is possible that a protection mechanism is activated in the macrophage cells when specific toxin concentrations are reached, which aids in cell survival. However, at higher toxin concentrations, this unknown mechanism(s) may be overwhelmed, which results in cytotoxicity effects.

The significant effects on macrophage viability led to the further investigation of mycotoxins *in vitro*. It was discovered that individually patulin, DON, ZEN and T-2 toxin all affect the ability of macrophages to respond to LPS activation, through analysis of

cytokine production. This cytokine production study demonstrated that mycotoxins have varying effects on the secretion of IL-6, IL-10, IL-27, IL-12p40, IL-1 β and TNF- α . These effects are dependent on toxin dosage and exposure to LPS stimulation. Interestingly, it was observed that 10 pg/mL of each of the toxins caused a large pro-inflammatory response with increases in the production of IL-27, IL-12p40, IL-1 β and TNF α . DON demonstrated a large overall pro-inflammatory response at high concentrations while some of the toxins suppressed pro-inflammatory cytokines at lower concentrations. Overall, it was apparent that individually these toxins have a dose-dependent effect on the modulation of cytokine secretion.

Understanding the effects of individual mycotoxin exposure is important but as mycotoxin contamination is so widespread, exposure to low levels of multiple toxins is almost unavoidable. Therefore, it is crucial to understand how low concentrations of multiple mycotoxins interact with the immune system. There is still a lack of understanding of how multiple mycotoxins interact with each other and the immune system. It is evident that the effects of mycotoxins can vary depending on concentration, combinations, exposure times as well as other environmental factors.

Chapter 4 built on data obtained in chapter 3 in order to investigate how binary combinations of these mycotoxins differ from their individual effects. From chapter 3, it was observed that while mycotoxins are not cytotoxic at very low concentrations they can still cause immune dysfunction. The cytokine production data detailed in chapter 4 clearly indicates that these mycotoxins have varying effects on the production levels of IL-6, IL-10, IL-12p40 and TNF- α , depending on mycotoxin concentration, combination and exposure to LPS. Exposure of macrophages to patulin, DON, ZEN and T-2 toxin resulted in a concentration and combination-dependent modulation of cytokine secretion. Specifically, it was observed that exposure to individual concentrations of DON and ZEN had no significant effect on the secretion levels of TNF- α following LPS stimulation, however, in all cases the combination of these toxins resulted in a largely significant suppression of TNF- α production. A similar effect was observed with the combination of ZEN and T-2 toxin, with each of these toxins having no effect on TNF- α but their combination caused suppression after LPS activation. While the individual concentrations of ZEN and T-2 toxin did result in suppression of IL-6, their combination produced a much greater suppression of the

cytokine's production level. Possibly the most interesting result arose from the combination of patulin and T-2 toxin. Here, the individual concentrations had no effect on IL-6 production after LPS activation but showed suppression when combined, and one of the combinations also significantly increased the production of IL-10 without LPS stimulation. However, the individual concentrations of patulin and ZEN suppressed the production of TNF- α , yet their combination increased the production of this cytokine. Overall, examples of these mycotoxins working additively, synergistically and antagonistically were observed depending on the concentrations and combinations. This is the first report on the effects of binary combinations of these mycotoxins on macrophage cells and it is evident that the toxins interact with each other to exert modulatory effects and disrupt macrophage function

It was clear from this data that binary combinations of mycotoxins can differ significantly from their individual effects with relation to their effect on cytokine secretion levels, but it was then important to examine their effects on other key aspects of macrophage function, such as cell surface marker expression and ability to phagocytose. Therefore, chapter 5 in this thesis used the data obtained from chapters 3 and 4 to select individual and combinations of mycotoxins to determine their effects on phagocytosis and the expression levels of CD80, CD86, TLR4 and MHCII. The cell surface marker data displayed in chapter 5 supports this data from chapter 4 and demonstrated that these mycotoxins, alone and in combinations, have varying effects on the expression levels of key cell surface makers, as well as phagocytosis. These effects are dependent on mycotoxin concentration, combination and exposure to LPS. Once again, it is apparent that these mycotoxins can be immunostimulatory or immunosuppressive depending on the concentration and combination. Notably, it was observed that 0.1 pg/mL DON increased phagocytosis after LPS stimulation but this was decreased without LPS challenge. The combinations of 0.01 pg/mL DON and 0.001 pg/mL ZEN showed an increase in phagocytosis without LPS, while the combinations of 0.1 pg/mL patulin and 0.001 pg/mL ZEN increased phagocytosis after LPS activation. ZEN (0.01pg/mL) caused an increased expression of MHCII, TLR4, CD80 and CD80 without LPS but after LPS activation the levels of all of these cell surface markers are decreased by this concentration. MHCII and CD80 levels are increased when exposed to 0.1pg/mL DON without LPS but a reduction in CD80 levels is seen after LPS stimulations compared to controls. Patulin appears to show suppression in the levels

of CD80 and CD80 at a number of concentrations (0.01, 0.1 and 1 pg/mL) both with and without LPS activation. Combinations of these patulin concentrations with DON, ZEN and T-2 show significant effects on the expression levels of all four surface makers. Overall, examples of these mycotoxins working additively, synergistically and agnostically were observed.

It is evident that mycotoxins, alone and in combinations, possess the ability to disrupt the signalling and functional ability of macrophages even at sub-lethal concentrations. The exact molecular processes of how these toxins cause this dysfunction are still not fully clear. However, this report has provided data which may aid in the understanding of how mycotoxins inhibit macrophage functions and, therefore, host defence systems. Evidence has been presented to show that even if a mycotoxin does not have an effect alone its combination with another can produce detrimental results. This has significant consequences for food safety monitoring. We must be able to account for the combinatory effects of multiple adulterants in contaminated food samples.

The results observed from Lab-in-a-Trench (LiaT) analysis are largely significant in this respect. Many of the effects observed in the flow cytometry analysis of CD80 and CD86 were also observed in LiaT analysis. The data also allows a direct comparison of the effects of individual mycotoxins versus their combinations. This successfully demonstrates the ability to measure the effects of multiple mycotoxins in a sample in 'real-time'. At present, there are no methods of doing this available. Currently, methods of mycotoxin analysis are based on the measurement of individual mycotoxins in samples and do not take into account the "cocktail effect" of multiple contaminants in a sample. Although LC-MS/MS can distinguish the presence of over 60 mycotoxins in a single sample the current novel approach provides a dynamic assay using a novel microfluidics-based strategy and has resulted in the new term 'mycofluidics' to describe the phenomenon. The LiaT offers a simple and robust method to measure potential additive and synergistic effects of multiple mycotoxins in 'real-time'. This analysis is not limited to mycotoxins analysis and has the potential to be used for any adulterants in a sample. The future of food analysis will require much more than simple individual quantification and a technology like LiaT can offer the characteristics needed to develop more sophisticated testing.

The initial part of this research project focused on the deregulation of immune system function by mycotoxins. Due to the obvious threat posed by mycotoxin exposure, regulatory limits have been introduced around the world. These limits are monitored by sophisticated analytical techniques such as LC-MS. The need for analysis method to account for the effect of multiple mycotoxin contamination has already been discussed, but the ability to quantify these toxins rapidly on-site is still a pressing issue. Assays must be designed that can compete with the gold standard techniques in terms of sensitivity and specificity to move mycotoxin monitoring from the lab to the field. A number of mycotoxin-specific antibodies have already been produced in the laboratory. However, no immune recombinant antibodies exist to patulin, OTA and AFM1. Therefore, chapters 6 and 7 of this these focus on the generation of recombinant immune libraries against patulin, OTA and AFM1, and the screening of these libraries for isolation of high affinity scFv to target the mycotoxins.

Initially, chapter 6 described the generation of a recombinant immune library to the mycotoxins patulin, OTA and AFM1. The immunisations of avian hosts were described and the difficulty in generating an immune response to patulin was highlighted. RNA was harvested from the avian spleen and converted to cDNA which was the template for amplification of the variable regions. The importance of polymerase choice was evident in these PCR's as the V_H region would not amplify from the cDNA of the patulin-immunised spleen using MyTaq™ Red Mix but successful amplification was achieved with GoTaq® polymerase. Following these successful amplifications the variable regions were joined by SOE-PCR. Here, it was demonstrated how crucial the annealing temperature is for the reaction as only slight changes (0.5 °C) had an impact on the amplification. A number of different conditions for the SOE reaction were investigated including use of a high fidelity polymerase and a two-step PCR, ultimately the optimal conditions were determined by use of a higher annealing temperature is due to the high T_m of the SOE primers. This allowed for the SOE product from each mycotoxin target to be amplified on large-scale and ligated into the pComb3XSS vector. This vector was they successfully transformed into XL1-Blue electrocompetent cells and scFv libraries were generated that could be screened for high affinity antibodies.

Chapter 7 then described the screening of these recombinant immune libraries. As previously outlined, chickens provided a number of advantages for recombinant antibody generation. A patulin-HS-BSA conjugate was synthesised in order to screen for this target and the conjugate was test using a commercial polyclonal antibody. Despite the conjugation appearing to be successful, bio-panning of this library could not be completed for when the colony pick PCR was checked the scFv inserts were not being carried through the panning rounds. This indicted that either there were not any clones present capable of binding the patulin conjugate, or the patulin conjugate was not of a high enough quality to allow scFv to bind. This issue may be due to the size and diversity of the original immune library. Initially, a poor immune response to the Patulin-HG-KLH conjugate was observed (Titre: 1 in 1,000). Patulin proved to be a very difficult toxin target, and there are very few reports of antibodies to target patulin in literature, with virtually no data on recombinant scFv development available. In the future, if new well-characterised patulin conjugates become available, the existing recombinant library could still be screened for novel binders. An isolated clone from this library would represent the only existing recombinant antibody to patulin. These results highlight the importance of each step in the generation process. From the very first immunisation to the final panning round, and the characterisation that follows all must involve the use of high quality and well-characterised reagents to ensure a successful output.

Even with the availability of this reagents, isolation of high affinity clones can still prove challenging. The initial immune response to OTA from the avian host with a good (Titre: 1 in 40,000) and a commercial OTA-BSA conjugate was available but even with enrichment observed in the polyclonal phage ELISA no binders could be identified with the monoclonal ELISA despite screening of 192 clones. This may be due to the diversity of the library being low and so many copies of the same scFv are present. The depletion process with BSA may also have been too severe and removed too many of the scFv from the original phage pool. This library still does, however, have the potential to produce high affinity scFv which would be useful to combine with other antibodies generated in the lab for multiplex detection.

Bio-panning of the immune library to AFM1 successfully identified a number of clones capable of being the toxin, and the H1 clone was characterised for its ability to bind in

a number of formats. This bio-panning process involved a unique depletion step in which the phage pool was depleted with an AFB1-BSA conjugate first. This would remove not only non-specific BSA-binders but also any scFv that target regions common to both AFB1 and AFM1, and ultimately allow for selection of clones that can bind AFM1 with little cross-reactivity to AFB1. Enrichment of the phage was observed after round 2 of panning so 192 clones from this round were screened and from this, 19 were identified as having good binding potential. These 19 scFv were then examined in a competitive format, from which 6 were determined capable of binding AFM1 in free solution. This is important as most mycotoxin immunoassays involve the use of competitive ELISAs. The titration profiles of these 6 clones were then examined and the H1 clone was selected based on its performance. The expression of the H1 clone was then optimised and the scFv was cultured in large-scale and purified by immobilised metal affinity chromatography, *via* an incorporated hexahistidine tag. The purification process was unsuccessful and this could be due to issues with the hexahistidine tag, possibly because of the conformation or folding of scFv preventing binding to the tag. Alternative purification techniques may need to be employed in future and further structural analysis and characterisation would be needed on the H1 scFv. There is also a potential to use genetic engineering methods such as chain shuffling or site-directed mutagenesis to improve the binding characteristics of any of the clones identified. These clones can then be incorporated into multiplex immunoassays for rapid detection of mycotoxins in the field.

Overall, this work has shown that naturally-occurring mycotoxins have the ability to cause macrophage and, therefore, immune dysfunction. Many of the molecular processes involved in this dysfunction are still not fully understood. However, this research work has shed some light on the mechanisms in which toxins inhibit macrophage and host defence functionality, through deregulation of cytokine secretion, cell surface marker expression and phagocytosis. Much more work is needed in this area to identify the exact pathways that these, and other, mycotoxins interact with and the effect these interactions have on immune function of humans and animals.

In addition, this work has also provided a proof-of-concept for a novel method of monitoring the “cocktail effect” of multiple mycotoxin contaminants through the use

of the Lab-in-a-Trench microfluidic platform for 'real-time' single cell analysis. This could prove highly significant in food safety monitoring as it accounts for the additive and synergistic effects of multiple contaminants in a sample which would help improve food safety. Further optimisation of the LiaT process is needed but in the future it could be combined with immunoassays in a device capable of monitoring the quantity of mycotoxin in a sample along with their effects.

The utility of recombinant antibody technology for the production of anti-mycotoxin antibodies was illustrated, and the importance of careful optimisation of each step in the production and screening of immune antibody libraries for the generation of anti-mycotoxin recombinant antibodies was highlighted. This work has produced recombinant immune libraries that, in the future, could be screened again to isolate high affinity antibodies. This project has also successfully employed depletion bio-panning with phage display technology to isolate a scFv with the ability to bind AFM1. Further characterisation of this clone is needed; such as examining binding kinetics with SPR, determining its sequence, and modelling its structure but it could now be used in immunoassay format to rapidly quantify AFM1 in food samples. It would be imperative to validate the assay in a matrix, to analyse whether sensitive AFM1 detection is possible in real samples, such as milk. These assays would then have to be correlated with currently-accepted detection methods, including HPLC and mass spectrometry.

Ultimately, the aim of this project was to utilise the insight gained from basic research to give novel diagnostic applications for a panel of mycotoxins, and to take mycotoxin analysis from the lab to the field. This research aimed to not only shed light on the how mycotoxins interact with the immune system, but to also use this information in their analysis by designing a way of monitoring the effects of multiple mycotoxins in a sample on immune cells, while also quantifying these toxins using recombinant antibodies. This work has provided important foundations for advancements in mycotoxin analysis research.

Chapter 9: Bibliography

- Abbès, S., Ben Salah-Abbès, J., Sharafi, H., Oueslati, R., Noghabi, K.A.** (2013). *Lactobacillus paracasei* BEJ01 prevents immunotoxic effects during chronic zearalenone exposure in Balb/c mice. *Immunopharmacol. Immunotoxicol.* **35(3)**, 341–348.
- Aderem, A.** (2003). Phagocytosis and the Inflammatory Response. *J. Infect. Dis.* **187**, S340-5.
- Al-Anati, L., and Petzinger, E.** (2006). Immunotoxic activity of ochratoxin. *A. J. Vet. Pharmacol. Ther.* **2**, 79-90.
- Alassane-Kpembé, I., Kolf-Clauw, M., Gauthier, T., Abrami, R., Abiola, F.A., Oswald, I.P. and Puel, O.** (2013). New insights into mycotoxin mixtures: The toxicity of low doses of type B trichothecenes on intestinal epithelial cells is synergistic. *Toxicol. Appl. Pharmacol.* **272(1)**, 191-198.
- Akira, S., Uematsu, S., and Takeuchi, O.** (2006). Pathogen recognition and innate immunity. *Cell.* **4**, 783-801.
- Ashcroft, G.S., Mills, S.J., Lei, K., Gibbons, L., Jeong, M.-J., Taniguchi, M., Burow, M., Horan, M.A., Wahl, S.M., Nakayama, T.** (2003). Estrogen modulates cutaneous wound healing by downregulating macrophage migration inhibitory factor. *J. Clin. Invest.* **111**, 1309–1318.
- Azzazy, H.M.E. & Highsmith, W.E.** (2002), Phage display technology: clinical applications and recent innovation, *Clin. Biochem.* **35(6)**, 425-445.
- Ball, R.W., Huie, J.M. and Coulombe Jr., R.A.** (1995). Comparative activation of aflatoxin B1 by mammalian pulmonary tissues. *Toxicol. Lett.* **75(1–3)**, 119-125.
- Barbas, C.F., 3rd, Burton, D.R., Scott, J.K., and Silverman, G.J.** (2001). Phage Display: A Laboratory Manual, 1st Edition. Cold Spring Harbor Laboratory Press, New York, USA.
- Barbas, C.F., 3rd, Bain, J.D., Hoekstra, D.M., and Lerner, R.A.** (1992). Semisynthetic combinatorial antibody libraries: a chemical solution to the diversity problem. *Proc. Natl. Acad. Sci. U.S.A.* **10**, 4457-4461.

- Bianco**, G., Russo, R., Marzocco, S., Velotto, S., Autore, G. and Severino, L. (2012). Modulation of macrophage activity by aflatoxins B1 and B2 and their metabolites aflatoxins M1 and M2. *Toxicon*. **59(6)**, 644–650.
- Bendtzen**, K. (1988). Interleukin 1, interleukin 6 and tumor necrosis factor in infection, inflammation and immunity. *Immunol. Lett.* **3**, 183-191.
- Boonen**, J., Malysheva, S.V., Taevernier, L., Diana Di Mavungu, J., De Saeger, S. and De Spiegeleer, B. 2012. Human skin penetration of selected model mycotoxins. *Toxicology*. **301(1–3)**, 21-32.
- Borrebaeck**, C.A.K. (2000). Antibodies in diagnostics – from immunoassays to protein chips. *Immunol. Today*. **21(8)**, 379-382.
- Bottalico**, A. (1998). Fusarium diseases of cereals: Species complex and related mycotoxin profiles. *Eur. J. Plant Pathol.* **80**, 85-103.
- Bruneau**, J.C., Stack, E., O’Kennedy, R. and Loscher, C.E. (2012). Aflatoxins B1, B2 and G1 modulate cytokine secretion and cell surface marker expression in J774A.1 murine macrophages. *Toxicol. In Vitro*. **26(5)**, pp.686-693.
- Bryksin**, A.V., Matsumura, I. (2010). Overlap extension PCR cloning: a simple and reliable way to create recombinant plasmids. *Biotechniques* **48**, 463–465.
- Bucci**, T.J., Howard, P.C., Tolleson, W.H., Laborde, J.B., and Hansen, D.K. (1998). Renal effects of fumonisin mycotoxins in animals. *Toxicol. Pathol.* **1**, 160-164.
- CAST** (Council for Agricultural Science and Technology). (2003). Mycotoxins: risks in plant, animal, and human systems. *Task Force Report*, Ames, Iowa, USA. **139**, 1-199.
- Capasso**, L., Longhin, E., Caloni, F., Camatini, M. and Gualtieri, M. (2015). Synergistic inflammatory effect of PM10 with mycotoxin deoxynivalenol on human lung epithelial cells. *Toxicon*. **104**, 65-72.
- Caputo**, D., de Cesare, G., Nascetti, A., Scipinotti, R., Pavanello, F., Arrigoni, R. (2014). DEMOCHEM: integrated system for mycotoxins detection. *Procedia. Eng.* **87**, 1354-1357.

- Clarke**, R., Connolly, L., Frizzell, C. and Elliott, C.T. (2014). Cytotoxic assessment of the regulated, co-existing mycotoxins aflatoxin B1, fumonisin B1 and ochratoxin, in single, binary and tertiary mixtures. *Toxicon*. **90**, 70-81.
- Conroy**, P.J., Hearty, S., Leonard, P. and O’Kennedy, R.J. (2009). Antibody production, design and use for biosensor-based applications. *Sem. Cell Dev. Biol.* **20(1)**, 10-26.
- Cooper**, A.M., Khader, S.A. (2007). IL-12p40: an inherently agonistic cytokine. *Trends Immunol.* **28**, 33–38.
- Couper**, K.N., Blount, D.G., Riley, E.M. (2008). IL-10: The Master Regulator of Immunity to Infection. *J. Immunol.* **180**, 5771–5777.
- Cousins**, M.A., Riley, R.T., and Pestka, J.J. 2005. Foodborne mycotoxins: chemistry, biology, ecology, and toxicology. In Foodborne pathogens: microbiology and molecular biology. 1st Edition. Editors, Fratamico P.M, Bhunia A.K, Horizon Scientific Press, Norfolk, UK. 164.
- Daly**, S.J., Keating, G.J., Dillon, P.P., Manning, B.M., O’Kennedy, R., Lee, H.A., and Morgan, M.R. (2000). Development of surface plasmon resonance-based immunoassay for aflatoxin B1. *J. Agric. Food Chem.* **11**, 5097-5104.
- Decken**, K., Köhler, G., Palmer-Lehmann, K., Wunderlin, A., Mattner, F., Magram, J., Gately, M.K., Alber, G. (1998). Interleukin-12 Is Essential for a Protective Th1 Response in Mice Infected with *Cryptococcus neoformans*. *Infect. Immun.* **66**, 4994–5000.
- Degen**, G.H. (2011). Tools for investigating workplace-related risks from mycotoxin exposure. *World Mycotoxin J.* **4(3)**, 315-327.
- De la Cruz**, S., Cubillos-Zapata, C., López-Calleja, I.M., Ghosh, S., Alcocer, M., González, I., Martín, R., García, T. (2015). Isolation of recombinant antibody fragments (scFv) by phage display technology for detection of almond allergens in food products. *Food Control* **54**, 322–330.
- Devegowda**, G., and Murthy, T.K.N. (2005). Mycotoxins: their adverse effects in poultry and some practical solutions. In The Mycotoxin Blue Book, 1st Edition. Editors, Diaz, D. E. Nottingham University Press, Nottingham, UK, 25-26.

- Dinarello, C.A.** (2000). Proinflammatory cytokines. *Chest*. **2**, 503-508.
- Dunne, L., Daly, S., Baxter, A., Haughey, S. and O'Kennedy, R.** (2005). Surface plasmon Resonance-Based immunoassay for the detection of aflatoxin B1 using Single-Chain antibody fragments. *Spectroscop. Lett.* **38(3)**, 229-245.
- Edite Bezerra da Rocha, M., Freire, F.d.C.O., Erlan Feitosa Maia, F., Izabel Florindo Guedes, M. and Rondina, D.** (2014). Mycotoxins and their effects on human and animal health. *Food Control*. **36(1)**, 159-165.
- Eckert, K.A., Kunkel, T.A.** (1991). DNA polymerase fidelity and the polymerase chain reaction. *PCR Methods Appl.* **1**, 17–24.
- Feng, X.M., Liu, N., Yang, S.G., Hu, L.Y., Chen, X.L., Fang, Z.H., Ren, Q., Lu, S.H., Liu, B., Han, Z.C.** (2008). Regulation of the class II and class I MHC pathways in human THP-1 monocytic cells by interleukin-27. *Biochem. Biophys. Res. Commun.* **367**, 553–559.
- Ferrante, M. C., Meli, R., Raso, G. M., Esposito, E., Severino, L., Di Carlo, G. and Lucisano, A.** (2002). Effect of fumonisin B on structure and function of macrophage plasma membrane. *Toxicol. Lett.* **129(3)**, 181–187.
- Ferrante, M. C., Raso, M. G., Bilancione, M., Esposito, E., Iacono, A. and Meli, R.** (2008). Differential modification of inflammatory enzymes in J774A.1 macrophages by ochratoxin A alone or in combination with lipopolysaccharide. *Toxicol. Lett.* **181(1)**, 40–46.
- Fodey, T., Delahaut, P. & Elliott, C.T.** (2007a), Use of antigen mimics to produce specific antibodies to anti-coccidial drugs, *J. Immunol. Methods*, **323(1)**, 31-38.
- Forgacs, J. and Carll W.T.** (1955). Preliminary mycotoxic studies on hemorrhagic disease in poultry. *Vet. Med.* **50**, 172.
- Gabay, C.** (2006). Interleukin-6 and chronic inflammation. *Arthritis Res. Ther.* **8**, S3.
- Gong, Y.Y., Egal, S., Hounsa, A., Turner, P.C., Hall, A.J., Cardwell, K.F., and Wild, C.P.** (2003). Determinants of aflatoxin exposure in young children from Benin and Togo, West Africa: the critical role of weaning. *Int. J. Epidemiol.* **4**, 556-562.

- Gordon, S.,** and Taylor, P.R. (2005). Monocyte and macrophage heterogeneity. *Nat. Rev. Immunol.* **12**, 953-964.
- Grenier, B.,** Oswald, I. (2011). Mycotoxin co-contamination of food and feed: meta-analysis of publications describing toxicological interactions. *World Mycotoxin J.* **4**, 285-313.
- Grinyó, J.M.,** Cruzado, J.M., Bestard, O., Vidal Castiñeira, J.R., Torras, J. (2012) Immunosuppression in the ERA of Biological Agents. *Adv. Exp. Med. Biol.* **741**, 60-72.
- Halbin, K.J.,** Kouakou, B., Dago, G. (2013). Low level of ochratoxin A enhances aflatoxin B1 induced cytotoxicity and lipid peroxidation in both human intestinal (caco-2) and hepatoma (HepG2) cell lines. *J. Nutr. Food Sci.* **2(6)**, 294-30.
- Han, K. N.,** Li, C. A. & Seong, G. H. (2013). Microfluidic Chips for Immunoassays. *Annu. Rev. Anal. Chem.* **6**, 119-141.
- Hawksworth, D.L.** (1991). The fungal dimension of biodiversity: magnitude, significance, and conservation. *Mycol. Res.* **95**, 641–655.
- Hermanson, G.T.** (2005), *Bioconjugate Techniques*, (2nd edn.), Academic Press, San Diego, USA.
- Holford, T.R.J.,** Davis, F., Higson, S.P.J. (2012). Recent trends in antibody based sensors. *Biosensors and Bioelectronics* **34**, 12–24.
- Holladay, S.D.,** and Blaylock, B.L. (2002). The mouse as a model for developmental immunotoxicology. *Hum. Exp. Toxicol.* **9-10**, 525-531.
- Holling, T.M.,** Schooten, E., van Den Elsen, P.J. (2004). Function and regulation of MHC class II molecules in T-lymphocytes: of mice and men. *Hum. Immunol.* **65**, 282–290.
- Hoogenboom, H.R.** (2002), Overview of antibody phage-display technology and its applications. *Method Mol. Biol.* **178**, 1-38.
- Hymery, N.,** Masson, F., Barbier, G. and Coton, E. 2014. Cytotoxicity and immunotoxicity of cyclopiazonic acid on human cells. *Toxicol. In Vitro.* **28(5)**, 940-947.

- Hu, Z.-Q., Li, H.-P., Wu, P., Li, Y.-B., Zhou, Z.-Q., Zhang, J.-B., Liu, J.-L., Liao, Y.-C. (2015).** An affinity improved single-chain antibody from phage display of a library derived from monoclonal antibodies detects fumonisins by immunoassay. *Anal. Chim. Acta* **867**, 74–82.
- Hussein, H.S. and Brasel, J.M. (2001).** Toxicity, metabolism, and impact of mycotoxins on humans and animals. *Toxicol.* **167(2)**, 101-134.
- Iyer, S.S., Cheng, G. (2012).** Role of Interleukin 10 Transcriptional Regulation in Inflammation and Autoimmune Disease. *Crit. Rev. Immunol.* **32**, 23–63.
- Jia, Z., Liu, M., Qu, Z., Zhang, Y., Yin, S. and Shan, A. (2014).** Toxic effects of zearalenone on oxidative stress, inflammatory cytokines, biochemical and pathological changes induced by this toxin in the kidney of pregnant rats. *Environ. Toxicol. Pharmacol.* **37(2)**, 580-591.
- Jiang, Y., Jolly, P.E., Ellis, W.O., Wang, J.S., Phillips, T.D., and Williams, J.H. (2005).** Aflatoxin B1 albumin adduct levels and cellular immune status in Ghanaians. *Int. Immunol.* **6**, 807-814.
- Johnston, B., Conly, J. (2006).** Tumour necrosis factor inhibitors and infection: What is there to know for infectious diseases physicians? *Can. J. Infect. Dis. Med. Microbiol.* **17**, 209–212.
- Kankkunen, P., Välimäki, E., Rintahaka, J., Palomäki, J., Nyman, T., Alenius, H., Wolff, H., Matikainen, S. (2014).** Trichothecene mycotoxins activate NLRP3 inflammasome through a P2X7 receptor and Src tyrosine kinase dependent pathway. *Human Immunol.* **75**, 134–140.
- Kew, M.C. (2003).** Synergistic interaction between aflatoxin B1 and hepatitis B virus in hepatocarcinogenesis. *Liver Int.* **23(6)**, 405–409.
- Klaric, M.Š., Rašić, D. and Peraica, M. (2013).** Deleterious effects of mycotoxin combinations involving ochratoxin A. *Toxins.* **5(11)**, 1965-1987.
- Kuiper-Goodman, T. (1995).** Mycotoxins: Risk assessment and legislation. *Toxicol. Lett.* **82–83**, 853-859.

- Lei, M., Zhang, N., Desheng, Q. (2013).** *In vitro* investigation of individual and combined cytotoxic effects of aflatoxin B1 and other selected mycotoxins on the cell line porcine kidney 15. *Exp. Toxicol. Pathol.* **63**, 1149-1157.
- Levisson, M., Spruijt, R.B., Winkel, I.N., Kengen, S.W.M., Oost, J. van der, 2014.** Phage Display of Engineered Binding Proteins, in: Protein Downstream Processing, Methods in Molecular Biology. Humana Press, Totowa, NJ, pp. 211–229.
- Li, P., Zhang, Q. and Zhang, W. (2009).** Immunoassays for aflatoxins. *Trends Anal. Chem.* **28(9)**, 1115-1126.
- Liu, B., Yu, F., Chan, M., and Yang, Y. (2002).** The effects of mycotoxins, fumonisin B1 and aflatoxin B1, on primary swine alveolar macrophages. *Toxicol. Appl. Pharmacol.* **3**, 197-204.
- Livonesi, M.C., Souto, J.T., Campanelli, A.P., Maffei, L., M, C., Martinez, R., Rossi, M.A., Silva, D., Santana, J. (2008).** Deficiency of IL-12p40 subunit determines severe paracoccidioidomycosis in mice. *Med. Mycol.* **46**, 637–646.
- Loftus, J.H., Kijanka, G.S., O’Kennedy, R. (2017).** Mycofluidics: Diagnostic Devices with Microfluidics, in: Diagnostic Devices with Microfluidics. Taylor & Francis Group, 6000 Broken Sound Parkway NW, Suite 300, Boca Raton, FL 33487-2742, pp. 75–88.
- Loftus, J.H., Kijanka, G.S., O’Kennedy, R., Loscher, C.E. (2016).** Patulin, Deoxynivalenol, Zearalenone and T-2 Toxin Affect Viability and Modulate Cytokine Secretion in J774A.1 Murine Macrophages. *Int. J. Chem.* **8**, 22-32.
- Luongo, D., Severino, L., Bergamo, P., De Luna, R., Lucisano, A., and Rossi, M. (2006).** Interactive effects of fumonisin B1 and alpha-zearalenol on proliferation and cytokine expression in Jurkat T cells. *Toxicol. In Vitro.* **8**, 1403-1410.
- Maggon, K. K., S. K. Gupta, and T. A. Venkitasubramanian. (1977).** Biosynthesis of aflatoxins. *Bact. Rev.* **41**, 822–855.
- Marin, S., Ramos, A.J., Cano-Sancho, G. and Sanchis, V. (2013).** Mycotoxins: Occurrence, toxicology, and exposure assessment. *Food Chem. Toxicol.* **60**, 218-237.

- Marroquín-Cardona**, A.G., Johnson, N.M., Phillips, T.D. and Hayes, A.W. (2014). Mycotoxins in a changing global environment – A review. *Food and Chem. Toxicol.* **69**, 220-230.
- Marzocco**, S., Russo, R., Bianco, G., Autore, G. and Severino, L. (2009). Pro-apoptotic effects of nivalenol and deoxynivalenol trichothecenes in J774A.1 murine macrophages. *Toxicol. Lett.* **189(1)**, 21–26.
- Min**, W.-K., Na, K.-I., Yoon, J.-H., Heo, Y.-J., Lee, D., Kim, S.-G., Seo, J.-H. (2016). Affinity improvement by fine tuning of single-chain variable fragment against aflatoxin B1. *Food Chem.* **209**, 312–317.
- Miyahira**, Y., Katae, M., Kobayashi, S., Takeuchi, T., Fukuchi, Y., Abe, R., Okumura, K., Yagita, H., Aoki, T. (2003). Critical contribution of CD28-CD80/CD86 costimulatory pathway to protection from *Trypanosoma cruzi* infection. *Infect. Immun.* **71**, 3131–3137.
- Molteni**, M., Gemma, S., Rossetti, C. (2016). The Role of Toll-Like Receptor 4 in Infectious and Noninfectious Inflammation. *Mediators Inflamm.* **2016**, 9.
- Moon**, E.Y., and Pyo, S. (2000). Aflatoxin B1 inhibits CD14-mediated nitric oxide production in murine peritoneal macrophages. *Int. J. Immunopharmacol.* **3**, 237-246.
- Moran**, K.L.M., Fitzgerald, J., McPartlin, D.A., Loftus, J.H., O’Kennedy, R., (2016). Chapter 4 - Biosensor-Based Technologies for the Detection of Pathogens and Toxins, in: Scognamiglio, V., Rea, G., Arduini, F., Palleschi, G. (Eds.), *Comprehensive Analytical Chemistry, Biosensors for Sustainable Food - New Opportunities and Technical Challenges*. Elsevier, pp. 93–120.
- Mosser**, D.M., Edwards, J.P., 2008. Exploring the full spectrum of macrophage activation. *Nat. Rev. Immunol.* **8**, 958–969.
- Muallem**, G., Wagage, S., Sun, Y., DeLong, J.H., Valenzuela, A., Christian, D.A., Pritchard, G.H., Fang, Q., Buza, E.L., Jain, D., Elloso, M.M., López, C.B., Hunter, C.A. (2017). IL-27 Limits Type 2 Immunopathology Following Parainfluenza Virus Infection. *PLOS Pathogens* **13**, e1006173.

- Müller**, G., Rosner, H., Rohrmann, B., Erler, W., Geschwend, G., Gräfe, U., Burkert, B., Möller, U., Diller, R., Sachse, K., Köhler, H. (2003). Effects of the mycotoxin ochratoxin A and some of its metabolites on the human cell line THP-1. *Toxicology* **184**, 69–82.
- Murata**, H., Sultana, P., Shimada, N., Yashioka, M. (2003). Structure–activity relationships among zearalenone and its derivatives based on bovine neutrophil chemiluminescence. *Vet. Hum. Toxicol.* **45 (1)**, 18–20.
- Murphy**, M., Jason-Moller, L., and Bruno, J. (2006). Using Biacore to measure the binding kinetics of an antibody-antigen interaction. *Curr. Protoc. Protein Sci.* **19**, 14.
- Niyo**, K.A., Richard, J.L., Niyo, Y., Tiffany, L.H. (1988). Effects of T-2 mycotoxin ingestion on phagocytosis of *Aspergillus fumigatus* conidia by rabbit alveolar macrophages and on hematologic, serum biochemical, and pathologic changes in rabbits. *Am. J. Vet. Res.* **49**, 1766–1773.
- O’Brien**, E. (2005). Microtoxins affecting the kidney. In *Toxicology of the Kidney*, 3rd Edition. Editors, Tarloff, J.B. and Lash, L.H. Taylor & Francis, London, UK. 895–936.
- Oh**, S.-Y., Cedergreen, N., Yiannikouris, A., Swamy, H.V.L.N., Karrow, N.A. (2017). Assessing interactions of binary mixtures of Penicillium mycotoxins (PMs) by using a bovine macrophage cell line (BoMacs). *Toxicol. and Appl. Pharmacol.* **318**, 33–40.
- O’Kennedy**, R., Fitzgerald, S., Murphy, C. (2017). Don’t blame it all on antibodies – The need for exhaustive characterisation, appropriate handling, and addressing the issues that affect specificity. *Trends Anal. Chem.* **89**, 53–59.
- Pestka**, J.J. (2003). Deoxynivalenol-induced IgA production and IgA nephropathy-aberrant mucosal immune response with systemic repercussions. *Toxicol. Lett.* **140-141**, 287-295.
- Pestka**, J.J., and Zhou, H.R. (2006). Toll-like receptor priming sensitizes macrophages to proinflammatory cytokine gene induction by deoxynivalenol and other toxicants. *Toxicol. Sci.* **2**, 445-455.
- Pestka**, J.J., Zhou, H.R., Moon, Y., and Chung, Y.J. (2004). Cellular and molecular mechanisms for immune modulation by deoxynivalenol and other trichothecenes: unraveling a paradox. *Toxicol. Lett.* **1**, 61-73.

- Quirino**, G.F.S., Nascimento, M.S.L., Davoli-Ferreira, M., Sacramento, L.A., Lima, M.H.F., Almeida, R.P., Carregaro, V., Silva, J.S. (2016). Interleukin-27 (IL-27) Mediates Susceptibility to Visceral Leishmaniasis by Suppressing the IL-17-Neutrophil Response. *Infect. Immun.* **84**, 2289–2298.
- Redford**, P.S., Murray, P.J., O’Garra, A. (2011). The role of IL-10 in immune regulation during *M. tuberculosis* infection. *Mucosal Immunol.* **4**, 261.
- Repique**, C.J., Li, A., Brickey, W.J., Ting, J.P.Y., Collins, F.M., Morris, S.L. (2003). Susceptibility of mice deficient in the MHC class II transactivator to infection with *Mycobacterium tuberculosis*. *Scand. J. Immunol.* **58**, 15–22.
- Richard**, J.L. (2007). Some major mycotoxins and their mycotoxicoses—An overview. *Int. J. Food Microbiol.* **119(1–2)**, 3-10.
- Rodríguez-Carrasco**, Y., Berrada, H., Font, G., Mañes, J. (2012). Multi-mycotoxin analysis in wheat semolina using an acetonitrile-based extraction procedure and gas chromatography-tandem mass spectrometry. *J. Chromatogr. A.* **1270**, 28-40.
- Routley**, C.E., Ashcroft, G.S. (2009). Effect of estrogen and progesterone on macrophage activation during wound healing. *Wound Repair Regen.* **17**, 42–50.
- Ryan**, A., Lynch, M., Smith, S.M., Amu, S., Nel, H.J., McCoy, C.E., Dowling, J.K., Draper, E., O’Reilly, V., McCarthy, C., O’Brien, J., Eidhin, D.N., O’Connell, M.J., Keogh, B., Morton, C.O., Rogers, T.R., Fallon, P.G., O’Neill, L.A., Kelleher, D., Loscher, C.E. (2011). A Role for TLR4 in *Clostridium difficile* Infection and the Recognition of Surface Layer Proteins. *PLOS Pathogens* **7**, e1002076.
- Salah-Abbès**, B., Abbès S., Houas, Z., Abdel-Wahhab, M.A., Oueslati, R. (2008). Zearalenone induces immunotoxicity in mice: possible protective effects of radish extract (*Raphanus sativus*). *J. Pharm. Pharmacol.* **60**, 761-70.
- Schüller**, S., Kügler, S., Goebel, W., 1998. Suppression of major histocompatibility complex class I and class II gene expression in *Listeria monocytogenes*-infected murine macrophages. *FEMS Immunol. Med. Microbiol.* **20**, 289–299.

- Shane, S.** (1994). Economic issues associated with aflatoxin. In D. L. Eaton and J. D. Groopman (Eds.). *The Toxicology of Aflatoxin: Human Health, Veterinary and Agricultural Significance*. Academic Press, Inc., Boston, Massachusetts, USA.
- Sharma, N., He, Q. and Sharma, R. P.** (2004). Augmented fumonisin B toxicity in co-cultures: Evidence for crosstalk between macrophages and non-parenchymatous liver epithelial cells involving proinflammatory cytokines. *Toxicol.* **203(1–3)**, 239–251.
- Sheedy, C., MacKenzie, R. C. & Hall, J.C.** (2007), Isolation and affinity maturation of hapten-specific antibodies, *Biotechnol. Adv.*, **25(4)**, 333-352.
- Smith, G.** (1985), Filamentous fusion phage: novel expression vectors that display cloned antigens on the virion surface, *Science*, **228(4705)**, 1315-1317.
- Snyderman, R., Pike, M.C., Fischer, D.G., Koren, H.S.** (1977) Biologic and biochemical activities of continuous macrophage cell lines P388D1 and J774A.1. *J. Immunol.* **119**, 2060-2066.
- Solhaug, A., Wisbech, C., Christoffersen, T.E., Hult, L.O., Lea, T., Eriksen, G.S. and Holme, J.A.** (2015). The mycotoxin alternariol induces DNA damage and modify macrophage phenotype and inflammatory responses. *Toxicol. Lett.* **239(1)**, 9-21.
- Stoev, S.D.** (2015). Foodborne mycotoxicoses, risk assessment and underestimated hazard of masked mycotoxins and joint mycotoxin effects or interaction. *Environ. Toxicol. Pharmacol.* **39(2)**, 794-809.
- Stornetta, A., Engeli, B.E., Zarn, J.A., Gremaud, G. and Sturla, S.J.** (2015). Development of a risk management tool for prioritizing chemical hazard-food pairs and demonstration for selected mycotoxins. *RTP.* **72(2)**, 257-265.
- Stow, J.L., Low, P.C., Offenhauser, C., and Sangermani, D.** (2009). Cytokine secretion in macrophages and other cells: pathways and mediators. *Immunobiol.* **7**, 601-612.
- Streit, E., Naehrer, K., Rodrigues, I., Schatzmayr, G.,** (2013). Mycotoxin occurrence in feed and feed raw materials worldwide: long-term analysis with special focus on Europe and Asia. *J. Sci. Food Agric.* **93**, 2892-2928.

Sullivan, G.W., Mandell, G.L. (1991). The role of cytokines in infection. *Current Opinion in Infectious Diseases* **4**, 344.

Turner, N.W., Bramhmbhatt, H., Szabo-Vezse, M., Poma, A., Coker, R. and Piletsky, S.A. (2015). Analytical methods for determination of mycotoxins: An update (2009–2014). *Anal. Chim. Acta* **1**, 1-22.

Turner, N.W., Subrahmanyam, S. and Piletsky, S.A. (2009). Analytical methods for determination of mycotoxins: A review. *Anal. Chim. Acta* **632(2)**, 168-180.

Ubagai, T., Tansho, S., Ito, T., and Ono, Y. (2008). Influences of aflatoxin B1 on reactive oxygen species generation and chemotaxis of human polymorphonuclear leukocytes. *Toxicol. In Vitro.* **4**, 1115-1120.

Vasanthi, S. and Bhat, R. (1998). Mycotoxins in foods - Occurrence, health & economic significance & food control measures. *Indian J. Med. Res.* **108**, 212-224.

Vasanthi, P., Nalini, G., Rajasekhar, G. (2007). Role of tumor necrosis factor-alpha in rheumatoid arthritis: a review. *APLAR J. Rheumatol.* **10**, 270–274.

Wang, S.-Z., Bao, Y.-X., Rosenberger, C.L., Tesfaigzi, Y., Stark, J.M., Harrod, K.S., 2004. IL-12p40 and IL-18 modulate inflammatory and immune responses to respiratory syncytial virus infection. *J. Immunol.* **173**, 4040–4049.

Welke J.E., Hoeltz M., Dottori H.A., Noll I.B. (2009) Quantitative analysis of patulin in apple juice by thin-layer chromatography using a charge coupled device detector. *Food Addit. Contam. Part A.* **26**, 754-758

White, M. (1999). Mediators of inflammation and the inflammatory process. *J. Allergy Clin. Immunol.* **3**, 378-S381.

Xu, F., Ren, K., Yang, Y., Guo, J., Ma, G., Liu, Y., Lu, Y., Li, X. (2015). Immunoassay of chemical contaminants in milk: A review. *J. Integrative Agric.* **14**, 2282–2295.

Xu, Y., Xiong, L., Li, Y., Xiong, Y., Tu, Z., Fu, J., Tang, X. (2015). Citrinin detection using phage-displayed anti-idiotypic single-domain antibody for antigen mimicry. *Food Chem.* **177**, 97–101.

Yeni, F., Acar, S., Polat, Ö.G., Soyer, Y. and Alpas, H. (2014). Rapid and standardized methods for detection of foodborne pathogens and mycotoxins on fresh produce. *Food Control*. **40**, 359-367.

Zain, M.E. (2011). Impact of mycotoxins on humans and animals. *J. Saudi Chem. Soc.* **15(2)**, 129-144.

Zhou, H.R., Islam, Z., and Pestka, J.J. (2003). Rapid, sequential activation of mitogen-activated protein kinases and transcription factors precedes proinflammatory cytokine mRNA expression in spleens of mice exposed to the trichothecene vomitoxin. *Toxicol. Sci.* **1**, 130-142.